

The  
GEOLOGICAL BULLETIN  
of the  
PUNJAB UNIVERSITY

Number 44

2009

C O N T E N T S

page

|  |   |     |
|--|---|-----|
| Crystallization History of the Kirana Volcanics, Sargodha, Pakistan.   | By Syed Alim Ahmad and Muhammad Nawaz Chaudhry  | 1   |
| Sedimentology of the Middle Jurassic Samana Suk Formation, Makarwal Section, Surghar Range, Trans Indus Ranges, Pakistan                         | By Abdur Rauf Nizami and Riaz Ahmad Sheikh  | 11  |
| Paleogene Biostratigraphy of Kohat Area, Northern Pakistan.  | By Shahid J. Sameeni, Mohammad Haneef, Obaid-Ur-Rehman and Jere H. Lipps                    | 27  |
| Allai Aggregate for Rehabilitation and Reconstruction of October 8, 2005 Earthquake Affected Allai-Banan Area, NWFP, Pakistan                    | By Naveed Ahsan, Muhammad Nawaz Chaudhry, Muhammad Munawar Iqbal Gondal and Zahid Karm Khan | 43  |
| Petrography and Mineralogy of Dolerites of Hachi Volcanics, Kirana Hills Area, Pakistan  | By Zahid Karim Khan, Naveed Ahsan, Abdul Mateen and Muhammad Nawaz Chaudhry                 | 55  |
| Microfacies Analysis and Diagenetic Settings of the Middle Jurassic Samana Suk Formation, Sheikh Budin Hill Section, Trans Indus Ranges-Pakistan | By Abdur Rauf Nizami and Riaz Ahmad Sheikh  | 69  |
| Foraminiferal Biostratigraphy and Reconnaissance Microfacies of Paleocene Lockhart Limestone of Jabri Area, Hazara, Northern Pakistan.           | By S. J. Sameeni, Nauman Nazir, Adnan Abdul-Karim and Humaira Naz                           | 85  |
| Engineering Properties of Potential Aggregate Resources From Eastern and Central Salt Range, Pakistan  | By Muhammad Munawar Iqbal Gondal Naveed Ahsan and Ahmad Zia Javid                           | 97  |
| Geochemistry and Tectonic Environments of Babusar Amphibolites in Southeast Kohistan, Pakistan.  | By Muhammad Ahmed Khan, Saif Ur Rehman, Muhammad Fahad Ullah and Naveed Ahsan               | 105 |
| Mangla Earthquake of March 10, 2006: Source Parameters and Nature of the Derived Fault   | By Talat Iqbal, Karam Khan, Muhammad Qaisar, Tariq Mahmood and Nasir Ahmad                  | 117 |
| Paleocurrent Analysis Of Dhok Pathan Formation, from Thathi Northeastern Potwar District Rawalpindi  | By Syed Mahmood Ali Shah, Amer Hafeez and Naveed Ahmad                                      | 123 |
| Sedimentology Of Dhok Pathan Formation from Thathi Area, Northeast Potwar District Rawalpindi  | By Syed Mahmood Ali Shah and Amer Hafeez  | 131 |
| Teaching staff list of the Institute of Geology, University of the Punjab 2009   |   | 139 |
| Non teaching staff members list of the Institute of Geology, University of the Punjab 2009   |   | 141 |



## CRYSTALLIZATION HISTORY OF THE KIRANA VOLCANICS, SARGODHA, PAKISTAN.

BY

SYED ALIM AHMAD

Institute of Geology, University of the Punjab, Quaid-i-Azam Campus,  
Lahore-54590 Pakistan

AND

MUHAMMAD NAWAZ CHAUDHRY

Postgraduate Centre for Earth Sciences, University of the Punjab, Quaid-e-Azam Campus, Lahore-54590 Pakistan.

**Abstract:** *The Neoproterozoic Kirana Volcanics represent bimodal volcanism in the Pakistani part of the Kirana-Malani Basin. Rhyolites predominate over the basalts/dolerites andesites and dacites. These volcanics represent the oldest remnants of widespread igneous activity within the so-called Kirana-Malani Basin and mark important Precambrian tectono-magmatic events in Pakistan. The acid volcanics are predominantly potassic; mafic representatives are characterized by the presence of plagioclase, augite and occasional olivine or magnetite. The felsic lavas are dominated by alkali feldspar and quartz. Amphibole and augite are also encountered in basalts/dolerites.*

### INTRODUCTION

The Kirana volcanics are an integral part of the world's largest felsic volcanic field known as 'Malani Volcanics' occupying tracks along the northwestern flank of the great Aravalli mountain ranges with scattered outcrops extending from Tosham in Haryana to other places in northern districts of Rajasthan. Thus, Kirana Malani may be described as volcanoplutonic province characterized by the widespread Late - Proterozoic tectono-magmatic activity (spanning over 950 Ma to 550 Ma) with distinct rhyolitic flows and associated granites.

The volcanic suites belong to tholeiitic basalt-andesite-rhyolite magma association (Ahmad, 2000, 2004). The volcanics are interbedded with intercalations of volcanogenic sediments and tuffs. The overlying metasedimentary units are Tuguwali phyllites and Asianwala quartzites respectively (Alam, 1987).

The volcanics and associated sedimentary rocks constitute a distinct cratonic rift assemblage and do not represent Indian Shield elements (Chaudhry et al., 1999) as previously believed by many workers (Heron, 1953; Davies and Crawford, 1971; Kochhar, 1984; Alam, 1987; Alam et al., 1992). The Kirana volcanics and volcanoplutonic rocks of Nagarparkar in Sindh were interpreted to have been emplaced in the extensional basins formed as a result of

mantle plume activity linked to the break-up of Rodinia Supercontinent. The extensional basin developed within the Late Proterozoic NE Gondwana part of Greater India is named as Malani-Kirana Basin (Chaudhry et al., 1999).

### CRYSTALLIZATION HISTORY

#### Dolerite and Microgabbros Associations

The minerals of some representative samples of dolerites, basalts, rhyolites, ignimbrites and welded tuffs have been analysed by microprobe analyzer at GeoScience laboratories, Islamabad.

Chemically these are classified as olivine-normative tholeiitic basalts/dolerites and their mineralogy may be conveniently described on the basis of olivine normative and quartz normative division. All lavas are examined; contain plagioclase, augite, olivine, ilmenite and apatite. Magnetite occurs only in the olivine-normative samples. The olivine normative lavas are aphyric, with some microphenocrystic olivine; plagioclase (up to 5%) and very minor augite are the phenocryst phases in the quartz normative lavas.

Olivine is an accessory phenocryst phase in the dolerite (olivine normative lava) and entirely absent in the quartz normative association of the Kirana Complex. The representative analyses of the olivines of the Kirana



**Table: 1.**  
Microprobe analysis of plagioclase in the Basalts/Dolerites from the Kirana Complex

| Sample#                                   | 135-72  | 134-72  | 143-72  | 144-72  | 149-72  | 162-72  | 163-72  | 177-72  | 178-72  | 181-72  |
|---|---------|---------|---------|---------|---------|---------|---------|---------|---------|---------|
| Lab No.                                   | C2/1-pl | C3-pl-C | C3-pl-R | C6-pl   | C4/2-Pl | C1/2-Pl | C4-Pl   | C5-Pl   | C1/2-Pl | C2/2-Pl |
| MAJOR OXIDE PERCENTAGE                    |         |         |         |         |         |         |         |         |         |         |
| TiO <sub>2</sub>                          | 0.072   | 0.039   | 0.066   | 0.089   | 0.620   | 0.059   | 0.072   | 0.065   | 0.412   | 0.051   |
| SiO <sub>2</sub>                          | 54.314  | 54.210  | 52.970  | 53.671  | 51.548  | 53.980  | 53.550  | 51.790  | 54.290  | 52.630  |
| Na <sub>2</sub> O                         | 4.213   | 5.310   | 3.950   | 4.540   | 2.995   | 4.280   | 3.990   | 5.160   | 6.210   | 3.187   |
| Cr <sub>2</sub> O <sub>3</sub>            | 0.034   | 0.024   | 0.023   | 0.019   | 0.013   | 0.029   | 0.018   | 0.019   | 0.018   | 0.024   |
| K <sub>2</sub> O                          | 0.150   | 0.140   | 0.012   | 0.140   | 0.088   | 0.170   | 0.149   | 0.149   | 0.103   | 0.130   |
| MgO                                       | 0.043   | 0.021   | 0.056   | 0.031   | 0.038   | 0.012   | 0.039   | 0.114   | 0.395   | 0.119   |
| MnO                                       | 0.036   | 0.034   | 0.000   | 0.021   | 0.011   | 0.052   | 0.047   | 0.023   | 0.019   | 0.004   |
| CaO                                       | 13.350  | 10.990  | 12.274  | 12.690  | 14.950  | 13.090  | 13.090  | 14.410  | 12.069  | 13.260  |
| Al <sub>2</sub> O <sub>3</sub>            | 27.723  | 29.120  | 29.456  | 28.504  | 29.900  | 28.110  | 29.150  | 28.056  | 25.490  | 29.410  |
| FeO                                       | 0.310   | 0.371   | 0.351   | 0.393   | 0.550   | 0.317   | 0.309   | 0.519   | 1.335   | 1.389   |
| NiO                                       | 0.000   | 0.048   | 0.001   | 0.000   | 0.017   | 0.000   | 0.002   | 0.049   | 0.089   | 0.077   |
| Total                                     | 100.173 | 100.268 | 99.093  | 100.009 | 100.110 | 100.040 | 100.344 | 100.289 | 100.018 | 100.230 |
| Mol.per cent                              |         |         |         |         |         |         |         |         |         |         |
| Ab  | 23.785  | 32.299  | 24.329  | 26.137  | 16.608  | 24.401  | 23.159  | 26.168  | 33.783  | 19.225  |
| An  | 75.368  | 66.849  | 75.597  | 73.057  | 82.904  | 74.629  | 75.977  | 73.077  | 65.657  | 79.990  |
| Or  | 0.847   | 0.852   | 0.074   | 0.806   | 0.488   | 0.969   | 0.865   | 0.756   | 0.560   | 0.784   |
| No. of cations on the basis of 32 oxygens |         |         |         |         |         |         |         |         |         |         |
| Ti  | 0.007   | 0.005   | 0.009   | 0.012   | 0.085   | 0.008   | 0.010   | 0.009   | 0.057   | 0.007   |
| Si  | 9.849   | 9.783   | 9.665   | 9.747   | 9.400   | 9.800   | 9.684   | 9.503   | 9.949   | 9.557   |
| Na  | 1.479   | 1.855   | 1.395   | 1.596   | 1.057   | 1.504   | 1.397   | 1.833   | 2.203   | 1.120   |
| Cr  | 0.005   | 0.003   | 0.003   | 0.003   | 0.002   | 0.004   | 0.003   | 0.003   | 0.003   | 0.003   |
| K   | 0.035   | 0.032   | 0.003   | 0.032   | 0.020   | 0.039   | 0.034   | 0.035   | 0.024   | 0.030   |
| Mg  | 0.012   | 0.006   | 0.015   | 0.008   | 0.010   | 0.003   | 0.010   | 0.031   | 0.108   | 0.032   |
| Mn  | 0.006   | 0.005   | 0.000   | 0.003   | 0.002   | 0.008   | 0.007   | 0.004   | 0.003   | 0.001   |
| Ca  | 2.594   | 2.125   | 2.400   | 2.469   | 2.921   | 2.546   | 2.536   | 2.833   | 2.370   | 2.580   |
| Al  | 5.914   | 6.183   | 6.323   | 6.090   | 6.415   | 6.004   | 6.202   | 6.056   | 5.495   | 6.283   |
| Fe  | 0.044   | 0.052   | 0.050   | 0.056   | 0.078   | 0.045   | 0.044   | 0.074   | 0.190   | 0.196   |
| Ni  | 0.000   | 0.007   | 0.000   | 0.000   | 0.002   | 0.000   | 0.000   | 0.007   | 0.013   | 0.011   |
| Total                                     | 19.936  | 20.051  | 19.854  | 20.004  | 19.908  | 19.954  | 19.917  | 20.378  | 20.357  | 19.815  |

SHIMADZU EPMA-8705 Q-II System installed at GeoScience Laboratory, GSP, Islamabad.

Conditions: Acc. Volt. = 15 kv Samp. Current = 1 Beam Dia = 10um

Satndards: TiO<sub>2</sub> Quartz, Albite, Cr<sub>2</sub>O<sub>3</sub> Sanidine, MgO, Rhodonite, Wollastonite, Al<sub>2</sub>O<sub>3</sub>, Fe<sub>2</sub>O<sub>3</sub>, Cobaltite, NiSi.



**Table:2.**  
Microprobe analyses of olivines in the Dolerites from the Kirana Complex

| Sample #                                 | K-209   | K-210   | K-211  | K-212   | K-213   | K-214   | K-215   | K-216  | K-217   | K-218   |
|--|---------|---------|--------|---------|---------|---------|---------|--------|---------|---------|
| Lab. #                                   | C1-ol   | C1-ol   | C1-ol  | C1-ol   | C1-ol   | C1-ol   | C1-ol   | C1-ol  | C1-ol   | C2/1-ol |
| SiO <sub>2</sub>                         | 35.654  | 36.735  | 35.560 | 35.678  | 35.112  | 36.225  | 36.122  | 35.225 | 36.445  | 36.665  |
| Al <sub>2</sub> O <sub>3</sub>           | 0.103   | 0.113   | 0.114  | 0.140   | 0.090   | 0.050   | 0.080   | 0.080  | 0.060   | 0.045   |
| FeO                                      | 27.570  | 26.056  | 26.311 | 27.786  | 26.889  | 25.558  | 25.489  | 27.410 | 25.523  | 24.470  |
| Na <sub>2</sub> O                        | 0.047   | 0.014   | 0.014  | 0.046   | 0.000   | 0.021   | 0.000   | 0.000  | 0.015   | 0.001   |
| C <sub>2</sub> O <sub>3</sub>            | 0.029   | 0.005   | 0.005  | 0.021   | 0.000   | 0.000   | 0.003   | 0.014  | 0.000   | 0.025   |
| K <sub>2</sub> O                         | 0.000   | 0.005   | 0.005  | 0.003   | 0.000   | 0.000   | 0.000   | 0.004  | 0.000   | 0.000   |
| MgO                                      | 36.227  | 36.560  | 36.763 | 36.113  | 37.428  | 37.072  | 37.450  | 36.175 | 37.145  | 37.257  |
| MnO                                      | 0.589   | 0.537   | 0.537  | 0.457   | 0.509   | 0.467   | 0.528   | 0.580  | 0.493   | 0.528   |
| CaO                                      | 0.024   | 0.068   | 0.068  | 0.055   | 0.036   | 0.038   | 0.049   | 0.020  | 0.039   | 0.029   |
| TiO <sub>2</sub>                         | 0.000   | 0.028   | 0.028  | 0.019   | 0.025   | 0.058   | 0.022   | 0.011  | 0.500   | 0.060   |
| CoO                                      | 0.047   | 0.030   | 0.030  | 0.000   | 0.000   | 0.898   | 0.593   | 0.073  | 0.080   | 0.630   |
| NiO                                      | 0.065   | 0.128   | 0.128  | 0.064   | 0.000   | 0.006   | 0.049   | 0.126  | 0.029   | 0.174   |
| Total                                    | 100.355 | 100.279 | 99.563 | 100.382 | 100.089 | 100.393 | 100.385 | 99.718 | 100.329 | 99.884  |
| No. of cations on the bases of 4 oxygens |         |         |        |         |         |         |         |        |         |         |
| Si                                       | 0.926   | 0.951   | 0.927  | 0.936   | 0.912   | 0.943   | 0.936   | 0.922  | 0.937   | 0.948   |
| Al                                       | 0.003   | 0.003   | 0.003  | 0.004   | 0.003   | 0.002   | 0.002   | 0.002  | 0.002   | 0.001   |
| Fe                                       | 0.558   | 0.521   | 0.534  | 0.556   | 0.549   | 0.511   | 0.512   | 0.559  | 0.511   | 0.493   |
| Na                                       | 0.002   | 0.001   | 0.001  | 0.002   | 0.000   | 0.001   | 0.000   | 0.000  | 0.001   | 0.000   |
| Cr                                       | 0.001   | 0.000   | 0.000  | 0.000   | 0.000   | 0.000   | 0.000   | 0.000  | 0.000   | 0.001   |
| K  | 0.000   | 0.000   | 0.000  | 0.000   | 0.000   | 0.000   | 0.000   | 0.000  | 0.000   | 0.000   |
| Mg                                       | 1.401   | 1.395   | 1.427  | 1.382   | 1.446   | 1.416   | 1.431   | 1.409  | 1.422   | 1.434   |
| Mn                                       | 0.013   | 0.012   | 0.012  | 0.010   | 0.011   | 0.010   | 0.011   | 0.013  | 0.011   | 0.012   |
| Ca                                       | 0.001   | 0.002   | 0.002  | 0.002   | 0.001   | 0.001   | 0.001   | 0.001  | 0.001   | 0.001   |
| Ti                                       | 0.000   | 0.001   | 0.001  | 0.000   | 0.000   | 0.001   | 0.000   | 0.000  | 0.010   | 0.001   |
| Co                                       | 0.001   | 0.001   | 0.001  | 0.000   | 0.000   | 0.018   | 0.012   | 0.002  | 0.002   | 0.013   |
| Ni                                       | 0.001   | 0.003   | 0.003  | 0.001   | 0.000   | 0.000   | 0.001   | 0.003  | 0.001   | 0.004   |
| Total                                    | 2.907   | 2.889   | 2.910  | 2.895   | 2.923   | 2.902   | 2.908   | 2.910  | 2.897   | 2.907   |



**Table: 3.**  
Microprobe analyses of augite in Gabbros and dolerites from the Kirana Complex

| Sample #                                 | K-209   | K-210   | K-211   | K-212   | K-213   | K-214   | K-215   | K-216   | K-217   | K-218    |
|--|---------|---------|---------|---------|---------|---------|---------|---------|---------|----------|
| Lab. #                                   | C1-aug  | C1-aug  | C1-aug  | C1-aug  | C1-aug  | C1-aug  | C1-aug  | C1-aug  | C1-aug  | C2/1-aug |
| SiO <sub>2</sub>                         | 49.710  | 52.345  | 47.106  | 51.990  | 49.291  | 52.490  | 49.790  | 48.420  | 49.215  | 51.646   |
| Al <sub>2</sub> O <sub>3</sub>           | 5.078   | 4.480   | 5.345   | 4.380   | 3.866   | 3.280   | 3.140   | 3.940   | 3.556   | 2.783    |
| FeO                                      | 11.820  | 8.780   | 11.193  | 7.840   | 8.007   | 8.330   | 7.750   | 9.800   | 8.600   | 7.124    |
| Na <sub>2</sub> O                        | 0.490   | 0.229   | 0.483   | 0.380   | 0.477   | 0.270   | 0.343   | 0.364   | 0.480   | 0.349    |
| C <sub>2</sub> O <sub>3</sub>            | 0.340   | 0.150   | 0.155   | 0.265   | 0.357   | 0.250   | 0.300   | 0.184   | 0.290   | 0.118    |
| K <sub>2</sub> O                         | 0.008   | 0.110   | 0.010   | 0.081   | 0.000   | 0.000   | 0.016   | 0.010   | 0.000   | 0.002    |
| MgO                                      | 13.090  | 14.580  | 13.699  | 14.990  | 15.639  | 12.940  | 15.550  | 14.640  | 14.870  | 14.960   |
| MnO                                      | 0.148   | 0.110   | 0.269   | 0.169   | 0.178   | 0.241   | 0.210   | 0.159   | 0.220   | 0.315    |
| CaO                                      | 17.670  | 19.223  | 19.126  | 18.234  | 20.860  | 21.090  | 20.840  | 20.970  | 21.440  | 22.128   |
| TiO <sub>2</sub>                         | 1.550   | 0.095   | 2.457   | 1.374   | 0.995   | 1.359   | 1.380   | 1.490   | 1.341   | 0.852    |
| CoO                                      | 0.355   | 0.149   | 0.294   | 0.542   | 0.640   | 0.000   | 0.495   | 0.016   | 0.000   | 0.000    |
| NiO                                      | 0.134   | 0.010   | 0.146   | 0.000   | 0.000   | 0.000   | 0.221   | 0.123   | 0.000   | 0.000    |
| Total                                    | 100.393 | 100.261 | 100.283 | 100.245 | 100.310 | 100.250 | 100.035 | 100.116 | 100.012 | 100.277  |
| NO. of cations on the basis of 6 oxygens |         |         |         |         |         |         |         |         |         |          |
| Si                                       | 1.835   | 1.835   | 1.756   | 1.892   | 1.823   | 1.921   | 1.844   | 1.804   | 1.828   | 1.909    |
| Al                                       | 0.165   | 0.165   | 0.244   | 0.108   | 0.177   | 0.079   | 0.135   | 0.173   | 0.140   | 0.091    |
| Al*                                      | 0.056   | 0.056   | 0.000   | 0.080   | 0.000   | 0.063   | 0.000   | 0.000   | 0.000   | 0.028    |
| Fe+2                                     | 0.371   | 0.272   | 0.217   | 0.243   | 0.088   | 0.260   | 0.133   | 0.133   | 0.112   | 0.171    |
| Fe+3                                     | 0.000   | 0.000   | 0.133   | 0.000   | 0.159   | 0.000   | 0.107   | 0.171   | 0.154   | 0.048    |
| Na                                       | 0.035   | 0.035   | 0.035   | 0.027   | 0.034   | 0.019   | 0.025   | 0.026   | 0.035   | 0.025    |
| Cr                                       | 0.010   | 0.010   | 0.005   | 0.008   | 0.010   | 0.007   | 0.009   | 0.005   | 0.009   | 0.003    |
| K  | 0.000   | 0.000   | 0.000   | 0.004   | 0.000   | 0.000   | 0.001   | 0.000   | 0.000   | 0.000    |
| Mg                                       | 0.719   | 0.719   | 0.758   | 0.812   | 0.861   | 0.705   | 0.857   | 0.812   | 0.822   | 0.808    |
| Mn                                       | 0.005   | 0.005   | 0.008   | 0.005   | 0.006   | 0.007   | 0.007   | 0.005   | 0.007   | 0.010    |
| Ca                                       | 0.699   | 0.699   | 0.775   | 0.711   | 0.827   | 0.827   | 0.827   | 0.837   | 0.853   | 0.860    |
| Ti                                       | 0.043   | 0.043   | 0.069   | 0.038   | 0.028   | 0.037   | 0.038   | 0.042   | 0.037   | 0.023    |
| Co                                       | 0.010   | 0.010   | 0.009   | 0.016   | 0.019   | 0.000   | 0.015   | 0.000   | 0.000   | 0.000    |
| Ni                                       | 0.004   | 0.004   | 0.004   | 0.000   | 0.000   | 0.000   | 0.007   | 0.004   | 0.000   | 0.000    |
| Total                                    | 3.952   | 3.853   | 4.013   | 3.943   | 4.032   | 3.926   | 4.005   | 4.013   | 3.997   | 3.976    |
| Atomic %ages                             |         |         |         |         |         |         |         |         |         |          |
| Mg                                       | 40.211  | 42.572  | 40.259  | 45.973  | 44.502  | 39.342  | 44.543  | 41.571  | 42.348  | 42.803   |
| Fe                                       | 20.722  | 16.068  | 18.589  | 13.778  | 12.776  | 14.507  | 12.492  | 15.573  | 13.705  | 11.630   |
| Ca                                       | 39.067  | 41.361  | 41.153  | 40.249  | 42.722  | 46.150  | 42.965  | 42.856  | 43.946  | 45.567   |
| mg*                                      | 65.992  | 72.599  | 68.412  | 76.941  | 77.695  | 73.059  | 78.098  | 72.748  | 75.550  | 78.635   |



**Table: 4.**  
Microprobe analyses of amphiboles in the dolerites from the Kirana Complex

| Sample #                                  | 131-72  | 147-72  | 150-72  | 151-72  | 157-72  | 158-72  | 165-72  | 167-72  | 172-72  | 173-72  |
|---|---------|---------|---------|---------|---------|---------|---------|---------|---------|---------|
| Lab. #                                    | C3-am-C | C3-am-C | C4/3-am | C5/1-am | C5/1-am | C4-am   | C2/1-am | C2/3-am | C4/1-am | C4-am   |
| SiO <sub>2</sub>                          | 44.120  | 43.334  | 43.12   | 41.25   | 43.220  | 41.450  | 42.889  | 44.120  | 43.110  | 41.330  |
| TiO <sub>2</sub>                          | 0.000   | 0.890   | 0.546   | 0.590   | 0.510   | 0.030   | 0.070   | 0.100   | 0.342   | 0.432   |
| Al <sub>2</sub> O <sub>3</sub>            | 10.120  | 9.260   | 9.34    | 10.230  | 9.330   | 9.780   | 8.340   | 8.660   | 9.340   | 9.230   |
| Cr <sub>2</sub> O <sub>3</sub>            | 0.010   | 0.060   | 0.02    | 0.420   | 0.230   | 0.030   | 0.000   | 0.020   | 0.040   | 0.080   |
| FeOT                                      | 20.340  | 19.334  | 19.334  | 20.560  | 23.230  | 22.445  | 22.445  | 22.140  | 23.120  | 20.230  |
| MnO                                       | 0.320   | 0.330   | 0.35    | 0.180   | 0.190   | 0.350   | 0.280   | 0.260   | 0.320   | 0.270   |
| MgO                                       | 9.340   | 12.220  | 10.34   | 10.550  | 9.340   | 10.220  | 9.340   | 10.320  | 11.450  | 12.090  |
| NiO                                       | 0.040   | 0.000   | 0.04    | 0.000   | 0.000   | 0.030   | 0.010   | 0.000   | 0.020   | 0.050   |
| CaO                                       | 15.223  | 14.221  | 16.37   | 16.230  | 14.230  | 15.920  | 15.450  | 13.950  | 12.340  | 16.300  |
| Na <sub>2</sub> O                         | 0.190   | 0.330   | 0.42    | 0.200   | 0.350   | 0.240   | 0.460   | 0.370   | 0.340   | 0.300   |
| K <sub>2</sub> O                          | 0.130   | 0.020   | 0.08    | 0.000   | 0.010   | 0.070   | 0.160   | 0.120   | 0.000   | 0.000   |
| Total                                     | 99.833  | 99.999  | 99.960  | 100.210 | 100.540 | 100.565 | 99.444  | 100.060 | 100.422 | 100.312 |
| No. of cations on the basis of 23 oxygens |         |         |         |         |         |         |         |         |         |         |
| Si <sup>4+</sup>                          | 6.571   | 6.391   | 6.483   | 6.191   | 6.378   | 6.259   | 6.530   | 6.497   | 6.373   | 6.333   |
| Al  | 1.420   | 1.609   | 1.517   | 1.809   | 1.622   | 1.741   | 1.485   | 1.503   | 1.627   | 1.667   |
| Al  | 0.356   | 0.000   | 0.138   | 0.000   | 0.000   | 0.000   | 0.000   | 0.000   | 0.000   | 0.000   |
| Ti <sup>4+</sup>                          | 0.000   | 0.099   | 0.062   | 0.067   | 0.057   | 0.003   | 0.008   | 0.011   | 0.038   | 0.050   |
| Cr <sup>3+</sup>                          | 0.001   | 0.007   | 0.002   | 0.050   | 0.027   | 0.004   | 0.000   | 0.002   | 0.005   | 0.010   |
| Fe <sup>3+</sup>                          | 0.144   | 0.378   | 0.000   | 0.189   | 0.854   | 0.114   | 0.271   | 0.873   | 0.608   | 0.000   |
| Fe <sup>2+</sup>                          | 2.389   | 2.007   | 2.431   | 2.391   | 2.013   | 2.720   | 2.565   | 1.853   | 2.250   | 2.592   |
| Mn <sup>2+</sup>                          | 0.040   | 0.041   | 0.045   | 0.023   | 0.024   | 0.045   | 0.036   | 0.032   | 0.040   | 0.035   |
| Mg <sup>2+</sup>                          | 2.074   | 2.687   | 2.318   | 2.360   | 2.055   | 2.301   | 2.104   | 2.266   | 2.523   | 2.762   |
| Ni <sup>2+</sup>                          | 0.005   | 0.000   | 0.005   | 0.000   | 0.000   | 0.004   | 0.001   | 0.000   | 0.002   | 0.006   |
| Ca <sup>2+</sup>                          | 2.429   | 2.247   | 2.637   | 2.609   | 2.250   | 2.576   | 2.501   | 2.201   | 1.954   | 2.676   |
| Na <sup>+</sup>                           | 0.055   | 0.094   | 0.122   | 0.058   | 0.072   | 0.070   | 0.135   | 0.106   | 0.097   | 0.089   |
| K <sup>+</sup>                            | 0.025   | 0.004   | 0.015   | 0.000   | 0.002   | 0.013   | 0.031   | 0.023   | 0.000   | 0.000   |
| Total                                     | 15.508  | 15.562  | 15.775  | 15.747  | 15.351  | 15.850  | 15.666  | 15.367  | 15.518  | 16.220  |



**Table: 5.**  
Microprobe analyses of orthoclases in the rhyolites from the Kirana Complex

| Sample No                                 | 21-vol-166 | 24-vol-166 | 26-vol-166 | 28-vol-166 | 32-vol-166 | 45-vol-166 | 46-vol-166 | 47-vol-166 | 50-vol-166 | 52-vol-166 |
|---|------------|------------|------------|------------|------------|------------|------------|------------|------------|------------|
| Rock Name                                 | C2-orth    | C2-orth    | C2-orth    | C1-orth    | C1-orth    | C2-orth    | C1-orth    | C-orth     | C1-orth    | C1-orth    |
| TiO <sub>2</sub>                          | 0.150      | 0.090      | 0.170      | 0.150      | 0.150      | 0.060      | 0.190      | 0.080      | 0.140      | 0.190      |
| SiO <sub>2</sub>                          | 70.800     | 79.850     | 80.690     | 76.810     | 79.700     | 84.650     | 67.840     | 81.980     | 83.610     | 72.240     |
| Na <sub>2</sub> O                         | 0.120      | 0.100      | 0.080      | 0.140      | 0.100      | 0.060      | 0.170      | 0.130      | 0.070      | 0.120      |
| Cr <sub>2</sub> O <sub>3</sub>            | 0.000      | 0.020      | 0.030      | 0.010      | 0.030      | 0.010      | 0.040      | 0.020      | 0.040      | 0.020      |
| K <sub>2</sub> O                          | 7.250      | 4.580      | 4.510      | 4.960      | 4.780      | 4.010      | 6.750      | 4.650      | 3.950      | 6.690      |
| MgO                                       | 0.820      | 0.550      | 0.620      | 0.670      | 0.570      | 0.460      | 0.940      | 0.480      | 0.400      | 0.780      |
| MnO                                       | 0.010      | 0.040      | 0.020      | 0.000      | 0.000      | 0.010      | 0.020      | 0.030      | 0.020      | 0.030      |
| CaO                                       | 0.000      | 0.000      | 0.020      | 0.030      | 0.010      | 0.000      | 0.000      | 0.010      | 0.030      | 0.010      |
| Al <sub>2</sub> O <sub>3</sub>            | 18.230     | 12.840     | 11.760     | 15.200     | 13.000     | 9.230      | 21.980     | 10.950     | 9.930      | 17.980     |
| FeO                                       | 1.908      | 1.269      | 1.599      | 1.812      | 1.482      | 1.301      | 1.546      | 1.215      | 1.770      | 1.716      |
| NiO                                       | 0.000      | 0.000      | 0.000      | 0.000      | 0.040      | 0.000      | 0.020      | 0.000      | 0.000      | 0.000      |
| Total                                     | 99.288     | 99.339     | 99.499     | 99.782     | 99.862     | 99.791     | 99.496     | 99.545     | 99.960     | 99.776     |
|   |            |            |            |            |            |            |            |            |            |            |
| Mol.%age                                  |            |            |            |            |            |            |            |            |            |            |
| ab  | 2.448      | 3.204      | 2.609      | 4.084      | 3.069      | 2.218      | 3.678      | 4.059      | 2.600      | 2.644      |
| an  | 0.000      | 0.000      | 0.361      | 0.484      | 0.170      | 0.000      | 0.000      | 0.173      | 0.617      | 0.122      |
| or  | 97.552     | 96.796     | 97.029     | 95.432     | 96.761     | 97.782     | 96.322     | 95.768     | 96.783     | 97.234     |
| No. of cations on the basis of 32 oxygens |            |            |            |            |            |            |            |            |            |            |
| Ti  | 0.020      | 0.012      | 0.022      | 0.019      | 0.019      | 0.008      | 0.025      | 0.010      | 0.018      | 0.025      |
| Si  | 12.470     | 13.625     | 13.756     | 13.171     | 13.572     | 14.240     | 11.929     | 13.926     | 14.095     | 12.594     |
| Na  | 0.041      | 0.033      | 0.026      | 0.046      | 0.033      | 0.020      | 0.058      | 0.043      | 0.023      | 0.040      |
| Cr  | 0.000      | 0.003      | 0.004      | 0.001      | 0.004      | 0.001      | 0.006      | 0.003      | 0.005      | 0.003      |
| K   | 1.630      | 0.998      | 0.982      | 1.086      | 1.039      | 0.861      | 1.515      | 1.008      | 0.850      | 1.489      |
| Mg  | 0.215      | 0.140      | 0.157      | 0.171      | 0.144      | 0.115      | 0.246      | 0.121      | 0.100      | 0.202      |
| Mn  | 0.001      | 0.006      | 0.003      | 0.000      | 0.000      | 0.001      | 0.003      | 0.004      | 0.003      | 0.004      |
| Ca  | 0.000      | 0.000      | 0.004      | 0.006      | 0.002      | 0.000      | 0.000      | 0.002      | 0.005      | 0.002      |
| Al  | 3.778      | 2.578      | 2.359      | 3.066      | 2.604      | 1.827      | 4.547      | 2.188      | 1.969      | 3.688      |
| Fe <sup>+2</sup>                          | 0.262      | 0.169      | 0.212      | 0.242      | 0.196      | 0.170      | 0.212      | 0.161      | 0.232      | 0.233      |
| Ni  | 0.000      | 0.000      | 0.000      | 0.000      | 0.005      | 0.000      | 0.003      | 0.000      | 0.000      | 0.000      |
| Total                                     | 18.397     | 17.550     | 17.503     | 17.789     | 17.601     | 17.235     | 18.518     | 17.456     | 17.284     | 18.255     |



Complex show small compositional variations. Compositions of olivine phenocrysts range from Fo<sub>73-70</sub>. Slight zoning to more fayalitic composition rims is observed as represented by Table: 1.

Olivine occurs as scattered microphenocrysts, but it is dominantly a groundmass phase in the olivine normative lavas. The microphenocrysts are normally zoned, the total compositional range being Fo<sub>48-61</sub>. Reaction rims of Ca-poor pyroxene have not been observed. Granular groundmass olivine is, within a given sample, compositionally similar to the coexisting microphenocryst rims, the observed range being Fo<sub>47-68</sub>. Al was detected only in a few samples. The trace element spectra are also similar. Cr is not detectable where as Ni and Co is detected in some samples. The CaO content in olivine is dependent on silica activity of magma; high silica activity promoting Ca poor olivine. Thus the most Ca-poor olivines in plutonic rocks should be expected in low-level undersaturated rocks.

The composition of plagioclase in basalt plots in the labradorite/bytownite field (Fig: 1). The structural formula of plagioclase is determined on the basis of 8 Oxygens. The Calcium contents in plagioclase vary from 67% to 79% and all feldspars are deficient in Al. The plagioclase from groundmass does not show any appreciable variation from the phenocrystal composition and plots in the labradorite field. The core of one of the phenocrysts plots near the boundary of labradorite-bytownite while the rim of the same is essentially of labradorite composition. As the composition of plagioclase in the groundmass does not show any appreciable variation, it is tempting to conclude that the magma ascended immediately after the formation of plagioclase phenocryst, allowing no time for further crystal fractionation in the residual melt.

Plagioclase represents phenocryst as well as groundmass phase in the dolerite, exhibiting relatively small compositional changes. Plagioclase crystals are slightly zoned and restricted in composition to labradorite to bytownite (An<sub>67</sub> to An<sub>82</sub>) field, however in the altered dolerites only albite is present (Fig. 1) The plagioclase from groundmass does not show any appreciable variation from phenocrystic composition and plots in the same fields.

The olivine normative lavas are characterized by a distinctly pink, granular groundmass of calcium rich augite, which shows rather restricted solid solution.

Microprobe analyses of the pyroxene from the Kirana basalts/dolerites clearly indicate that all the analysed samples fall within the field of augite, when plotted on the Ca-Mg-Fe diagram (Fig: 2) after Morimoto, et al (1988). Calcic augite is the dominant phenocryst and groundmass phase following plagioclase in the dolerites of the Kirana Complex. Analyses of pyroxenes (Table: 3) calculated on

the basis of 6 oxygens and 4 cations. The chemical data indicates that the clinopyroxene mainly formed under low pressure conditions as documented by their low Al<sup>6</sup> value as represented in Table: 3.

The microprobe analyses of the amphibole are given in Table: 4. All the samples fall in "Fe-hornblende" to "Mg-hornblende" fields, when plotted on the Si versus Mg/(Mg+Fe<sup>2+</sup>) diagram (Fig: 3) after Leake et al (1997). It occurs as phenocrysts as well as in the groundmass. The amphibole is rich in Ca to be hornblende enriched in Fe and Mg to be classified as Fe-hornblende to Mg-hornblende. The chemistry of the amphibole follows the parameters of Ca-amphibole i.e. Ca<sup>2+</sup> > 1.50; (Na+K) < 0.50 (after Leake et al, 1997). All the samples fall in the "Magmatic amphibole" field, when plotted on the Si versus Ca+Na+K diagram (Fig: 4) after Leake et al (1971).

### Felsic and Silicic Associations

Rhyolites are phenocryst free (5% total volume of samples) with two-feldspars plus quartz. Orthoclase, (the dominant feldspar, generally in excess of plagioclase in at least 5:1 proportion) ranges in composition from 95% to 98% (Table: 5). Individual crystals show minor oscillatory zoning of plagioclase. Plagioclase is predominantly sodic oligoclase and individual phenocrysts show oscillatory normal zoning typically with less than 5% total variation. Samples from the different flows show small variations in their total compositional range.

Wide variation exists in the K-Na content of the alkali feldspar in the different samples. The two phenocrysts of alkali feldspars from rhyolite represent almost end members with 94% K Al Si<sub>3</sub>O<sub>8</sub>, and 98% Na Al Si<sub>3</sub>O<sub>8</sub> (Fig: 1). The maximum albite contents of K-feldspar from rhyolite is 45%, with less than 2wt% anorthite, K-feldspar is found to co-exist with pure albite.

The maximum albite content of k-feldspar in the granites is 3% with <0.5% anorthite (Table:5). The iron contents of the K-feldspar ranges from 1.26% to 1.91% as FeO. Wide variations exist in K-Na content of the alkali feldspar in the rhyolites of the Malani volcanics (India). Bhushan (1989) presented analyses exhibiting 94%KAlSi<sub>3</sub>O<sub>8</sub>.

### DISCUSSION

It is a generally accepted fact that felsic volcanics predominate over the mafics within bimodal complexes (e. g. Yellowstone and Medicine lake in Western, USA, Iceland, Western Scotland and Southern Queens land of Australia, Malanis, India; Nagarparkar Complex, Pakistan). Ahmad (2000) and Ahmad (2004) based on geochemical constraints suggest that the rhyolites of the Kirana and Nagarparkar complexes are not differentiated products of



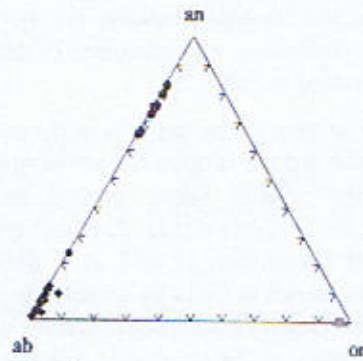


Fig: 1

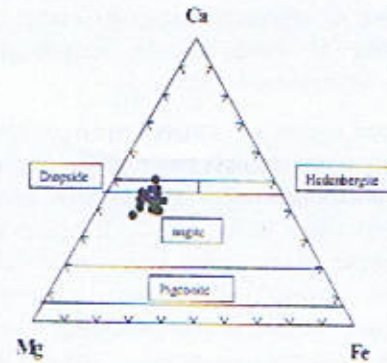


Fig: 2

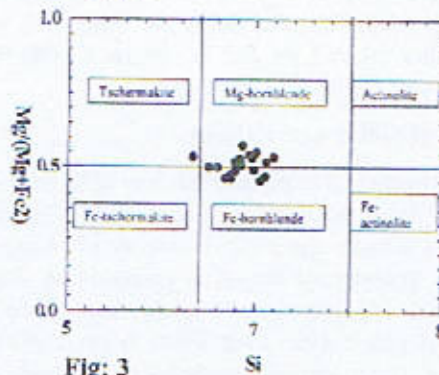


Fig: 3

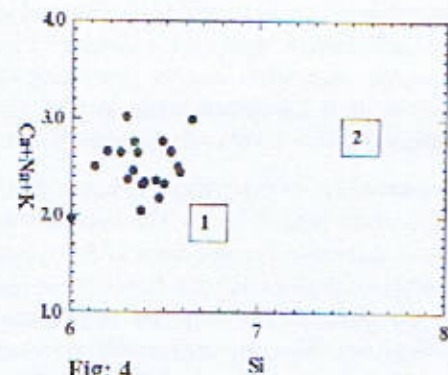


Fig: 4

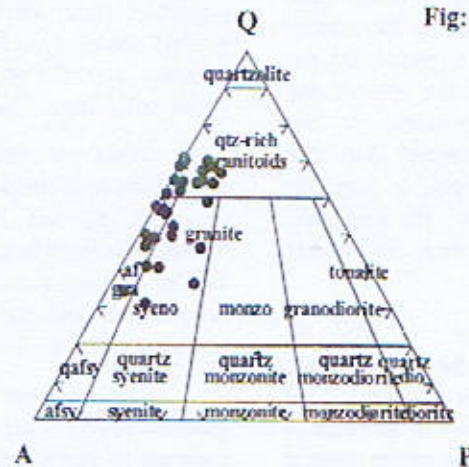


Fig: 5

Fig: 1. Plots of microprobe analyses of feldspar (mol per cent), from the rhyolites and dolerites of the Kirana Complex. Dolerites/basalts (rounded) show bytownite to labradorite composition. Rhyolites contain orthoclase (triangle). Filled diamonds are albitised plagioclase from altered dolerite.

Fig: 2. Microprobe plots of clinopyroxene in the dolerite from the Kirana Complex (Mg-Ca-Fe diagram) indicating augite to diopside composition (after Morimoto et al, 1988).

Fig: 3. Amphibole composition (plotted after Leake et al., 1997) from dolerite of the Kirana Complex. Composition of the representative samples fall in Ca-amphibole from Fe-hornblende to Mg-hornblende.

Fig: 4. Plot of Si versus Ca+Na+K for amphibole from the Kirana Complex. Fields after Leake (1971), 1 = magmatic amphibole, 2 = metamorphic amphibole. All the representative samples fall in the field of magmatic amphibole.

Fig. 5. Plots of Q-Ab+Or-An normative data of rhyolite from the Kirana Complex, plotted on the Q-A-P diagram, using fields established by Streckeisen (1976) for his modal Quartz-Alkalifeldspar-Plagioclase plot. The rhyolite of the Kirana Complex is falling in the fields of Alkali granite (alkali rhyolite), Granite (rhyolite) to Quartz rich granitoids (quartz rich rhyolite) fields.



basaltic magmatism. Near absence of intermediate members between the basaltic and rhyolitic flows and presence of voluminous rhyolitic rocks suggests that the rhyolites are not differentiated products of basaltic magmas (Bhushan, 1989). Only a small proportion of rhyolitic material as a fractionate may be generated by the differentiation of basic magma. Hence their formation by fractionation from basalt is not considered feasible. Evidently the generation of silicic magma should be related to partial melting of a preexisting crust, enriched in silica, alumina and alkalis (McBurney, 1984). The presence of bipyramidal quartz and K-feldspar as phenocrysts is indicative of high temperature of crystallization (Deer et al., 1992). The long-lived magmatism in the Neoproterozoic Kirana-Malani Basin necessitates the geochemical and geodynamic conditions that enable melting and igneous activity for extended

periods of time. The observed variations in the chemical compositions of Kirana volcanics require that they be derived by different degrees of melting from heterogeneous mantle source.

#### ACKNOWLEDGEMENTS

The authors are highly obliged to Prof. J. P. Burg, Director, Institute of Geology, E. H. Zurich, Switzerland for his guidance during the course of this research project. This research work was carried out under partial support of Punjab University research grant no 8/2001-R-1 and 211-222-P&D dated 25 6 99. Pakistan Institute of Engineering and Applied Sciences (PIEAS), Islamabad and GeoScience Laboratories, Islamabad, are acknowledged for providing analytical support in the laboratories and logistics during the fieldwork.

#### REFERENCES

- Ahmad, S. A., 2000. Geology and geochemistry of Neoproterozoic Kirana Volcanics, Sargodha district, Pakistan. *Geol. Bull. Punjab Univers.*, **35**: 59-71.
- Ahmad, S. A., 2004. Geology, Petrology and Geochemistry of the Neoproterozoic Indian Shield rocks extension in Pakistan, Ins. Geol. Lahore, Pakistan. *Ph. D thesis.*, 478.
- Alam, G.S., 1987. Geology of Kirana Hills, Sargodha, Punjab, Pakistan. *Information release no.201. GSP. Quetta, Pakistan*:1-37.
- Alam, G.S., Jaleel, A. and Ahmad, R. 1992. Geology of the Kirana area, District Sargodha Punjab, Pakistan. *Acta Miner. Pak* **6**: 93-100.
- Bhushan, S.K., 1989. Mineral chemistry and petrogenetic aspects of Malani Volcanics, Western Rajasthan. *Indian Minerals.*, **43**: 3&4: 325-338.
- Chaudhry, M.N., Ahmad, S.A. and Mateen, A., 1999. Some postulates on the tectonomagmatism, tectonostratigraphy and economic potential of Kirana-Malani-Basin, Indo-Pakistan. *Pakistan Jour. Hydrocarbon. Res. Islamabad, Pakistan.*, **11**: 52-68.
- Davies, R.G. and Crawford, A.R., 1971. Petrography and age of the rocks of Buland Hills, Sargodha Districts West Pakistan. *Geol. Mag.*, **108**: **3**: 235-246.
- Heron, A. M., 1953. The Geology of Central Rajputana. *Mem. Geol. Surv. India.*, **79**: 1-339.
- Kochhar, N., 1984. Malani igneous suite: Hotspot magmatism and Cratonization of the northern part of Indian Shield. *Journal of Geological Survey of India.*, **25**, (3): 155-161.
- Leak, B.E., 1971. On aluminous edenitic and hornblendes. *Mineral. Mag.*, **42**: 389-407.
- Leak, B.E., Wooley, A. R., Arps, C.E.S., Birch, W. D., Gilbert, M.C., Grice, J.D., Hawthorne, C., Kato, A., and others., 1997. Nomenclature of amphiboles: Report of the subcommittee on amphiboles of the International Mineralogical Association, Commission on new minerals and mineral names. *Amer. Mineral.*, **82**: 1019-1037.



## SEDIMENTOLOGY OF THE MIDDLE JURASSIC SAMANA SUK FORMATION, MAKARWAL SECTION, SURGHAR RANGE, TRANS INDUS RANGES, PAKISTAN

BY

ABDUR RAUF NIZAMI AND RIAZ AHMAD SHEIKH

Institute of Geology, University of the Punjab, Quaid-i-Azam Campus,  
Lahore-54590 Pakistan  
Email: raufnizami@yahoo.com

**Abstract:** *The sedimentology of the Middle Jurassic Samana Suk Formation, Makarwal Section, Surghar Range, Trans Indus Ranges, was investigated to elaborate its microfacies and diagenetic settings. The Samana Suk Formation is mainly composed of limestones and dolomitic limestones with some dolomite and intercalations of marl and shale at different levels. A detailed study was conducted after collecting systematically a total of 98 rock samples and studying selected 72 thin sections. To investigate its sedimentology, microfacies package and diagenetic settings the petrographic study of unstained and stained thin sections has been executed. Detailed field observations and laboratory investigations revealed that it contains microfacies forming SMF zones and is comprised of oolitic, peloidal, cortoidal and skeletal grainstones, bioclastic, ooidal and peloidal packstones, bioclastic wackstones, bioclastic mudstones and mudstones microfacies along with presence of dolomite at certain stratigraphic levels. This research work also demonstrates the presence of various cement types and their morphologies and diagenetic overprinting. The dolomitization has developed at different horizons as cement as well as replacement and as stylocumulate along stylolites. The dedolomitization has, also, been recorded along with incorporation of iron into calcite and dolomite at some later diagenetic stage. The Samana Suk Formation is widely exposed in the Upper Indus Basin of Pakistan. The microfacies analysis and diagenetic settings lead towards the conclusion that the formation was deposited in shallow shelf environment with open and restricted marine conditions.*

### INTRODUCTION

The Samana Suk Formation is a recognized as the most prominent stratigraphic unit in the Upper Indus Basin of Pakistan. It is integral part of the Mesozoic strata of Trans Indus Ranges, Cis-Indus Salt Ranges, Hazara Mountains, Kohat Tribal Range, Samana Range and Kala Chitta Range as the most important lithological package of carbonates. Further towards the west the Chiltan Formation and Mazar Drick Formation, exposed at a number of sections in the Sulaiman Fold and Thrust Belt and Murree Brewery Gorge near Quetta, Balochistan, Pakistan, are correlated with it. The Makarwal Section is located near Makarwal, District Mianwali, at a distance of 5km (Fig. 1). This section is located approximately at Latitude 32° 55' 35" N and Longitude 71° 08' 50" E on Toposheet No. 38 P/1 (Survey of Pakistan, Rawalpindi). It lies in the north

trending southern part of the Surghar Range and is striking in the NS direction near Makarwal. The Makarwal, a coal miners' small town, is accessible from the Kalabagh, Kamar Mashani and Isakhel through Mianwali-Bannu Road. A detailed study was conducted after collecting systematically a total of 98 rock samples and studying selected 72 thin sections to investigate sedimentology of the Samana Suk Formation exposed at this section. Here the formation is 37.98m thick. The present paper concentrates on sedimentology of the Samana Suk Formation. This contribution forms part of the doctoral thesis of the principal author.

### PREVIOUS INVESTIGATIONS

Earlier workers named this formation as Kioto Limestone (Cotter, 1933), Samana Suk Limestone (Davies,



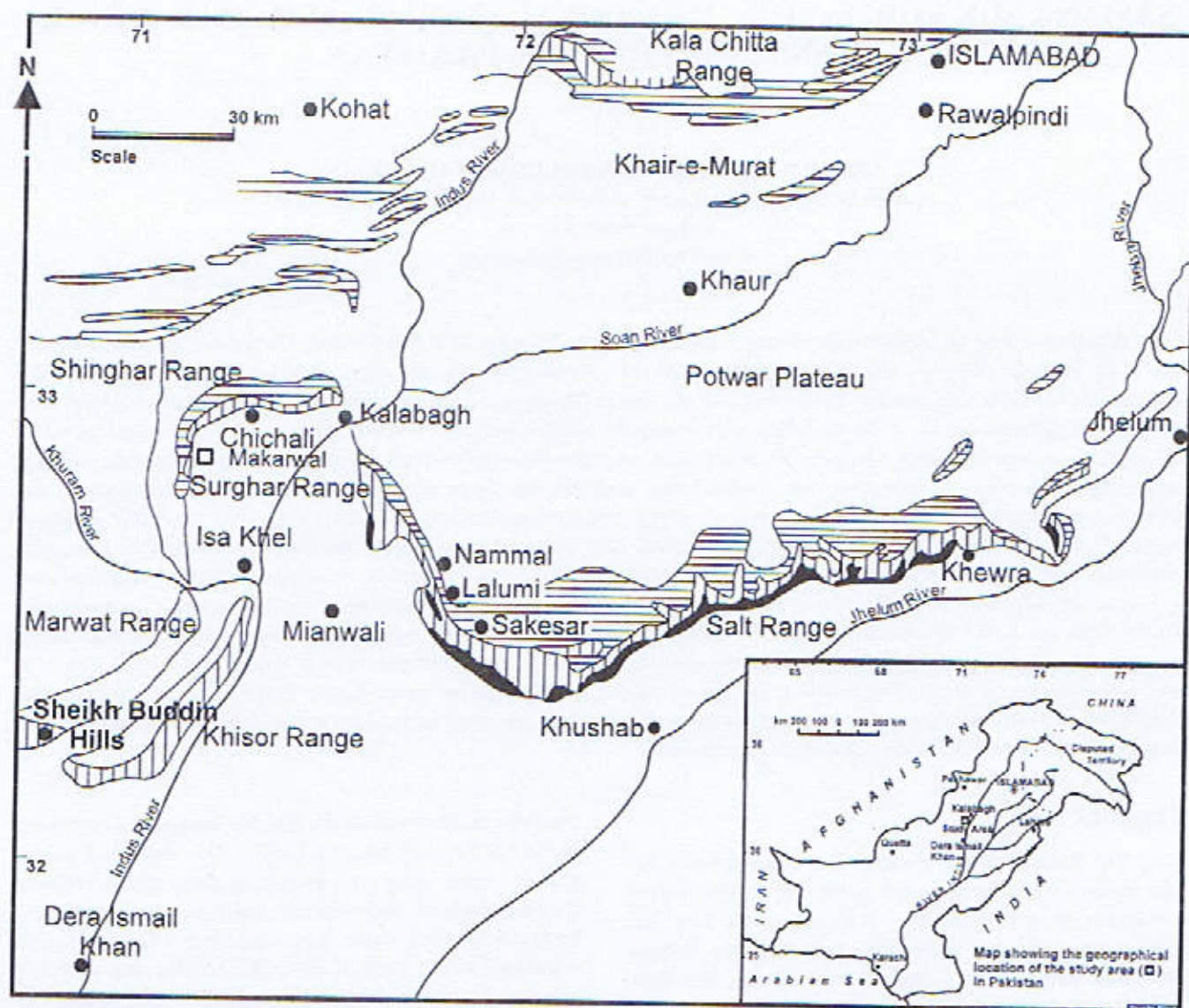


Fig.1 Map showing the location of Sheikh Buddin Hills Section (□) in the Trans Indus Ranges (Modified after Gee, 1989)



1930) and Broach Limestone (Gee, 1947). The name, Samana Suk Formation, was formalized in 1974 by Fatmi, et al., 1990. In the Upper Indus Basin, where the Trans Indus Ranges are situated (Anwar, et al., 1992 and Gee, 1989), the Jurassic strata is composed of Datta Formation, Shinawari Formation and Samana Suk Formation (Shah, 1977). According to Bender and Raza (1995) the lower part (relatively much thinner) of Chichali Formation is part of this Jurassic sequence. The upper part of Jurassic column is occupied by the Samana Suk Formation, which is a shallow water marine carbonate rock (Fatmi, et al., 1990). Mensink, et al. (1988), Fatmi, et al. (1990) and Mertmann and Ahmad (1994) reported that the Jurassic rock formations are exposed at a number of localities in the Trans Indus Ranges, particularly in the Surghar and Marwat Ranges. A number of previous workers executed commendable investigations on the Samana Suk Formation of middle Jurassic age. Trans Indus Ranges with different angles. Mensink, et al. (1988), Fatmi, et al. (1990) and Mertmann and Ahmad (1994) worked on its microfacies and depositional environments in a broad spectrum covering these ranges on regional scale. Danilchick and Shah (1987) investigated the stratigraphy and coal reserves of the Makarwal area, Surghar Range. The facies development during Jurassic of Trans Indus Ranges was investigated by Mensink, et al. (1988) based on the study of geological sections of Gulakhel, Broach Nala and Chichali Pass. Fatmi, et al. (1990) executed investigations on the occurrence of lower Jurassic Ammonoids from the Surghar Range and revised the nomenclature of the Mesozoic rocks of the Salt Range and Trans Indus Ranges on the basis of their research findings. The Jurassic shelf sedimentation and sequence stratigraphy of the Surghar Range was discussed by Ahmed, et al. (1997). Akhtar (1983) gave a brief account of stratigraphy of Surghar Range. The literature survey shows that no detailed work on sedimentology of the Samana Suk Formation was carried out in the host area of Makarwal Section, Surghar Range. Therefore a detailed investigation on microfacies analysis and diagenetic settings of the Samana Suk Formation was carried out by the present authors.

The parameters, like, field observations, section measurement, sampling, field photography, laboratory investigations (thin sections studies using petrographic microscope, chemical staining with Alizarin Red S and Potassium Ferricyanide) and digital photomicrography have been applied in the present research work.

#### SAMANA SUK FORMATION

In Makarwal Section the Samana Suk Formation is comprised of thin, medium to thick and massive

limestones/dolomites beds, which are uneven to wavy at places in the stratigraphic stacking. It is mainly composed of limestone and dolomitic limestone with intercalated calcareous shales/marls, present at a number of stratigraphic horizons. These argillaceous contents are deposited due to the periodic influxes of clay in response to small scale and distant tectonic uplift and erosion or climatic change on an area acting as provenance. The shale/marl breaks and intercalations present at different levels are irregular and do not show any cyclic deposition. The limestones are light grey and yellowish grey and at places dark grey and are mostly dense, hard and compact. Micritic and oolitic limestones are very fine to coarse grained. The general topographic impression of these limestones is that of a ridge former. These limestones also form steep slopes and impassable cliffs in the studied area. The Samana Suk Formation is stratigraphically sandwiched between the Shinawari Formation and Chichali Formation (Table 1). The lower contact with the Shinawari Formation is conformable and transitional one. The top most sandstone bed of the Shinawari Formation is marked here as the lower stratigraphic contact (Akhtar, 1983 and Mertmann and Ahmed, 1994). The upper contact with the Chichali Formation is disconformable and sharp and is marked by hard ground with lateritic encrustation (Mertmann and Ahmed, 1994 and Sheikh, 1991). Two hard ground surfaces have been recorded in this section, which mark the presence of regressive cycles and periods of non erosion-non deposition. According to Spath (1939) the age of this formation in the Trans Indus Ranges is Late Jurassic (Late Callovian) on the basis of cephalopod fauna present, however, its age is considered Early to Middle Callovian (Middle Jurassic) based on the occurrence of Middle Callovian Ammonites in highly fossiliferous sections of the Datta Nala, Punnu Nala, Landa Nala, Mallakhel and Makarwal areas in Surghar Range (Fatmi, 1972).

#### MICROFACIES

The microfacies analysis of this section revealed that the developed microfacies here include: bioclastic, peloidal, ooidal and cortoidal grainstones, bioclastic, ooidal and peloidal packstones, bioclastic wackestones, bioclastic mudstones and mudstones.

#### Grainstones

The following types of grainstones have been elaborated on the bases of petrographic analysis:

**Bioclastic grainstones:** This microfacies is composed of skeletal shells and fragments of organisms, sometimes in association with other carbonate grains (Plates 5a and d).



Table 1

Stratigraphic sequence of the Makarwal Section, Surghar Range, Trans Indus Ranges, Pakistan, showing the position (**bold**) of Samana Suk Formation (Hemphill and Kidwai, 1973, Akhtar, 1983, Danilchik and Shah, 1987 and Warwick, et al., 1995).

| ERA          | AGE          | GROUP          | FORMATION            |
|--------------|--------------|----------------|----------------------|
| CENOZOIC     | EOCENE       | CHHARAT GROUP  | Sakesar Formation    |
|              |              |                | Nammal Formation     |
|              | PALEOCENE    | MAKARWAL GROUP | Patala Formation     |
|              |              |                | Lockhart Formation   |
|              |              |                | Hangu Formation      |
| UNCONFORMITY |              |                |                      |
| MESOZOIC     | CRETACEOUS   | SURGHAR GROUP  | Lumshiwal Formation  |
|              |              |                | Chichali Formation   |
|              | UNCONFORMITY |                |                      |
|              | JURASSIC     | BROACH GROUP   | Samana Suk Formation |
|              |              |                | Shinawari Formation  |
|              |              |                | Datta Formation      |
|              | UNCONFORMITY |                |                      |
|              | TRIASSIC     | MUSAKHEL GROUP | Kingrialli Formation |

**Peloidal grainstones:** The peloidal grainstones have been recorded at a number of stratigraphic levels in the measured section and are predominantly represented. This sub microfacies consists of faecal pellets and peloidal grains which are micritized and have no internal micro architecture (Plates 1a and 6a). The other carbonate grains are also found in associations with peloids (e.g., foraminifera) in these grainstones (Plate 1a).

**Ooidal grainstones:** The ooids present in these grainstones have concentric laminar microfabrics (Plate 4c). Various skeletal grains act as nuclei in these ooids. Peloid and skeletal grains have also been recorded in association with ooids (Plate 4c).

**Cortoidal grainstones:** The cortoids are coated grains covered by micritic envelope and constitute a type of non-laminated coated grains (Tucker and Wright, 1990). This sub microfacies of grainstones has been found only at one horizon in this section (Plate 3a and 7b). The frequency of appearance of cortoids in other microfacies is relatively low.

#### Packstones

The packstone microfacies, commonly, display various types of grains as their components. These grains include skeletal grains, ooids and peloids. The following microfacies of packstone have been documented in this section.

**Bioclastic packstones:** This microfacies is composed of skeletal grains of different sorts. The frequency of occurrence of various bioclasts, shells, tests, and biodebris shows a variety of component skeletal grains (Plates 3b and d). This microfacies mainly exhibits skeletal shells and grains of mollusks, forams and brachiopods.

**Ooidal packstones:** It has been recorded only at two horizons in the investigated section (Plate 1c). The recorded ooids generally have concentric laminae.

**Peloidal packstones:** The peloidal packstones are present at few levels in the investigated section (Plates 4a and 5c). However, the frequency of appearance of peloids in association with other grains in other microfacies is low.

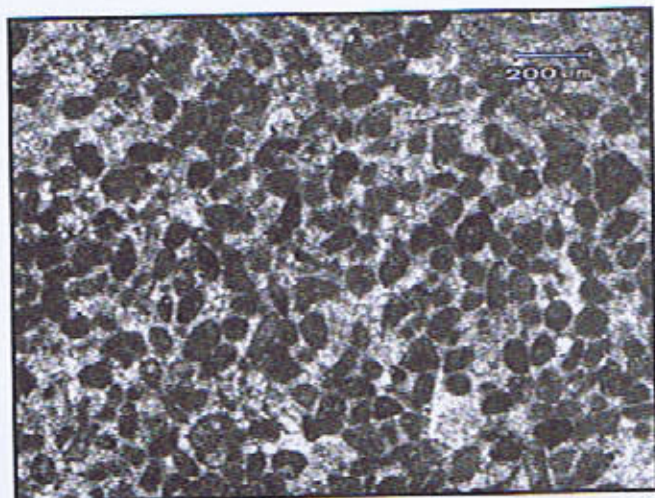
#### Wackestones

A microfacies with more than 10% carbonate grains set in micrite is categorized as wackestone according to Dunham classification (1962) of the carbonate microfacies. Only the bioclastic wackestones have been found here.

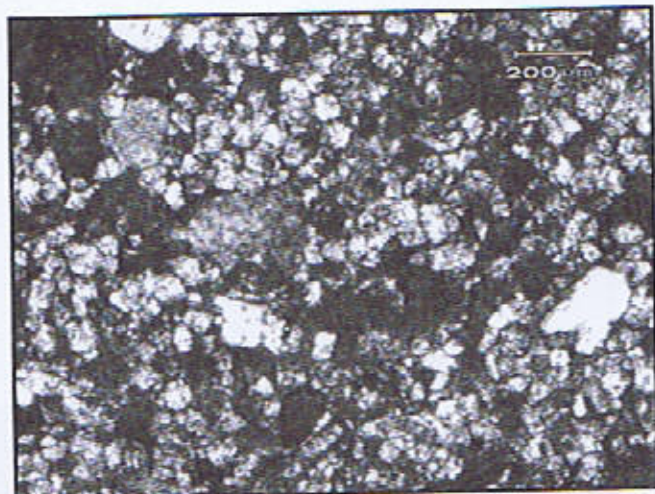
**Bioclastic wackestones:** The bioclastic wackestones have been documented at various levels in the studied section. The faunal diversity has also been noted in these wackestones (Plate 4d). The skeletal shells and fragments of mollusks are commonly found in this microfacies.



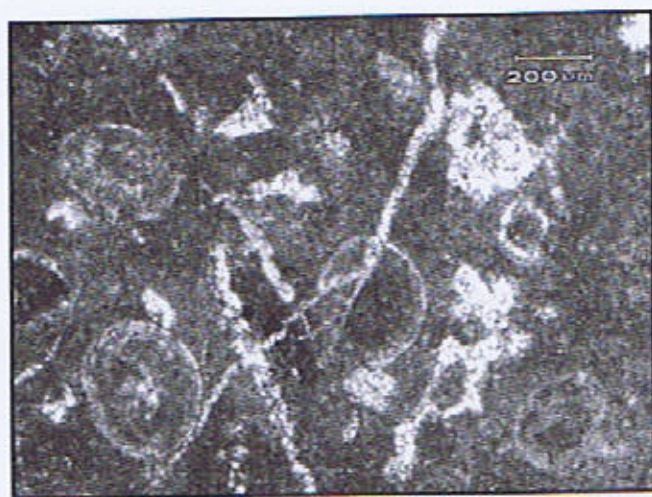
## Plate 1



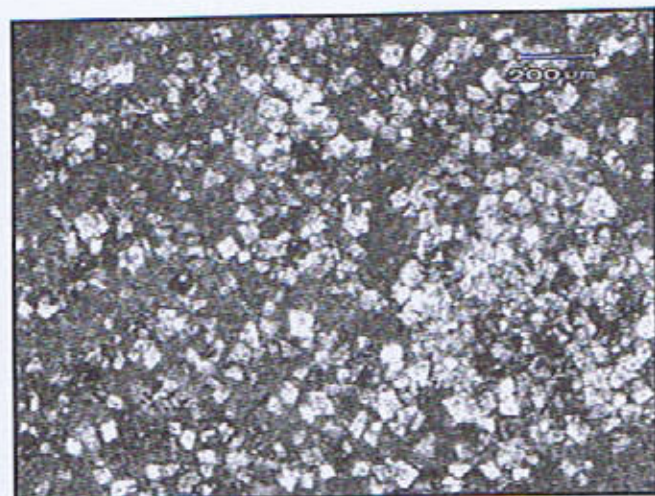
a.



b.



c.



d.

a. Photomicrograph showing peloidal grainstone cemented by intergranular cement (C) with drusy mosaic of crystals. A few associated foraminifers' shells (F) are present as well. (PPL, stained) Sample No. MKW-11T

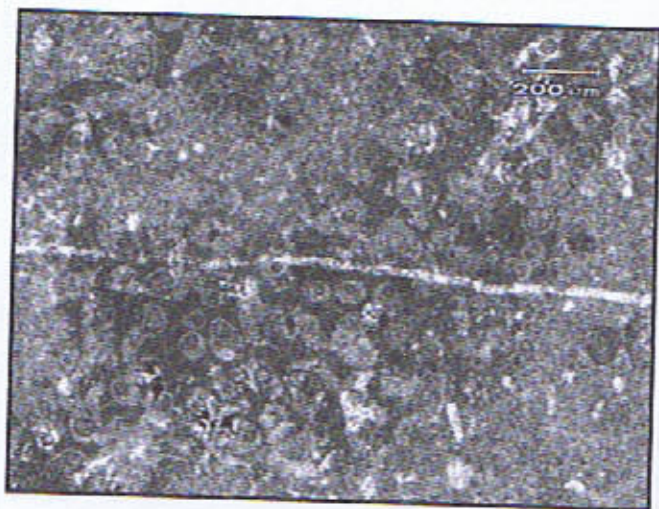
b. Photomicrograph showing dedolomitization/calcitization in a dolomitized horizon. The neomorphosed calcite (NC) is a non-ferroan calcite with pink stain colour. The dolomite crystals display a hypidiomorphic mosaic of crystals. (PPL, stained) Sample No. MKW-19

c. Photomicrograph displaying fractures (FR) bearing ooidal packstone with associated indeterminate skeletal grains (SK). The ooids (O) have concentric microfabrics. (PPL, stained) Sample No. MKW-12T

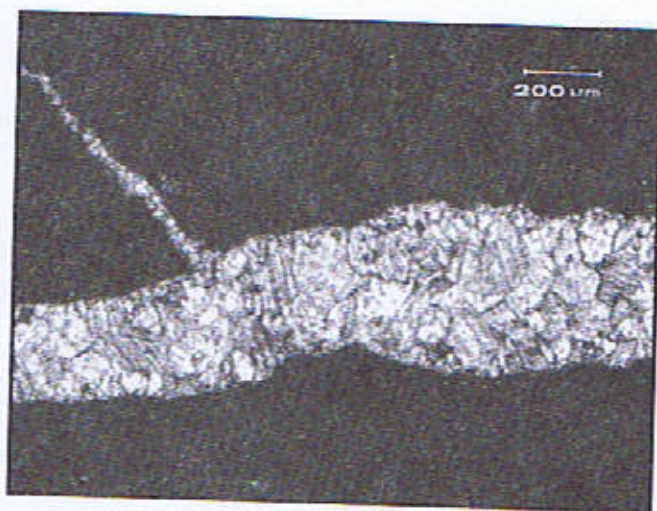
d. Photomicrograph showing dedolomitization/calcitization (NC) with pink stain colour. The dolomite crystals display well developed crystal faces. (PPL, stained) Sample No. MKW-21M



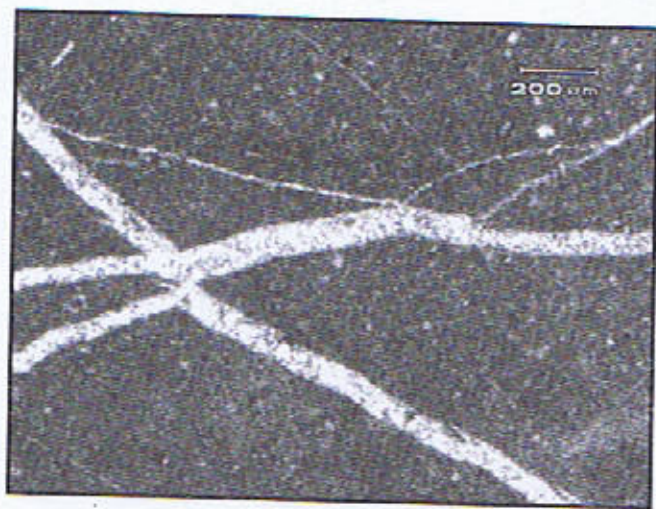
## Plate 2



a.



b.



c.



d.

a. Photomicrograph showing bryozoan (BZ) bioclastic packstone. A small fracture (FR) is cutting across the slide. (PPL, stained) Sample No. MKW-22

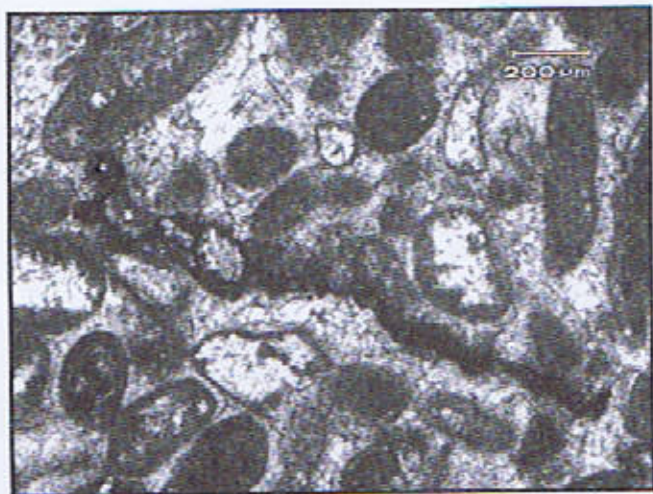
b. Photomicrograph showing a large fracture (FR) and its splay occluded by calcite in mudstone. (PPL, stained) Sample No. MKW-35

c. Photomicrograph displaying a highly fractured mudstone. The fractures (FR) are now filled with calcite and belong to multi phase fracturing. (PPL, stained) Sample No. MKW-36

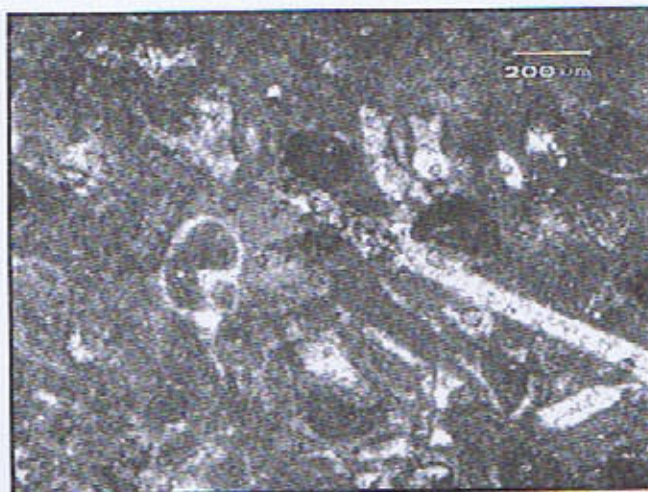
d. Photomicrograph showing bioclastic mudstone. The skeletal grains belong to pelecypod (P) and gastropod (G). (PPL, stained) Sample No. MKW-48M



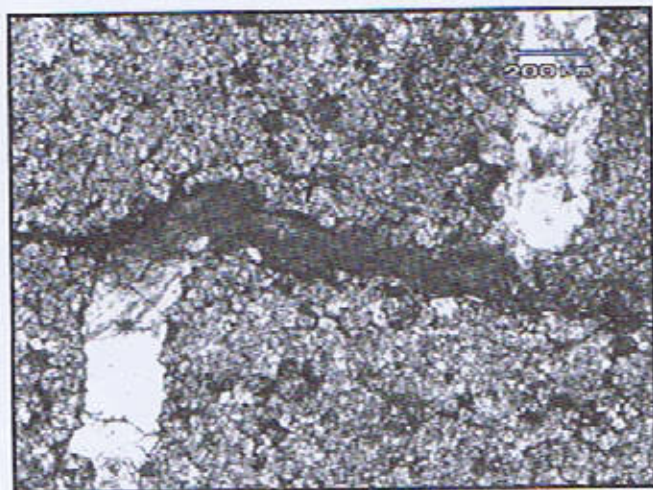
## Plate 3



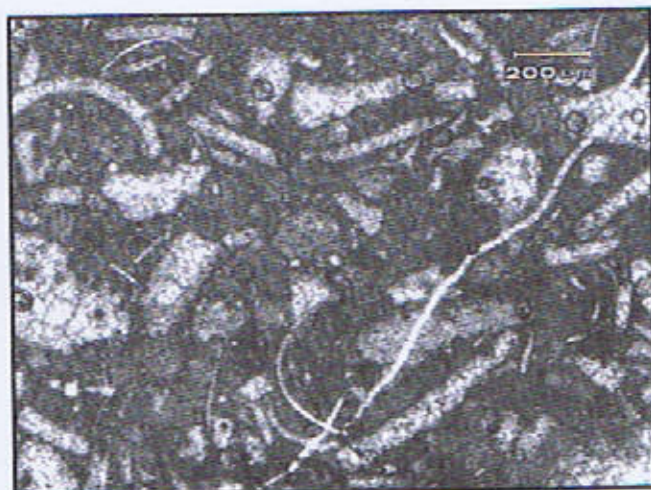
a.



b.



c.



d.

a. Photomicrograph displaying cortoidal grainstone. The dog tooth cement has nucleated cortoids. The coated grains (CT) have micritic envelopes (E), which serve to protect morphology of these grains. (PPL, stained) **Sample No. MKW-49**

b. Photomicrograph showing bioclastic packstone. Gastropod (G) shells and brachiopod (BR) grains are present. (PPL, stained) **Sample No. MKW-75U**

c. Photomicrograph showing dolomite, in which a stylolite (ST) is cutting a fracture (FR), thus is postdating this fracture. (PPL, stained) **Sample No. MKW-76**

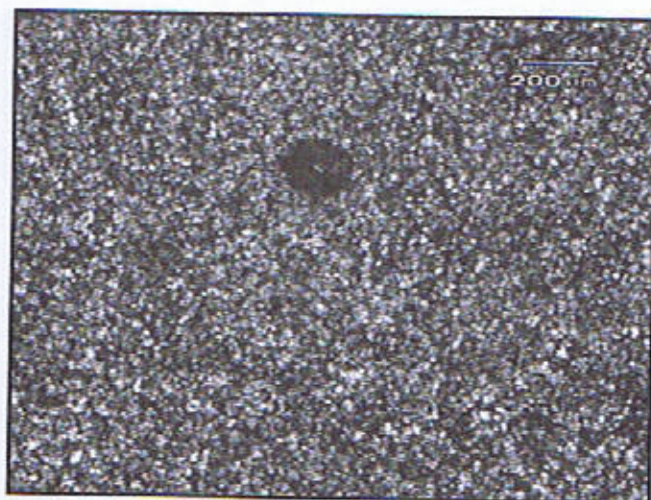
d. Photomicrograph showing bioclastic packstone. Shells of pelecypod (P), gastropod (G) and algae (A) are present. A small fracture (FR) is cross cutting all the grains. (PPL, stained) **Sample No. MKW-79**



## Plate 4



a.



b.



c.



d.

a. Photomicrograph showing peloidal packstone bearing a fracture (FR) occluded by ferroan dolomite (FD) with turquoise stain colour. (PPL, stained) Sample No. MKW-87U

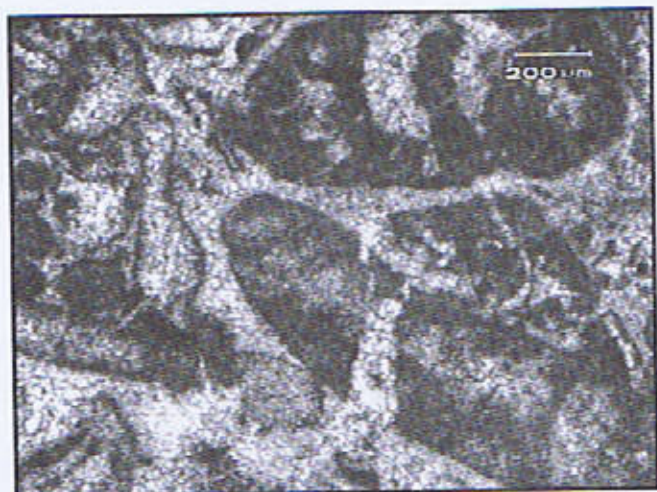
b. Photomicrograph showing dedolomitization/calcitization (NC) with pink stain colour in microdolomite. (PPL, stained) Sample No. MKW-18

c. Photomicrograph displaying ooidal grainstone in association with algae (A) and other bioclasts. The ooids (O) have concentric laminae. An indeterminate calcitized grain, having aragonitic composition originally, converted to sparry calcite (SP) for aragonite is metastable and dissolves first of all. The grain has lost internal structure due to dissolution/precipitation phenomenon and now possesses micritic envelope (E), which serve to preserve its outline. (PPL, stained) Sample No. MKW-28

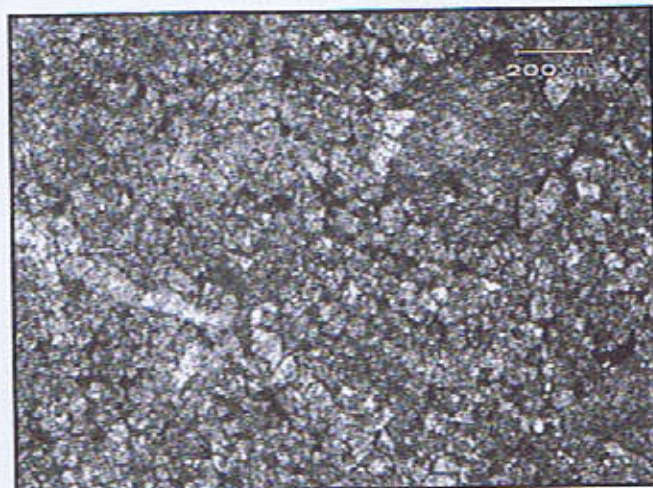
d. Photomicrograph showing fabric/grain selective dolomitization in a bioclastic wackestone. The present shells belong to gastropods (G). (PPL, stained) Sample No. MKW-20L



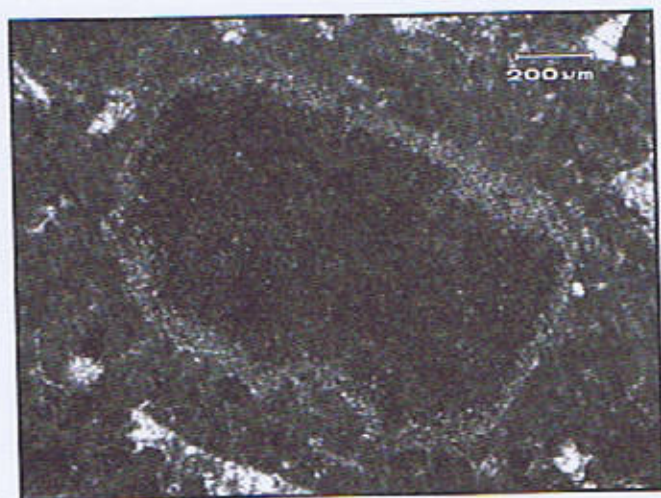
## Plate 5



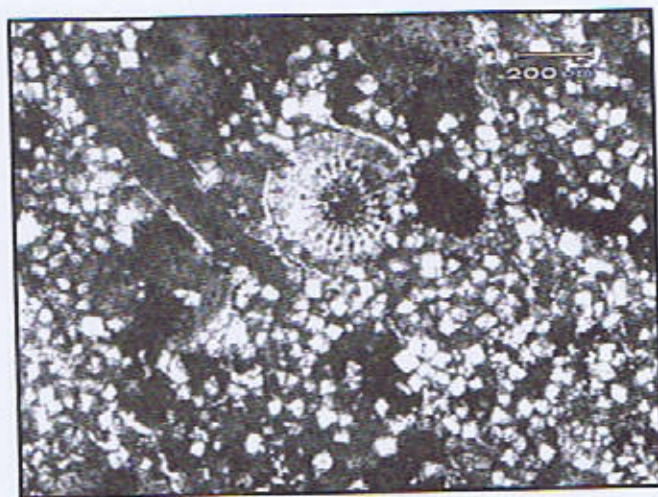
a.



b.



c.



d.

a. Photomicrograph showing bioclastic grainstone in association with grapestones (GR). Broken clasts exhibit signs of mechanical compaction (MC). (PPL, stained) Sample No. MKW-56

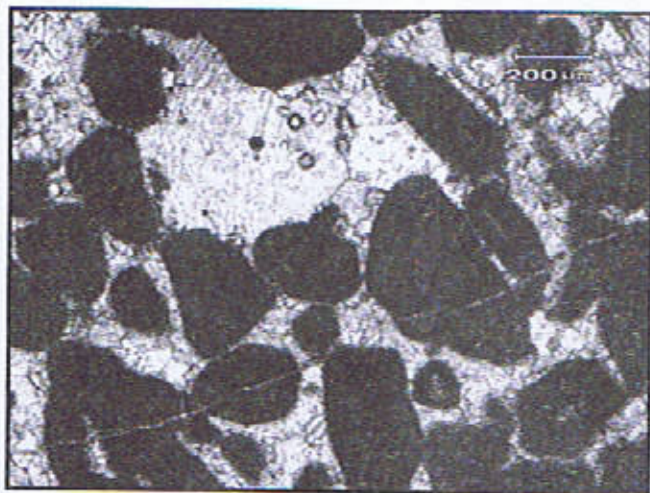
b. Photomicrograph showing a ferroan calcite (FC) with mauve stain colour and a fracture (FR) in dolomite. (PPL, stained) Sample No. MKW-76

c. Photomicrograph showing peloidal packstone. Syntaxial rim cement (SR) developed in optical continuity on an echinoderm (EC) grain is shown as well. The grain is exhibiting characteristic single crystal extinction and uniform coarse porous structure. (XN, stained) Sample No. MKW-81.

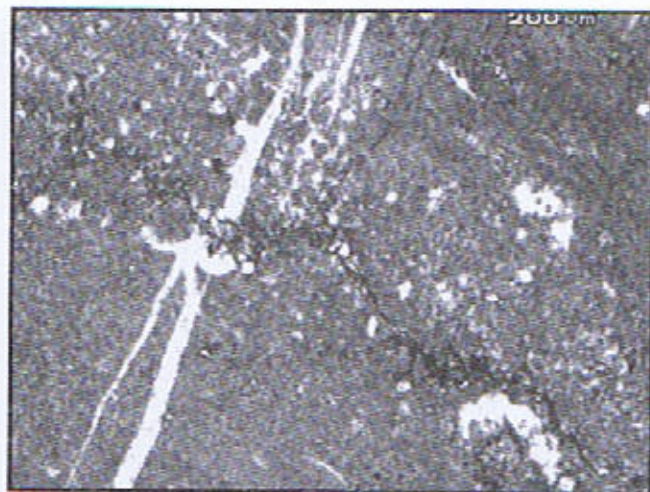
d. Photomicrograph displays pervasive dolomitization of bioclastic grainstone. The dolomite crystals display well developed crystal faces. The cross section of echinoderm spine (ES) shows very characteristic lacy pattern. A test of algae (A) is present too. (PPL, stained) Sample No. MKW-27



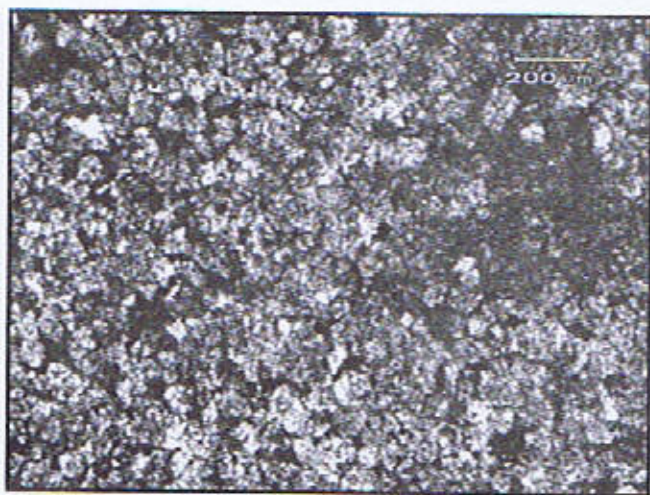
## Plate 6



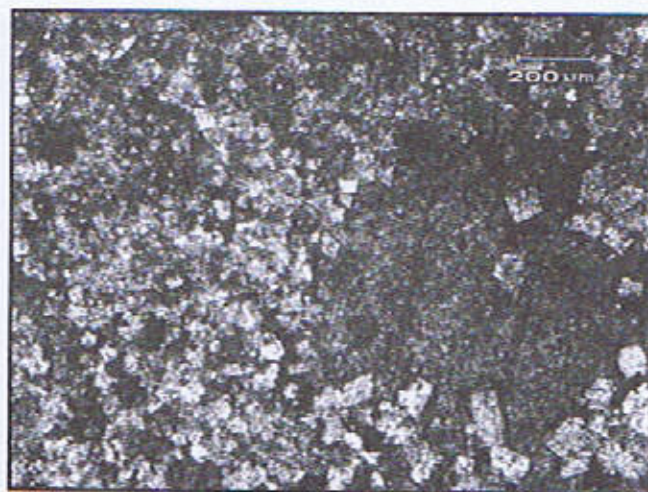
a.



b.



c.



d.

a. Photomicrograph showing younger poikilotopic cement (PC) and older circumgranular columnar (arrowed) cement in peloidal grainstone. A very small fracture (FR) is cutting grains and cement and is postdating the cement and grains. (PPL, stained) Sample No. MKW-26

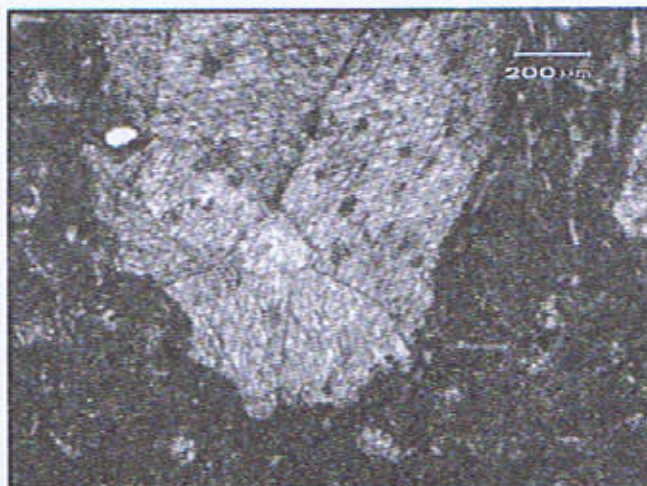
b. Photomicrograph showing mudstone. A fracture (FR) is being cross cut by stylolite (ST), thus predating it. (PPL, stained) Sample No. MKW-36

c. Photomicrograph displaying dedolomitization/calcitization in a dolomitized horizon. The pink stain color displays the neomorphosed non-ferroan calcite (NC). The dolomite crystals exhibit a xenotopic mosaic of crystals. (PPL, stained) Sample No. MKW-20M

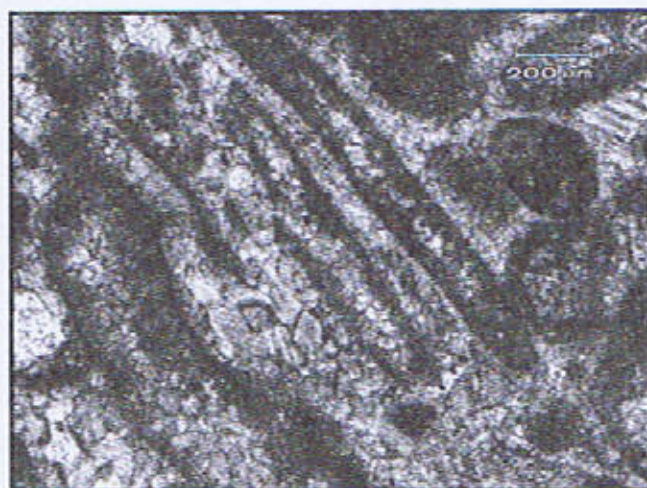
d. Photomicrograph showing dolomite and dedolomitization. The calcite is now ferroan calcite (FC) due to incorporation of iron afterwards. (XN, stained) Sample No. MKW-74



## Plate 7



a.



b.

**a.** Photomicrograph showing late stage ferroan calcite (FC) with purple stain colour and ferroan dolomite (FD) with turquoise stain colour in peloidal packstone. (PPL, stained) **Sample No. MKW-87L**

**b.** Photomicrograph showing cortoidal grainstone. The tests of algae (A) are present. The broken algal grains exhibit signatures of mechanical compaction (MC). Younger circumgranular dogtooth (arrowed) cement (IG) has developed over a grain and older intergranular cement has occluded the interstices. (PPL, stained) **Sample No. MKW-49**



## Mudstones

This microfacies is also found at different levels in the measured section. These mudstones are sometimes highly fractured and fractures are filled with calcite. Mudstones devoid of any skeletal grain have been recorded in Plates 2b and c. A fractured mudstone with a medium amplitude stylolite, postdating these fractures, is shown in Plate 6b. Mudstones with skeletal grains are described in the following lines.

**Bioclastic mudstones:** The bioclastic mudstones found in this section are composed predominantly of bioclasts of molluscan shells and their fragments (Plate 2d). These are found at a number of horizons in the studied formation.

## STANDARD MICROFACIES (SMFs)

The microfacies found in this section have been compared with the Standard Microfacies (SMFs) of Wilson (1975) and Flugel (1982), which include: SMF Nos. 8, 9, 11, 15, 16 and 23.

## DIAGENESIS

The petrographic analysis of diagenetic settings of the studied formation exposed at this section revealed the following diagenetic features:

### Micritic envelopes

These envelopes develop on carbonate grains with original aragonitic mineral composition. Aragonite, being metastable among carbonate minerals, is dissolved in the first phase of diagenesis of carbonate sediments and replaced by calcite (Plate 4c). Micritic envelopes serve to preserve the outline and morphology of the grains.

### Cements

Cementation of the carbonate sediments is an important diagenetic process, which endows strength and stability to the concerned microfacies. The well developed cement, always, resists physical, as well as, chemical compaction and fracturing episodes. Early diagenetic cement precipitates as fibrous aragonite. While dog tooth cement (circumgranular equant cement), dolomite cement, drusy mosaic cement, poikilotopic cement and radial cements precipitate as later diagenetic cements. Various stages of cement formation and stratigraphy are shown in Plates 6a and 7b. The following cement types have been found at different levels and in different microfacies of the Samana Suk Formation from the studied section:

**Circumgranular cement:** The following two types of this cement have been found.

i. **Dog tooth cement:** The dog tooth cement is circumgranular equant cement which precipitates as later diagenetic cements, such as dolomite cement, drusy mosaic cement, poikilotopic cement, etc. Its examples are given in Plates 3a and 7b.

ii. **Syntaxial rim cement:** The syntaxial rim cement grows over the host grain in optical continuity. It is common in many carbonate rocks. It usually develops on echinoderm (crinoids and echinoids) shells/grains in optical continuity and is recognized by simultaneous extinction. It has been observed in Plate 5c.

**Intergranular cement:** The intergranular cement is found at a number of horizons of Samana Suk Formation (Plate 1a and 7b). According to Sheikh (1992) it is the next phase of carbonate diagenesis regarding cement stratigraphy.

**Poikilotopic cement:** This cement develops after the pervasive dolomitization and development of intergranular cements. In this type of cement coarse crystals enclose fine grains, which look like speks. It develops in phreatic environment commonly in burial regime and is shown in Plate 6a.

### Fractures

Different phases of fracturing, open or filled with calcite/dolomite and belonging to one or more episodes were recorded in this section (Plates 1c, 2b and c and 5b). Fracturing along with stylolites observed in this section show that stylolites developed in the carbonate mudstone and other microfacies disrupted the fractures/veins (Plates 3c and 6b). Mudstones particularly bear fractures, which at places are highly fractured with several phases of fracturing sometimes (Plates 2c and 6b). Fractures are also found in other microfacies, for example in Plates 1c, 2a and 3c. Imprints of mechanical compaction (broken grains) are shown in Plate 5a and 7b.

### Stylolites

The stylolites have been observed at various levels of the formation. Examples are shown in Plates 6b and 3c). The stylolites are found mostly in mudstones. Some of the stylolites are found cutting across the filled fractures and thus postdate the fracturing of that microfacies (Plates 6b and 3c). The recorded stylolites indicate the signatures of chemical compaction, which might be result of one or both tectonic stresses and overburden pressure.

### Dolomitization

It is developed at various levels in this section. The following three types of dolomitization have been observed here:

**Pervasive dolomitization:** It is formed as a result of extensive process of dolomitization in limestones. In this type the dolomitization is not texture selective and attacks



fabric of the rock and the whole of the rock gets dolomitized (Plate 5d).

**Microdolomitization:** Very small and fine crystals of dolomite are produced in this diagenetic process and sometimes larger magnification is required to observe these crystals (Plate 4b). The Plates 3c and 4b exhibit good examples of microdolomites.

#### **Dedolomitization**

It is a reverse process in which during diagenesis the dolomite is calcitized. It is a common phenomenon in carbonate rocks. The dedolomitization/calcitization has been observed in the Samana Suk Formation of investigated section in Plates 1b and d, 4b and 6c).

#### **Incorporation of iron in calcite and dolomite**

Incorporation of iron in calcite and dolomite is a late stage diagenetic phenomenon. Ferroan calcite (Plates 5b, 6d and 7a) and ferroan dolomite (Plates 4a and 7a) have been recorded from this section.

#### **DIAGENETIC EVENTS' SUCCESSION**

The diagenetic event's succession of different diagenetic processes and their products depending on time hierarchy of presently discussed section is described here.

##### **Micritic envelopes**

It is the first diagenetic phase, which takes place in the marine diagenesis of limestones. Micritic envelopes develop around fauna which have original aragonitic mineralogical composition. These envelopes serve to define and preserve the outline and morphology of the carbonate grains over which these envelopes develop.

##### **Dissolution of aragonite**

In the second phase the aragonite dissolves in the faunal grains having aragonitic mineralogy and is precipitated as sparite. Sometimes the internal structure of the skeletal grains is totally destroyed and no relict structure is observed at all. However, the outline and morphology of these grains is preserved.

##### **Fabric selective dolomite**

The fabric selective dolomitization is the next phase of the diagenetic history of limestones, in which only the dolomitization of matrix takes place and component grains/allocherts takes place.

##### **Fracturing and physical compaction**

The physical compaction of the carbonate sediments is the next diagenetic event. Under this diagenetic process the inter-grain space reduces, which results in the overall reduction of porosity of the rock. In case of poorly cemented sediments the component grains may break due to physical compaction process. This and other factors produce fractures and ultimately enhance the porosity and permeability of the rock.

#### **Chemical compaction**

In this phase as a result of increasing compaction first the grain to grain contacts take place and then simple grain contacts developed into sutured grain contacts. Later on dissolution of grains starts at these contacts. Sometimes the embayment of one grain into the other is, also, observed.

#### **Stylolitization**

It is the last diagenetic event. The stylolites are actually manifestation of a diagenetic phenomenon, named as pressure-dissolution or chemical compaction.

#### **Dedolomitization**

It is also a late stage diagenetic process, in which dolomite is converted into calcite. It is also known as calcitization.

#### **Incorporation of iron into calcite and dolomite**

It is the last event in the course of diagenesis of carbonate sediments and is related with the late stage uplifting and/or unconformity surface. The leached out iron in this environment gets incorporated into calcite (rendering it into ferroan calcite) and dolomite (rendering it into ferroan dolomite) as per demand of the prevailing environmental conditions.

#### **DISCUSSION**

The Samana Suk Formation in Makarwal Section is comprised of limestones, dolomitic limestones and dolomites with calcareous shales/marls breaks appearing at a number of levels. These shale/marl breaks and intercalations are irregular and do not show any cyclic deposition. The limestones are light grey and yellowish grey and at places dark grey and are mostly dense, hard and compact and contains faunal and floral tests, shells and grains. Two hard ground surfaces, recorded in this section, mark the presence of regressive cycles and periods of non erosion/non deposition. The microfacies developed here include bioclastic, peloidal, ooidal and cortoidal grainstones, bioclastic, ooidal and peloidal packstones, bioclastic wackestones, bioclastic mudstones and mudstones. The bioclastic microfacies form the predominant component of limestones of this section. These bioclastic microfacies host from small to very large skeletal shells and fragments of foraminifera, brachiopoda, gastropoda, pelecypoda, sponges, corals, echinoderma and algae. The cement types found at different levels and in different microfacies are dog tooth cement, intergranular cement, poikilotopic cement and syntaxial rim cements. Important diagenetic phases noted include dissolution, replacement, alteration, dolomitization, dedolomitization and incorporation of iron into calcite and dolomite as late stage diagenetic events.



## CONCLUSIONS

The following conclusions have been drawn:

The Samana Suk Formation exposed at this section is predominantly composed of fine to coarse grained hard and compact limestones, dolomitic limestones and dolomites with thin intercalations of calcareous shales and marls.

Hard ground surfaces are present at two different levels showing the regressive cycles during deposition of this formation and mark the periods of non erosion/non deposition.

The microfacies types found here include bioclastic, peloidal, ooidal and cortoidal grainstones, bioclastic, ooidal and peloidal packstones, bioclastic wackestone, bioclastic mudstones and lime mudstones devoid of any fossils. The faunal and floral assemblage present in the bioclastic microfacies consists of shells and grains of foraminifera,

brachiopoda, gastropoda, pelecypoda, sponges, corals, echinoderma and algae.

Through a number of diagenetic episodes the development of different cement types (dog tooth cement, intergranular cement, poikilotopic cement and syntaxial rim cements), dissolution and replacement minerals, alteration products, fracturing, mechanical and chemical compactional features (broken component grains, dissolution seams and stylolites), dolomitization and dedolomitization and incorporation of iron into calcite and dolomite were produced at different levels and in different microfacies of this section.

It is inferred by the analytical studies of depositional fabric, microfacies and diagenetic settings of the Samana Suk Formation found at this section that it was deposited in the open marine environments of shallow (outer and inner) shelf with open and restricted marine conditions.

## REFERENCES

- Ahmad, S., D. Mertmann and E. Manutsoglu, 1997, "Jurassic Shelf Sedimentation and Sequence Stratigraphy of the Surghar Ranges, Pakistan", *Jour. Nepal Geol. Soc.*, **15**, 15-22, Nepal
- Akhtar, M., 1983, "Stratigraphy of Surghar Range", *Geol. Bull. Punjab Uni.* **18**, 32-45, Lahore, Pakistan
- Anwar, M., Fatmi, A. M. and Hyderi, I. H., 1992, "Revised Nomenclature and Stratigraphy of Musakhel and Baroch Groups in Surghar Range, Pakistan" *Jour. of Geol.*, **1**, 15-28 Pakistan
- Bender, F. K. and Raza, H. A., 1995, "Geology of Pakistan", Gebruder, Borntraeger Berlin, 414p Germany
- Cotter, G. de P., 1933, "The Geology of the Part of the Attock District, West of Longitude 72° 45' E", *India Geol. Surv. Mem.*, **55**, 63-161, Calcutta, India
- Danilchik, W., and S. M. I. Shah, 1967, "Stratigraphic Nomenclature of Formations in Trans-Indus Mountains, Mianwali District, West Pakistan", U.S. Geol. Surv., Proj. Report (IR) PK-33, p45, USA
- Davies, L. M., 1930, "The Fossil Fauna of the Samana Range and Some Neighbouring Areas", Part I: An Introductory Note, *Geol. Survey India, Mem. Palaeont.*, N. S. **15**, 15, Calcutta, India
- Dunham, R. J., 1962, "Classification of Carbonate Rocks According to the Depositional Texture", In: *Classification of Carbonate Rocks, Amer. Assoc. Petrol. Geol. Mem.* **1**, 108-121, USA
- Fatmi, A. N., 1972, "Stratigraphy of the Jurassic and Lower Cretaceous rocks and Jurassic ammonites from northern areas of West Pakistan", *British Mus. Nat. Hist. Bull. (Geol.)*, **20** No. 7, 299-380 UK
- Fatmi A. N., I. H. Hyderi, and M. Anwar, 1990, "Occurrence of the Lower Jurassic Ammonoid Genus *Bouleiceras* from the Surghar Range with a Revised Nomenclature of the Mesozoic Rocks of the Salt Range and Trans Indus Ranges (Upper Indus Basin)", *Geol. Bull. Punjab Univ.*, **25**, 38-46, Pakistan
- Flügel, E., 1982, "Microfacies Analysis of Limestones", Springer-Verlag, Berlin, 633p, Germany
- Gee, E. R., 1947, "The Age of the Saline Series of the Punjab and of Kohat", *India Mat. Sci. Proc. Sec.*, B **14**, 269-310, Calcutta, India
- Gee, E. R., 1989, "Overview of the Geology and Structure of the Salt Range with Observations on Related Areas of Northern Pakistan", In: *Tectonics of the western Himalayas* (Eds. L. L. Malinconico, and R. J. Lillie), *Geol. Soc. Amer. Spec. Papers*, **239**, 52-112, Boulder, USA
- Hemphill, W. R., and Kidwai, A. H., 1973, "Stratigraphy of the Bannu and Dera Ismail Khan areas, Pakistan", *US Geol. Surv., Prof. Paper* **716-B**, 36 USA



- Mensink, V. H., D. Mertmann, Bochum and S. Ahmad, 1988, "Facies Development during the Jurassic of the Trans Indus Ranges, Pakistan", *N. Jb. Geol. Palaont. Mh.*, H. 3, 153-166, Germany
- Mertmann D. and S. Ahmad, 1994, "Shinawari and Samana Suk Formations of the Surghar and Salt Ranges, Pakistan: Facies and Depositional Environments", *Z. dt. Geol. Ges.*, 145, 305-317, Germany
- Shah, S. M. I., 1977, "Stratigraphy of Pakistan", *Mem. Geol. Surv. Pakistan*, Quetta, 12, 138p Pakistan
- Sheikh, R. A., 1991, "Deposition and Diagenesis of the Samana Suk Formation, Kala Chitta Range, North Pakistan", *TERRA Abstracts*, An Official Journal of the European Union of Geosciences, VI, 3, No. 1, France
- Sheikh, R. A., 1992, "Deposition and Diagenesis of Mesozoic Rocks, Kala Chitta Range, Northern Pakistan", Ph.D. dissertation, Imperial College, London, 360p UK
- Spath, L. F., 1939, "The Cephalopoda of the Neocomian Belemnite Beds of Salt Range", *Indian Geol. Surv., Mem. Palaeont. Indica, New Series*, 25, No. 1, 154, India
- Tucker, M. F. and Wright, V. P., 1990, "Carbonate Sedimentology", Blackwell Scientific Publication, Oxford, London 482p, UK.
- Wilson, J. L., 1975, "Carbonate Facies in Geological History", Springer-Verlag, Berlin, 471p, Germany



## PALEOGENE BIOSTRATIGRAPHY OF KOHAT AREA, NORTHERN PAKISTAN.

BY

**SHAHID J. SAMEENI**

Institute of Geology, University of the Punjab, Quaid-i-Azam Campus,  
Lahore-54590 Pakistan

**MOHAMMAD HANEEF, OBAID-UR-REHMAN**

Department of Geology, University of Peshawar, Peshawar, Pakistan.

AND

**JERE H. LIPPS**

Museum of Paleontology, University of California, Berkeley, CA-94720, U.S.A.

**Abstract:** The Kohat area of north Pakistan has a thick sequence of Paleogene strata. As a part of this study, four stratigraphic sections were measured and sampled for biostratigraphic studies. At present, the established stratigraphic sequence of Kohat area is after Shah, 1977, for the first time, the age of the units is established on the basis of Alveolinids. Shallow Benthic Biozones commonly referred as SB zones.

|                  |  |
|------------------|--|
| Eocene           | Kohat Formation (SB-13-14)<br>Kuldana/Mamikhel (SB-10-12) based on its position<br>Shekhan Formation/Jatta Gypsum (SB-8-10)<br>Panoba Shale/Bahadurkhel Salt & Gypsum (SB-6-8) |
| Paleocene-Eocene | Patala Formation (SB-4-6)  |
| Paleocene        | Lockhart Limestone (SB-3)<br>Hangu Formation (SB-3)  |




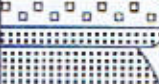



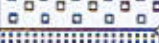













The data presented in this study will provide a basis for global correlation, sequence stratigraphy and paleobathymetry, important tools for surface and sub-surface hydrocarbon exploration.

### INTRODUCTION


The Kohat basin is the most complex tectonic area of northern Pakistan. It is a tilted plateau with a moderate to steeper dips and asymmetrical structures formed by a large number of thrust/normal faults. It has been interpreted as formed by transgressional tectonics based on salt affected or basement involved thrust/reverse faulting (Paracha, 2001). The exposed stratigraphic sequence comprised of clastic, carbonate and evaporite strata ranging in age from Jurassic to Quaternary constitute a thickness in excess of 4 km (Table.1)


The earlier literature on the geology of Kohat and adjacent area is mainly focused on the salt deposits (Brunes, 1832; Fleming, 1853; Oldham and Thomas, 1864). Later work on the stratigraphy and structure include that of Eames (1952) Rashid et. al. (1965) Khan (1967) Meissner et. al. (1968; Meissner, et. al. (1974). Gardezi, et al., (1976) discussed the geology of the Darra Adam Khel. District Kohat with the observations on the facies changes and their tectonic implications. Tanoli, et. al. (1993) has done a detailed study of the Eocene sedimentary sequence in Kohat Basin.





| Era      | Period     | Epoch       | Group         | Unit Thickness   | Formation  | Log  |  |                    |  |
|----------|------------|-------------|---------------|------------------|--|--|--|--------------------|--|
| Cenozoic | Quaternary | Pleistocene |               | 170m             | Soan Fm  |    |  |                    |  |
|          | Tertiary   | Pliocene    | Siwalik Group | 1666m            | Dhok Pathan Fm   |    |  |                    |  |
|          |            |             |               | 2651m            | Nagri Fm   |    |  |                    |  |
|          |            |             |               | 934m             | Chinji Fm  |    |  |                    |  |
|          |            | Miocene     |               | Kawalpindi Group | 565m   | Karnial Fm   |    |                    |  |
|          |            |             |               |                  | 101m   | Murree Fm  |    |                    |  |
|          |            |             |               | Cherat Group     | 173m   | Kohat Fm   |    |                    |  |
|          |            |             |               |                  | 70m  | Mami Khel Clay   |    |                    |  |
|          |            |             |               |                  | 95m  | Jatta Gypsum   |    |                    |  |
|          |            | Eocene      |               |                  | 227m   | Shekhan Fm<br>Bahadur Khel Salt<br>Panoba Shale                                      | <br><br> |                    |  |
|          |            |             |               |                  | Palaeocene   | Makarwal Group   | 127m   | Patala Fm          |   |
|          |            |             |               |                  |  |  | 103m   | Lockhart Limestone |  |
|          |            |             |               |                  |  |  | 121m   | Hangu Fm           |  |
|          |            | Mesozoic    | Cretaceous    |                  | 91m  | Kawagarh Fm  |    |                    |  |
|          |            |             |               |                  | 115m   | Lumshiwal Fm   |    |                    |  |
|          |            |             |               |                  | 15m  | Chichali Fm  |    |                    |  |
| Jurassic |            |             | 153m          | Samana suk Fm    |  |  |  |                    |  |
|          |            |             | 357m          | Datta Fm         |  |  |  |                    |  |
|          |            |             |               |                  |  |  |  |                    |  |
|          |            |             |               |                  |  |  |  |                    |  |

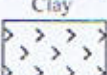
INDEX

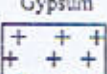
 Sandstone


 Conglomerate


 Shale

 Clay

 Gypsum

 Salt

 Limestone

 Unconformity

## INDEX



Sandstone



Conglomerate



Shale



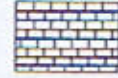
Clay



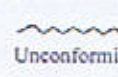
Gypsum



Salt



Limestone



Unconformity

Table 1. Generalized stratigraphy of the Kohat Plateau (Based on data from Meissner et. al, 1974, Kadri et.al, 1995).



## REGIONAL STRATIGRAPHY:

The study area mostly lies in the eastern side of Kohat city (Fig.1) i.e. Shekhan Nala section, Tarkhobi section and Panoba section while only one section under study is the Uch Bazar section which is in the west of Kohat town.

The nomenclature of the stratigraphic units exposed in the area, adopted by the Stratigraphic Committee of Pakistan (Fatmi, 1973) are as follows.

| Age               | Old Names  | Present Names   |
|-------------------|--|---|
| Eocene            | Kohat Limestone & Sirki Shales<br>Kuldana Series/Lr. Chharat Series<br>Shekhan Lst./Jatta Gypsum<br>Green Shales/Kohat Saline Series | Kohat Formation<br>Kuldana Formation/Mamikhel Clay<br>Shekhan Lst./Jatta Gypsum<br>Panoba Shale/Bahadur Khel Salt |
| Paleocene- Eocene | Tarkhobi Shales  | Patala Formation  |
| Paleocene         | Tarkhobi Limestone<br>Hangu Shale & Sst  | Lockhart Limestone<br>Hangu Formation   |

### Hangu Formation

The name "Hangu Shale" and "Hangu Sandstone" was first used by Davies in 1930 which was laterally formulized by the Stratigraphic Committee of Pakistan (Fatmi, 1973) as "Hangu Formation".

The formation consists of light gray to reddish brown, weathers dark rusty brown, fine to coarse-grained sandstone, medium to thick-bedded with gray shale intercalations in the upper part. The thickness of the formation in the Uch Bazar section is 71 meters (Fig.2).

### Lockhart Limestone

Davies in 1930 introduced the name "Lockhart Limestone" for a Paleocene Limestone unit for the Tarkhobi Limestone of Eames (1952) in Kohat area which was later on formulized by the Stratigraphic Committee of Pakistan (Fatmi, 1973). In the study area, the formation consists of light gray to dark gray, medium to thick-bedded and massive limestone. In the Tarkhobi area, the limestone contains shale interbeds in its lower part and is nodular in its upper part having a thickness of around 150 meters while it is only 48 meters thick in the Uch Bazar section (Fig. 2).

### Patala Formation

The name "Patala Shale" was introduced by Davies and Pinfold (1937) for Paleocene shales of the Salt Range area. Later, the Stratigraphic Committee of Pakistan (Fatmi, 1973) formulized it as "Patala Formation" and extended this name to the "Tarkhobi Shales" of Eames (1952) in the Kohat area. The formation consists of gray, splintery shale with beds of silty shale and argillaceous limestone with

Eocene forams in the upper limestone. The formation is exposed in all the measured stratigraphic sections carried out during this study. A thickness of 45 meters (Panoba section), 188 meters (Tarkhobi section), 20 meters (Shekhan Nala section) and 32 meters was recorded in the study area (Fig.2).

### Panoba Shales

Eames (1952) introduced the name Panoba Shale for the previously named Green Shales of Parson (1926). The name was later on adopted by the Stratigraphic Committee of Pakistan (Fatmi, 1973). The formation consists of greenish grey to light grey shale, slightly silty and calcareous at the base with flaggy limestone interbeds at some places. A thickness of 110 meters at Panoba section, 68 meters at Tarkhobi section, 60 meters at Shekhan Nala section and 172 meters at Uch Bazar section is recorded during present study. The Bahadur Khel Salt is the lateral facies of the Panoba Shale exposed in the southern side of the Kohat area.

### Shekhan Formation

The name Shekhan Limestone was introduced by Davies in 1930 which was later formulized by the Stratigraphic Committee of Pakistan (Fatmi, 1973) as Shekhan Formation.

The formation consists of yellowish gray to gray, thick bedded to massive and nodular limestone with interbeds of shale, which is gypsiferous at places. At Panoba, a thin bed of gypsum is also present (Fig.2). The formation is not exposed in the Uch Bazar section where the Kohat Formation has a disconformable upper contact with the Panoba Shales. A thickness of 74 meters at Panoba



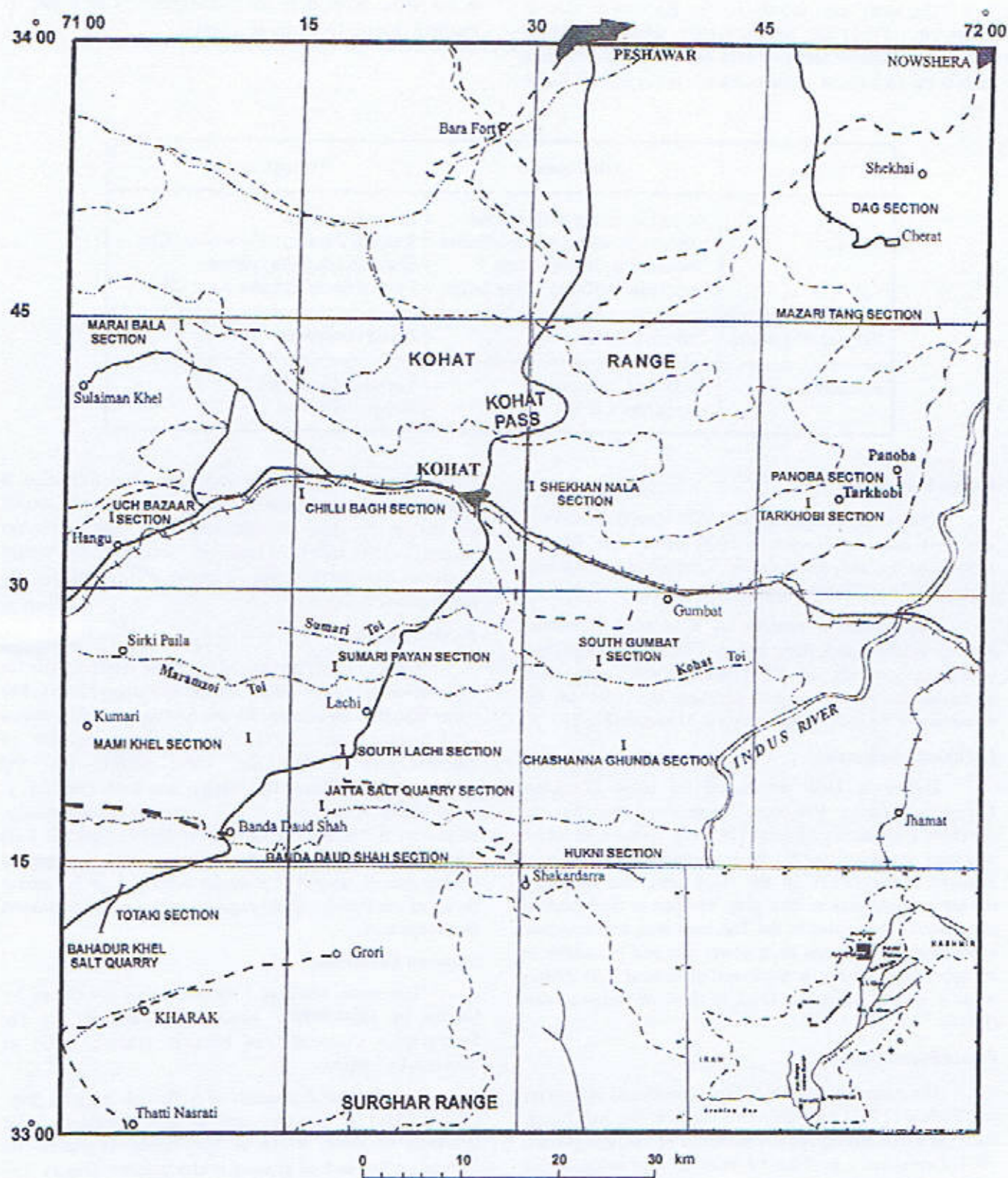


Fig. 1. Location map (after Meissner et al 1974)



section, 65 meters at Tarkhobi section and 52 meters at Shekhan Nala section were observed. The Jatta Gypsum is the lateral facies of Shekhan Formation in the southern side of Kohat.

#### Kuldana Formation

The name Kuldana Formation was first used by Latif (1970) to the Kuldana Series of Middlemiss (1896) and later on the name was formulized by the Stratigraphic Committee of Pakistan (Fatmi, 1973). The same name was extended to "Lower Chharat Series" of Eames (1952) in the Kohat area. The formation is comprised of brownish red to red shale which is calcareous and silty with thin beds of sandstone. The Kuldana Formation records the southward progression of a fluvial/deltaic system that introduced red shales, sandstones and local conglomerates in the basin. It has a continental fluvial origin and was deposited in a semi-arid basin at the end of a marine regression by rapidly flowing streams (Abbassi & McElory, 1991). The formation is only exposed in the Panoba section and the Shekhan Nala section. Its thickness is 21 meter at Panoba and 120 meters at Shekhan Nala. The Mamikhel Clay is regarded as its lateral facies equivalent in other parts of the Kohat area.

#### Kohat Formation

The name Kohat Shales and Kohat Limestone is used by Eames (1952) and has been formulized by the Stratigraphic Committee of Pakistan (Fatmi, 1973) as Kohat Formation. Meissner *et al.* (1968) divided the formation into three members as Kaladand Member as lower one, Sadkal Member as upper one while the third one Habib Rahi Member is the lower member of the Kirthar Formation of the Sulaiman Province, exposed here in Kohat area. The formation is composed of limestone and shale interbeds. The Kaladand Member is mainly composed of light gray, thin-bedded limestone with intercalations of shale in its lower part while the upper Sadkal Member is composed of calcareous, greenish gray shale and gray limestone. The formation is not exposed in the Tarkhobi area. A thickness of 61 meters in Panoba section, 95 meters in Shekhan Nala section and 191 meters in Uch Bazar section were measured.

#### Kirthar Formation

The Habib Rahi Member of the Kirthar Formation is exposed in the studied sections and is composed of pale gray to brownish limestone. In the Shekhan Nala section, it is overlain by the Murree Formation. Its thickness varies from 47 m in Panoba section, 38m in Shekhan Nala section and 41m in the Uch Bazar section.

#### Methodology

As a part of this study, four, previously known (Meissner, *et al.* 1974), stratigraphic sections of the

Paleogene succession were selected in Kohat area. Three of these sections, Panoba, Tarkhobi and Shekhan Nala are located in the east while the Uch Bazar section lies in the west of Kohat city (Fig.1). Paleocene and Eocene succession was logged and about 100 samples were collected from these rocks for the preparation of thin sections. Loose specimens of larger foraminifers were also collected for detailed study and identification of age diagnostic foraminiferal species.

#### OBSERVATIONS

After detailed study of thin sections and loose specimens, the following age diagnostic species of larger foraminifers are recorded.

- Alveolina elliptica* (SOWERBY), 1840
- Alveolina stercusmeris* MAYER-EYMAR, 1886
- Alveolina frumentiformis* SCHWAGER, 1883
- Alveolina aff. canavarii* HOTTINGER, 1974
- Alveolina pasticillata* SCHWAGER, 1883
- Alveolina indicatrix* HOTTINGER, 1960
- Nummulites mamillatus* (FICHEL and MOLL)
- Nummulites atacicus* LEYMERIE
- Nummulites globulus* LEYMERIE
- Nummulites pengaroensis* VERBEEK
- Discocyclina dispansa* (SOWERBY)
- Assilina laminosa* GILL

#### SYSTEMATIC PALEONTOLOGY

##### Genus *Alveolina* D'Orbigny, 1826

- Alveolina elliptica* (SOWERBY) 1840  
(Plate-II, Figs-a-c)

- Fasciolites elliptica* SOWERBY W., 1840, pl. 24, fig. 17.
- Alveolina javana* VERBEEK R., 1891, p. 111, pl. 1, figs. 4-7.
- A. (Flosculina) pillai* CHECCHIA-RISPOLI G., 1909, p. 69, pl. 3, fig. 12, text fig. 8.
- Fasciolites elliptica* SOWERBY, BAKX L. A., 1932, p. 229, pl. 3, figs. 15-17.
- Fasciolites javana* VERBEEK, BAKX L. A., 1932, p. 231, pl. 4, figs. 21-25.
- Alveolina (Fasciolites) subpryenaica* var. *flosculina* SILVESTRI A., 1939, p. 30, pl. 7, figs. 4-5.
- A. elliptica nutalli* DAVIES L., 1940, p. 219, 221, pl. 12, figs. 1-4.
- A. elliptica* (SOWERBY) var. *flosculina* SILVESTRI, SMOUT A. H., 1954, p. 82, pl. 14, figs. 8-12.
- Alveolina elliptica* (SOWERBY), HOTTINGER L., 1960, p. 146, pl. 12, figs. 1-3.
- A. elliptica nutalli* DAVIES, HOTTINGER L., 1960, p. 146, pl. 12, fig. 4.

REMARKS:- This species is recorded from middle and upper part of the Kohat Formation from Panoba, Shekhan



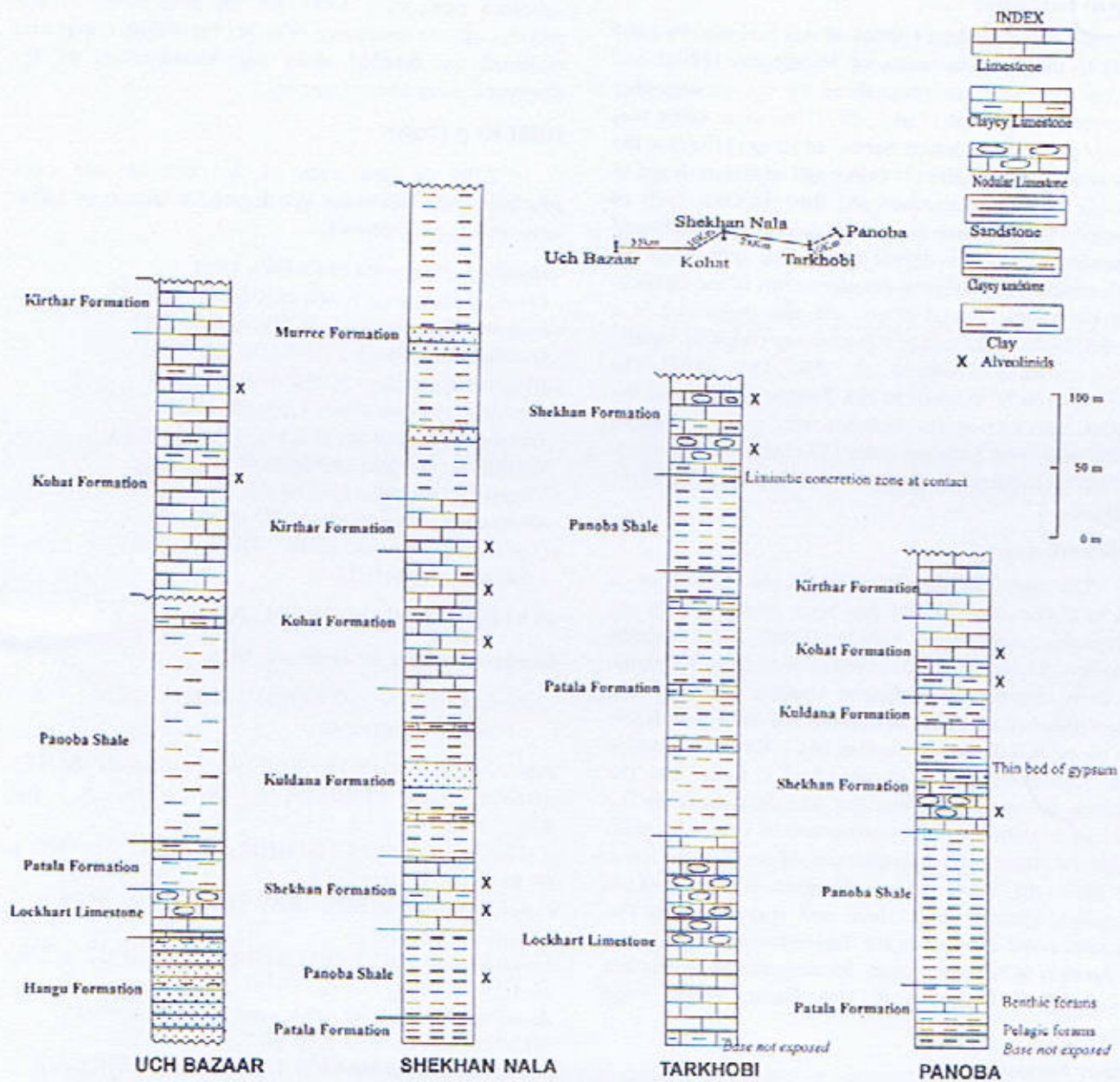


Fig.2. Stratigraphic columns of the measured sections Paleogene succession in Kohat area.



Nala and Uch Bazar sections. It is also recorded from the Habib Rahi Member of the Kirthar Formation in the Shekhan Nala section. The stratigraphic range of the species is *A. stipes* zone to *A. prorecta* zone (Fig. 3).

-*Alveolina stercusmeris* MAYER-EYMAR, 1886.

(Plate-II, Fig-c)

*Alveolina stercusmeris* MAYER-EYMAR K., 1886, table 1.

*Alveolina stercusmeris* MAYER-EYMAR. HOTTINGER L., 1960, p. 147, (no figure)

REMARKS: Oval shape, medium sized with rounded to slightly truncated poles, can be separated from *Alveolina elliptica* in lack of flosculinization. This species is recorded from the Kohat Formation of the Shekhan Nala section. The stratigraphic range of this species is *A. stipes* zone (Fig. 3).

-*Alveolina frumentiformis* SCHWAGER, 1883

(Plate-II, Fig-d)

*Alveolina frumentiformis* SCHWAGER C., 1883, p. 100, pl. 2, fig. 4.

*Alveolina frumentiformis* SHWAGER. HOTTINGER L., 1960, p. 152, pl. 10, figs. 15-18, text fig. 82.

REMARKS: This species is recorded from the middle and upper part of the Kohat Formation from Panoba and Shekhan Nala sections. The stratigraphic range of this species is *A. stipes* zone (Fig. 3).

-*Alveolina* aff. *canavarii* HOTTINGER, 1974

(Plate-III, Fig-a)

*Alveolina* sp. aff. *Alveolina canavarii*, n. sp. 2, HOTTINGER L., 1974, p. 51, pl. 58, Figs. 1-3.

REMARKS: This species is recorded from the middle and upper part of Shekhan Formation from Tarkhobi and Shekhan Nala sections. The stratigraphic range of this species is *A. trempina* zone (SB-9) to the lower part of the *A. oblonga* zone (SB-10) Fig. 3.

-*Alveolina pasticillata* SHWAGER, 1883

(Plate-III, Fig-b)

*Alveolina pasticillata* SCHWAGER C., 1883, p. 104, pl. 26, fig. 2.

*Alveolina pasticillata* SCHWAGER. HOTTINGER L. 1958, figs. 7d, e.

*Alveolina pasticillata* SHWAGER. HOTTINGER L., 1960, p. 88, pl. 4, figs. 26-33. Text figs. 44-45.

REMARKS: This species is recorded from Panoba Shale of the Shekhan Nala area. The stratigraphic range of this species is from *A. ellipsoidalis* zone (SB-6) to the lower part of *A. carhrica* zone (SB-8) Fig. 3.

-*Alveolina indicatrix* HOTTINGER, 1960.

(Plate-IV, Fig-a)

*Alveolina indicatrix* HOTTINGER L., 1960, p. 100, pl. 5, figs. 1-2, text figs. 51a, b, 52.

REMARKS: This species is recorded from the upper part of the Shekhan Formation from Tarkhobi and Shekhan Nala sections. The stratigraphic range of this species is from the upper part of *A. trempina* zone (SB-9) to *A. oblonga* zone (SB-10) Fig. 3.

#### Genus *Nummulites* Lamarck, 1801

*Nummulites globulus* LEYMERIE

(Plate-IV, Fig-b)

*Nummulites globulus* LEYMERIE, 1846, p. 359, pl. XIII, figs. 14a, 14d.

REMARKS: This species is recorded from the Shekhan Formation and the Kohat Formation from Tarkhobi and Shekhan Nala sections. The stratigraphic range of this species is from lower to middle Eocene.

-*Nummulites mamillatus* (FICHTEL & MOLL)

(Plate-III, Fig-c)

*Nummulites mamilla* (FICHTEL & MOLL), NUTTAL, 1925, p. 445, pl. 27, figs. 1-3.

REMARKS: This species is recorded from the uppermost part of the Patala Formation in the Panoba section. The stratigraphic range of this species is from lower to middle Eocene.

-*Nummulites atacicus* LEYMERIE

(Plate-III, Fig-f)

*Nummulites atacicus* LEYMERIE, 1846, p. 358, pl. 13, fig. 13.

REMARKS: This species is recorded from the lower part of the Shekhan Formation of the Shekhan Nala section. The stratigraphic range of this species is from lower to middle Eocene.

-*Nummulites pengaroensis* VERBEEK

(Plate-IV, Fig-c)

*Nummulites pengaroensis* VERBEEK. NAGAPPA, 1951, p. 181, pl. 10, figs. 3-5.

REMARK: This species is recorded from the Kohat Formation and the Habib Rahi Member of the Kirthar Formation of Shekhan Nala section. The stratigraphic range of this species is from middle to upper Eocene.

#### Genus *Discoeyclina* Gumbel, 1870

-*Discoeyclina dispansa* (SOWERBY)

(Plate-IV, Fig-d)

*Discoeyclina dispansa* (SOWERBY), NUTTAL, 1926, p. 157, pl. 7, figs. 1-3, 5.

REMARKS: This species is recorded from the Panoba Shale of Shekhan Nala section. The stratigraphic range of this species is from lower to middle Eocene.



| Age       |           | Shallow Benthic Biozones (SB) | Alveolinids Zones | elliptica Group  |  | vredenburgi Group                                      | canavarii Group  | pasticillata Group                                     |                  |
|-----------|-----------|-------------------------------|-------------------|--|--|--|--|--|------------------|
|           |           |                               |                   | A. elliptica   | A. stereusmeris  | A. frumentiformis                                      | A. aff. canavarii                                      | A. pasticillata<br>A. indicatrix                       |                  |
| Eocene    | Lutetian  | SB-15                         | A. prorrecta      | <br> <br> <br> <br> <br> <br> <br> <br> <br> <br> <br> | <br> <br> <br> <br> <br> <br> <br> <br> <br> <br> <br> | <br> <br> <br> <br> <br> <br> <br> <br> <br> <br> <br> | <br> <br> <br> <br> <br> <br> <br> <br> <br> <br> <br> | <br> <br> <br> <br> <br> <br> <br> <br> <br> <br> <br> |                  |
|           |           | SB-14                         | A. munieri        |  |  |  |  |  |                  |
|           |           | SB-13                         | A. stipes         |  |  |  |  |  |                  |
|           | Ypresian  | Cusian                        | SB-12             |  |  |  |  |  | A. voilae        |
|           |           |                               | SB-11             |  |  |  |  |  | A. dainelli      |
|           |           |                               | SB-10             |  |  |  |  |  | A. oblonga       |
|           |           | Herdian                       | SB-9              |  |  |  |  |  | A. trempina      |
|           |           |                               | SB-8              |  |  |  |  |  | A. carbrica      |
|           |           |                               | SB-7              |  |  |  |  |  | A. moussoulensis |
|           |           |                               | SB-6              |  |  |  |  |  | A. ellipsoidalis |
|           |           |                               | SB-5              |  |  |  |  |  | A. vredenburgi   |
|           |           |                               | SB-4              |  |  |  |  |  | A. (G.) levis    |
|           | Paleocene | Danian                        | SB-3              |  |  |  |  |  | A. (G.) primaeva |
| SB-2      |           |                               |                   |  |  |  |  |  |                  |
| SB-1      |           |                               |                   |  |  |  |  |  |                  |
| Thanetian |           |                               |                   |  |  |  |  |  |                  |

Fig. 3. Stratigraphic range of Alveolinids recorded.



| Age       |           |         | Shallow Benthic Biozones (SB) | Alveolinids Zones | Formation                                |                   |
|-----------|-----------|---------|-------------------------------|-------------------|--|-------------------|
| Eocene    | Lutetian  |         | SB-15                         | A. prorrecta      | Kirthar Formation<br>(Habib Rahi member) |                   |
|           |           |         | SB-14                         | A. munieri        |  |                   |
|           |           |         | SB-13                         | A. stipes         | Kohat Formation                          |                   |
|           | Ypresian  | Cusian  |                               | SB-12             | A. voilae                                | Kuldana Formation |
|           |           |         |                               | SB-11             | A. dainelli                              |                   |
|           |           | Berrian |                               | SB-10             | A. oblonga                               | Shekhan Formation |
|           |           |         |                               | SB-9              | A. trempina                              |                   |
|           |           |         |                               | SB-8              | A. carbrica                              | Panoba Shale      |
|           |           |         |                               | SB-7              | A. moussoulensis                         |                   |
|           |           |         |                               | SB-6              | A. ellipsoidalis                         | Patala Formation  |
|           |           |         |                               | SB-5              | A. vredenburgi                           |                   |
| Paleocene | Danian    |         | SB-4                          | A. (G.) levis     | Lockhart Limestone<br>Hangu Formation    |                   |
|           |           |         | SB-3                          | A. (G.) primaeva  |  |                   |
|           | Thanetian |         | SB-2                          |                   |  |                   |
|           |           |         | SB-1                          |                   |  |                   |

Fig. 4. Chronostratigraphy of Paleogene succession of Kohat area on the basis of Alveolinids



## DISCRIPTION OF PLATES

## PLATE-I

*Alveolina elliptica* group, from Kohat Formation.

## PLATE-II

Fig. a,b,c : *Alveolina elliptica* (Sowerby), 1840, from Kohat Formation.

Fig. e: *Alveolina stercumeris* (Mayer-Eymar), 1886, from Kohat Formation.

Fig. d: *Alveolina frumentiformis* Schwager, 1883, from Kohat Formation.

## PLATE-III

Fig. a: *Alveolina* aff. *canavarii* Hottinger, 1974, from Shekhan Formation.

Fig. b: *Alveolina pasticillata* Schwager, 1883, from Panoba Shale.

Fig. c: *Nummulites mamillatus* (Fichtel & Moll), from Patala Formation.

Fig. d: *Nummulites ataecius* Leymerie, from Patala Formation.

Fig. e: *Assilina laminosa* Gill, from Panoba Shale.

## Plate-IV

Fig. a: *Alveolina indicatrix* Hottinger, 1960, from Shekhan Formation.

Fig. b: *Nummulites globulus* Leymerie, from Kohat Formation.

Fig. c: *Nummulites pengaroensis* Verbeek, frm Kohat Formation.

Fig.d: *Discocyclina dispansa* (Sowerby), from Panoba Shale

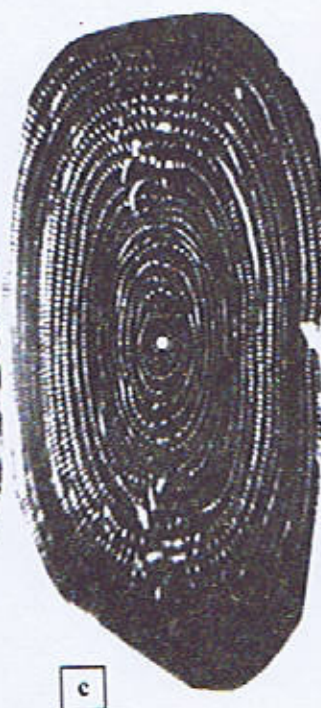
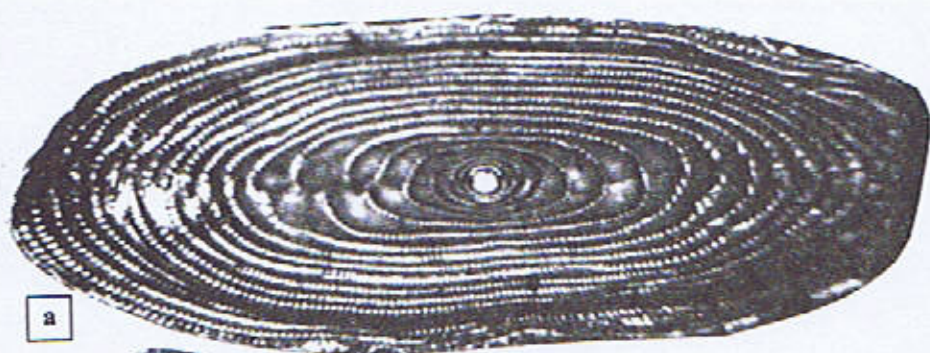


Plate- I



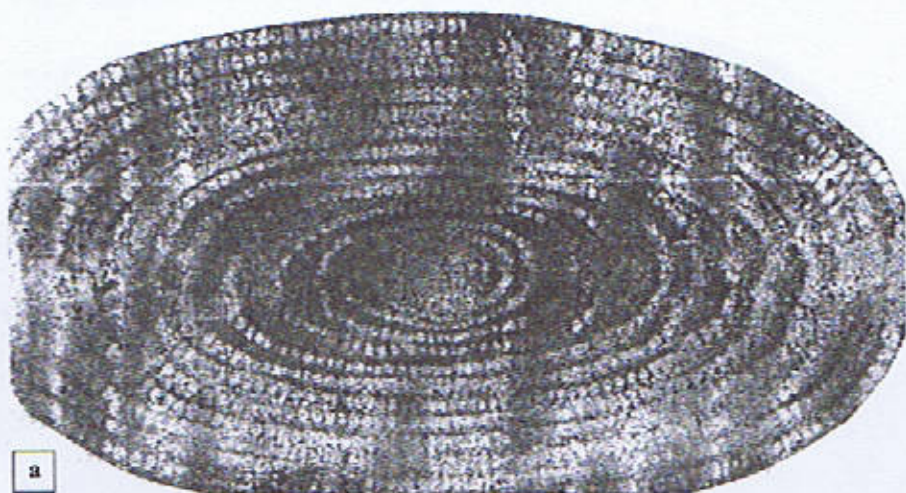


## Plate-II





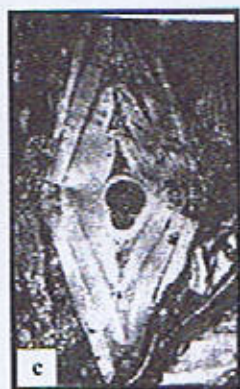
## Plate-III



a



b



c



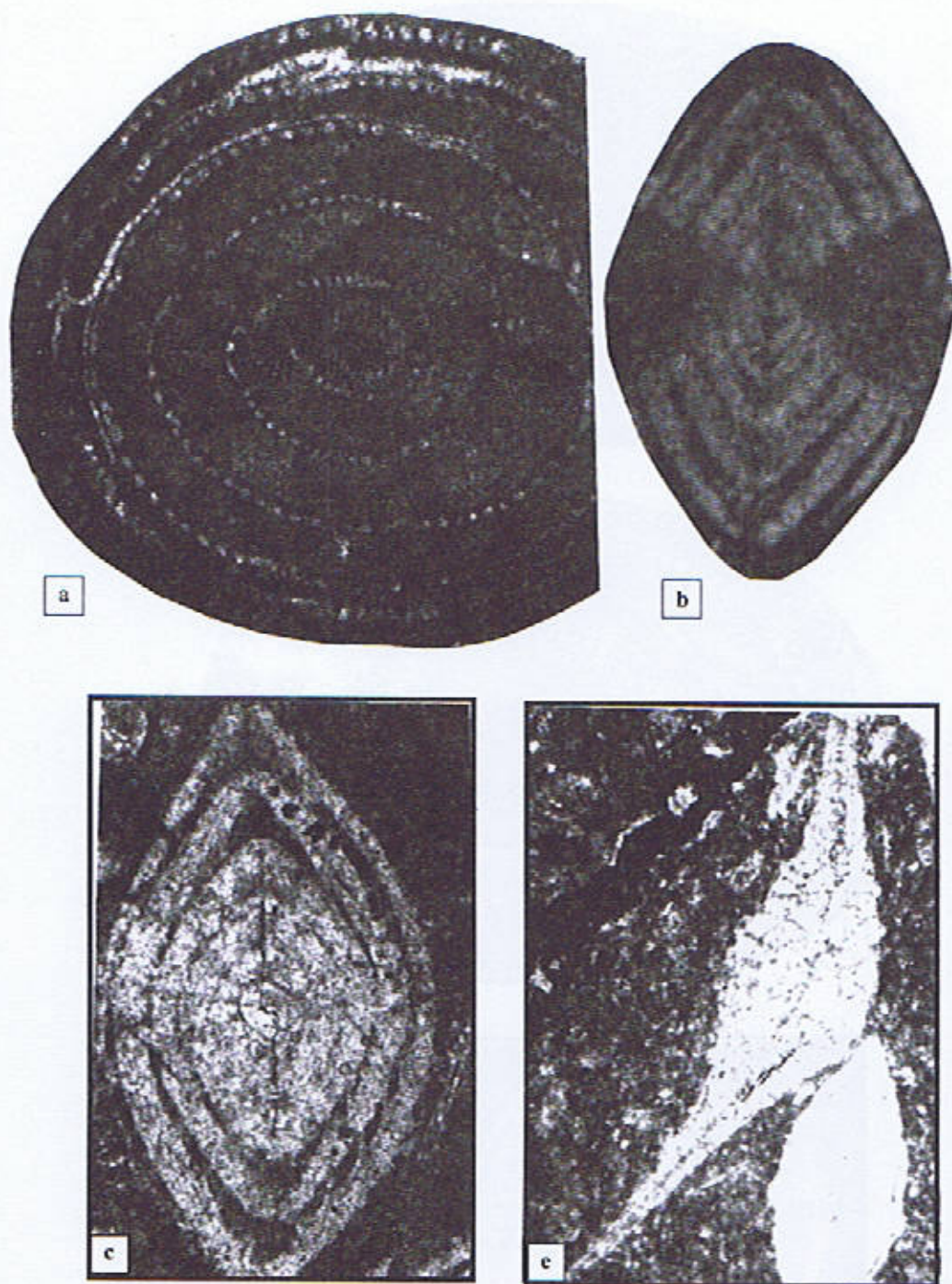
d



e



## Plate-IV





## Genus *Assilina* D'orbigny, 1826

*-Assilina laminosa* GILL.

(Plate-III, Fig-e)

*Assilina laminosa* GILL., 1953, p. 83, pl. 13, figs. 14-17.

REMARKS: This species is recorded from Panoba Shale of the Shekhan Nala section. The stratigraphic range of this species is lower Eocene.

## CONCLUSIONS

Chronostratigraphy of the Paleogene rocks of Kohat area is established according to the modern Shallow Benthic Biozones (SB zones) on the basis of Alveolinids (Fig. 4). The Hangu Formation and Lockhart Limestone are upper Paleocene rocks as they contain upper Paleocene fauna. The Lockhart Limestone belongs to *A. (G.) primaeva* zone (SB-3) due to the presence of *Alveolina (Glomalveolina) dachelensis*. The base of the Patala Formation is not exposed in Panoba section, the lower part in this area contains planktons of P-5 zone which is equivalent to *Alveolina vredenburgi* zone (SB-5) and the

upper part of the Patala Formation in this area contains *Nummulites mamillatus* which belongs to lower Eocene i.e. *Alveolina ellipsoidalis* zone (SB-6). Due to the presence of *Alveolina pasticillata* in the Panoba Shale, this Formation ranges from *Alveolina ellipsoidalis* zone to *Alveolina carbrica* zone (SB-6 to SB-8). *Alveolina aff. canavarii* and *Alveolina indicatrix* are recorded from the Shekhan Formation, so this formation ranges from *Alveolina carbrica* zone to *Alveolina oblonga* zone (SB-8 to SB-10). *Alveolina elliptica*, *Alveolina stercusmeris* and *Alveolina frumentiformis* are recorded from middle and upper part of Kohat Formation which show the range of Kohat Formation from *Alveolina stipes* zone to *Alveolina muniere* zone (Fig. 4). *Alveolina elliptica* is also present in the HabibRahi member of Kithar Formation so the boundary between the Kohat Formation and the Kithar Formation is in between *Alveolina muniere* zone. The Kuldana Formation is lacking Alveolinids so because of its position, it ranges from *Alveolina oblonga* zone to *Alveolina voilae* zone (SB-10 to SB-12).

## REFERENCES

- Abbasi, I. A., and Mc Elory, R., 1991. Thrust kinematics in the Kohat Plateau, Trans Indus Salt Range, Pakistan. *J. Str. Geol.*, 1B, 319-327.
- Brunes, A., 1832. Some account of salt mines of the Punjab. *Asiatic Soc. Bengal J.*, 1, 145-147.
- Cecchia-Rispoli, G., 1905. Sopra alcune Alveoline eoceniche della Sicilia. *Paleontogr. Ital.* 11, 147-165.
- Davies, L. M., 1926. Notes on the geology of Kohat, with reference to the homotexial Position of the salt marl at Bahadur Khel. *Asiatic Soc. Bengal J., Proc., New Series*, 20, 207-224.
- Davies, L. M., 1930. The fossil fauna from Samana Range and some neighbouring areas. The Paleocene Foraminifera. *Ibid. Mem. Paleont. Indica, New Series*, 15, 1-13.
- Davies, L. M. and Pinfold, E. S., 1937. The Eocene beds of the Punjab Salt Range. *Geol. Surv. Mem., Paleont. Indica, New series*, 24 (1), 1-79.
- Eames, F. E., 1952. A contribution to the study of the Eocene in western Pakistan and Western India. Part a., The geology of the standard sections in the western Punjab and in the Kohat District. *Geol. Soc. London. Quart. J.*, 107: 159-172.
- Fleming, A., 1853. On the Salt Range of the Punjab. *J. Geol. Soc. London*, 10, 1-80.
- Fichtel, L. V. and Moll, J. P. C., 1798. *Testacea Microscopia*.
- Gill, W. D., 1953. the genus *Assilina* in Laki Series (Lower Eocene) of the Kohat Potowar basin, north-west Pakistan. *Contr. Cushman Found. Forum. Res.*, 4, 76-84.
- Gumbel, C. W., 1870. Beitrage zur Foraminiferen fauna der nordalpinen Eocangebilde. K. Bayer. *Akad. Wiss. Abhandl.*, 10, 581-770.
- Hottinger, L., 1960. Recherches sur les Alveolines du Paleocene et de l'Eocene. *Mem. Suiss. Pal. Bale.* 75/76, 1-237.
- Hottinger, L., 1974. Alveolinida, Cretaceous-Tertiary Larger Foraminifera. *EPR-E-I SP* 74, 1-84.
- Gardezi, A. H., Ghazanfar, M. and Shakoor, A., 1976. Geology of Darra Adam Khel area, Chat Division, N.W.F.P. with observation on the facies changes and their tectonic implications. *Geol. Bull. Punj. Univ.*, 12, 97-102.



- Khan, M. A. 1967. Stratigraphic sections on the southern slope of Handyside Fort, Kohat, Western Pakistan. *Geol. Bull. Peshawar Univ.* **3(1)**, 15-18.
- Lamarck, J. B. P. A. De, 1801. 'System des Animaux sans Vertebres', 1<sup>re</sup> ed.
- Latif, M. A. 1970. Explanatory notes on the geology of southern Hazara to accompany The revised Geological Map. *Wein Jb. Geol. B. A., Sonderb.* **15**, 5-20.
- Leymerie, A., 1846. Mem. Sur le Terrain a Nummulites des Corbieres, etc., *Mem. Soc. Geol. France*, (2), **1**, 337-373.
- Meissner, C. R., Master, J. M., Rashid, M. A. and Sethi, U. B. 1968. Stratigraphy of Kohat Quadrangle, west Pakistan. *USGS Proj. Rep. (IR) PK-20*, 1-86.
- Meissner, C. R., et. al. 1974. Stratigraphy of Kohat Quadrangle, Pakistan. *USGS Prof. Paper* **716-D**, 1-30.
- Middlemiss, C. S. 1896. The geology of Hazara and Black Mountains. *Geol. Surv. Mem. India*, **26**, 1-302.
- Nagappa, Y., 1959. Foraminifera biostratigraphy of Cretaceous-Eocene succession in India, Pakistan and Burma regions. *Micropal.*, **5** (2), 145-192.
- Nuttall, W. L. F., 1925. The Stratigraphy of Laki Series, *Quart. J. Geol. Soc. London*, **LXXXI**, 417-453.
- Oldham, T. 1864. Memorandum on the results of a cursory examinations of the Salt Range and parts of the districts of Bannu and Kohat with a special view to the Mineral resources of those districts. *Rees., Govt. India*, **64**, 126-156.
- Orbigny, A. D., 1826. Tableau Methodique de la Classe des Cephalopods., *Ann. Sci. nat.*, **VII**.
- Parson, E., 1926. The structure and stratigraphy of the north-west Indian oil fields. *Inst. Petroleum Tech. J.*, **12**, 439-505.
- Pinfold, E. S., 1918. Notes on structure and stratigraphy in the north-west Punjab. *India Geol. Surv., Rees.*, 137-160.
- Rashid, M. A., Hussain, M., Masteb, J. M. and Meissner, D. R., 1965. Mineral deposits of eastern Kohat region, west Pakistan. *Geol. Surv. Pakistan, Rec. XIII*, part. 2: 1-16.
- Schwager, C., 1883. Die Foraminifera aus den Eocenablagerungen der Libyschen Wüste und Aegyptens., *Paleontographica*, **XXX**, 78-153.
- Silvestri, A., 1937. Foraminiferi del dell'Eocene della Somalia. *Paleontologi Somalia*, **32** (3), 49-89.
- Smout, A. H., 1954. Lower Tertiary Foraminifera of Qatar Peninsula. *British Mus. (N.H.) London*, 1-79.
- Sowerby, J. De C., 1840. Systematic description of organic remains of Cutch., *Trans. Geol. Soc. London*, **2**, (V), 327-329.
- Tanoli, S. K., Abbasi, I. A., Rehman, O., Riaz, M. and Iqbal, H., 1992. Early Cenozoic deltaic sedimentation in Kohat Basin. *Abstract, First south Asian Geol. Cong. Islamabad*.
- Vredenburg, E. W., 1909. Note on the stratigraphy of the Ranikot Series., *Pal. Indica, N. S.*, **III**, Mem. 1: 5-19.



## ALLAI AGGREGATE FOR REHABILITATION AND RECONSTRUCTION OF OCTOBER 8, 2005 EARTHQUAKE AFFECTED ALLAI-BANAN AREA, NWFP, PAKISTAN

BY

NAVEED AHSAN

Institute of Geology, University of the Punjab, Quaid-i-Azam Campus,  
Lahore-54590 Pakistan  
E-mail: naveedahsan@ymail.com

MUHAMMAD NAWAZ CHAUDHRY

College of Earth and Environmental Sciences, University of the Punjab, Lahore-54590

MUHAMMAD MUNAWAR IQBAL GONDAL

Road Research and Material Testing Institute, Lahore-54590

AND

ZAHID KARM KHAN

Institute of Geology, University of the Punjab, Lahore-54590

**Abstract:** The October 8, 2005 earthquake destroyed infrastructure of Allai-Banan area and large quantity of aggregate is required for the relocation, restoration, construction of buildings, bridges and roads. Moreover a number of hydroelectric projects with a total hydroelectric potential between 500 to 1000 MW are likely to be built on the Allai river and its tributaries that will require hundreds of thousands of cubic meter of fine and coarse aggregate. The Allai river and its tributaries flow across the Higher Himalaya, igneous and metamorphic rocks of the Lesser Himalaya, Tethyan Himalaya, Indus Suture Zone and part of adjoining Kohistan Island Arc and contains substantial quantity of aggregates that can be utilized for construction. The geology of the area reveals a very complex lithostratigraphic and lithotectonic set up that explain a very heterogeneous nature of aggregates derived from this terrain.

Engineering properties of the gravel and associated sand deposits of Allai river, terraces, bars and its tributaries fulfill the parameters specified in the standards. However, the aggregates of Allai river system contain mylonites, slates, phyllites, microcrystalline quartz and highly strained quartz. These potentially reactive rock types can initiate alkali aggregate reaction that will damage the infrastructures if preventive measures are not considered.

### INTRODUCTION

Allai valley located at lat. 34° 50' 14" and long. 73° 04' 08" (Toposheet No. 43 F/1) is one of two thesils of district Batgram. The valley is accessible from Besham via Kond Saiyidan and Thakot located on Karakoram Highway and its width varies from 0.5 km to 5 km. Allai river, main stream of the area, confluences the River Indus near Besham at Kond Saiyidan. The October 8, 2005 earthquake (Ahmad et al., 2008; Mona Lisa et al., 2008) destroyed the built infrastructure leaving devastating impacts on human life in northern Pakistan including Allai and its union council Banan. Earthquake rehabilitation and reconstruction

programme of Pakistan's Government aims at improving the lives of quake-ravaged people and construction of buildings, schools, dispensaries, hospitals, roads and bridges, etc.

In the areas of Allai-Banan, huge quantity of aggregate will be required for the relocation, restoration, construction and modernization of civil infrastructures. In addition to this, a number of hydroelectric power projects with a total hydroelectric potential of 500 to 1000 MW are likely to be built on the Allai river and its tributaries that will require hundred of thousands of cubic meter of fine and coarse aggregate for the weir/dam and related civil



structures. The gravel and associated sand occurs in the bed of the Allai River and its tributaries near Allai and Banan. Besides gravel and sand deposits of river and its tributaries, coarse aggregate can be manufactured by crushing suitable rock types (Bell, 2007) to meet the demands of civil works.

In service performance of civil infrastructure depends on a number of factors (Sarkar and Actin, 1990; Neville, 2000; Ilango et al., 2008) that may include engineering properties of coarse and fine aggregates, proportion of aggregate and cement paste, paste-aggregate bond characteristics, etc. In this context, durable aggregate is preferred that may have the ability to maintain its engineering properties without momentous deterioration in strength during an extensive period of time (Neville, 1981; Lafrenz, 1997; Smith and Collis, 2001). Along with suitable physical and mechanical properties, it is indispensable that the aggregate should be innocuous with respect to deleterious alkali aggregate reaction potential (ASTM C 295, Bell, 2007) especially where it has to perform in humid conditions. In Pakistan, aggregates for construction are manufactured by crushing rocks extracted from outcrops (Tepordei, 1999; Ahsan et al., 2000; Gondal, 2006a, b) through open excavation. In addition to this crushed and uncrushed river, terrace and pit run gravels (Chaudhry et al., 1997; 2001) and in some cases recycled aggregates (Deal, 1997; Wilburn and Goonan, 1998), consisting mainly of crushed concrete and asphalt pavements, are also used when crushed rock aggregate is not available or is economically unsuitable.

Deposits of sand and gravel (Collins and Dunne, 1990; Kondolf, 1997; Bolen, 1999) are widely exploited as construction aggregate for reinforced concrete, concrete products (such as blocks, bricks, pipes, etc), plaster and gunite sands, roofing granules, road pavements, riprap, railroad ballast and filter blankets for drainage through out the world (Bell, 2007). These fluvial deposits have been subjected to lengthy transportation processes (e.g. abrasion and attrition) in streams that remove all the weak materials leaving behind durable, sub rounded to rounded and well sorted gravels (Barksdale, 1991). Generally these graveliferous aggregate deposits can be quarried from river beds, flood plains and river terraces. In Allai area, floodplain and channel deposits are topographically lowest areas along river and tributaries beds that contain substantial quantity of aggregates as active and abandoned channel fill, small alluvial fans and bar deposits. Thickness and horizontal extent of the deposits varies considerably and is paleo-topographically controlled. Besides these, few terrace deposits, such as Banan Terrace, are located at higher elevations and present day river channel is cutting through these. The depth of incision by river itself and its tributaries varies from point to point. Alluvial fans and bars are few in the area and predominantly contain gravels.

The Allai river and its terraces are the only potential resource, keeping in view apparent quantity and close proximity to transportation routs, economics and end users, for the development of gravel and sand quarries in the area. However, for extraction of aggregates from these prospective deposits some processing will be required. At places minor over-burden and/or vegetation occurs but can be removed. The boulders and gravels will require crushing to meet up the specified gradation, texture and grain morphological parameters. From gravel fans and terraces, aggregates can be transported to Allai for crushing and sizing. The crushed gravel can be sized by using vibratory sieves so that high efficiency and capacity are met. The sieved out as well as oversized material may require the removal of deleterious materials like clay, mud and organic matter, etc.

The present study is mainly aimed:

- to locate the potential resources of sand and gravel for the remote area of Allai and Banan,
- to find out the engineering characteristics of Allai river aggregates,
- to determine the modal mineralogical composition of fine and coarse aggregates,
- to properly investigate and recognize potentially reactive aggregates prior to construction and
- to suggest the remedial measures to avoid the deleterious alkali aggregate reaction.

Representative samples for the evaluation of physical, petrographical and chemical properties of Allai aggregate were collected from river bed, terraces and bars.

## ORIGIN OF AGGREGATES

Allai river and its tributaries flow across the Higher Himalaya, igneous and metamorphic rocks of the Lesser Himalaya, Tethyan Himalaya, Indus Suture Zone (ISZ) and part of adjoining Kohistan Island Arc. The Allai river drainage system derives S-type porphyritic cordierite bearing two mica granites, high grade pelitic and psammitic schists, pegmatites, vein quartz and dolerites/metadolerites from Lesser Himalaya igneous and metamorphic zones which lies between the Punjal Fault and Main Central Thrust (MCT; Chaudhry and Ghazanfar, 1990). The non-porphyritic garnetiferous granites, quartzites, marbles, pelites, psammites metadolerites (amphibolites) and pegmatites are derived from the upper amphibolites facies of the Higher Himalaya. Slates, phyllites and slightly metamorphosed limestones are derived from fault slices/zones of the upper Mesozoic and lower Paleozoic Tethyan sediments. This zone that lay between Thakot Fault and ISZ is now imbricated. In addition to these rock types, dunites/peridotite and basic rock fragments as well as meta-argillites are derived from the ISZ. Amphibolites, diorites and norites have their origin in the Kohistan Island Arc that lies north of the ISZ.



## GEOLOGY OF THE AREA

The area of Allai-Banan is situated on eastern and northeastern part of the Besham Syntaxis (Treloar et al., 1989; Williams, 1989). The Besham Syntaxis is one of the many domal structures of the Higher Himalaya and is bounded on the east by Thathakot Fault and on the west by the Puran Fault (Chaudhry et al., 1980). Both, Thathakot and Puran faults trend NS. The lower Proterozoic Higher Himalaya Crystalline (HHC) comprises upper amphibolite facies, pelites, psammites, quartzites and marbles along with garnet mica non-porphyritic granitoids (Chaudhry et al., 1994). The HHC structures in this region lay NS as against EW predominant trend in the Lesser Himalaya (Chaudhry et al., 1997). The area has suffered lower Proterozoic, Pan African and Himalayan orogenies in which gneisses and mylonites were developed.

The Lesser Himalaya drained by Allai river system is composed of pelites, psammites and S-type porphyritic two mica tourmaline and cordierite granites. The Lesser Himalaya suffered Pan African orogeny and developed mylonites during Himalayan orogeny.

A unique feature of this area is a kidney shaped outcrop of the Tethyan Himalaya. The Tethyan Himalayan sediments are only slightly metamorphosed and comprise limestones, meta-argillites (slates and subphyllites). This zone that lay between the Trans Hhimadri Fault and the ISZ is now imbricated. The Tethyan Himalaya has been discussed in detail by Ghazanfar (1993).

The structural zone (ISZ) in Allai is a rare and unique section in the sense that in addition to ultramafics and pillow basalts, it also contains low grade siliclastics meta-turbidites deposited in the fore arc basin. To the north of this fore arc basin lies the deeply eroded parts of Kohistan Island Arc. The Allai river system cuts across the amphibolites, diorites and barely accesses norites.

The brief description of geology of the area given above reveals a very complex lithostratigraphic and lithotectonic set up (Treloar et al., 1989; Williams, 1989) and helps to explain a very heterogeneous nature of aggregates derived from this terrain. The geology may vary from one tributary to the other. Therefore, the aggregate deposits may vary widely in comparison and physical properties. However, in this publication by far the biggest and better mixed deposits of Allai-Banan area were studied.

## ENGINEERING CHARACTERISTICS OF COARSE AGGREGATE

As engineering properties of aggregates determine their performance in mortar, concrete and unbound and bound pavement (e.g. Neville and Chatterton, 1981; Winslow 1994, Pigeon and Plateau, 1995; Neville, 2000;

Smith and Collis, 2001) therefore it is common practice to work out desirable properties through tests mentioned in literature (e.g. Neville, 2000) standards (e.g. BS, ASTM, etc.).

## Texture and Grain Morphology

Surface texture plays a vital role in bond between aggregate and cementing material and depends upon the mineralogy of the aggregate particle. Generally, the aggregate with rough surface texture is desired in engineering projects (Nevelli, 2000; Fletcher et al., 2002) as it produces a stronger bond thereby creating a stronger cement concrete or hot mix asphalt concrete and avoid stripping of asphalt (Maupin, 1987). Aggregate particles of the Allai river do not indicate considerable variation in surface texture and dominantly texture is rough. Amphibolites, diorites, granite, S-type granite gneiss, granite mylonites, mylonites, pegmatites, schists, vein quartz, norites and dunites show rough texture whereas marbles give smooth texture.

The gravel of the Allai river consists of naturally rounded particles resulting from disintegration and abrasion of parent rocks. They present three aspects of grain morphology that include shape, sphericity and roundness. Allai aggregates are subangular to well rounded (Pettijohn, et al., 1987; Ahn, 2000; Tucker, 2001; Neville, 2000) and generally they show low to high sphericity. The morphology of grains depends on mineralogy, degree of weathering and degree of abrasion during transportation (Ritter, et al., 2000; Bell, 2007). Rounded particles are undesirable in cement and asphalt concrete as they impede the bond between aggregates and cementing material (Hu and Stroeve, 2006). In addition to this rounded aggregate continue to compact, shove and rut after construction. Similarly, elongated and flat particles break under impact and reduce strength (Smith and Collis, 2001; Jamkar and Rao, 2004). In present case, Allai aggregate is predominantly angular to rounded and degree of sphericity is low it may, therefore, prove a good aggregate for cement and asphalt concrete. However, crushing is recommended prior to its use in construction and it will help to get the desired gradation.

## Bulk Density and Specific Gravity

It gives the mass of the aggregate in given volume and is required for the volume method of mixture proportioning (Neville, 2000; BS 812). The well-graded and densely packed aggregates have higher value of the density as compared to loosely packed aggregates (Mehta and Monteiro, 1993). The values of loose bulk density range from 89 lbs/cft to 91 lbs/cft. Specific gravity gives a weight volume relationship so that an appropriate concrete design mix can be determined (AASHTO T 85). The



specific gravity of Allai aggregate on oven-dried basis is 2.70. The use of bulk density has declined due to availability of mix designs (Smith and Collis, 2001).

### Water Absorption

The water absorption affects the specific gravity of the aggregate as well as in service behaviour of concrete. It is considered an indirect measure of permeability of aggregate that affects other physical characteristics such as mechanical strength, soundness and its general durability potential (Smith and Collis, 1993; Neville, 2000). Aggregates having high water absorption are unsuitable unless they are found to be acceptable based on other properties such as strength, impact and hardness tests (Schmidt and Graf, 1972; Graf, 1986). The water absorption of the Allai river gravel varies from 0.9% to 1.1% that is within the specified limits.

### Strength and Durability

Aggregates under go wear and tear through out their performance life and it is required that they should resist crushing, degradation and disintegration when used in sub base, base course, hot mix asphalt and plain cement concrete (Roberts et al., 1996; Wu et al., 1998). In addition to this aggregates should be resistant to abrasion and polishing otherwise they will cause skidding on the roads. Fookes et al., (1988) recommend using the combination of impact value and Los Angeles abrasion resistance to assess the performance and durability of aggregates. In addition to this, work by Bullas and West (1991) shows that aggregate crushing value helps to separate suitable and unsuitable aggregate for bitumen macadam road base as compared to aggregate impact value.

Aggregate impact value (AIV) indicates relative measure of mechanical resistance of an aggregate to sudden shock (Smith and Collis, 2001). The percentage loss in Allai gravel is 25.3% and this value is within safe limits for concrete and asphalt. Another parameter to assess toughness and abrasion resistance of the aggregate is aggregate crushing value (ACV) and Los Angeles abrasion value, LAV, (Smith and Collis, 2001). The aggregate crushing value is 22.9% and Los Angeles abrasion value is 24.6% for Allai gravels that are within safe limits for construction purposes. Roberts et al., (1996) show values of 10% fines for igneous rock indicating %age loss of 27-49 for granite, 33-55 for gneiss and 20-35 for quartzites. Similarly, Bell (2007) indicates that AIV, ACV and LAV for basalt, granite, micro-granite and quartzite range from 12% to 20%. In this study ACV and AIV for quartzite and granite is 20% i.e. maximum. Although AIV, ACV, and LAV are within safe limits according to AASHTO and BS but they are high as compared to the values calculated by Bell (2007). This is probably due to the presence of mylonite, gneiss and schist clasts in Allai gravels.

Another parameter, soundness test (ASTM C 88), mentioned in published literature (e.g. Smith and Collis, 2001; Neville, 2000) is the resistance of aggregate to disintegrate when subjected to attacks by salts and freeze and thaw action during extreme weathering conditions (Wu, et al, 1998; ASTM C 88). The loss of Allai gravel when tested in  $\text{Na}_2\text{SO}_4$  solution (AASHTO T 104) ranges from 3.32% to 3.25% thereby indicating a sound aggregate for construction. In a study carried out for Alabama, Georgia, North and South Carolina, aggregates mainly composed of granite indicate soundness value in the range from 0% to 2.2% (Cooley, Jr. et al., 2002). The values of Allai gravels are relatively high as it contains some weak rock clasts as mylonite, gneiss and schist clasts.

### ENGINEERING PROPERTIES OF FINE AGGREGATE

The river bed and terraces contain variable amount of sand. It can be used in cement concrete, unbound and bound pavements after processing. Like coarse aggregates, many properties of the fine aggregate depend entirely on the properties of the parent rock, for example, chemical and mineral composition, petrologic character, specific gravity, hardness, strength, physical and chemical stability, pore structure and colour (Neville, 1981; Smith and Collis, 2001; Dilek and Leming, 2004).

A number of sieve analyses of the Allai River bed and associated sand deposits show that it does not conform to the overall limits of BS 882: 1992; ASTM C 33. The sand is poorly graded and its gradation varies from place to place. It is coarse grained (FM=3.8) where it occurs as point bar deposits and sand associated with terraces is fine grained (FM=0.9). The amount of fine aggregate, generally passing the #50 and #100 sieves, affects the characteristics of cement concrete like workability and bleeding (Dilek and Leming, 2004). Besides this, it is believed that appropriate quantity of fine aggregate is needed for good cohesiveness and plasticity (Quiroga and Fowler, 2003). Improved overall grading of sand can be achieved by blending experiments (Chaudhary et al., 2000; Ahsan et al., 2000). The sand for blending can be obtained as a by-product if coarse aggregates were manufactured by crushing innocuous oversized associated gravels.

The other properties of fine aggregate include bulk density (BS 812), specific gravity and water absorption (BS 812), soundness (ASTM C 33) and Los Angeles abrasion value (ASTM C 131) are 85Lbs/cft-89Lbs/cft, 2.70-2.73, 0.5%-0.9%, 2.32%-2.96%, and 28.7%-29.3%, respectively. All these values are well below the time honoured standards that are referred in construction industry for specifications. However, Allai sand contains 1.21%-1.30% silt and clay and when tested in accordance to ASTM C 142, Allai sand contains 0.5% to 1.1% clay lumps. Such pieces may be



problematic in concrete in cold climates. The sands contain dried leaves, wood pieces and grass shoots as organic impurities but are free from chloride contents (Neville, 2000).

#### PETROGRAPHY OF COARSE AGGREGATE

ASTM C 295 recommends petrographic examination (Watters, 1969; Nixon and Sims, 2006; Tremblay, 2008) of aggregates to "determine the physical and chemical characteristics, identification of types and varieties of rocks present in potential aggregates, establish whether the aggregate contains chemically unstable minerals such as soluble sulfates, unstable sulfides that may form sulfuric acid or create distress in concrete exposed to high temperatures during service, or volumetrically unstable materials such as smectites and potentially alkali-silica reactive and alkali-carbonate reactive constituents, determine such constituents quantitatively, and recommend additional tests to confirm or refute the presence in significant amounts of aggregate constituents capable of alkali reaction in concrete". In addition to this petrography is implied to identify promising occurrence of contaminants in aggregates, such as synthetic glass, cinders, clinker, coal ash, magnesium oxide, calcium oxide, or both, gypsum, soil, hydrocarbons, chemicals that may affect the setting behavior of concrete or the properties of the aggregate (ASTM C 295). Moreover, animal excrement, plants or rotten vegetation, and any other contaminant that may harm the performance of concrete is also undesirable (Neville, 2000). For petrographic evaluation fine and coarse fractions (10 samples of each) of Allai aggregate were studied under the microscope to, particularly, predict in service performance of gravel and sand with respect to alkali aggregate reaction potential. The petrographic results of coarse and fine aggregates are presented in Table 1 and 2, respectively. However Table 2 show modal analysis of coarse fraction associated with fine sand.

The gravels of the river and its tributaries are composed of amphibolites, diorite, granite, S-type granite gneiss, granite mylonite, marble, mylonite, pegmatite, schist, vein quartz, norite and dunite. The fine fraction of river bed, bars and terraces is composed of granite/granodiorite, diorite/tonalite/amphibolite, quartzite, phyllite/slate, greywacke group, chert, quartz mica schist/gneiss, quartz/polygrain quartz, feldspar, biotite, muscovite, amphibole, epidote, magnetite, garnet, tourmaline and zircon. In addition to this petrographic modal analysis of 6 samples was carried out and average composition of rocks present in these samples are: amphibolite (14.5%), diorite (25.1%), granite (13.81%), granite gneiss (4.0%), marble (10.3%), mylonite (3.5%), pegmatite (1.0%), schist (11.4%), vein quartz (1.3%), psammite (6.7%), slate (2.3%), greenstone/meta-basalt (3.8%), norite (2.0%) and dunite/peridotite (0.3%).

#### ALKALI AGGREGATE REACTION POTENTIAL

Alkali aggregate reaction (AAR) was first reported by Thomas Stanton (1940) as a reaction of alkalis released by cement paste ( $\text{Na}_2\text{O}$  and  $\text{K}_2\text{O}$ ) and California aggregates that contained opal. This reaction later on named as alkali silica reaction (ASR) produces a gel that will expand in presence of moisture and induces cracks in aggregate and cement paste (Diamond, 1989; Hobbs, 1978, 1988; Swamy, 1992; West, 1996). ASTM C 33 indicates that alkali silica reactive constituents present in aggregates are opal, chalcedony, cristobalite, tridymite, highly strained quartz, microcrystalline quartz, volcanic glass, and synthetic siliceous glass. In addition to this aggregate materials containing glassy to cryptocrystalline intermediate to acidic volcanic rocks, some argillites, phyllites, graywacke, gneiss, schist, gneissic granite, vein quartz, quartzite, sandstone, and chert are also potentially deleterious with respect to AAR (Mindness and Young, 1981; Wenk, 1998; Codey et al., 1994; Gress, 1996).

Published literature indicates (Frany and Kosmatka, 1997; Chaudhry and Zaka, 1998; Neville, 1996, 2000) that ASR will not occur when the equilibrium internal relative humidity in the concrete is less than 75% (Pedneault, 1996), in the absence of sufficient alkali in the pore solutions (Nixon and Sims, 1992) and absence of pessimum proportion of reactive aggregates (CSA, 2000). Moreover, if any one of these three factors is absent, then ASR will not proceed (Stark, 1991).

In Pakistan structural damage in Warsak Dam was recognized due to the occurrence of ASR (Chaudhry and Zaka, 1998) and major repair of dam was carried out. Similarly, ASR in Tarbela Dam (TAM Report, WAPDA, 1965) damaged the power tunnels. In case of Warsak Dam aggregates containing potentially reactive volcanics were used with ordinary Portland cement (OPC) and in Tarbela Dam aggregate extracted from the River Indus were involved in reaction with OPC, twelve years after completion. Chaudhry and Zaka (1994) petrographically indicated the presence of strained quartz and other rock types, particularly meta greywackes, that were slowly reacting with aggregates to produce ASR. Shrimmer (2003) reported malfunction in gates of a 47 years old dam in southern British Columbia due to AAR and in all 125 affected sites have been identified through out British Columbia. Mostly quartzite, andesite, chert and opal were identified to be involved in AAR (Shrimmer, 2003).

Allai gravels contain mylonites and slates as deleterious constituents with respect to AAR. Coarser fragments associated with Allai sand that are potentially reactive are phyllite/slate, greywacke group and chert. It is evident from published literature (e.g. TAM Report, WAPDA, 1965; Charwood and Solymar, 1994; Chaudhry



**Table 1**  
Petrographic modal analysis of coarse aggregate of Allai gravel

| Rock /Sieve            | >2in   | 1 1/2 in | 1 in   | 3/4 in | 1/2 in | 3/8 in | No. 4  |
|------------------------|--------|----------|--------|--------|--------|--------|--------|
| Amphibolite            | 20.00% | 9.10%    | 15.60% | 12.00% | 2.10%  | 10.00% | 7.10%  |
| Diorite                | 27.20% | 24.40%   | 24.50% | 31.50% | 0.00%  | 28.10% | 27.50% |
| Granite                | 5.00%  | 19.50%   | 8.20%  | 10.30% | 10.20% | 14.90% | 10.40% |
| Granite Gneiss S-Type* | 9.60%  | 4.90%    | 7.20%  | 4.30%  | 3.20%  | 4.00%  | 6.30%  |
| Marble                 | 7.50%  | 15.90%   | 17.20% | 10.40% | 22.30% | 12.00% | 10.10% |
| Mylonite*              | 3.20%  | 6.80%    | 2.50%  | 3.60%  | 2.30%  | 2.60%  | 3.00%  |
| Pegmatite*             | 2.50%  | 2.70%    | 1.00%  | 2.30%  | 1.10%  | 2.10%  | 2.10%  |
| Schist                 | 1.10%  | 2.30%    | 20.50% | 14.50% | 18.50% | 13.60% | 14.90% |
| Vein Quartz            | 1.00%  | 0.00     | 2.50%  | 0.60%  | 1.00%  | 0.70%  | 3.70%  |
| Psammite*              | 5.10%  | 9.50%    | 0.00%  | 5.40%  | 4.50%  | 8.30%  | 9.60%  |
| Slate*                 | 2.00%  | 0.40%    | 0.80%  | 1.20%  | 1.40%  | 3.70%  | 3.00%  |
| Greenstone             | 5.60%  | 4.50%    | 0.00%  | 1.80%  | 5.00%  | 1.00%  | 1.10%  |
| Norite                 | 5.10%  | 0.00%    | 0.00%  | 0.00%  | 25.40% | 0.00%  | 0.00%  |
| Dunite                 | 5.10%  | 0.00%    | 0.00%  | 2.10%  | 3.00%  | 0.00%  | 1.2%   |

\*Potentially deleterious constituents with ASR potential

**Table 2**  
Petrographic modal analysis of rock fragments associated with fine aggregate from Allai river

| Rock fragments /sieve        | NO.8   | NO.16  | NO.30  | NO.50  | NO.100 |
|------------------------------|--------|--------|--------|--------|--------|
| Granite/granodiorite         | 22.20% | 22.10% | 34.30% | 42.00% | 53.60% |
| Diorite/tonalite/Amphibolite | 6.30%  | 8.30%  | 4.70%  | 4.60%  | 8.40%  |
| Quartzite                    | 1.50%  | 1.60%  | 1.30%  | 1.70%  | 2.00%  |
| Phyllite/slate*              | 2.40%  | 1.40%  | 1.40%  | 1.60%  | 2.4%   |
| Greywacke group*             | 1.60%  | 3.70%  | 0.90%  | 2.30%  | 2.80%  |
| Chert*                       | 1.40%  | 1.50%  | 1.60%  | 1.80%  | 1.80%  |
| Quartz mica schist/gneiss*   | 1.20%  | 1.30%  | 1.00%  | 1.40%  | 3.00%  |
| Schist*                      | 1.10%  | 1.20%  | 1.20%  | 1.40%  | 1.20%  |

\*Potentially deleterious constituents with ASR potential

**Table 2 (Cont.)**  
Petrographic modal analysis of fine aggregate from Allai river

| Mineral grains/ sieve   | NO.8   | NO.16  | NO.30  | NO. 50 | NO. 100 |
|-------------------------|--------|--------|--------|--------|---------|
| Quartz/polygrain quartz | 23.50% | 16.30% | 9.60%  | 6.10%  | 0.90%   |
| Feldspar                | 3.40%  | 4.90%  | 0.30%  | 0.50%  | 0.20%   |
| Biotite                 | 12.40% | 9.90%  | 8.80%  | 8.10%  | 8.60%   |
| Muscovite               | 15.50% | 20.40% | 17.00% | 18.40% | 7.20%   |
| Amphibole               | 0.80%  | 0.40%  | 1.10%  | 0.40%  | 0.40%   |
| Epidote                 | 0.90%  | 0.10%  | 0.60%  | 0.50%  | 0.80%   |
| Magnetite               | 5.40%  | 3.30%  | 8.50%  | 8.30%  | 8.10%   |
| Garnet                  | 0.00%  | 3.10%  | 7.10%  | 0.00%  | 0.00%   |
| Tourmaline              | 23.50% | 16.30% | 9.60%  | 6.10%  | 0.90%   |
| Zircon                  | 3.40%  | 4.90%  | 0.30%  | 0.50%  | 0.20%   |
| Clay lumps              | 12.40% | 9.90%  | 8.80%  | 8.10%  | 8.60%   |



and Zaka, 1994; 1998) that use of these gravels will create a major durability crisis that will result in premature deterioration of concrete structures. The present study shows that Allai sands are deleterious as far as ASR is concerned. They contain more than 20% highly strained quartz. In addition to this, ASTM C 1260, quick mortar bar test shows an expansion of 0.30% at 28 days that verifies the conclusion of petrographic test, ASTM C 295.

As far as Allai aggregate is concerned it is the only source of aggregate available in the area of Allai and Banan. As the area is located in tectonically deformed Himalayan ranges and the aggregate is extracted from the rocks including granites, granodiorites, quartzites and metamorphic rocks such as slates, gneisses, etc. therefore it is not possible to avoid their use as aggregates. Moreover, if aggregate is transported from innocuous sources like limestones, cost of the project will increase manifolds. However, it is possible to use suitable crushed rock aggregate after petrographical evaluation for construction that in turn may increase the cost.

Best way to avoid AAR is to use innocuous aggregate so that proper performance life of a structure may be assured. However, in the absence of safe aggregate, published literature (Thomas et al., 1997; Afrani and Rogers 1994; Rogers and Hooton 1992; Thomas and Innis, 1998; Thomas 1996; Malver et al., 2002, 2003; Malver and Lenke, 2005) suggests preventive measures that can be taken in to account when use of potentially reactive aggregate is inevitable. One such measure is use of low alkali cement (alkali content of less than 0.60%  $\text{Na}_2\text{O}$  equivalent; Nevelli, 2000; Rogers et al., 2004). Blast furnace slag cement (Douglas et al., 1992; Rogers et al., 2000) and fly ash (Malvar and Lenke, 2005, 2006; Lenke and Malvar, 2005) have been used effectively to prevent ASR (Donnelly, 1990) in Canada. However, use of slag cement retards strength gain in cold climates (Rogers et al., 2000), like Allai. In Lower Notch Dam (North America) in 1971, use of argillites was permitted with high alkali cement with fly ash as additive and dam performed well for 30 years (Rogers et al., 2000). Another preventive measure is use of chemical admixtures or cement additives such as lithium compounds (Stark, 1992, 1993; Gajda, 1996; Ober, 2002). When lithium compounds (hydroxide,  $\text{LiOH}$ ; lithium nitrate,  $\text{LiNO}_3$ ; or lithium carbonate,  $\text{LiCO}_3$ , etc.) are added to cement it forms a lithium bearing gel that greatly reduces

potential for expansion. Moreover blended aggregates can be used to minimize the percentage of potentially deleterious rock types (Chaudhry, 2000). Besides these silica fumes and natural pozzolans (such as diatomite, pumicite) can be used to control ASR (Bérubé and Duchesne, 1992; Boddy et al., 2003)

## CONCLUSIONS AND RECOMMENDATIONS

The life performance of civil structures mainly depends upon the physical and chemical properties of aggregates. Beside these properties, mineralogy of aggregates controls the extent of ASR. It is imperative that potentially reactive aggregates are identified and appropriately scrutinized prior to construction, as there is no technique to avert the ASR after the concrete has been placed. The main focus of this study was the huge aggregate deposits of Allai-Banan near Banan on Allai river that would be used in the reconstruction of earthquake affected Allai area.

- The Allai aggregates meet engineering properties/parameters/requirements. However, both fine and coarse have ASR potential.
- The reactive constituents, recognized by petrography, are mylonites, slates, phyllites, microcrystalline quartz and highly strained quartz.
- ASTM C 1260, quick mortar bar test shows an expansion of 0.30% at 28 days. This test verifies the conclusion of petrographic test, ASTM C 295.
- It is recommended that the Allai aggregates may be used with low alkali cement, fly ash, slag, microsilica or pozzolana. For this purpose, a concrete mix design should be developed with additives.
- Since the geology of the area is highly heterogeneous, the aggregates of all major tributaries of Allai river should be studied to find out the presence of non deleterious aggregates.
- Innocuous crushed rock aggregate could be blended with Allai gravel to reduce/avert ASR potential.

## ACKNOWLEDGEMENT

We are thankful to HEC for supplying fund under the project "Analysis and interpretation of geotechnical properties, alkali aggregate reaction potential and provenance of indus aggregate".

## REFERENCES

- Afrani, I., and Rogers, C. 1994. The effect of different cementing materials and curing regimes on the scaling resistance of concrete. *Cement Concrete and Aggregates*, 16(2), pp. 132-139.
- Ahn, N., 2000. An Experimental Study on the Guidelines for Using Higher Contents of Aggregate Microfines in Portland Cement Concrete, Ph.D. Dissertation, University of Texas at Austin,.



- Ahsan, N., Chaudhry, M.N., Majid, M. 2000. Strength Evaluation of Blends of Lawrencepur, Chenab and Ravi Sands with Lockhart and Margala Hill Limestones for use in Concrete. Special Issue Pak. Muse. Nat. Hist. Pakistan Science Foundation, pp. 213-240.
- American Standard for Testing and Materials C 1260. Test Method to evaluate aggregate reactivity in presence of deicer solutions.
- American Standard for Testing and Materials C 131. Resistance to abrasion of small size coarse aggregate by use of the Los Angeles machine.
- American Standard for Testing and Materials C 295. Standard Guide for Petrographic Examination of Aggregates for Concrete.
- American Standard for Testing and Materials C 88. Soundness of Aggregates by Use of Sodium Sulfate or Magnesium Sulfate.
- American Standard for Testing and Materials: C 227. Potential alkali reactivity of aggregates (chemical method).
- American Standard for Testing and Materials: C 33. Tentative specifications for concrete aggregates.
- Barksdale, R.D. 1991. The aggregate handbook. National Stone Association, Washington, DC.
- Bell, F. G., 2007. Engineering Geology. Butterworth-Heinemann, Oxford, UK, 581pp.
- Bérubé, M.A., Duchesne, J., 1992. Evaluation of testing methods used for assessing the effectiveness of mineral admixtures in suppressing expansion due to alkali-aggregate reaction. *Proceedings of the Fourth International Conference on Fly Ash, Silica Fume, Slag, and Natural Pozzolans in Concrete*, (Ed. V.M. Malhotra), ACI SP132, Vol. 1, American Concrete Institute, Detroit, MI, pp. 549-575.
- Boddy, A.M., Hooton, R.D., and Thomas, M.D.A. 2003. The effect of the silica content of silica fume on its ability to control alkali-silica reaction. *Cement and Concrete Research*, Vol. 33, pp. 1263-1268.
- Bolen, W.P., 1999. Sand and gravel (construction): U.S. Geological Survey Mineral Commodity Summaries, p. 146-147.
- British Standard: 812. Method for determination of water-soluble chloride salts.
- British Standard: 882. Specification for aggregate, from natural source for concrete.
- Bullas, J.C. and West, G., 1991. Specifying Clean, Hard and Durable Aggregate for Bitumen Macadam Roadbase. *Research Report 284*, Transport and Road Research Laboratory, Department of Transport (British).
- Canadian Standards Association (CSA), 2000. Guide to the Evaluation and Management of Concrete Structures Affected by Alkali-Aggregate Reactions, **CSA A864-00**, Ontario, Canada.
- Charlwood, R.G., and Solymar Z.V., 1994. A Review of Alkali-Aggregate Reaction in Dams. *Dam Engineering*, Vol. V, Issue 2, pp. 31-62.
- Chaudhry, M. N., and Zaka, K. J., 1994. Tarbela Dam: A Discussion on the Discrepancy Between the Laboratory Testing and Inservice Behaviour of Indus Aggregate in Concrete", *Dam Engineering*, Vol. V, 1, pp. 63-80.
- Chaudhry, M. N., and Zaka, K. J., 1998. Petrographic Evaluation of Alkali Aggregates Reaction in Concrete Structures of Warsak Dam, N.W.F.P.- A Case Study", *Proceedings Eighth International Congress, Association of Engineering Geology and Environment*, pp. 2841-46.
- Chaudhry, M.N. and Ghazanfar, M., 1990. Position of the Main Central Thrust in the tectonic framework of Western Himalaya, *Tectonophysics*, 174, pp. 321-329.
- Chaudhry, M.N., Ahsan, N., Majid, C.M. and Gondal, M.M.I. 2001. Petrographic evaluation of Jalipur mollase as construction raw material. 4th Pakistan Geological Congress, February 27-28, Islamabad, National Geological Society of Pakistan, PMNH (Pakistan Science Foundation).
- Chaudhry, M.N., Ahsan, N., Zaka, K.J. and Majid, C.M. 1997. Alkali aggregate reaction potential of Indus gravel and sand between Riakot bridge and Kalabagh, Pakistan. National Symposium on Economic Geology of Pakistan, April 2-3, 1997. PMNH, Pakistan Science Foundation.



- Chaudhry, M.n., Ashraf, M. and Hussain, S.S. 1980. General geology and economic significance of the Lahor granite and rocks of southern ophiolite belt in Allai Kohistan area. Proc. Int. Geodynamics. Group 6, meeting, Peshwar, Nov. 23-29, 1979. Special Issue, *Geol. Bull. Univ. Peshwar*, 13, pp. 25-44.
- Chaudhry, M.N., Baloch, I.H., Ahsan, N. and Majid, Ch. M. 1999. Engineering properties, Mineralogy, Alkali Aggregate Reaction Potential and Provenience of Lawrencepur Sand Pakistan, Special Issue Pak. Muse. Nat. Hist. Pakistan Science Foundation, pp. 241-254.
- Chaudhry, M.N., Ghazanfar, M., Spencer, D.A. Hussain, S.S. and Dawood H., 1997. The Higher Himalaya in Pakistan – A tectono Stratigraphic Synopsis. *Geol. Bull. Punjab Univ.* 31 & 32, pp. 21-41.
- Cody, R. D., Spry, P. G., Cody, A. M., and Gan, G., 1994. The Role of Magnesium in Concrete Deterioration," Iowa DOT HR-335. Final Report.
- Collins, B. and Dunne, T. 1990. Fluvial geomorphology and river-gravel mining: a guide for planners, case studies included. Calif. Depart. Conserv., *Div. Mines Geol., Spec. Pub.* 98. 29 pp.
- Cooley, Jr. L. A., Huner, M. S. and James, R. H. 2002. Micro-Deval Testing of Aggregates In The Southeast, National Center for asphalt technology, Auburn University, Alabama, *NCAT Report No. 02-09*, pp32.
- Deal, T.A., 1997. What it costs to recycle concrete: C&D Debris Recycling. September/October, pp. 10-13.
- Diamond, S. 1989. ASR- Another look at mechanisms. Proceedings of the 8<sup>th</sup> International Conference on Alkali-Aggregate Reaction, (Ed. K.Okada, S. Nishibayashi, and M. Kawamura), Kyoto, Japan, pp. 83-94.
- Dilek, U. and Leming, M. L., 2004. Relationship between Particle Shape and Void Content of Fine Aggregate. *Cement, Concrete and Aggregates*, Vol. 26, No. 1, American Society of Testing and Materials, West Conshohocken, PA. pp 14-20.
- Douglas, E., Bilodeau, A., Malhotra, V. M., 1992. Properties and Durability of Alkali Activated Slag Concrete, *ACI Materials Journal*, V. 89, No 5. September-October 1992. pp 509-516
- Farny, A. J. and Kosmatka, H.S. 1997. Diagnosis and Control of Alkali-Aggregate Reactions in Concrete. Concrete Information Series No. IS413.01T. Portland Cement Association. Skokie, IL. ISBN 0 89312 146 0. 24 pp.
- Farny, James A., and Steven H. Kosmatka (1997). Diagnosis and Control of Alkali Aggregate Reactions in Concrete. Concrete Information Series No. IS413.01T. Portland Cement Association. Skokie, IL. ISBN 0 89312 146 0. 24 pp.
- Fletcher, T., Chandan, C., Masad, E., Sivakumar, K., 2002. Measurement of Aggregate Texture and its Influence on HMA Permanent Deformation. *In Proceedings of the 81<sup>st</sup> Annual Meeting of the Transportation Research Board*, Washington, DC.
- Fookes, P.G. and Revie, W.A. 1982. Mica in Concrete --- in a case history from Eastern Nepal; *Concrete*, 16, No.3, pp. 12-16.
- Fookes, P.G. and Coolis, L. 1975. Aggregate and the Middle East, *Concrete*, 9, No.11, pp. 14-19.
- Fookes, P.G., Gourley, C.S., and Ohkere, C., 1988. Rock Weathering in Engineering Time," *The Quarterly Journal of Engineering Geology* (British), Vol. 21.
- Gajda, John, Development of a Cement to Inhibit Alkali-Silica Reactivity, Research and Development Bulletin RD115, Portland Cement Association, Skokie, Illinois, 1996.
- Ghazanfar, M. 1993. Petrotectonic Elements and Tectonic Framework of Northwest Himalaya. Ph.D thesis, University of the Punjab, Vol.1 & 2, pp. 1-380.
- Gondal, M.M.I., Javaid, A.Z., Ahsan, N. and Chaudhry, M.N. 2006b. Engineering Evaluation of Gravel Deposits from Mauza Kalary District Dera Ghazi Khan. Geological Material & Aggregates of Pakistan. Publ: National Geological Society of Pakistan.
- Gondal, M.M.I., Javaid, A.Z., Chaudhry, M.N. and Ahsan, N. 2006a. Geotechnical Investigation of Nullah Sanghar Gravel Deposits, District Dera Ghazi Khan, Punjab, Pakistan. Geological Material & Aggregates of Pakistan. Publ: National Geological Society of Pakistan.



- Gress, D. 1997. Early Distress in Concrete Pavements. FHWA-SA-97-045, Federal Highway Administration, Washington, DC. January. 53 pp.
- Hobbs, D.W. 1988. Alkali-silica reaction in concrete. Thomas Telford Ltd., London, UK.
- Hobbs, D.W. 1978. Expansion of concrete due to the alkali-silica reaction: an explanation. *Mag. Concr. Res.*, **30**, pp. 215-220.
- Hu, J. and Stroeve, P., 2006. Shape Characterization of Concrete Aggregate. *Image Analysis and Stereology*, **25**, pp. 43-53.
- Hussain, A. Yeats R. S. and MonaLisa, 2008. Geological setting of the 8 October 2005 Kashmir earthquake, *Jour. Seismol.* DOI 10.1007/s10950-008-9101-7
- Ilangoval, R., Mahendran, N. and Nagamanib, K., 2008. Strength and durability properties of concrete containing quarry rock dust as fine aggregate. *ARPJ Journal of Engineering and Applied Sciences*, Vol. **3**, No. **5**, pp. 20-26.
- Jamkar, S.S., Rao, C.B.K. 2004. Index of Aggregate Particle Shape and Texture of coarse aggregate as a parameter for concrete mix proportioning. *Cement and Concrete Research* Vol. **34** Num. **11** 2021-2027.
- Kelly, T.D., 1998. The substitution of crushed cement concrete for construction aggregates: U.S. *Geological Survey Circular* **1177**, 15 p.
- Kondolf, G. M., 1997. Hungry Water: Effects of Dams and Gravel Mining on River Channels. *Environmental Management*. Vol. **21**, No. **4**, pp. 533-551
- Lafrenz, J.L., 1997. "Aggregate Grading Control for PCC Pavements: Improving Constructability of Concrete Pavements by Assuring Consistency of Mixes," *Proceedings, Fifth Annual International Center for Aggregates Research Symposium*, Austin, Texas.
- Lenke, L. R., and Malvar, L. J., 2005, "Fly Ash Efficiency For Alkali- Silica Reactivity (ASR) Mitigation," *Proceedings, Texas Section ASCE, Fall Meeting*, El Paso, Tex.
- Malvar, L. J. Cline, G. D.; Burke, D. F.; Rollings, R.; Sherman, T. W.; and Greene, J., 2002, "Alkali Silica Reaction Mitigation: State-of-the-Art and Recommendations," *ACI Materials Journal*, V. **99**, No. **5**, Sept.-Oct., pp. 480-489.
- Malvar, L. J., and Lenke, L. R., 2005, "Minimum Fly Ash Cement Replacement to Mitigate Alkali Silica Reaction," *Proceedings, World of Coal Ash (WOCA 2005)*, Lexington, Ky., <http://www.flyash.info/2005/170mal.pdf>.
- Malvar, L. J., and Lenke, L. R., 2006. Efficiency of Fly Ash in Mitigating Alkali-Silica Reaction Based on Chemical Composition, *ACI Materials Journal*, Title no. **103-M35**, pp. 319-326
- Malvar, L. J.; Cline, G. D.; Burke, D. F.; Rollings, R.; Sherman, T. W.; and Greene, J., 2003, Closure to discussion of "Alkali Silica Reaction Mitigation: State-of-the-Art and Recommendations," *ACI Materials Journal*, V. **100**, No. **4**, July-Aug., pp. 346-350.
- Maupin, G., Jr. 1987. Final report: The use of hydrated lime as an antistripping additive. VTRC Report No. 87-R16. Charlottesville, Va.: Virginia Transportation Research Council.
- McKeen, R. G., Lenke, L. R. and Pallachulla, K.K., 1998. Mitigation of Alkali-Silica Reactivity in New Mexico. Research Bureau New Mexico State Highway and Transportation Department and U.S. Department of Transportation Federal Highway Administration
- Mehta, P. K. and Monteiro, P. J. M., 1993. Concrete Structure, Properties, and Materials, Prentice-Hall, Inc., Englewood Cliffs, NJ.
- Mindess, S., and Young, J. F. 1981. Concrete. Prentice-Hall, Inc., Englewood Cliffs, NJ. 671 pp.
- Mindess, S., and Young, J.F., 1981. Concrete, Prentice Hall, Inc., New Jersey.
- Mona Lisa, Khwaja, A.A. and Jan, M. Q. 2008. The 8 October 2005 Muzaffarabad earthquake: Preliminary seismological investigations and probabilistic estimation of peak ground accelerations. *Current Science*, **94**, NO. **9**, pp. 1158-1166.
- Neville A. M., and Chatterton M., 1979. New Concrete Technologies and Building Design, Longman Inc.,
- Neville A. M., 1981. Properties of Aggregates, Pitman Books Limited.



- Neville, A. M. 1996. *Properties of Concrete*. John Wiley and Sons, Inc., New York, New York.
- Neville, A.M. 2000 *Properties of Concrete* 4<sup>th</sup> ed. Pearson Education Asia Pte. Ltd. Edinburgh, U.K. 844p.
- Neville, A.M., and Brooks, J.J. 1999. *Concrete Technology* Longman Group U.K. First ISE reprint 1999 Edinburgh, U.K. 438p.
- Nixon, P.J., and Sims, I., 2006. Alkali-reactivity and Prevention – Assessment, Specification, and Diagnosis of Alkali-reactivity, International Union of Laboratories and Experts in Construction Materials, Systems and Structures (RILEM), International Specification to Minimise Damage from Alkali Reactions in Concrete: Part 1 Alkali-Silica Reaction, *RILEM TC 191-ARP AAR-7.1*.
- Nixon, P.J., Sims, I., 1992. RILEM TC106 Alkali Aggregate Reaction – Accelerated Tests Interim Report and Summary of Survey of National Specifications,” *Proceedings of the Ninth International Conference on Alkali-Aggregate Reaction in Concrete, Concrete Society, Slough, Vol. 2*, pp. 731–738.
- Ober, J.A., 2002. United States Geological Survey (USGS) Mineral Commodity Summaries. Oberholster, R.E., Davies, G., “An Accelerated Method for Testing the Potential Reactivity of Siliceous Aggregates,” *Cement and Concrete Research*, Vol. 16, 1986, pp. 181–189.
- Pedneault, A., 1996. Development of Testing and Analytical Procedures for the Evaluation of the Residual Potential of Reaction, Expansion, and Deterioration of Concrete Affected by ASR,” M.Sc. *Memoir, Laval University*, Québec City, Canada, 133 pp.
- Pettijohn, F.J., Potter, P.E., Siever, R., 1987. *Sand and sandstone*. 2<sup>nd</sup> edition, Berlin (Springer), pp. 1- 553.
- Pigeon, M., and Plateau, R. 1995. *Durability of Concrete in Cold Climates*. E and FN Spon. ISBN: 0-419-19260-3. 244 pp.
- Quiroga, P.N., and Fowler, D.W., 2003. The Effects of Aggregates Characteristics on the Performance of Portland Cement Concrete. Report ICAR 104-1F, The University of Texas, Austin, pp. 382.
- Ritter, D.F., Kochel, R.C., and Miller, J.R., 2000. *Process Geomorphology*, 3rd edition: Dubuque, Iowa, Wm.C. Brown Publishers, 546 p.
- Roberts, F. L., Kandhal, P. S., Brown, E. R., Lee, D., and Kennedy, T. W., 1996. *Hot Mix Asphalt Materials, Mixture Design, and Construction*, 2nd Edition, Napa Education Foundation, Lanham, MD.
- Rogers, C., Grattan-Bellew, P.E., Hooton, R. D., Ryell, J. and Thomas M.D.A., 2000. Alkali-aggregate reactions in Ontario. *Can. Jour. Civ. Eng.* 27(2): 246-260.
- Rogers, C.A., and Hooton, R.D. 1992. Comparison between laboratory and field expansion of alkali-carbonate reactive concrete. *Proceedings of the 9th International Conference on Alkali- Aggregate Reaction in Concrete*, London, U.K., July 1992, pp. 877–884.
- Sarkar, S. L. and Aitcin, P-C. 1990. Importance of Petrological, Petrographical and Mineralogical Characteristics of Aggregates in Very High Strength Concrete. *ASTM Special Technical Publication*, No. 1061, pp. 129-144.
- Shrimer, F.H., 2003, Investigation for alkali-aggregate reaction in a dam in southern British Columbia: Western Conference of American State Dam Safety Officials, Oklahoma City, Okla., 2003, *Proceedings*, p. 83–95.
- Smith, M. R. and Collis, L. 2001. *Aggregates – Sand, Gravel and Crushed Rock Aggregates for Construction Purposes* (3rd edition). The Geological Society London, pp.199-224.
- Stanton, T. E. 1940. Expansion of concrete through reaction between cement and aggregate.” *Proceedings, ASCE*, vol. 66, pp. 1781-1811.
- Stark, D. (1991). *Handbook for the Identification of Alkali-Silica Reactivity in Highway Structures*. SHRP-C/FR-91-101. Strategic Highway Research Program, Washington, DC.
- Stark, D., 1993. Eliminating or Minimizing Alkali-Silica Reactivity, SHRP-C-343, Strategic Highway Research Program, Washington, D. C., 1993. Also PCA Publication LT178.



- Stark, David C., 1992. Lithium Salt Admixture—An Alternative Method to Prevent Expansive Alkali-Silica Reactivity." Proceedings of the 9th International Conference on Alkali Aggregate Reaction in Concrete, The Concrete Society, London, July, 1992. Also PCA Publication RP307.
- Swamy, R.N., 1992. The Alkali-Silica Reaction in Concrete, Blackie, London.
- TAMS Report, 1965, Concrete Studies, Tarbela Dam Project. WAPDA, Pakistan.
- Tepordei, V.V., 1999. Stone (crushed): U.S. Geological Survey Mineral Commodity Summaries 1999, p. 162–163.
- Thomas, M.D.A. 1996. Field studies of fly ash concrete structures containing reactive aggregates. Magazine of Concrete Research, 48 (177): 265–279.
- Thomas, M.D.A., and Innis, F.A. 1998. Effect of slag on expansion due to alkali-aggregate reaction in concrete. American Concrete Institute, ACI Materials Journal, November/December, pp. 1–9.
- Thomas, M.D.A., Hooton, R.D., and Rogers, C.A. 1997. Prevention of damage due to alkali-aggregates reaction in concrete construction - Canadian approach. *Cement, Concrete and Aggregates*, 19(1): 26–30.
- Treloar, P.J., Broughton, R.D., Williams, M.P., Coward, M.P., Coward, M.P. and Windley, B.F., 1989. Deformation, metamorphism and imbrication of the Indian Plate, south of the Main Mantle Thrust, north Pakistan. *Jour. Met. Geol.*, 7, pp. 111-125.
- Tremblay, C., Berube, M., A., Fournier, B., Thomas, M.D.A. and Folliard, K.J., 2008. Use of the Accelerated Mortar Test to Evaluate the Effectiveness of LiNO<sub>3</sub> Against Alkali silica Reaction Part 2: Comparison With Results from the Concrete Prism Test, Accepted for publication, *Cement and Concrete Research*, March 2008.
- Tucker, M.E., 2001. Sedimentary Petrology. 3<sup>rd</sup> Edition. Blackwell Science, Oxford, pp. 1 - 262p
- Watters, W.A., 1969. Petrological examination of concrete aggregates. Proceedings of the National Conference on Concrete Aggregates, Hamilton, June 1969. N.Z. Portland Cement Association, Wellington, pp 49-54.
- Wenk, H.R. 1998. Deformation of Mylonites in Palm Canyon, California, Based on Xenolith Geometry. *Journal of Structural Geology*, Vol. 20, No. 5, pp. 559-571.
- Wenk, H.R., Pannetier, J. 1990. Texture Development in Deformed Granodiorites from the Santa Rosa Mylonite Zone, Southern California." *Journal of Structural Geology*, Vol. 12, No. 2, pp. 177-184.
- West, G., 1996. Alkali-Aggregate Reaction in Concrete Roads and Bridges, Thomas Telford, London.
- Wilburn, D.R., and Goonan, T.G., 1998. Aggregates from natural and recycled sources: U.S. Geological Survey Circular 1176, 36 p.
- Williams, M.P., 1989. The geology of Besham area, Northern Pakistan: Deformation and imbrication in the footwall of Main Mantle Thrust. *Geol. Bull. Univ. Peshwar*, 22, pp. 65-52.
- Winslow, D. N. 1994. The Pore System of Coarse Aggregates." Significance of Tests and Properties of Concrete and Concrete-Making Materials. STP 169C. Publication Code No. 04-169030-07. American Society for Testing and Materials. Philadelphia, PA. pp. 429-437.
- Wu, T., F. Parker, and P.S. Kandhal. 1998, Aggregate Toughness/Abrasion Resistance and Durability/Soundness Tests Related to Asphalt Concrete Performance in Pavements. Transportation Research Board, Transportation Research Record 1638.



## PETROGRAPHY AND MINERALOGY OF DOLERITES OF HACHI VOLCANICS, KIRANA HILLS AREA, PAKISTAN

BY

**ZAHID KARIM KHAN, NAVEED AHSAN**

Institute of Geology, University of the Punjab, Quaid-i-Azam Campus,  
Lahore-54590 Pakistan

**ABDUL MATEEN**

Department of Environmental Sciences, COMSATS Institute of Information Technology, Abbottabad, Pakistan

AND

**MUHAMMAD NAWAZ CHAUDHRY**

College of Earth and Environmental Sciences, University of the Punjab, Lahore, Pakistan

**Abstract:** *The Kirana Hills outcrop in the Punjab plains and represent remnants of the widespread Precambrian igneous activity within the Kirana-Malani basin of NE Gondwana. These volcanics comprise mainly of mafic and felsic rocks belonging to the tholeiitic basalt-rhyolite magma association with intercalated meta-sediments. Present study deals with petrography and mineralogy of the dolerites from the Hachi volcanics representing Precambrian bimodal volcanism. The dolerites suffered hydrothermal alteration and low-grade metamorphism. Electron-microprobe analyses were carried out of plagioclase, pyroxene, amphibole, chlorite, epidote, opaque oxides and calcite. Petrography and compositional variations of mineral phases are discussed in terms of metamorphic and hydrothermal alteration, igneous differentiation and temperature - pressure estimations.*

### INTRODUCTION

The Kirana Hills volcanics, Neoproterozoic in age, represent isolated outcrops of volcanic and sedimentary rocks scattered in the Punjab plain areas from Chiniot to Sargodha (Shah, 1977). The volcanics are the remnants of the widespread Precambrian igneous activity within the Kirana-Malani basin of NE Gondwana (Chaudhry et al., 1991). The Kirana Hills are very important economic sources of aggregates in the Punjab province (Khan and Chaudhry, 1991; Khan, 2004).

Published literature (e.g. Heron, 1913; Shah, 1977; Alam, 1987; Khan and Chaudhry, 1991; Alam et al., 1992; Chaudhry et al., 1999; Ahmad et al., 2000) indicates that a variety of rocks are exposed in the area that includes volcanics and meta-sedimentary rock groups. They, according to stratigraphic classification of Chuhadry et al., (1999), are Hachi Volcanics and Machh Super Group. (Table 1). These two packages i.e. the lower predominantly volcanic package (Hachi Volcanics) and the upper sedimentary sequence (Machh Super Group) were formed

in two distinct petrotectonic environments and represent two distinct petrotectonic assemblages (Ahmad et al., 2000).

The Hachi Group is comprised of volcanics that contain felsic and mafic volcanics. Felsic volcanics are composed of andesites, dacites, dacitic tuff, rhyolites and rhyolitic tuff and mafic volcanics are comprised of dolerites belonging to tholeiitic basalts and basaltic andesites (Chuhadry et al., 1999; Khan, 2000). These are sub volcanic and intrusive sheet like bodies that are generally concordant to semi concordant. Whereas, Machh sedimentary group is composed of Chak 112 Conglomerate, Tuguwali, Asianwali, Hadda and Sharaban formations that mainly consist of phyllites and quartzites with subordinate quartz wackes/arenaceous slates, lithic greywackes and conglomerates (Chuhadry et al., 1999; Khan, 2000).

The main purposes of this study are: to provide detailed study of petrography and mineralogy of dolerites, belonging to Hachi Group, and to understand the compositional variations within the dolerites related to



**Table 1**  
Stratigraphic Classification of Kirana area (Chaudhry et al., 1999)  
Top not preserved

| Group             | Formation              | Description  |
|-------------------|------------------------|--|
| Machh Super Group | Sharaban Formation     | Conglomerates with slate intercalations.   |
|                   | Hadda Formation        | Calcareous quartzites  |
|                   | Asianwala Formation    | Mainly quartzites with sub ordinate quartz wackes / arenaceous slates, gritty quartzites and slates, often showing cross bedding and ripple marks. |
|                   | Tuguwali Formation     | Slates, fine grained quartz wackes / arenaceous slates   |
|                   | Chak 112 Conglomerates | Polymict conglomerate with clasts of dolerite and acid volcanics.  |
| Hachi Volcanics   | Volcanogenic slates    | Often interbedded with rhyolite / rhyolitic tuff and dolerite  |
|                   | Volcanics              | Dolerites, andesites, dacites, dacitic tuff, rhyolites and rhyolitic tuff.   |

Base not exposed

**Table 2**  
Modal mineralogy of dolerites from Bulland Hill and Sheikh Hill quarries of Kirana

| Mineralogy (%age)   | Bulland Hill |      |      |      |      | Sheikh Hill |      |      |        |      |
|---------------------|--------------|------|------|------|------|-------------|------|------|--------|------|
|                     | C-2          | C-9  | C-12 | C-13 | C-15 | C-36        | C-52 | C-72 | BIH101 | C-69 |
| Quartz              | 8.0          | 9.0  | 8.0  | 5.0  | 3.0  | 3.0         | 0.0  | 2.0  | 1.0    | 7.3  |
| Plagioclase         | 25.0         | 27.0 | 25.0 | 26.0 | 23.0 | 26.5        | 37.0 | 21.5 | 31.5   | 32.7 |
| Pyroxene            | 3.0          | 0.0  | 3.0  | 8.5  | 10.0 | 0.0         | 0.0  | 5.0  | 1.5    | 3.5  |
| Amphibole           | 25.5         | 17.0 | 25.5 | 19.5 | 13.0 | 8.3         | 16.0 | 29.5 | 15.0   | 18.0 |
| Sphene              | 4.5          | 3.0  | 4.5  | 2.0  | 2.5  | 1.0         | 0.0  | 3.0  | 3.0    | 5.0  |
| Epidote             | 0.0          | 2.0  | 0.0  | 2.5  | 1.5  | 2.5         | 1.0  | 4.0  | 3.0    | 2.0  |
| Chlorite            | 23.5         | 22.0 | 23.5 | 17.0 | 12.0 | 23.2        | 23.0 | 26.0 | 23.5   | 5.0  |
| Calcite             | 6.5          | 13.0 | 6.5  | 12.0 | 28.0 | 29.0        | 17.0 | 3.5  | 13.8   | 19.4 |
| Ilmenite/ leucoxene | 1.0          | 3.0  | 1.0  | 3.5  | 3.0  | 5.0         | 4.0  | 3.0  | 5.0    | 3.1  |
| Hydromica           | 3.0          | 4.0  | 3.0  | 4.0  | 4.0  | 1.5         | 2.0  | 2.5  | 2.7    | 4.0  |



magmatic differentiation and subsequent metamorphic and hydrothermal alterations.

### Sampling of dolerites

The dolerites of the Kirana volcanics investigated in this study include all the mafic rock suites in the compositional range of  $\text{SiO}_2$  upto 55 wt%. The rock suites categorized as dolerites consist of tholeiitic basalts, basaltic andesites and microgabbros. The dolerites are present in quarries situated around the Bulland Hill, 126, Sheikh Hill, 116, Chak 123 and Kila Minor, 128. In all, 10 samples were collected from Bulland Hill and Sheikh Hill (Table 2) to determine modal mineralogy and carry out microprobe analyses. In addition to this, mineralogy of two samples (C-12 and C-36) was checked and analyzed by X-ray diffraction.

### X-RAY DIFFRACTION IDENTIFICATION

Whole rock representative samples of dolerites were crushed to a  $< 10\mu\text{m}$  powder to obtain x-ray diffraction patterns for the identification of primary igneous minerals and their alteration products. Composition of the mineral grains was subsequently determined by microprobe analysis.

Petrographic observations have clearly indicated variable alteration of dolerites. X-ray diffraction patterns of typical representative dolerite samples C-12 and C-36 are displayed in Fig. 1. The secondary alteration assemblage in dolerites is identified as chlorite, epidote, feldspar (albite) and possible clay minerals. The altered dolerites lack olivine and pyroxene. The mafic rock suites have suffered alteration to considerable degree due to chloritization, epidotization, calcitization and sericitization.

### PETROGRAPHY

Modal mineralogy data for dolerite samples studied are given in Table 2. The dolerites of the Kirana volcanics investigated include all mafic rock suites, consisting of tholeiitic basalts, basaltic andesites and microgabbros.

The dolerites invariably show alteration, though unaltered dolerites are recognized at places. The dolerites can be grouped into two varieties. Unaltered dolerites are generally holocrystalline, rarely porphyritic and lack directional texture. The altered dolerites are fine to medium grained and lack olivine and pyroxene. The rock suites have suffered alteration due to extensive chloritization, calcitization, sericitization and epidotization. The altered dolerites are comprised of chlorite, amphibole, plagioclase, quartz, sericite, calcite, epidote, ilmenite/leucosene, sphene and hematite (Fig. 2).

The dolerites are generally fine to medium grained and dark green to light green in color. They have been extensively altered due to hydrothermal activity. The volcanic rocks of the Kirana hills have been

metamorphosed to low-temperature mineral assemblage that includes chlorite, epidote, albite, sericite and carbonates. However, clinopyroxene, amphibole and opaque (ilmenite) grains are the primary magmatic phases. Plagioclase is replaced by epidotes, carbonate and sericite, while pyroxene and olivine are replaced by chlorite and actinolitic hornblende. The dolerites have suffered low grade metamorphism and autometasomatism. Some dolerites contain relics of clinopyroxene and calcic plagioclase phenocrysts (Alim et al., 2000). The altered dolerites are holocrystalline and composed of chlorite  $\pm$  epidote  $\pm$  amphibole + albite + quartz + calcite  $\pm$  ilmenite/leucosene.

The dolerite bodies are, at places, cut by quartz (Fig. 3) and carbonate veins. They may exhibit flow structures with parallel to sub-parallel orientation of feldspar laths and microphenocrysts. Texture ranges from intersertal, intergranular, subophitic to ophitic in dolerites. Plagioclase is variably saussuritized. Plagioclase twinning and grain-boundaries have been obliterated. Interstitial material, consisting mainly of chlorite is common within the dolerites and was probably derived from the pyroxene and amphibole. Primary oxide grains occupy the interstices between feldspar laths. Interstitial chlorite is widespread and appears to have replaced primary ferromagnesian material.

According to Davies and Crawford (1971), the dolerites of the Kirana Hills are autometasomatic types that have produced late stage concentrations of hydrothermal carbonate-rich fluids. The late hydrothermal activity caused breakdown and albitization of plagioclase feldspar and breakdown of ferromagnesian minerals. The migration of hydrothermal fluids into the neighbouring pre-existing rhyolites was responsible for alteration and accompanied by deposition of quartz, ankeritic carbonates, calcite and hematite in the available fractures, cavities and pore-spaces. A few thin doleritic intrusions contain plagioclase with rather altered pyroxene and brown olivine relicts.

Pyroxenes in less altered dolerites are generally subhedral to eumorphic and may occur as discrete crystals as well as aggregates. The phenocrysts often enclose subophitically, laths of calcic-plagioclase of andesine composition. Cracks and fractures of pyroxene may be filled by secondary calcite. Pyroxene is generally augite and may marginally alter to hornblende. However, pyroxene and olivine are rare minerals and may occur only as relics in dolerites.

Hornblende occurs as euhedral to subhedral phenocrysts as well as smaller crystals in the groundmass. Hornblende may also ophitically enclose laths of calcic-plagioclase. Rarely acicular to columnar aggregates of actinolite may also occur. Hornblende may show marginal alteration to chlorite.



Plagioclase is subhedral to eumorphic and occurs as well formed prismatic crystals. Plagioclase occurs both as phenocrysts as well as smaller crystals in the groundmass. The crystals of plagioclase are well twinned on albite law. Combined carlsbad-albite twins are rare. The plagioclase is variably and erratically saussuritized/calcsitised. The products of this alteration are epidote, sericite and calcite. Sericite, epidote and calcite are the major components of this alteration. Plagioclase crystals and laths are sometimes traversed by epidote, calcite and chlorite veinlets. These veinlets are in fact late stage and post consolidation fracture fillings.

Chlorite varies widely in this unit. It may occur as pseudomorphs after amphibole or may develop as aggregates of small flaky crystals. It is strongly pleochroic from neutral green to bright green and shows a variety of interference colours, most common being tobacco green and bluish green. It appears to be Fe-Mg-rich chlorite. It is generally very fine to fine grained and occurs as flake and fibre like aggregate.

Epidote is usually anhedral and occurs as an alteration product of plagioclase and amphibole. It may occur as smaller grains, or granular masses. It varies from colourless to pale. The interference colours show that both zoisite and clinozoisite are present, since both normal and anomalous interference colors are observed. Size of epidote grains ranges from 0.01 mm to 0.52 mm in general.

Calcite is a secondary mineral and occurs as anhedral to subhedral crystals of widely variable size. Its amount varies widely and it may, therefore, occur as an accessory to essential mineral. It either forms extremely fine-grained microcrystalline aggregates or occurs as clear and well-formed discrete crystals and their aggregates. It may also occur as fracture filling mineral within plagioclase.

Ilmenite and leucoxene are anhedral occurring as aggregates as well as discrete crystals. Alteration of ilmenite to leucoxene is very prominent.

## MINERALOGY OF DOLERITES

The mineralogy of dolerites of the Kirana Hills has been investigated for seeking information on the nature of mineral phases of primary igneous crystallization and subsequent alteration products developed by hydrothermal activity. The mineral compositions were determined on two dolerite samples, relatively unaltered dolerite (Sample No. 12) and altered dolerite (Sample No. 36). Microprobe analyses of minerals were carried out on electron microprobe (Jeol Super probe JXA-8600, Leicester University, UK). The mineral phases have been recalculated on a stoichiometric basis of oxygen and cations following the recommendations of the International

Association Subcommittee on the nomenclature of minerals.

The purpose of microprobe analysis has been to understand the nature of primary magmatic mineral and to identify the alteration products. The compositional variations in the mineral phases are interpreted in terms of magmatic differentiation and extent of alteration of dolerites.

## Plagioclase

Mineralogical data of plagioclase in the dolerite is quite unusual and fall in the field of sodium-rich phases Albite-oligoclase rather than Ca-rich member of plagioclase generally expected in the igneous mafic suites. The dolerite samples analyzed (Sample No. 36) from the quarries are altered dolerites. Compositional variations in terms of An-Ab-Or components of the plagioclase analysed are shown in Figure 4 a. Plagioclase ranges in composition from  $An_{24}$  to  $An_{15}$  in sample 12, while plagioclase in the highly altered dolerite sample 83 is almost albitic ( $An_{0.9}$   $Ab_{98.7}$   $Or_{0.4}$   $Ab_{96.6}$   $Or_{0.9}$ , Figure. 4a). The observed plagioclase compositions in the altered dolerites may be interpreted in terms of complete alteration of primary dolerites (basalts and basaltic andesites). Plagioclase exhibits fine laminar intergrowth of two phases of Ca-rich and Na-rich composition. The Ca-rich plagioclase is most susceptible to hydrothermal alteration to more sodic varieties due to late stage action of hydrothermal solutions (Deer et. al., 1992). Late stage magmatic and metasomatic process may also shift the composition of Ca-rich plagioclase towards Na-rich albite phase. Accordingly dolerites (normal basalts and basaltic andesites) must have suffered alteration and albitized to spilitic mineralogy. Thus albite is the stable phase in the altered dolerites.

Plagioclase in bleached zone differs markedly by having a composition close to pure albite. Figure 4 b displays a plot of mole % An versus mole % albite which clearly shows that the bleached plagioclase tends to be albitic. Evidently the alteration causing bleaching is associated with the removal of Ca, which must have crystallized as carbonate, as indicated by the frequent occurrence of carbonate-filled microfractures in these zones.

## Pyroxene

The pyroxene grains from dolerite samples 12 and 36 were analyzed. The compositions have been recalculated on the basis of 4 cations and 6 oxygen atoms.  $Fe^{3+}$  is estimated using stoichiometric criteria according to the method of Droop (1987). Pyroxene compositions are plotted in terms of Q-J diagram for preliminary fall in the domain of Quad (Fig. 5 a.) The pyroxene compositions are also plotted on the recommended amplified Quad



classification diagram (Figure 5 b) after Rock (1990) in terms of Ca-Fe-Mg. The pyroxene compositions fall within the Fe-rich augite to subcalcic augite fields. Pigeonitic pyroxene is absent.

Pyroxenes display narrow compositional variation as shown in Q-J and quadrilateral diagrams which summarize the compositional ranges of pyroxenes for the dolerites (Figure 5 a, b). The composition falls in the range of Fe-rich augite ( $Wo_{25.8} En_{26.2} Fs_{48.0}$ ). Their Fe/(Fe+Mg) ratios lie between 0.17 to 0.5. The alumina varies from 1.1 wt.% to 5.4 wt.%.  $TiO_2$  contents are variably low in the range from 0.03 to 0.9 wt.% in sample 12, while the sample 83 has extremely low  $TiO_2$  content falling in 0.0 to 0.23 wt.%.

Kushiro (1960) proposed that during magmatic crystallization, the proportion of Si increases in the pyroxene structure whereas that of Al in tetrahedral site decreases.  $^{IV}Al > ^{VI}Al$  is somewhat typical for pyroxene formed at high temperature. These two characteristics combined suggest that the pyroxene in the Kirana dolerites probably crystallized at relatively moderate temperature (Figure 5 c). Pyroxene appears crystallizing after olivine and plagioclase in dolerites (basalts and basaltic andesites), after or simultaneously with plagioclase in more evolved rocks, but always before opaque Fe-Ti oxide minerals.

### Amphibole

Amphibole compositions have Si atoms per formula unit (apfu) ranging from 7.25 to 7.58 apfu and can be classified in the IMA nomenclature (Leake et al., 1997) as actinolite to magnesio-hornblende (calcic amphibole). Optical mineralogy also confirms the presence of actinolite patches. In the cationic  $Mg/(Mg + Fe^{2+})$  versus (Si) and  $Ca_{II}$  versus  $(Na+K)_A$  diagrams (Figure 6 a, b), the amphiboles from dolerite samples show a trend from actinolite to edenite.

Two distinct variations in chemical compositions of amphibole phases in dolerite may be related to magnesio-hornblende (Sample No. 12) and ferro-actinolite (sample 36) representing basalt and basaltic andesite suites respectively. Hornblende is characteristic mineral of intermediate igneous rocks and may also occur as primary crystallization of basic rocks such as basaltic andesites (Deer et al. 1992). Nevertheless, actinolitic hornblende association is generally developed in low-grade greenschist facies metamorphism of mafic rocks. The occurrence of magnesio-hornblende and ferro-actinolite in the Kirana mafic suite supports their secondary origin. The amphiboles may have been derived from primary pyroxene through magmatic-hydrothermal activity. Also hornblende and some Fe-Ti oxides may be subsolidus products from breakdown of pyroxene in dolerites.

Compositional limit for igneous amphiboles is shown in Figure 7 with respect to (Ca+Na+K) and Si formula unit (Leake, 1971; Wones and Gilbert, 1982). The (Ca+Na+K) versus Si plot allows chemical discrimination between igneous and metamorphic amphiboles (Leake, 1971). The amphiboles from dolerites plot in the igneous as well as metamorphic field of the diagram. This behaviour is interpreted as an indication that amphiboles are igneous actinolite to magnesio-hornblende however their chemistry has been partially affected by reaction with the hydrothermal fluids causing compositional modification.

### Chlorite

Incipient alteration of igneous mica and amphibole to chlorite is widespread, thus making chlorite minerals among the most dominant product of alteration in dolerites. The number of cations in the unit cell were calculated on the basis of 28 oxygens [based on chlorite formula  $Y_1Z_4O_{20}(OH,F)_{16}$ : Y and Z represent octahedral and tetrahedral cations respectively]. Compositional variations of chlorite are plotted in terms of binary relationships of Fe/(Fe + Mg) ratios versus cationic Si and Al in T-site as shown in Figure 8 and 9. Most of the microprobe data points fall within the pycnochlorite field. The analyzed chlorite shows a restricted range of composition from ripidolite-pycnochlorite to diabantic (according to the classification of Foster, 1962).

As shown in Figure 9, chlorite of the Kirana dolerites defines comparable compositional range of Mg-Fe chlorites (Deer et al., 1992) of the stable metamorphic chlorite field (Bailey, 1987). Ca, Na and K contents are negligibly low which are suggested to occur as impurities in chlorite (Albee, 1962). These elements are occasionally absorbed or occur as interlayer cations in the chlorites (Czamanske et al., 1981).

Chlorites have been extensively studied in the igneous environment (Eggletton and Banfield, 1985; Abdel-Fattah and Abdel-Rahman, 1995) in meta volcanics (Al Dahan et al., 1988; Bettison and Schiffman, 1988) and hydrothermal ore deposits (Kranidiotis and Maclean 1987; Shikazono and Kawahata, 1987; Nutt, 1989). The relationship of Mg and Fe contents provides best discriminant between the chlorites phases occurring in igneous suites (Figure 9.) The chlorite from the dolerites of Kirana volcanics exhibit compositional range which is comparable to the chlorites in the calc-alkaline rocks. Fe/(Fe+Mg) ratios vary in the range of 0.398 to 0.501. The pycnochlorites indicate a trend toward increasing Fe that appear to correspond to the degree of alteration. Intense chloritization in felsic igneous rocks represent the first alteration stage after quartz dissolution. The chlorite of this generation consists of pseudomorphs after biotite. The chlorite generations are crystallized at temperatures 300-200°C at a constant pressure of 1 Kbar (Walsche, 1986).



Microprobe data indicate a restricted range of chemical composition falling around Mg-Fe chlorite (comparison with analyses reported by Deer et al., (1992). Chlorite is a widespread secondary phase of dolerites particularly with a composition of altered basalt and basaltic andesites in Kirana. Extensive development of chlorite phase in the mafic suites is due to hydrothermal alteration of primary crystallizing phase of ferromagnesian minerals. Chlorite may be interpreted to have been formed by hydrothermal replacement of pyroxene and amphibole. The compositional range can be related to primary Mg-Fe silicate phases of pyroxene and amphibole crystallizing in the mafic suites of Kirana hills.

### Epidote

Microprobe data indicate that all the epidotes are Fe-rich. The atomic%  $\text{Fe}^{3+}$  ( $\text{Fe}^{3+} + \text{Al}$ ) ratio expressed, as Pistacite contents ( $\text{Ps} = 100 \times \text{Fe}^{3+} / (\text{Fe}^{3+} + \text{Al})$ ) varies in the range of  $\text{Ps}_{16.4}$  to  $\text{Ps}_{31.6}$  for the magmatic epidote in the Kirana dolerites. The Ps values are mostly comparable with a variation equivalent to that of epidote phenocryst in the calc-alkalic dykes of the Front Range of Colorado (Dawes and Evans, 1991) that is one of the strongest example of magmatic epidote. Similar compositional range is found in magmatic epidotes of granodioritic plutons (Rogers, 1988; Owen, 1991; Farrow and Barr, 1992).

MnO contents range from 0.0 to 0.24 wt.% while MgO contents are very low upto 0.21 wt.% while  $\text{TiO}_2$ ,  $\text{Na}_2\text{O}$  and  $\text{K}_2\text{O}$  contents are negligible. Fe-rich epidotes generally indicate low-grade greenschist facies metamorphic conditions (Cooper, 1972).

Microprobe data show that the epidote in dolerite is slightly rich in  $\text{Fe}^{2+}$  and can be distinguished from amphibole by its characteristic pleochroism. Presence of epidote indicates that the dolerites have suffered low-grade metamorphism. The contents of epidote have been derived from the plagioclase. Amphibole + epidote + chlorite + albite mineral assemblage in the dolerite aggregate of Kirana Hills area provides strong evidence of alteration and low-grade green schist facies metamorphism.

### Fe-Ti Oxide

Titano-magnetite and ilmenite are opaque mineral phases ubiquitously present in dolerite samples. The cationic compositions have been calculated on the basis of 3 oxygen and 2 cations for titano-magnetite and ilmenite respectively. A typical feature of the titano-magnetite is that it has very low contents of MnO compared to that of ilmenite. From the inspection of the data, the Fe-Ti oxides in the dolerites appear to have been extensively re-equilibrated. Magnetite and ilmenite pairs in igneous rocks are of particular importance because of their potential to yield information about magmatic temperatures.

Unfortunately the analyzed Fe-Ti oxides are exsolved. The Buddington and Lindsley (1964) magnetite-ilmenite geothermometer/oxygen barometer is of very limited use for the compositions. The compositions merely indicate that the oxides re-equilibrated during the cooling to temperature of 530°C.

The more fractionated dolerites (Sample 36) contain magnetite with high  $\text{TiO}_2$  content in the range from 10 to 18.3 wt.%. As a result these oxides can be called titanomagnetites. The range of  $\text{TiO}_2$  (and equivalent Ulvospinel  $\text{Fe}_2\text{TiO}_4$ ) in magnetite is well within the range of the basaltic volcanic rocks worldwide (Buddington and Lindsley, 1964). The titanomagnetite of volcanic rocks coexists with ilmenites that have substantially higher values of  $\text{Fe}_2\text{O}_3$ . This is due to greater degree of oxidation of the volcanic rocks as a result of subsolidus oxidation by solutions at relatively low temperatures.

The main opaque oxide phase is titanomagnetite. Although there exists a complete solid solution between ilmenite and hematite, the compositions of Ti-Fe oxide phase do not show typical igneous ilmenite-magnetite phase relationship with ulvospinel component. The compositions of Ti-Fe oxides phase indicate that it contains appreciable contents of  $\text{SiO}_2$  and CaO. The alteration of primary igneous Ti-Fe oxide phase may have taken place at various stages of post-magmatic hydrothermal activity in the Kirana volcanics. The alteration products may be mixtures of amorphous Fe-Ti oxides and leucosene (Deer et al. 1992).

### Titanite (Sphene)

The cationic compositions have been calculated on the basis of 3 cations and 5 oxygens. Analysed sphenes are slightly low in titanium and contain appreciable contents of aluminium and iron. The compositions may be compared with gothite variety of sphene (Deer et al., 1992). Sphene is an essential accessory phase in dolerites and exhibits weak pleochroism in yellowish to brown colours.

### Calcite

Calcite is relatively free from Mg and Fe contents (low in MgO = 0.26 wt% and FeO = 0.67 wt%). The composition is fairly close to pure calcite. The presence of calcite phase in dolerite is due to hydrothermal activity in the Kirana volcanics. Crystallization of calcite in dolerites is secondary and represents late stage hydrothermal precipitation.

### TEMPERATURE AND PRESSURE ESTIMATION

The estimates of temperature for Kirana dolerites are made using pyroxene thermometry (Lindsley, 1983) Figure 5 c displays the plot of pyroxene data on graphical thermometer, calibrated for 1 atmosphere pressure. It



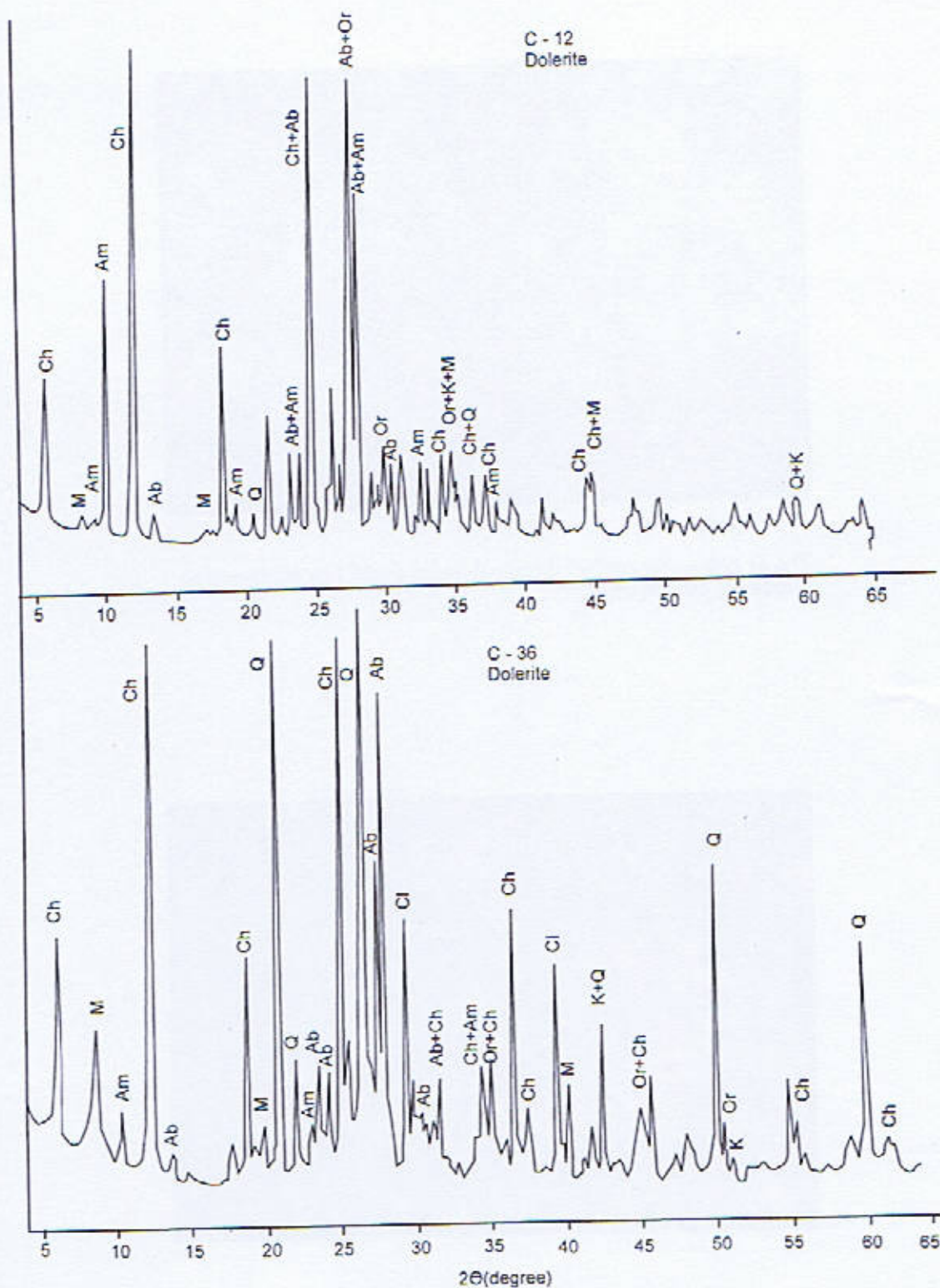


Fig. 1. X-ray diffractogram for the whole-rock dolerite powder samples, Kirana Hills





**Fig. 2.** Autometasomatised dolerite showing assemblage of plagioclase-amphibole-chlorite-quartz.



**Fig. 3.** Quartz veins cutting dolerite sills in Bulland Hill 126 quarry.



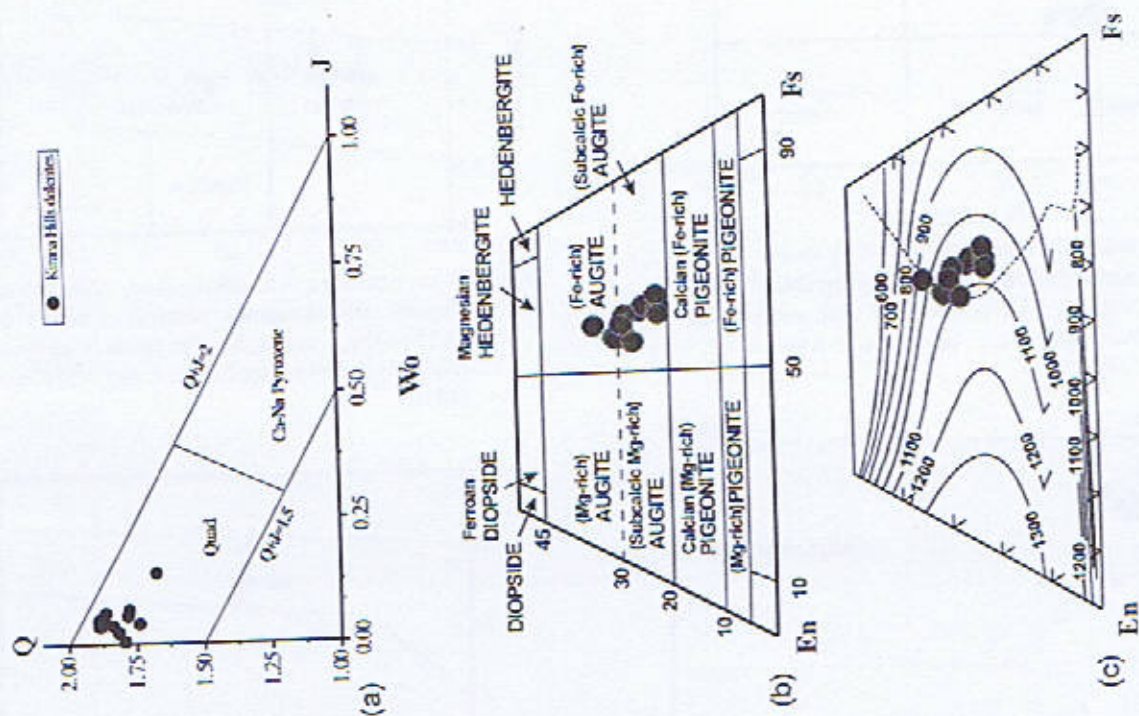
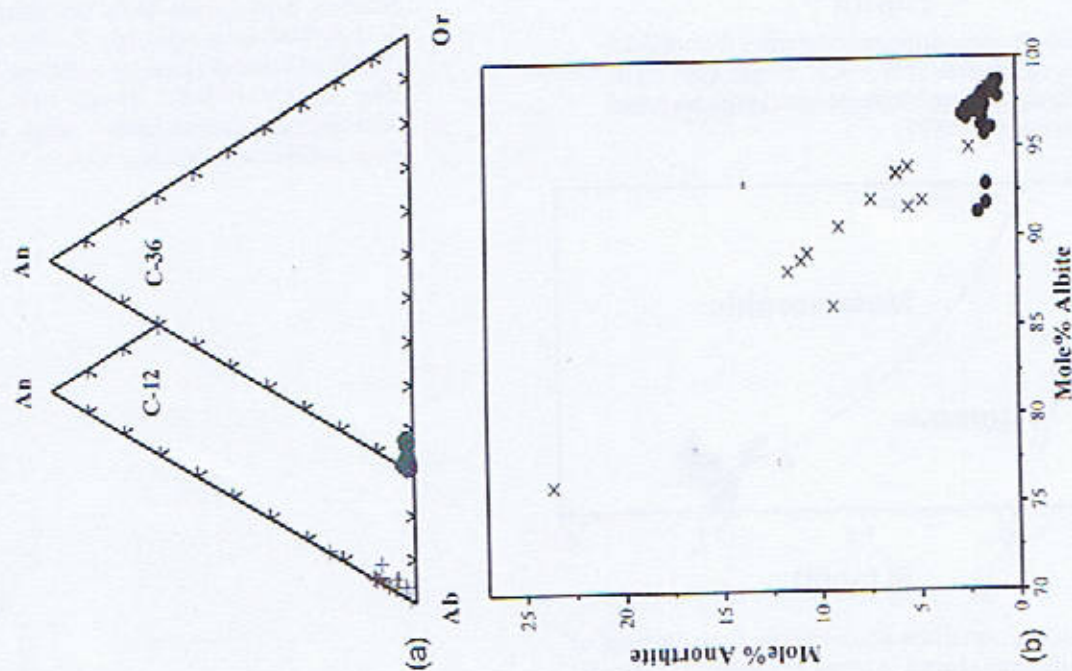


Fig. 5. Pyroxene compositions of dolerites from Kirana Hills area plotted on the classification diagram (a) Q-J diagram, (b) Ca-Mg-Fe (Quad Wo-En-Fs) diagram; after Rock (1990) and (c) Graphic projection of pyroxene thermometry (Lindsley, 1983) for temperature estimation



**Fig. 4.** Compositional variations of plagioclase from dolerite of Kirana Hills (a) plotted in terms of normative Ab-Or-An triangular diagram (b) Mole % Anorthite versus Mole % Albite



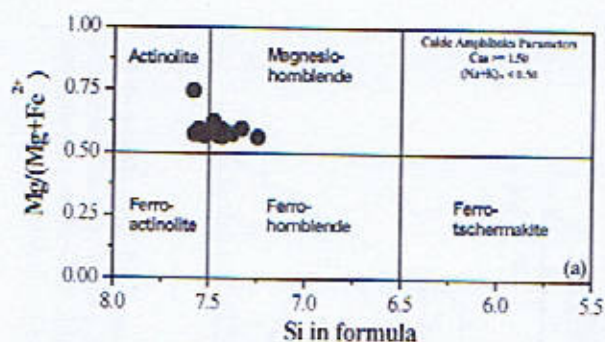


Fig. 6 (a): Amphibole compositions of dolerites from Kirana Hills area plotted as of  $Mg/(Mg+Fe^{2+})$  versus Si. The boundaries and amphibole nomenclature are based on Leake et al., (1997)

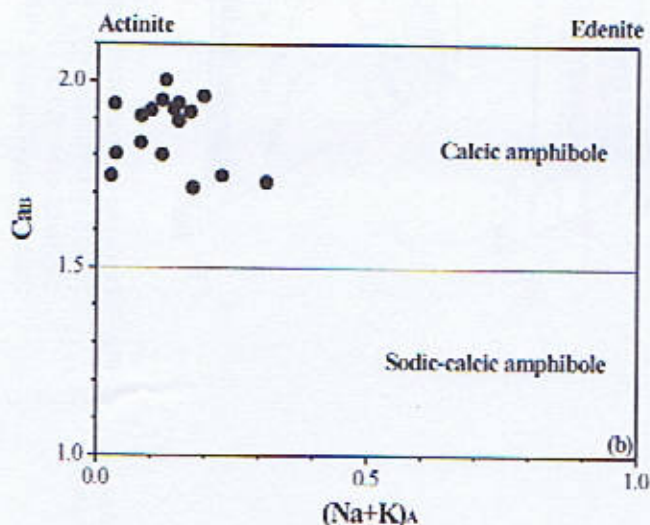


Fig. 6 (b): Amphibole compositions of dolerites from Kirana Hills area plotted,  $(Na + K)^A$  versus  $Ca^B$ . The boundaries and amphibole nomenclature are based on Leake et al., (1997)

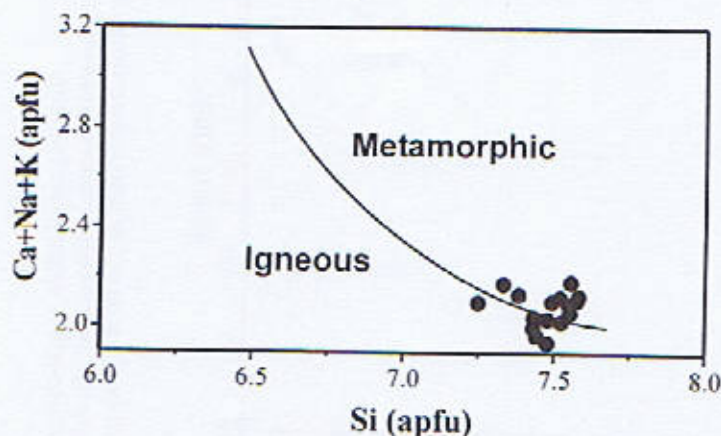


Fig. 7: Compositional variations of amphibole from dolerites of Kirana Hills area plotted in terms of cations  $(Ca+Na+K)$  versus Si (apfu) diagram after Giret et al., (1980)

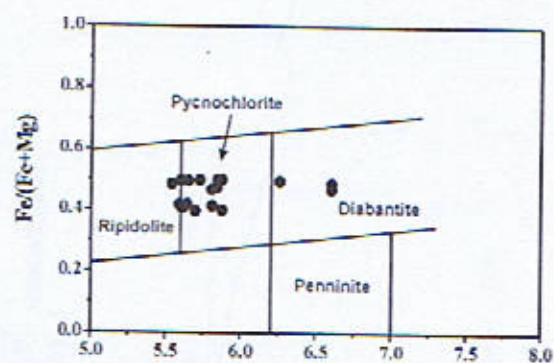


Fig. 8: Compositional variations from dolerites of Kirana Hill Volcanics plotted in terms of  $Fe/(Fe+Mg)$  versus Si. The fields of chlorite minerals defined after Bettison and Schiffman (1988)

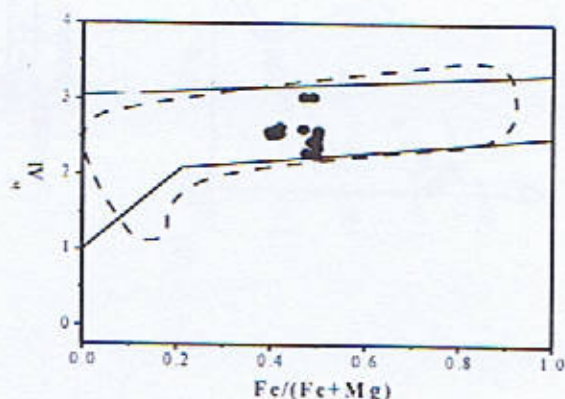


Fig. 9: Plot of ivAl versus  $Fe/(Fe+Mg)$  for the dolerites from Kirana Hills Volcanics. The field defined by a solid line is after Hayes (1970) and that defined by a dashed line is after Bailey (1988). These two fields represent the compositional range of the more stable metamorphic chlorites



indicates a complex cooling history through a wide range of temperatures, for the Kirana dolerites. A temperature range of 1100°C to 800°C is established from the graph of Lindsley (1983). Similarly temperature estimate spectrum have been established for the tholeiitic dolerites in alkaline provinces elsewhere (Hall and Hughes, 1986).

The total Al content of amphibole can be used to estimate the pressure of solidification of this phase in dolerites. Successive empirical and experimental calibrations (Hammarstrom and Zen, 1986; Johnson and Rutherford, 1989; Schmidt, 1992) improved this barometer.

According to Johnson and Rutherford (1989) calibration was obtained by performing experiments on natural samples under  $\text{CO}_2 + \text{H}_2\text{O}$  volatile pressures. Presence of magmatic episode implies a low  $\text{CO}_2$  activity during crystallization of the post magma (Ghent et al., 1991; Helmy, 2004). Therefore, Schmidt (1992) calibration was applied. The dolerite samples studied vary in Al from 0.494 to 1.006 apfu. If the entire Al in this phase is ascribed to pressure and Schmidt equation is used, pressures of solidification in the 5-7 K bar range are obtained from amphibole study.

## REFERENCES

- Abdel-Fattah and Abdel-Rahman, 1995. Chlorites in a Spectrum of Igneous Rocks: Mineral Chemistry and Paragenesis. *Mineralogical Magazine*, **59**, pp. 129-141.
- Ahmad, S. A., Mateen, A., Khan, Z.K. and Chaudhry, M.N., 2000. Geology and geochemistry of Neoproterozoic Kirana Volcanics, Sargodha district, Punjab, Pakistan, *Geol. Bull. Punjab Univ.*, **35**, 59-71.
- Alam, G.S. 1987. Geology of Kirana Hills District Sargodha, Punjab 1, Pakistan, *G.S.P. Quetta*, Pakistan, 1-37.
- Alam, G.S., Jaleel, A. and Ahmad, R. 1992. Geology of the Kirana area, District Sargodha Punjab, Pakistan. *Acta Mineralogica Pakistanica*, **6**, 93-100.
- Albee, A.L., 1962. Relationship between the mineral association, chemical composition and physical properties of the chlorite series. *American Mineralogist*, **47**, pp. 851-870.
- Al-Dahan, A.A.Ounchanum, P., and Morad, S., 1988. Chemistry of micas and chlorite in Proterozoic acid metavolcanics and associated rocks from the Hästefält area, Norberg ore district, central Sweden. *Contributions to Mineralogy and Petrology*, **13**, pp. 457-492.
- Bailey, D. K., 1987. Mantle metasomatism: perspective and prospect. In: Fitton, J. G. and Upton, B. G. J. (eds.) *Alkaline Igneous Rocks*. Blackwell, London, pp.1-33.
- Bettison, L.A. and Schiffman, P., 1988. Compositional and structural variations of phyllosilicates from the Point Sal ophiolite, California. *American Mineralogist*, **73**, 62-76.
- Brown, G.C., Thorpe, R.S. and Webb, P.C., 1984. The geochemical characteristics of granitoids in contrasting arcs and comments on magma sources. *Jour. Geol. Soc. Lond.*, **141**, 411-426.
- Buddington A.F. and Lindsley D.H., 1964. Iron-titanium oxide minerals and synthetic equivalents. *Journal of Petrology*, **5**, 310-357.
- Chaudhry, M.N., Ahmad, S.A. and Mateen, A., 1999. Some postulates on the tectanomagmatism, tectanostratigraphy and economic potential of Kirana-malani-Basin, Indo-Pakistan, *Pakistan Journal of Hydrocarbon Research*, **11**, 52-68.
- Cooper, A. F., 1972. Progressive metamorphism of metabasic rocks from the Haast Schist Group of southern New Zealand. *Journal of Petrology*, **13**, pp. 457-492.
- Czamanske, G.K., Ishihara, S. and Atkin, S.A., 1981. Chemistry of rock-forming minerals of the Cretaceous-Paleocene Batholith in southwestern Japan and implications for magma genesis. *Journal of Geophysical Research*, **86**, 10431-10469.
- Davies, R.G. and Crawford, A.R., 1971. Petrography and age of the rocks of Buland hills, Sargodha Districts West Pakistan, *Geological Magazine*, **108**, pp. 235-246.
- Dawes, R.L. and Evans, B.W., 1991. Mineralogy and geothermometry of magmatic epidote bearing dikes, Front Range, Colorado. *Geological Society of America Bulletin*, **103**, 1017-1031.
- Deer, W. A., Howie, R. A., and Zussman, J., 1992. *An Introduction to the Rock Forming Minerals*, 2nd ed., Longman, London, 696pp.



- Droop, G. T. R., 1987. A general equation for estimating Fe<sup>3+</sup> concentrations in ferromagnesian silicates and oxides from microprobe analyses using stoichiometric criteria. *Mineralogical Magazine*, **51**, 431-435.
- Eggleton, R. A. and Banfield, J. F., 1985. The alteration of granitic biotite to chlorite. *American Mineralogist*, **70**, 902-910.
- Farrow, C. E. G. and Barr, S. M., 1992. Petrology of high-alumina hornblende- and magmatic epidote-bearing plutons, southeastern Cape Breton Highlands, Nova Scotia. *Canadian Mineralogist*, **30**, 377-392.
- Foster, M. D., 1962. Interpretation and a classification of the chlorite. *US Geological Survey professional paper*, **414A**, pp. 1-33.
- Ghent, E. D., Nicholls, J., Siminy, P. S., Seigniny, H. H. and Stout, M. Z., 1991. Hornblende geobarometry of the Nelson Batholith, Southeastern British Columbia: tectonic implications. *Canadian Journal of Earth Science*, **28**, 1982-1991.
- Giret, A., Bonin B. and Léger J. M., 1980. Amphibole compositional trends in oversaturated and undersaturated alkaline plutonic ring complexes. *Canadian Mineralogist*, **18**, 481-495.
- Hall, R. P. and Hughes, D. J., 1986. Complex sequential pyroxene growth in tholeiitic hypabyssal rocks from southern West Greenland. *Mineralogical Magazine*, **50**, 491-502.
- Hammarstrom, J. M. and Zen, E., 1986. Aluminium in hornblende: an empirical igneous geobarometer. *American Mineralogist*, **71**, 1297-1313.
- Hayes, P. T., 1970. Mesozoic stratigraphy of the Mule and Huachuca Mountains, Arizona: *U.S. Geological Survey Professional Paper*, **658-A**, 27 p.
- Helmy, H. M., Ahmed, A. F., Mahallawi, M. M. El. and Ali, S. M., 2004. Pressure, temperature and oxygen fugacity conditions of calc-alkaline granitoids, Eastern Desert of Egypt, and tectonic implications. *Journal of African Earth Sciences*, **38**, 255-268.
- Heron, A. M., 1913. The Kirana and other hills in the Jeeb and Rachna Doabs. *Memoirs, G.S.I. Records*, **43**, Pt. 3, 229-236.
- Johnson, M. C., and Rutherford, M. J., 1989. Experimental calibration of the aluminum-in-hornblende geobarometer with application to Long Valley caldera (California) volcanic rocks: *Geology*, **17**, p. 837-841.
- Khan, Z. K., 2004. Classification of base and sub-base of road aggregates in Kirana area, districts Jhang and Sargodha, Punjab. Workshop on Geological Materials/Aggregates of Pakistan, June 10, 2004, Islamabad. National Geological Society of Pakistan & Pakistan Museum of Natural History (Pakistan Science Foundation).
- Khan, Z. K., 2000. Study of the geology of Kirana Group, Central Punjab and evaluation of its utilization and economic potential as aggregate. Ph. D. thesis, University of the Punjab, Lahore, 1-240.
- Khan, Z. K. and Chaudhry, M. N., 1991. Engineering Geological and Petrographic Evaluation of Metadolerites of Buland Hill and Chak 123 Quarries of Kirana Hills, District, Sargodha, Pakistan. *Kashmir Journal of Geology*, **8-9**, 181-184.
- Khan, Z. K., 2004. Classification of base and sub-base of road aggregates in Kirana area, districts Jhang and Sargodha, Punjab. Workshop on Geological Materials/Aggregates of Pakistan, June 10, 2004, Islamabad. National Geological Society of Pakistan & Pakistan Museum of Natural History (Pakistan Science Foundation).
- Kranidiotis, P. and MacLean, W. H., 1987. Systematics of chlorite alteration at the Phelps Dodge massive sulfide deposit, Matagami, Quebec. *Economic Geology*, **82**, 1898-1911.
- Kushiro, I., 1960. Si-Al relations in clinopyroxenes from igneous rocks: *American Journal of Science*, **258**, 548-554.
- Leake, B. E., Woolley, A. R., Arps, C. E. S., Birch, W. D., Gilbert, M. C., Grice, J. D., Hawthorne, F. C., Kato, A., Kisch, H. J., Krivovichev, V. G., Linthout, K., Laird, J., Mandarino, J., Maresch, W. V., Nickel, E. H., Rock, N. M. S., Schumacher, J. C., Smith, D. C., Stephenson, N. C. N., Ungaretti, L., Whittaker, E. J. W. and Youzhi, G., 1997. Nomenclature of amphiboles: Report of the subcommittee on amphiboles of the international Mineralogical Association Commission on new minerals and mineral names. *Mineralogical Magazine*, **82**, 1019-1037.
- Leake, B. E., 1971. On aluminous and edenitic hornblendes. *Mineralogical magazine* **38**, 389-405.
- Lindsley, D. H., 1983. Pyroxene geothermometry. *American Mineralogist*, **68**, 477-493.



- Nutt, C.J. 1989. Chloritization and Associated Alteration at the Jabiluka Unconformity-Type Uranium Deposit, Northern-Territory, Australia. *Canadian Mineralogist*, **27**, 41-58.
- Owen, J.V., 1991. Significance of epidote in orbicular diorite from the Grenville Front Zone, eastern Labrador. *Mineralogical Magazine*, **55**, 173-181.
- Rock, N. M. S., 1990. The International Mineralogical Association (IMA/CNMMN) pyroxene nomenclature scheme: computerization and its consequences. *Mineralogy and Petrology*, **43**, 99-119.
- Rogers, H. D. 1988. Field relations, petrography, and geochemistry of granitoid plutons in the Shelburne area, southern Nova Scotia; *Geological Survey of Canada*, Open File **1835**.
- Schmidt, M. A., 1992. Amphibole composition in tonalite as a function of pressure: an experimental calibration of the Al-in-hornblende barometer. *Contributions to Mineralogy and Petrology*, **110**, 304-310.
- Shah, S.M.I., 1977. Stratigraphy of Pakistan: *Geol. Surv. Pakistan*, Quetta, Mem. No. **12**, 1-138.
- Shikazono, N. and Kawahata, H. 1987. Compositional differences in chlorite from hydrothermally altered rocks and hydrothermal ore deposits. *Canadian Mineralogist*, **25**, 465-474.
- Walshe, J.L., 1986. A six-component chlorite solid solution model and the condition of chlorite formation in hydrothermal and geothermal systems. *Economic Geology*, **81**, 681-703.
- Wones, D. and Gilbert, M. C. 1982. Amphiboles in the igneous environment. In: Veblen, D. R. and Ribbe, P. H. (eds) *Amphiboles: Petrology and Phase Relations*. *Mineralogical Society of America*, Reviews in Mineralogy **9B**, 355-389.



## MICROFACIES ANALYSIS AND DIAGENETIC SETTINGS OF THE MIDDLE JURASSIC SAMANA SUK FORMATION, SHEIKH BUDIN HILL SECTION, TRANS INDUS RANGES-PAKISTAN

BY

ABDUR RAUF NIZAMI AND RIAZ AHMAD SHEIKH

Institute of Geology, University of the Punjab, Quaid-i-Azam Campus,

Lahore-54590 Pakistan

Email: raufnizami@yahoo.com

**Abstract:** A detailed study on the microfacies analysis and diagenetic settings of the Middle Jurassic Samana Suk Formation exposed at the Sheikh Budin Hill Section, Marwat Range, Trans Indus Ranges, was conducted. The Samana Suk Formation is mainly comprised of limestones and dolomitic limestones along with some dolomite and intercalations of marl and shale at different levels. The investigation was carried out after collecting systematically a total of 210 rock samples and studying selected 140 thin sections from 136 individual beds. The petrographic study of unstained and stained thin sections have been carried out to investigate its sedimentology, microfacies assemblages and diagenetic sequence. Detailed work in the field and in the laboratory revealed that it contains microfacies forming SMF zones and exhibits frequent oolitic, peloidal and skeletal grainstone microfacies along with presence of dolomite at various horizons. The grainstone microfacies constitute a predominant part in this section in comparison to other sections towards east of Sheikh Budin Hill. A variety of cement morphologies and diagenetic features have been elaborated. Dolomitization has developed at various levels as cement as well as replacement and as stylocumulates. The incorporation of iron into calcite and dolomite at some later diagenetic stage has been recorded. The dedolomitization has, also, been noted. The Samana Suk Formation is widely exposed in various sedimentary basins of Pakistan. The detailed microfacies analysis and its diagenetic settings show that this formation was deposited in an environment of shallow shelf with open and restricted marine conditions as carbonate platform depositional product.

### INTRODUCTION

The Samana Suk Formation is a distinctive stratigraphic unit recognizable over a wide area of northern Pakistan. It is the most prominent lithological package of carbonates in the Mesozoic strata of Trans Indus Ranges, Cis-Indus Salt Range, Hazara Mountains, Kohat Tribal Range, Samana Range and Kala Chitta Range. Further towards the west the Chiltan Formation, exposed at a number of sections in the Sulaiman Range and Kirthar Range, is taken as an equivalent carbonate rock unit of the Samana Suk Formation. In Sheikh Budin Hill Section the Samana Suk Formation presents strata sets, comprising thin bed, medium to thick beds and massive limestone beds. Within the vertical stacking of beds at places the bedding thickness is uneven to wavy. The most part of the formation consists of relatively larger number of coarse grained limestone

horizons. The Sheikh Budin Hill Section is located near Pezu Pass, District Laki Marwat at a distance of 7 km (Fig. 1). The approximate location of this section is at Latitude 32° 17' 11" N and Longitude 70° 43' 51" E (Toposheet No. 38 L/15 of Survey of Pakistan). The Pezu Pass could be approached from Dera Ismail Khan in south and Laki Marwat in northwest via Indus Highway. Field work was carried out in the Sheikh Budin Hill area, Marwat Range during March, 2006 and a total of 210 rock samples were collected from 136 individual beds and 140 thin sections were selected for present research work. The thickness of this formation at the studied section is 87.57m. The paper demonstrates the investigations on the sedimentology, microfacies analysis and diagenetic settings of this formation. The research work presented here is extracted from the doctoral dissertation of the first author.



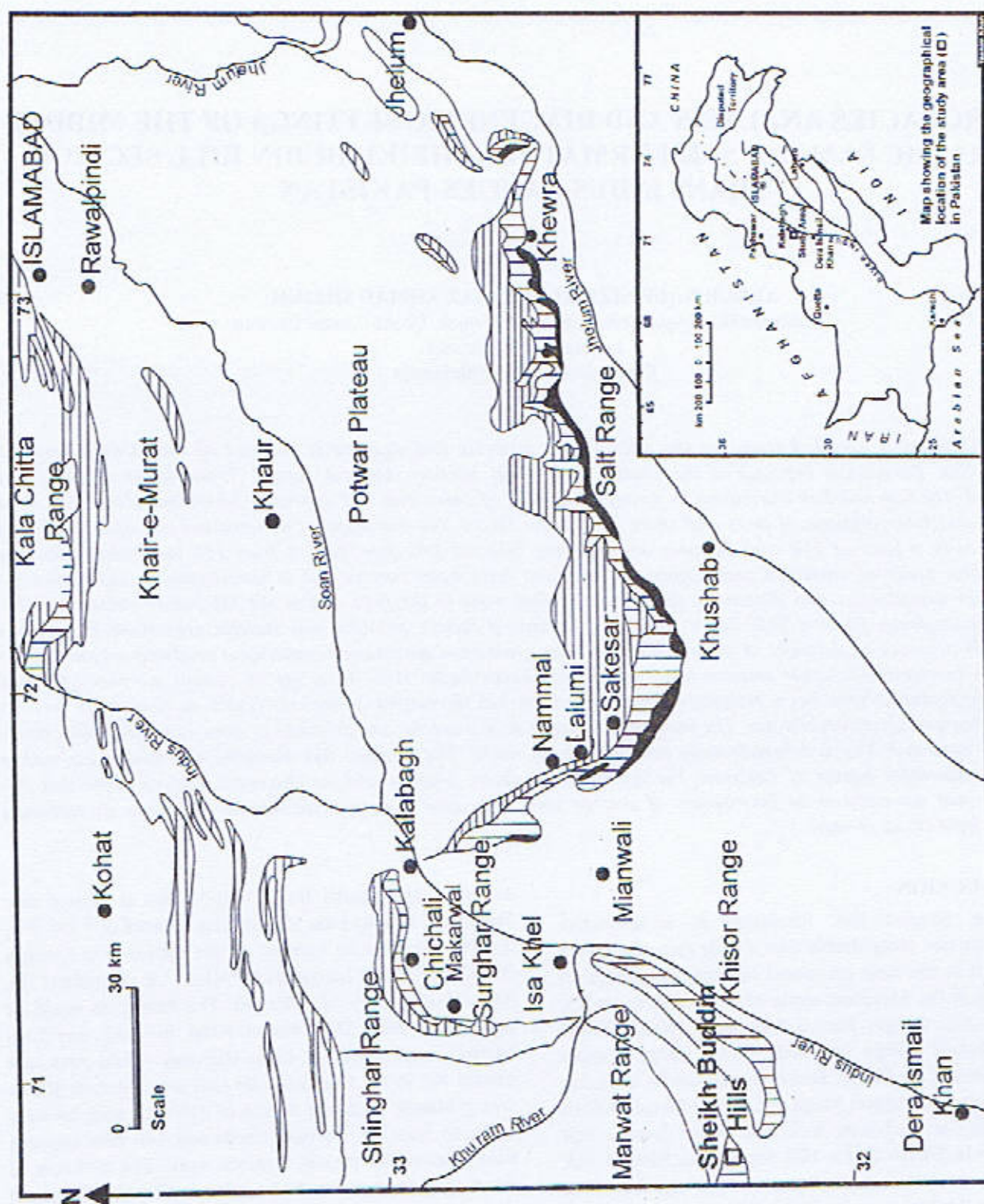


Fig.1. Map showing the location of Sheikh Buddin Hills Section (□) in the Trans Indus Ranges (Modified after Gee, 1989)



## PREVIOUS INVESTIGATIONS

Previously this formation was named as Kioto Limestone by Cotter (1933) and Gee (1947), Samana Suk Limestone by Davies (1930) and Baroch Limestone by Gee (1947). In 1974 the name, Samana Suk Formation, was formalized by Fatmi et al., 1990. According to Shah (1977) in the Upper Indus Basin, where the Surghar and Marwat Ranges are situated (Anwar, et al., 1992 and Gee, 1989), the Jurassic sequence contains Datta Formation, Shinawari Formation and Samana Suk Formation. Bender and Raza (1995) added that the lower part (relatively much thinner) of Chichali Formation is part of this Jurassic sequence. Fatmi, et al. (1990) indicated that the upper part of Jurassic sequence is represented by the Samana Suk Formation and it is a shallow water marine carbonate rock. Mensink, et al. (1988), Fatmi, et al. (1990) and Mertmann and Ahmad (1994) described that the rocks of the Jurassic sequence are exposed at a number of localities in the Trans Indus Ranges, particularly in the Surghar and Marwat Ranges. A commendable work has been done on the various aspects of Samana Suk Formation of Jurassic age, Trans Indus Ranges, by Mensink, et al. (1988), Fatmi, et al. (1990) and Ahmad, et al. (1997) on its microfacies and depositional environments in a broad spectrum. Hemphill and Kidwai (1973) gave an account on the stratigraphy of Bunnu and Dera Ismail Khan including the geology of Sheikh Budin Hill and that of the Samana Suk Formation as well. From above it is obvious that no detailed work on sedimentology of the Samana Suk Formation was carried out in the area of Sheikh Budin Hill, Marwat Range. Therefore a detailed microfacies analysis and diagenetic interpretation of the Samana Suk Formation were undertaken.

The following parameters have been taken into consideration for this research work: Outcrop observations and field study, section measurement, field photography, laboratory investigations including thin sections studies using petrographic microscope, chemical staining with Alizarin Red S and Potassium Ferricyanide and digital photomicrography.

## SAMANA SUK FORMATION

The Samana Suk Formation exposed at the Sheikh Budin Hill in the Marwat Range is mainly composed of limestones, dolomitic limestones and dolomites with interbedded calcareous shales/marls, which are present at various levels and are the result of periodic influxes of clay due to small scale and distant tectonic uplift and erosion or climatic change on a distant land mass. The limestones are mostly hard, compact, grey and yellowish grey and at places dark grey in colour, micritic, oolitic and dense to coarse grained. Generally the topographic impression of limestone is a ridge former, however it also forms steep slopes and impassable cliffs in the host area. Here it comprises limestone as a dominant lithology with dolomite,

marl and shale intercalations. The Samana Suk Formation conformably overlies the Shinawari Formation and disconformably underlies the Chichali Formation (Table 1). The lower contact with Shinawari Formation is transitional one. The top most sandstone bed of the Shinawari Formation is marked here as the lower stratigraphic contact (Akhtar, 1983 and Mertmann and Ahmed, 1994). The upper contact with the Chichali Formation is sharp and is marked by hard ground with lateritic encrustation (Mertmann and Ahmed, 1994 and Sheikh, 1991). The shale/marl breaks and intercalations present at different levels do not show any regular or alternative cyclic deposition. Three well developed hard ground surfaces were found and recorded. These surfaces mark the presence of regressive cycles and periods of non erosion-non deposition. Mostly the bed forms are planar, however few beds exhibit uneven thickness. In Trans Indus Ranges the age of this formation was determined Late Jurassic (Late Callovian) on the basis of cephalopod fauna described by Spath (1939), however, Fatmi (1972) considers its age to be Early to Middle Callovian (Middle Jurassic) on the basis of Middle Callovian Ammonites that occur in richly fossiliferous sections of the Datta, Punnu Nala, Landa Nala, Mallakhel and Makarwal areas, Surghar Range. This formation is correlated with the Mazar Drick Formation and Chiltan Formation in the Sulaiman Fold and Thrust Belt and Murree Brewery Gorge near Quetta, Balochistan, Pakistan.

## MICROFACIES

For the microfacies analysis of the Samana Suk Formation the microfacies classification scheme suggested by Dunham (1962) has been followed. To interpret coquina limestone facies Embry and Klovan (1971) scheme has been adopted, who further subdivided the boundstone microfacies of Dunham into two categories: Autochthonous limestones and allochthonous limestones. Allochthonous limestones are classified as floatstones, in which component bioclasts are matrix-supported, larger than 2mm in dimensions and more than 10% in numbers whereas rudstones have grain-supported texture with bioclasts larger than 2mm as well (Scoffin, 1987). The Samana Suk Formation as measured in this section is dominated with bioclastic microfacies from bioclastic mudstone to bioclastic grainstone and floatstone/rudstone facies along with peloidal and ooidal grainstones. Ten microfacies have been identified and compared with the Dunham classification and Embry and Klovan extended scheme. The interpreted microfacies include bioclastic, peloidal, cortoidal and ooidal grainstones, grapestones, bioclastic rudstone and floatstone, bioclastic and peloidal packstones, bioclastic wackestone, bioclastic mudstone and mudstone. In the following pages details of microfacies and Standard Microfacies (SMFs) recorded from this section are presented:



Table 1

Stratigraphic successin of the Sheikh Budin Hill area, Marwat Range, Trans Indus Ranges, showing the position (**bold**) of Samana Suk Formation

| ERA          | AGE                      | GROUP         | FORMATION             |
|--------------|--------------------------|---------------|-----------------------|
| CENOZOIC     | PLIOCENE-<br>PLEISTOCENE | SIWALIK GROUP | Dhok Pathan Formation |
|              |                          |               | Nagri Formation       |
| UNCONFORMITY |                          |               |                       |
| MESOZOIC     | CRETACEOUS               | SURGHAR GROUP | Lumshiwal Formation   |
|              |                          |               | Chichali Formation    |
|              | UNCONFORMITY             |               |                       |
|              | JURASSIC                 | BROACH GROUP  | Samana Suk Formation  |
|              |                          |               | Shinawari Formation   |
|              |                          |               | Datta Formation       |

### Grainstones

The petrographic analysis revealed the following microfacies of grainstone. Diversity of bioclastic grains has commonly been observed in all grainstones. An excellent display of grainstone assemblages is present in this section, which is estimated up to 32% and it is a higher value relative to the other studied sections of the Samana Suk Formation towards east in the Surghar Range (Nizami and Sheikh, 2007).

**Bioclastic grainstones:** This type of grainstone consists of skeletal shells, tests and fragments of different organisms sometimes in association with intraclasts (Plates 2a and d). These shells and grains mostly belong to foraminifera, algae and sponges.

**Peloidal grainstones:** The frequency of appearance of peloidal grainstones is relatively higher in this section and is found at a number of levels. It is commonly composed of faecal pellets and peloidal grains, having micritic composition (Plates 3a, 6d and 7b). These grainstones are also found in associations with foraminifera (Plate 3a).

**Cortoidal grainstones:** The cortoids are one of types of coated grains and are covered by micritic envelope only. These grains actually constitute a type of non-laminated coated grains (Tucker and Wright, 1990). This microfacies of grainstone has been recorded in (Plate 1d). The frequency of their appearance in other microfacies is relatively low.

**Ooidal grainstones:** The ooids found are generally of concentric and radial concentric type (Plates 2b and c). The chemical compaction has intensely affected this microfacies. The boundaries between ooids are mostly sutured and embayments of one ooid into the other are present (Plate 7c). Due to over burden pressure brittle deformation has been noted in the form of broken and spalled off ooids (Plate 4a). In connection with the late void and micro fracture filling spars some calcareous spars related to the deep burial environments are precipitated between these spalled off cortices of ooids.

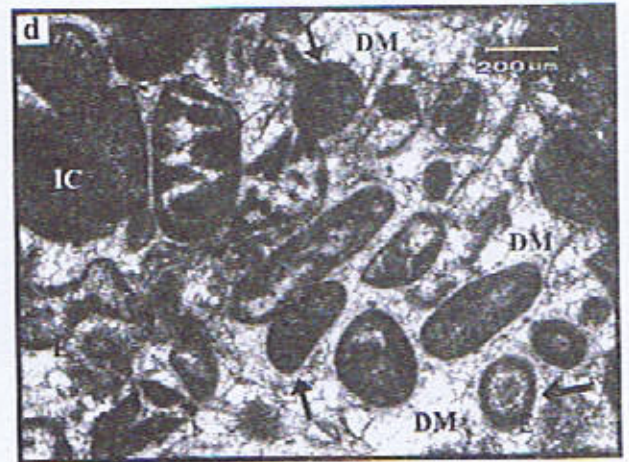
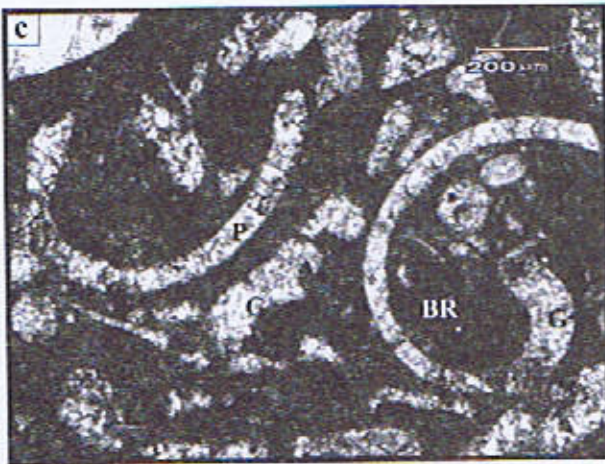
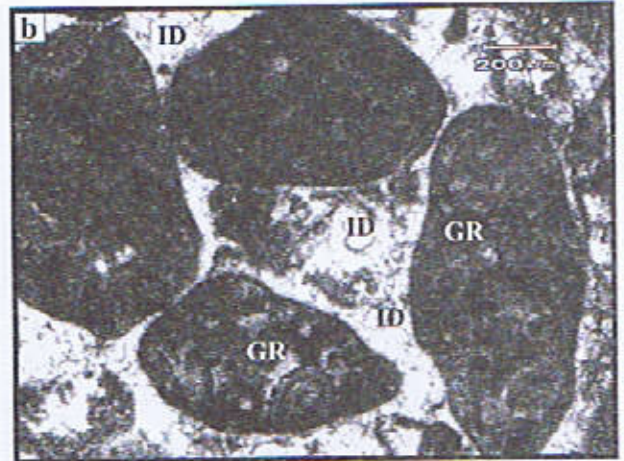
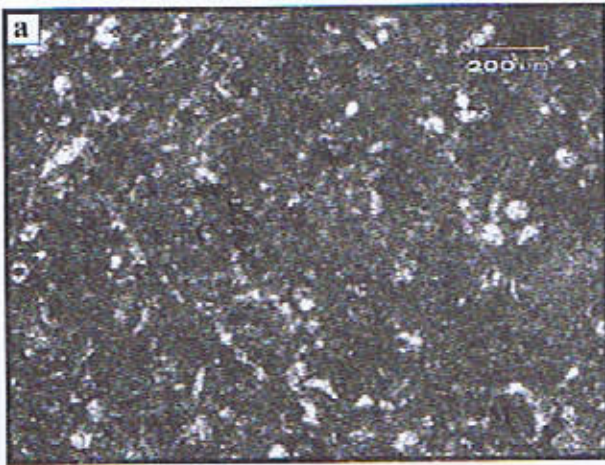
**Grapestone grainstones:** Grapestones are actually aggregate grains and are commonly encountered in the grainstone microfacies of Samana Suk Formation at this section. The grainstones comprised entirely of grapestones has been recorded in Plate 1b. The grapestones are also found in other microfacies, however the frequency of their appearance is not very high.

### Bioclastic rudstones

According to Embry and Kalovan (1971) rudstone is mainly composed of more than 2mm larger shells and grains of organisms and is a grain supported sub-microfacies of allochthonous (derived) limestones. The rudstones found in this section are composed predominantly of bioclasts of mollusks and bryozoans shells, tests and their fragments with more than 3mm in length and 2mm in

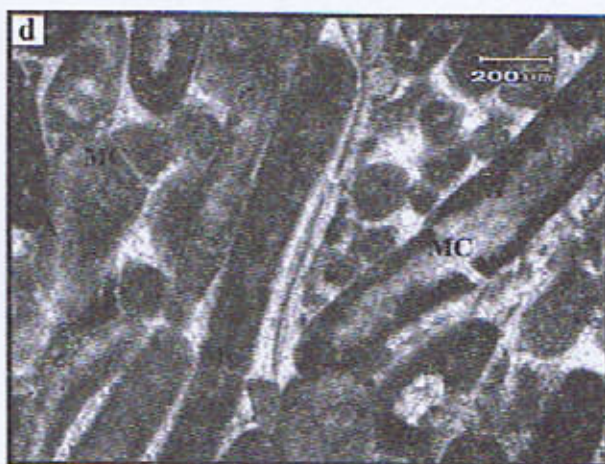
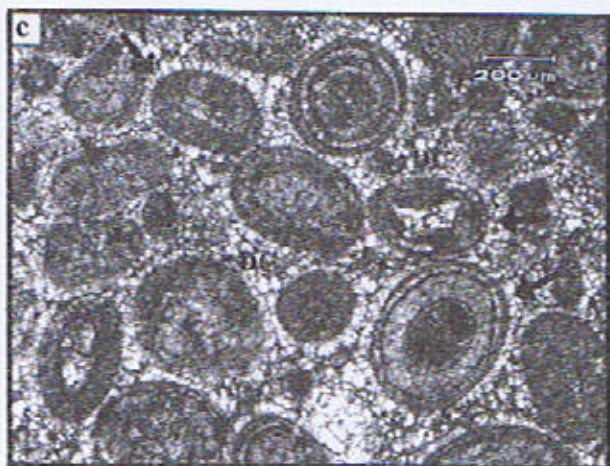
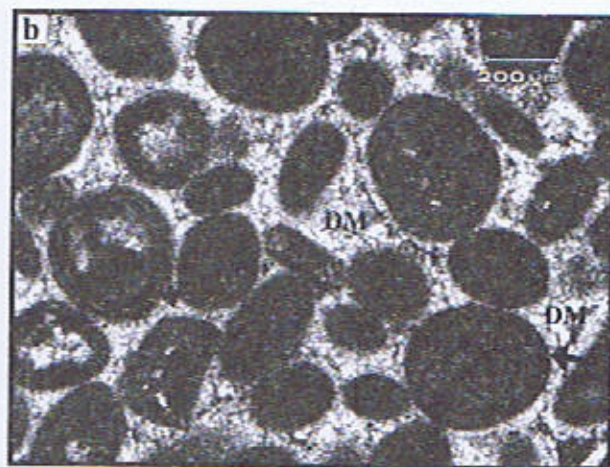
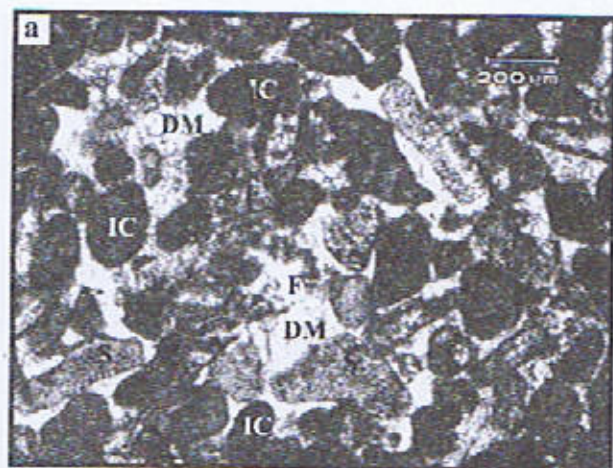


## Plate 1



- a.** Photomicrograph showing peloidal packstone, wherein skeletal grains of echinoderm (EC) and mollusks (M) in association with peloids are present. (XN, stained) **Sample No. SBH-23B**
- b.** Photomicrograph showing a grainstone composed of grapestones (GR) cemented by intergranular dolomite (ID) cement. (PPL, stained) **Sample No. SBH-24T**
- c.** Photomicrograph exhibits bioclastic wackestone with well preserved shells and fragments of brachiopod (BR), gastropod (G) and pelecypod (P). (PPL, stained) **Sample No. SBH-42L**
- d.** Photomicrograph displays cortoidal grainstone with circumgranular columnar (arrowed) cement and intergranular drusy mosaic (DM) cement. The skeletal grains have lost internal structure due to dissolution-precipitation phenomenon and now possess micritic envelopes (E), occasional intraclasts (arrowed) are present. (PPL, stained) **Sample No. SBH-42U**





a. Photomicrograph showing a bioclastic grainstone. Several shells of sponge (S) and a few shells of foraminifera (F) are present along with intraclasts (IC) cemented by drusy mosaic cement (DM). The signatures of mechanical compaction (MC) are present as well. (PPL, stained) Sample No. SBH-46

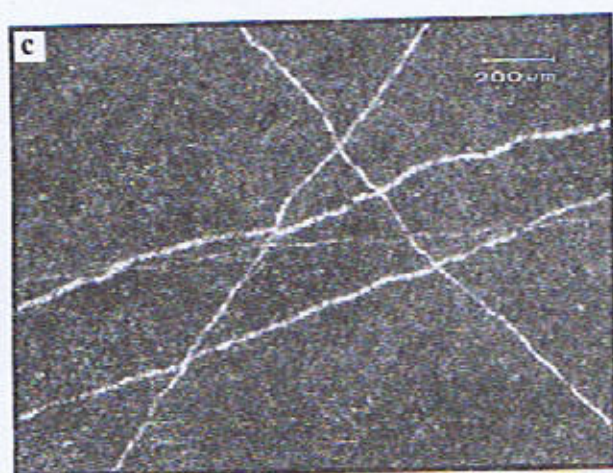
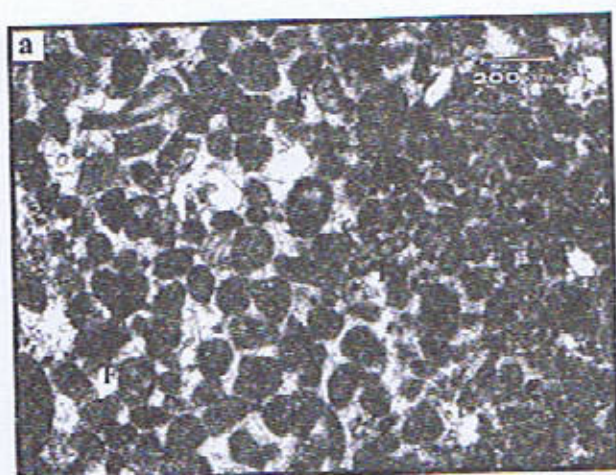
b. Photomicrograph showing an ooidal grainstone cemented by dolomite having drusy mosaic (DM) of crystals. Ooids are concentric. Dogtooth cement (arrowed) has nucleated few ooids. (PPL, stained) Sample No. SBH-49

c. Photomicrograph showing an ooidal grainstone with pervasive dolomitization attacking matrix and allochems (ooids). Ooids are concentric and are retaining morphology. Intergranular dolomite cement (DC) with partial incorporation of Fe and circumgranular columnar (arrowed) cement is present. (PPL, stained) Sample No. SBH-49

d. Photomicrograph exhibiting signatures of mechanical compaction (MC) in a bioclastic grainstone, shown by broken bioclasts of algae (A). (PPL, stained) Sample No. SBH-71B



## Plate 3



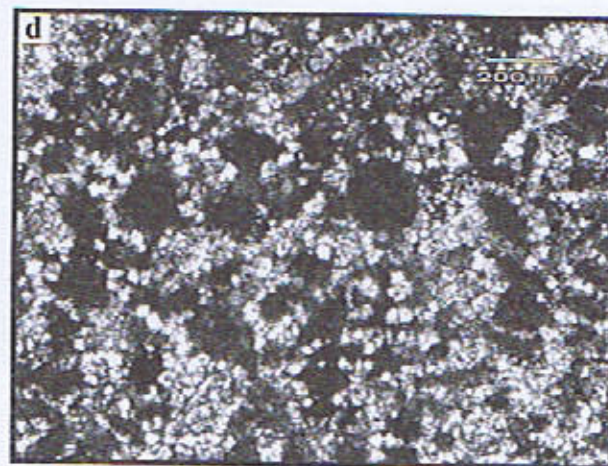
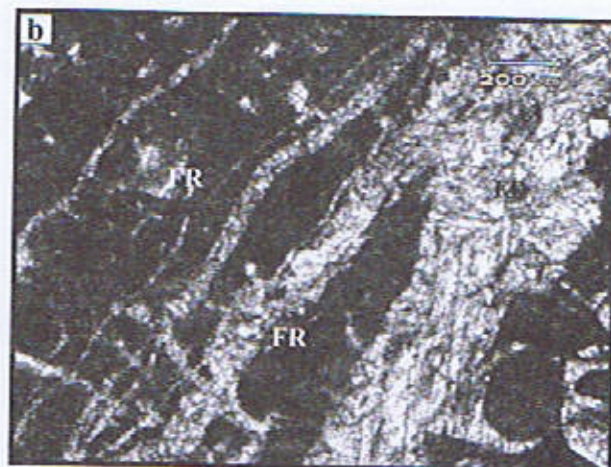
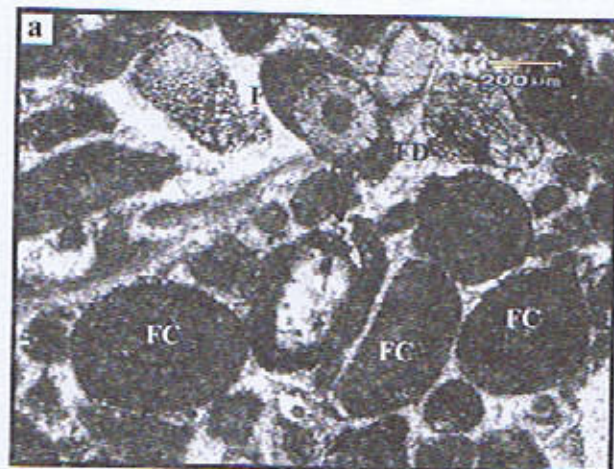
a. Photomicrograph displaying a peloidal grainstone with associated foraminiferal (F) tests. The intergranular drusy mosaic (DM) cement has partially altered into ferroan calcite with light royal blue stain colour. (PPL, stained) Sample No. SBH-74B

b. Photomicrograph displaying a bioclastic packstone. Bryozoan (BZ) colony is prominently present. (PPL, stained) Sample No. SBH-89

c. Photomicrograph showing a highly fractured mudstone bearing the multi-stage fracturing, well displayed by cross cutting relationship of these fractures. (PPL, unstained) Sample No. SBH-96L.

d. Photomicrograph displaying a large and a small micritic envelope (E) in a bioclastic floatstone. (XN, stained) Sample No. SBH-93





a. Photomicrograph displaying spalled off cortices (**arrowed**) of ooids in an ooidal grainstone. Incorporation of iron in calcite (**FC**) is shown by maroon stain colour of ooids. Iron also partially incorporated in the intergranular dolomite (**FD**) cement with turquoise stain colour. (PPL, stained) **Sample No. SBH-122B**

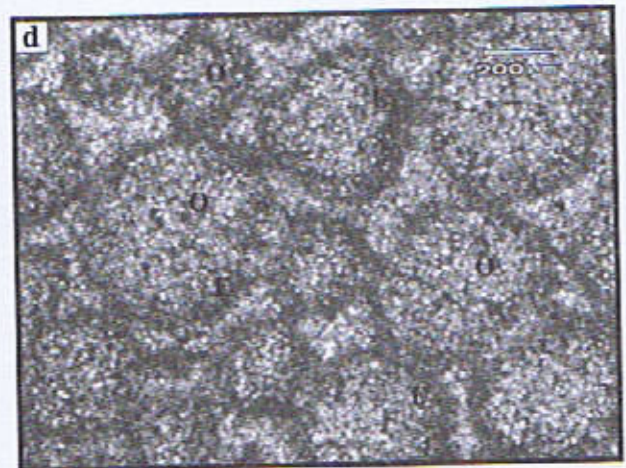
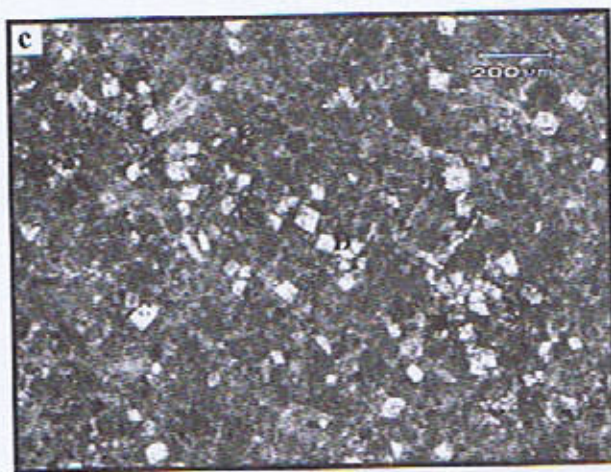
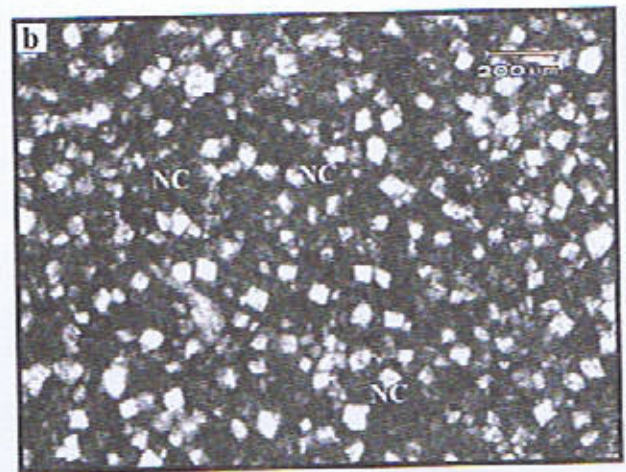
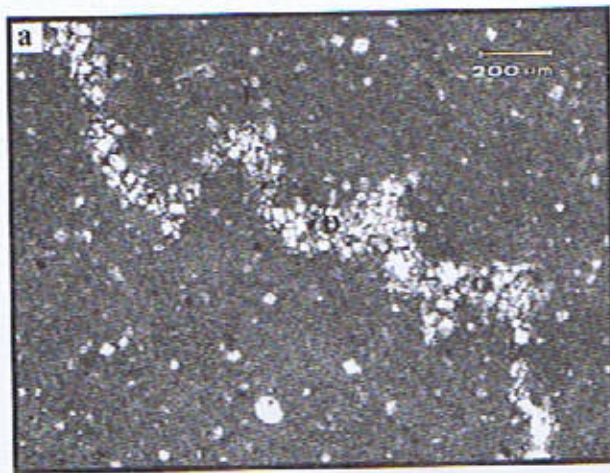
b. Photomicrograph displaying ferroan dolomite (**FD**) with turquoise stain colour precipitated along fractures in a bioclastic packstone. (PPL, stained) **Sample No. SBH-12**

c. Photomicrograph displaying a bioclastic mudstone. A high amplitude stylolite (**ST**) is cutting across the slide. (PPL, stained) **Sample No. SBH-11L**

d. Photomicrograph showing initially fabric selective dolomitization which after wards changed into pervasive dolomitization in a bioclastic grainstone, wherein bioclasts are indeterminate due to this replacement phenomenon. Some dolomite crystals have been dedolomitized (**NC**) with pink stain colour. (PPL, stained) **Sample No. SBH-5T**

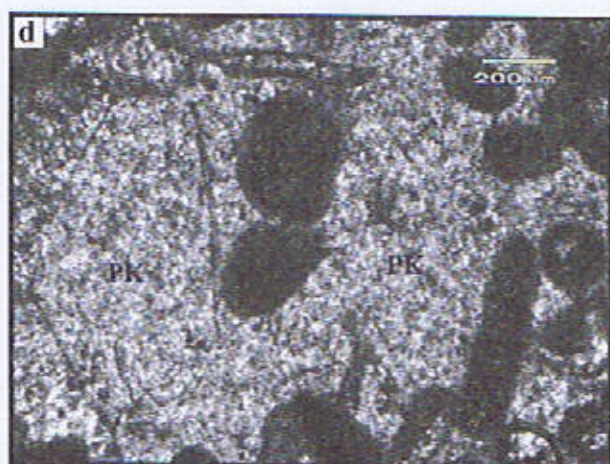
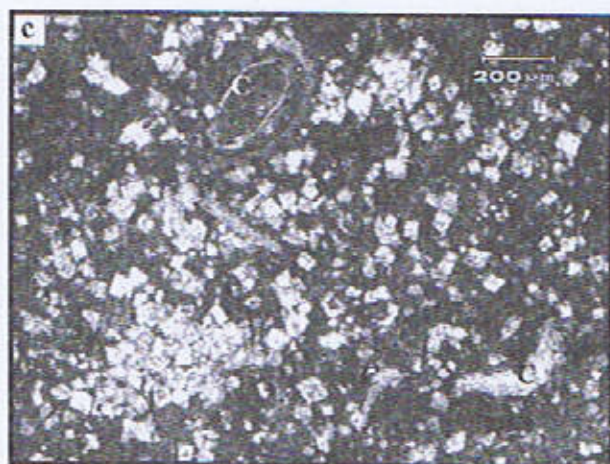
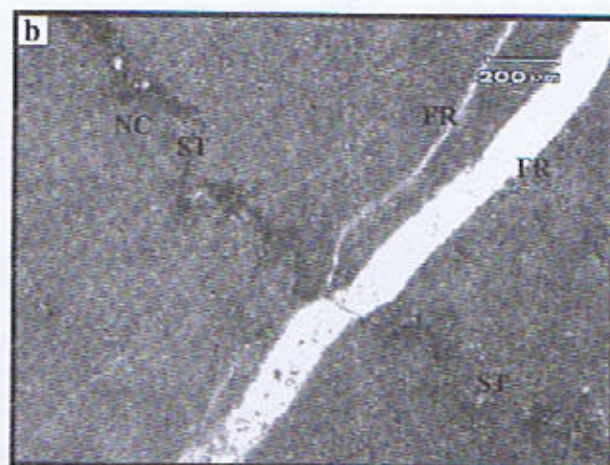
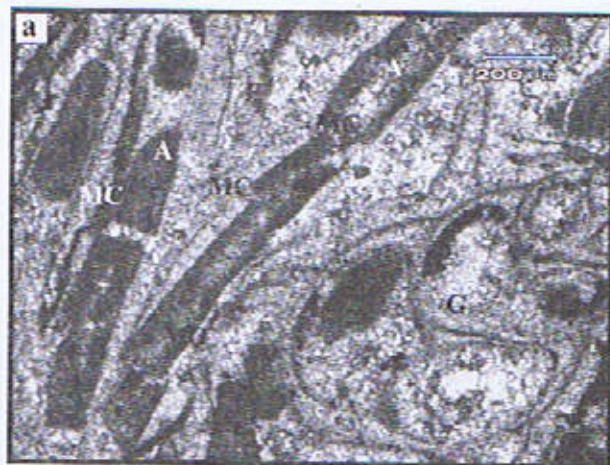


## Plate 5



- a. Photomicrograph showing stylolite along with dolomite stylolite (D) in a partially dolomitized mudstone. (PPL, stained) Sample No. SBH-13B
- b. Photomicrograph showing dolomitization and dedolomitization (NC) with pink stain colour in a bioclastic grainstone. (PPL, stained) Sample No. SBH-18L
- c. Photomicrograph showing dolomite stylolite (D) in a partially dolomitized peloidal packstone. (PPL, stained) Sample No. SBH-19T
- d. Photomicrograph showing pervasive dolomitization in ooidal grainstone converting it to microdolomite. The ghosts of ooids (O) are identifiable due to present micritic envelopes (E). (PPL, stained) Sample No. SBH-24B

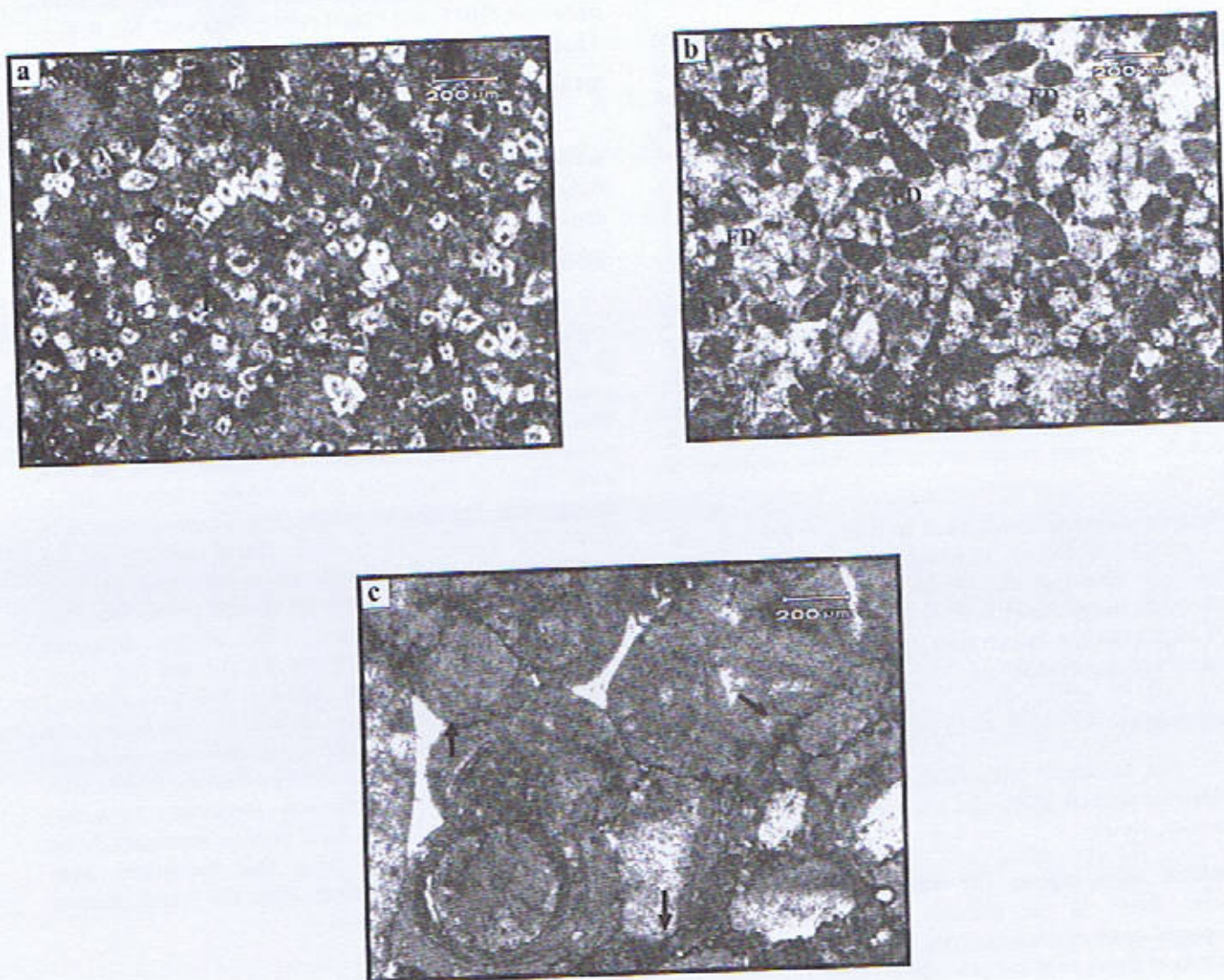




- a.** Photomicrograph showing a bioclastic rudstone, wherein mechanical compaction (MC) prior to cementation is exhibited by broken algal (A) shells. A large gastropod (G) shell is present too. (PPL, stained) **Sample No. SBH-31**
- b.** Photomicrograph displaying fractures (FR) and a low amplitude stylolite (ST) in mudstone. Stylolite is cutting across fractures and thus postdating these ones. (PPL, stained) **Sample No. SBH-56T**
- c.** Photomicrograph displaying matrix selective dolomitization in a bioclastic mudstone. The skeletal grains are composed of calcite (C) with pink stain colour. (PPL, stained) **Sample No. SBH-63L**
- d.** Photomicrograph displaying poikilotopic (PK) cement with characteristic large calcite crystal developed in a peloidal grainstone. (PPL, unstained) **Sample No. SBH-92**



## Plate 7



- a.** Photomicrograph displaying zoned dolomite in a mudstone. The zoning (**arrowed**) in dolomite indicates changes in the geochemistry of formation fluids during the course of crystallization. (PPL, unstained) **Sample No. SBH-115B**
- b.** Photomicrograph showing ferroan dolomite (**FD**) with turquoise stain colour and calcite (**C**) with pink stain colour in a peloidal grainstone. (PPL, stained) **Sample No. SBH-124T**
- c.** Photomicrograph displaying a chemically compacted ooidal grainstone. The tightly compacted facies exhibits sutured grain contacts (**arrowed**) approaching to pressure solution seams. (PPL, unstained) **Sample No. SBH-130**



width. It is found only at one horizon in the studied formation (Plate 6a).

### Bioclastic floatstones

Floatstone is a matrix supported sub-microfacies of allochthonous (derived) limestones. It consists of shells and grains of organisms more than 2mm in size (Embry and Kalovan, 1971). This microfacies is also found at only one horizon in the studied section (Plate 3d). Shells and bioclasts of mollusks and sponges have mostly been recorded.

### Packstones

The following microfacies of packstone have been identified.

**Bioclastic packstones:** This sub-microfacies of packstone is commonly composed of skeletal grains of different species (Plates 3b and 4b). However at only one horizon a bioclastic packstone comprised of bryozoans is shown in Plate 3b.

**Peloidal packstones:** It has been recorded at few levels in the investigated section as shown in Plates 1a and 5c. Peloids are found in association with skeletal grains of echinoderm and mollusks in Plate 1a. Peloids in association with other grains in various microfacies are found with low frequency of appearance.

### Wackestones

The carbonate microfacies with more than 10% skeletal/nonskeletal grains are categorized as wackestones (Dunham, 1962).

**Bioclastic wackestones:** The wackestones are found at various levels in the Samana Suk Formation. The interpreted bioclastic wackestones are mainly composed of bioclasts of gastropods and pelecypods (Plate 1c).

### Mudstones

Mudstones, without any component grain have been found in the studied formation and are highly fractured (Plate 3c). Subsequently these fractures got filled with calcite. A highly fractured mudstone with a small amplitude stylolite, which is cross cutting these fractures and hence, postdating these fractures, is shown in Plate 6b. Such mudstones are present at few horizons in the investigated formation. Partially dolomitized mudstones have also been recorded (Plate 5a and 7a).

**Bioclastic mudstones:** Bioclastic mudstones are present at a number of levels in the measured section. Representatively the bioclastic mudstones are shown in Plates 4c and 6c.

## STANDARD MICROFACIES (SMFs)

The recorded microfacies from this studied section have been compared with the Standard Microfacies (SMFs) of Wilson (1975) and Flugel (1982). The SMF No. 8, 9, 11, 15, 16, 17, 23 and 24 have been documented here.

## DIAGENETIC SETTINGS AND SEQUENCE

The following diagenetic features, developed in this section, have been observed. A detailed account of the sequence of various diagenetic phases and their products depending on time hierarchy is presented here:

### Micritic envelopes

It is the first diagenetic phase, which takes place in the marine diagenesis of limestones. Micritic envelopes develop around fauna which have original aragonitic mineralogical composition. Such grains are very much prone to develop these envelopes. As aragonite is a metastable carbonate mineral. It is dissolved in the very early phase of diagenesis of carbonate sediments and is subsequently replaced by calcite. These envelopes serve to define and preserve the outline and morphology of the carbonate grains over which these envelopes develop. These envelopes may be found on skeletal and non-skeletal grains in different microfacies. The micritic envelopes found here are shown in Plates 1d, 3d and 5d. These envelopes, recorded in the Samana Suk Formation of studied section, are similar to those described by Kendal and Skipwith (1969) from the recent carbonate sediments and resemble with those illustrated by Bathurst (1964) from the Jurassic and Carboniferous limestone. However, according to Sheikh (1992) fossil micritic envelopes found in the Shinawari and Samana Suk formations from Kalachita Ranges are different from the recent micritic envelopes.

### Dissolution of aragonite

In the second phase the aragonite dissolves in the faunal grains having aragonitic mineralogy and is precipitated as sparite. Sometimes the internal structure of the skeletal grains is totally destroyed and no relict structure is observed at all. However, the outline and morphology of these grains is preserved.

### Cements

Cement endows strength and stability to the carbonate microfacies and sediments. The well developed cement, always, resists physical, as well as, chemical compaction and fracturing episodes. Hence, the cementation of carbonate sediments is taken as an important diagenetic process. Early diagenetic cement precipitates as fibrous aragonite, while dog tooth cement (circumgranular eque cement), dolomite cement, drusy mosaic cement and



poikilotopic cement precipitate as late diagenetic cements. Intergranular cement is the next phase of carbonate diagenesis. The sparry calcite cement with drusy mosaic of crystals is product of meteoric phreatic environment (Tucker, 1988). The following cement types have been recorded at different levels and in different microfacies:

**Circumgranular cements:** The documented two types of this cement are elaborated here:

**Dog tooth cement:** The dog tooth cement precipitates as late diagenetic cement as do dolomite cement and poikilotopic cement in a late diagenetic phase. It is circumgranular equant cement and has been recorded in Plate 2b.

**Columnar or prismatic cement:** It commonly precipitates in the mixed meteoric/marine phreatic environments (Tucker, 1988). This circumgranular cement found in the studied formation is shown in Plate 1d.

**Drusy calcite cement:** It is a pore filling cement and commonly precipitates in grainstones. It might be composed of sparry calcite or dolomite. Its crystals are of small size at margins and gets larger towards the centre of pore as per available accommodation space. It has been recorded in Plate 1d.

**Poikilotopic cement:** The diagnostic texture of poikilotopic cement is elucidated as that the coarse cement crystals enclose component allochems, which look like specks in crystals mosaic. It develops after the phase of pervasive dolomitization and development of intergranular cements and precipitates in phreatic environment, commonly, in burial regime. It has been found at various horizons and is shown representatively in Plate 6d.

### Mechanical compaction

Mechanical compaction of the carbonate sediments is the next diagenetic event. Under this diagenetic process the inter-grain and interstitial space reduces, which results in the overall reduction of porosity of the rock. In case of poorly cemented sediments the component grains may break due to increased mechanical compaction (Plate 2d and 6a). This and other factors produce fractures and ultimately enhance the porosity and permeability of the rock.

**Fractures:** The presence of different types of fractures, veins and broken allochems display the imprints of both tectonic stresses and overburden pressure pre-and-post cementation phases. Fractures are commonly found at various horizons in the measured section. Different phases of fracturing, sometimes along with stylolitization, filled with one or more episodes of calcite/ferroan calcite and dolomite/ferroan dolomite have been identified here (Plates 3c, 4b and 6b). The stylolites developed in the lime

mudstone microfacies have been noted disrupting the fractures (Plate 6b). Mudstones particularly bear fractures, which at places are highly fractured with several phases of fracturing sometimes (Plate 3d). Fractures have been recorded in other microfacies too (Plate 4b). The effective porosity and permeability is thought to be enhanced in the presently investigated section due to the occurrence of various phases of fracturing, which cause to provide interconnectivity. More over during and after uplifting of the host area most probably the creation of additional porosity took place by dissolution and fracturing. The signatures of mechanical compaction have been noted in Plate 2d.

### Chemical compaction

In this late stage diagenetic phase as a result of increasing compaction due to overburden and tectonic stresses first the grain to grain contacts take place and then simple grain contacts developed into planar and sutured grain contacts. Later on dissolution of grains starts at these contacts. Sometimes the embayment of one grain into the other is, also, observed (Plate 7c).

**Stylolites:** The stylolites develop in the last diagenetic events. These are actually manifestation of a diagenetic phenomenon, named as pressure-dissolution or chemical compaction. The continued dissolution of compacted grains at planar and sutured contacts results in the formation of stylolites or so called dissolution seams/pressure solution seams. The recorded point, planar and sutured grain contacts, pressure solution seams and stylolites all are indicators of chemical compaction due to both tectonic stresses and overburden pressure. The observed stylolites at various levels of this formation range from low amplitude (Plate 6b) to high amplitude stylolites (Plate 4c) and are found mostly in mudstones, however these have been recorded in other microfacies as well (Plate 5c and 7c). The stylolites have also developed in association with different episodes of fracturing. The stylolites, developed in mudstone microfacies, have cross cutting relationship with calcite filled fractures and postdate these fractures (Plate 6b). The Plate 7c shows the sutured grain contacts approaching to pressure solution seams.

### Dolomitization

The matrix selective, in other words, texture preserving dolomitization is the next phase of the diagenetic history of limestones, in which only the dolomitization of matrix takes place and component grains/allochms are not dolomitized. The diagenetic process of dolomitization results in the formation of dolomite of secondary nature. It is a common feature of carbonate sediments, particularly that of limestones, during the continuation of various diagenetic phases. In the investigated section the dolomitization is relatively fairly extensive and has



developed at its different horizons. Dolomite has also been recorded as stylocumulate along microstylolites (Plates 5a and c), while dolomite as cement has been found in Plate 2b and c. The following types of dolomitization have been observed in the studied section:

**Texture preserving dolomitization:** It has been documented in the studied formation at a few horizons. It is a texture preserving non-mimic dolomitization process and remains restricted to the matrix. It attacks the matrix and destroys it (Plate 6c), that is why it is referred to as matrix selective dolomitization.

**Pervasive dolomitization:** It is an extensive dolomitization process in limestones, in which the dolomitization is not texture selective and attacks the fabric of rock, hence whole of the rock gets dolomitized with the passage of time (Plates 2c, 4d and 5d).

**Microdolomitization:** Microdolomitization is such a type of diagenetic process, in which crystals of dolomite develop in a very small size. Microdolomite is noted in Plate 5d.

**Zoned dolomitization:** It has developed in the upper part of this formation at a number of levels. The zoning in dolomite is indicative of changes in the geochemistry of formation fluids during the growth of dolomite crystals. The noted zoned dolomitization has partially affected the concerned microfacies (Plate 7a). It is related to uplift of the basin and/or to the unconformity surface.

#### **Dedolomitization**

Dedolomitization is also among the last diagenetic events, during which the dolomite is calcitized under the prevailing diagenetic conditions, such that, the dolomitization is reversed and dolomite is converted into calcite. This diagenetic process is also termed as calcitization. It is a common phenomenon in carbonate rocks and is thought to be a recent phenomenon, most probably related to the Holocene age. The recorded dedolomitization in the Samana Suk Formation is shown in Plates 4d and 5b.

#### **Incorporation of iron into calcite and dolomite**

It is the last diagenetic setting in which the leached out iron from various sources gets incorporated into calcite (rendering it into ferroan calcite) and dolomite (rendering it into ferroan dolomite) as per demand of the prevailing environmental conditions. This setting is related with the late stage uplifting and/or unconformity surface. It is the post uplift diagenetic phase. The leached out iron is incorporated in calcite and renders it into ferroan calcite (Plate 4a). The ferroan dolomite (Plates 4a and b and 7b) is formed by the same diagenetic process.

#### **DISCUSSION**

The Samana Suk Formation was deposited as significant carbonate litho-package comprised of limestones, dolomitic limestones and dolomites along with

some siliciclastic contents in the form of shale/marl breaks. The limestones range from lime mudstones (unfossiliferous and poorly fossiliferous) to grainstones and are dolomitized at several horizons. The found dolomites are micro to macro and dedolomitized at a number of stratigraphic levels. The formation is predominantly composed of coarse grainstone microfacies, wherein a variety of diagenetic settings has been documented. These settings are represented by different cement types, neomorphic mineral products, mechanical and chemical compaction, stylolites and by the incorporation of iron in calcite and dolomites. The formation experienced a number of episodes of fracturing during its geologic history, in which swarms of fractures of different nature and size were produced. Later on these fractures were filled by secondary calcite/dolomite. This sequence of carbonate sediments is highly fossiliferous at certain levels and contains very large faunal and floral tests, shells and bioclasts approaching to coquina lithofacies. The main character of this formation exposed at the measured section is determined to be the porous and permeable coarse grained carbonate unit.

#### **CONCLUSIONS**

The conclusions drawn are given as under:

The Samana Suk Formation at this section is comprised predominantly of dolomitized limestones and dolomites frequently fractured and stylolitized along with minor shale and marl component.

The noted microfacies include bioclastic rudstones and floatstones, bioclastic, pelloidal, ooidal, cortoidal and grapestone grainstones, bioclastic and pelloidal packstones, bioclastic wackestones, bioclastic mudstones and unfossiliferous mudstones.

The component skeletal grains of the bioclastic microfacies are predominantly shells, tests and particles of benthonic foraminifers, echinoderms, mollusks, brachiopods, corals, sponges, bryozoa and algae.

The diagenetic settings were prone to produce a variety of features, like, cements from early marine to late diagenetic cements, micritization, neomorphism, different types and phases of dolomitization and dedolomitization, incorporation of iron to calcite/dolomite, compaction features and dissolution fabric.

Three hard ground surfaces have been recorded in this section at different levels. These surfaces represent the periods of non erosion/non deposition and mark regressive cycles during deposition of this formation.

The analytical studies of depositional texture and microfacies exhibit that the Samana Suk Formation was deposited in the shallow shelf open marine environments in outer and inner shelf and in lagoon.

The formation's coarse grained texture, larger dolomitic contents, highly fractured horizons and dissolution fabric point towards its reservoir potential.



## REFERENCES

- Ahmad, S., D. Mertmann and E. Manutsoglu, 1997, "Jurassic Shelf Sedimentation and Sequence Stratigraphy of the Surghar Ranges, Pakistan", *Jour. Nepal Geol. Soc.*, **15**, 15-22, Nepal
- Akhtar, M., 1983, "Stratigraphy of Surghar Range", *Geol. Bull. Punjab Uni.* **18**, 32-45, Lahore, Pakistan
- Anwar, M., Fatmi, A. M. and Hyderi, I. H., 1992, "Revised Nomenclature and Stratigraphy of Musakhel and Baroch Groups in Surghar Range, Pakistan" *Jour. of Geol.*, **1**, 15-28 Pakistan
- Bathurst, R.G.C., 1964, "The Replacement of Aragonite to Calcite in the Molluscan Shell Wall", In: *Approaches to Palaeoecology* (Ed. J. Imbrie, and N. D. Newell), John Wiley and Sons, New York 357-376, USA
- Bender, F. K. and Raza, H. A., 1995, "Geology of Pakistan", Gebruder, Borntraeger Berlin, 414 p Germany
- Cotter, G. de P., 1933, "The Geology of the Part of the Attock District, West of Longitude 72° 45' E", *India Geol. Surv. Mem.*, **55**, 63-161, Calcutta, India
- Davies, L. M., 1930, "The Fossil Fauna of the Samana Range and Some Neighbouring Areas", Part I: An Introductory Note, *Geol. Survey India, Mem. Palaeont., N. S.* **15**, 15, Calcutta, India
- Dunham, R.J., 1962, "Classification of Carbonate Rocks According to the Depositional Texture", In: *Classification of Carbonate Rocks*, *Amer. Assoc. Petrol. Geol. Mem.* **1**, 108-121, USA
- Embry, A.F. and Klovan, J.E., 1971, "A Late Devonian Reef Tract on North Eastern Banks Island, North West Territories", In: Scoffin, P.T. (1987), "An Introduction to Carbonate Sediments and Rocks", Chapman and Hall, New York 9-10 USA
- Fatmi, A. N., 1972, "Stratigraphy of the Jurassic and Lower Cretaceous rocks and Jurassic ammonites from northern areas of West Pakistan", *British Mus. Nat. Hist. Bull. (Geol.)*, **20** No. 7, 299-380 UK
- Fatmi A. N., I. H. Hyderi, and M. Anwar, 1990, "Occurrence of the Lower Jurassic Ammonoid Genus *Bouleiceras* from the Surghar Range with a Revised Nomenclature of the Mesozoic Rocks of the Salt Range and Trans Indus Ranges (Upper Indus Basin)", *Geol. Bull. Punjab Univ.*, **25**, 38-46, Pakistan
- Flügel, E., 1982, "Microfacies Analysis of Limestones", Springer-Verlag, Berlin, 633p, Germany
- Gee, E. R., 1947, "The Age of the Saline Series of the Punjab and of Kohat", *India Mat. Sci. Proc. Sec.*, **B 14**, 269-310, Calcutta, India
- Gee, E. R., 1989, "Overview of the Geology and Structure of the Salt Range with Observations on Related Areas of Northern Pakistan", In: *Tectonics of the western Himalayas* (Eds. L. L. Malinconico, and R. J. Lillie), *Geol. Soc. Amer. Spec. Papers*, **239**, 52-112, Boulder, USA
- Hemphill, W. R., and Kidwai, A. H., 1973, "Stratigraphy of the Bannu and Dera Ismail Khan areas, Pakistan", *US Geol. Surv., Prof. Paper* **716-B**, 36 USA
- Kendall, C. G. St. C. and P. A. d'E. Skipwith, 1969, "Holocene Shallow Water Carbonate and Evaporite Sediments of Khor al-Bazam, Abu Dhabi, Southwest Persian Gulf", *Bull. Amer. Ass. Petrol. Geol.*, **53**, 841-869, Tulsa, USA
- Mensink, V. H., D. Mertmann, Bochum and S. Ahmad, 1988, "Facies Development during the Jurassic of the Trans Indus Ranges, Pakistan", *N. Jb. Geol. Palaont. Mh.*, **H. 3**, 153-166, Germany
- Mertmann D. and S. Ahmad, 1994, "Shinawari and Samana Suk Formations of the Surghar and Salt Ranges, Pakistan: Facies and Depositional Environments", *Z. dt. Geol. Ges.*, **145**, 305-317, Germany
- Nizami, A. R. and R. A. Sheikh, 2007, "Microfacies analysis and diagenetic setting of the Samana Suk Formation, Chichali Nala Section, Surghar Range, Trans Indus Ranges-Pakistan", *Geol. Bull. Punjab Univ.*, **43**, 37-52 Pakistan
- Scoffin, T. P., 1987, "An Introduction to Carbonate Sediments and Rocks", Blackie and Sons, Ltd., 7-Leicester Place, London, 274p UK
- Shah, S. M. I., 1977, "Stratigraphy of Pakistan", *Mem. Geol. Surv. Pakistan*, Quetta, **12**, 138p Pakistan



- Sheikh, R. A., 1991, "Deposition and Diagenesis of the Samana Suk Formation, Kala Chitta Range, North Pakistan", *TERRA Abstracts*, An Official Journal of the European Union of Geosciences, VI, 3, No. 1, France
- Sheikh, R. A., 1992, "Deposition and Diagenesis of Mesozoic Rocks, Kala Chitta Range, Northern Pakistan", Ph.D. dissertation, Imperial College, London, 360p UK
- Spath, L. F., 1939, "The Cephalopoda of the Neocomian Belemnite Beds of Salt Range", *Indian Geol. Surv., Mem., Palaeont. Indica, New Series*, 25, No. 1, 154p, India
- Tucker, M., 1988, "Techniques in Sedimentology", Blackwell Scientific Publications, Oxford, London, 394p, UK
- Tucker, M. F. and Wright, V. P., 1990, "Carbonate Sedimentology", Blackwell Scientific Publication, Oxford, London 482p, UK
- Wilson, J. L. 1975, "Carbonate Facies in Geological History", Springer-Verlag, Berlin, 471p, Germany



# FORAMINIFERAL BIOSTRATIGRAPHY AND RECONNAISSANCE MICROFACIES OF PALEOCENE LOCKHART LIMESTONE OF JABRI AREA, HAZARA, NORTHERN PAKISTAN.

BY

S. J. SAMEENI, NAUMAN NAZIR, ADNAN ABDUL-KARIM  
Institute of Geology, University of the Punjab, Quaid-i-Azam Campus,  
Lahore-54590 Pakistan

AND

HUMAIRA NAZ  
Department of Geology, University of Sindh, Jamshoro, Pakistan.

**Abstract:-** The Lockhart Limestone of Paleocene age is well exposed in Jabri area. A section along the Lora-Maqsood road is measured and sampled for foraminiferal and microfacies studies. The total thickness is 73 meters and total 12 samples were collected at different intervals. Ten species of Benthic Foraminiferas are observed including age diagnostic *Miscellanea miscella* and *Lockhartia haimei* along with *Bigenerina* sp. and *Milliolids*. Three major types of microfacies are observed including Mudstone, Packstone and Wackstone. The variation in faunal assemblages are used to recognize subenvironments within the shelf. The age of the Lockhart Limestone on the basis of observed fauna is Thanetian (Upper Paleocene).

## INTRODUCTION

The Hazara mountains form the northern border of Potowar Basin, it is a NE-SW trending acute trough situated along the northern margin of Indo-Pakistan Plate and has been formed as a continent to continent collision. The Jabri area of southern Hazara is easily accessible from Rawalpindi-Islamabad via Ghora Gali, located on Lora-Maqsood road (long. 73° 10' 15", lat. 35° 54' 45") where rocks exposed from Jurassic to Eocene are as follows.

|            |   |
|------------|---|
| Eocene     | Margala Hill Limestone  |
| Paleocene  | Patala Formation<br>Lockhart Limestone<br>Hangu Formation       |
| Cretaceous | Kawagarh Formation<br>Lumshiwal Formation<br>Chichali Formation |
| Jurassic   | Samana Suk Formation  |

Davies (1930a) gave the name "Lockhart Limestone" to the Paleocene limestone unit in Kohat area and this name was extended by the Stratigraphic Committee

of Pakistan (Fatmi 1973) to the "Mari Limestone" of Latif (1970a) in Hazara area. Waagen and Wynne (1872) are the pioneers of the work in this area, they have explained the basic geology of this area. Wynne (1873) had worked on the geology of the northern Punjab. Wynne (1874) had explained the geology of the Murree Hills and its surroundings. Waggen (1895) had given the comprehensive study of the geology of Sirban mountains near Abbottabad. Middlemiss (1896) had given a brief description of the geology of the Hazara and Black Mountains. Pinfold (1918) had explain the structure and stratigraphy of the north western Punjab. Cotter (1933) had given a brief description of the geology around the Attock area. Eames (1952) had explained the Eocene rocks of the Western Pakistan. Latif (1970, 1970a, 1970c) had mapped the Hazara area and explained the detailed stratigraphy and micropaleontology of all rocks from Pre-Cambrian to Recent. Latif (1976) has given a comprehensive account of the micropaleontology of Gallis Group of Hazara. Butt (1972) had discussed the problems of the stratigraphic nomenclature of the Hazara area. Shahnawaz and Sameeni et. al. (1992) have describe the preliminary microfacies of the Margala Hill Limestone of Jabri area. Sameeni (1993) have given a comprehensive study of the microfauna of the Margala Hill Limestone of



Bandi area. Kamran and Sameeni et. al. (2000) explained the stratigraphy and microfauna of the Patala Formation of the Jabri area only. Munir et. al. (2006) have explained the stratigraphy and microfauna of the Paleogene rocks of Hazara and Kashmir area. First time the comprehensive study of the microfauna and reconnaissance microfacies of Lockhart Limestone of Jabri area is carried out.

## OBSERVATIONS

The Lockhart Limestone is well exposed on both sides of Harro River in Jabri area. A section on the northern bank of the river is selected for the present study (Fig-1) where its lower contact with Hangu Formation and upper contact with Patala Formation are sharp and conformable. The total thickness of Lockhart Limestone is 73 meters. Its lithology from bottom to top as observed is, in its lower part, 05 meters thick bedded dark grey, fossiliferous limestone is exposed, followed by 01 meter thick greenish grey shale having no fossils, then 14 meters thick massive, nodular, grey to dark grey fossiliferous limestone is present, 02 meters thick arenaceous unfossiliferous limestone of grey colour, 18 meters thick massive grey coloured nodular poorly fossiliferous limestone, 04 meters thick bedded limestone of grey to dark grey in colour with less fossils, 12 meters thick massive fossiliferous limestone of grey to dark grey in colour, 01 meter thick band of light grey calcareous shale with no fossils, 04 meters thick bedded fossiliferous limestone of dark grey colour, 01 meter thick band of light grey shale and at the top 01 meter thick band of dark grey sandy/shaly limestone is exposed (Fig-2). Total 12 samples were collected from bottom to top at different levels as shown in fig-2 and total 30 thin sections were prepared for micropaleontological and microfacies studies. The recorded species of foraminifera are as follows.

- *Miscellanea miscella* (d'Archaic & Haime)
- *Lockhartia haime* (Davies)
- *Lockhartia conditi* (Nuttall)
- *Lockhartia tipperi* (Davies)
- *Ranikotalia sindensis* (Davies)
- *Ranikotalia sahnii* (Davies)
- *Operculina salsa* Davies & Pinfold
- *Operculina patalensis* Davies & Pinfold
- *Assilina subspinosa* Davies & Pinfold
- *Discocyclina ranikotensis* Davies
- *Bigenerina* sp.
- *Millioides*

## SYSTEMATIC PALEONTOLOGY

*Miscellanea miscella* (d'Archaic & Haime)  
(Figs.A,B Plate 1)

*Miscellanea miscella* (d'Archiac and Haime), Pfender 1934. Bull. Soc. Geol. France, vol. IV, pp.231-235 and Text figs. 1-4, pl. 11, figs. 6-7, pl.13, figs. 2-4.

Remarks: This is the most common species present throughout the formation from bottom to top. Microspheric and megalospheric both types were observed.

*Lockhartia haime* (Davies)  
(Figs.A Plate 2)

*Lockhartia haime* (Davies) Davies & Pinfold 1937. Mem. Geol. Surv. India, Pal. Indica, New Series, vol.24(1), pl.7, figs.9-13,15.

Remarks: This species is a guide fossil for upper Paleocene rocks so very common in this formation from bottom to top.

*Lockhartia conditi* (Nuttall)  
(Figs. B,D Plate 2)

*Lockhartia conditi* (Nuttall) Davies 1932. Trans. Roy. Soc. Edin. Vol.57Pl. 2, fig. 7; Pl. 4, fig.7.

Remarks: This species is common to upper Paleocene and lower Eocene and is observed throughout the formation from bottom to top.

*Lockhartia tipperi* (Davies)  
(Figs. D Plate 3)

*Lockhartia tipperi* (Davies) Davies 1932. Trans. Roy. Soc. Edin., vol. 57.

Remarks: This species is recorded from the upper half of the formation where it is common.

*Ranikotalia sindensis* (Davies)  
(Figs.C,D,E Plate 1)

*Nummulites sindensis* (Davies), Davies & Pinfold 1937. Mem. Geol. Surv. India, Pal. Indica, New Series, vol.24(1), pl.4, fig. 21.

Remarks: This species is common to the upper Paleocene and lower Eocene deposits and recorded from the formation from bottom to top.

*Ranikotalia sahnii* (Davies)  
(Figs. A,B Plate 3)

*Nummulites sahnii* Davies 1927, Quart. Journ. Geol.Soc. Lond, vol.83, pl. 19, figs.10-13.

Remarks: This species is not so common, only recorded from the middle upper part of the formation.

*Operculina salsa* Davies & Pinfold  
(Figs. C Plate 3)

*Operculina salsa* Davies & Pinfold 1937. Mem. Geol. Surv. India, Pal. Indica, New Series, vol.24(1), pl.5, figs. 1,3, 7,10,15.

Remarks: This species is recorded from the upper part of the formation.



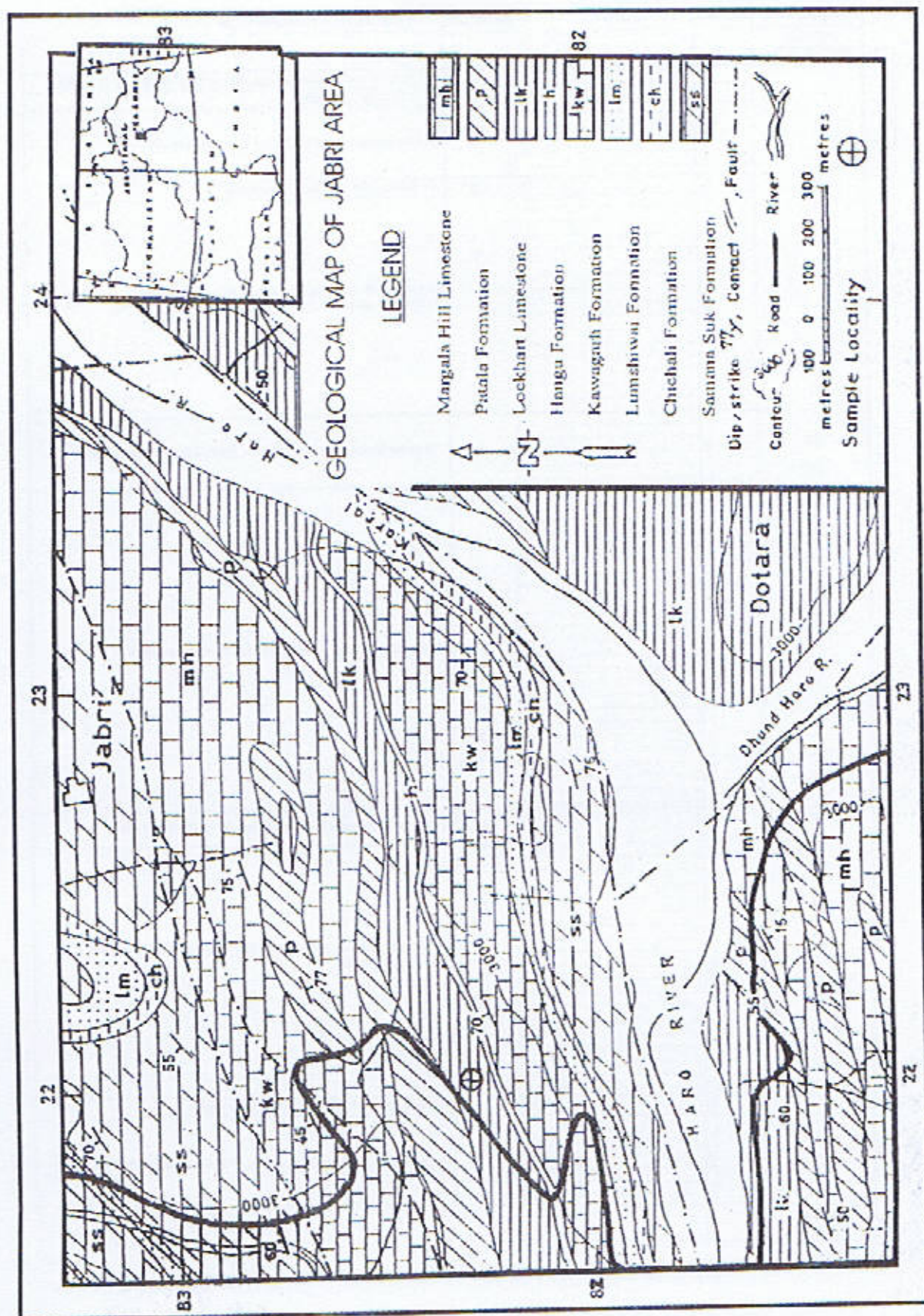


Fig. 1.



| FORMATIONS         | METERS | LITHOLOGY | SAMPLES | LITHOLOGIC DESCRIPTION   |
|--------------------|--------|-----------|---------|--|
| PATALA FORMATION   |        |           |         |  |
| LOCKHART LIMESTONE | 01     |           | ●       | 01 m thick poorly fossiliferous dark grey shaly/sandy limestone                        |
|                    | 01     |           | ●       | 01 m thick light grey shale.   |
|                    | 04     |           | ●       | 04 thick bedded limestone of dark grey colour fossiliferous                            |
|                    | 01     |           | ●       | 01 m thick light grey calcareous shale   |
|                    | 12     |           | ●       | 12 meter thick, massive fossiliferous limestone of grey to dark grey in colour         |
|                    | 04     |           | ●       | 04 meter thick bedded grey in color, fossiliferous of grey to dark                     |
|                    | 18     |           | ●       | 18 m thick massive nodular poorly fossiliferous limestone                              |
|                    | 2      |           | ●       | 2 m thick arenaceous grey colour limestone unfossiliferous.                            |
|                    | 14     |           | ●       | 14 m thick Massive, grey to dark grey limestone slightly nodular, having less fossils. |
|                    | 1      |           | ●       | 1m thick greenish grey shale having no fossils.  |
|                    | 6      |           | ●       | Thick bedded fossiliferous limestone of dark grey colour 6 meter thick.                |
| PATALA FORMATION   |        |           |         |  |

Fig. 2. Stratigraphic column of Lockhart limestone, Jabri, Hazara



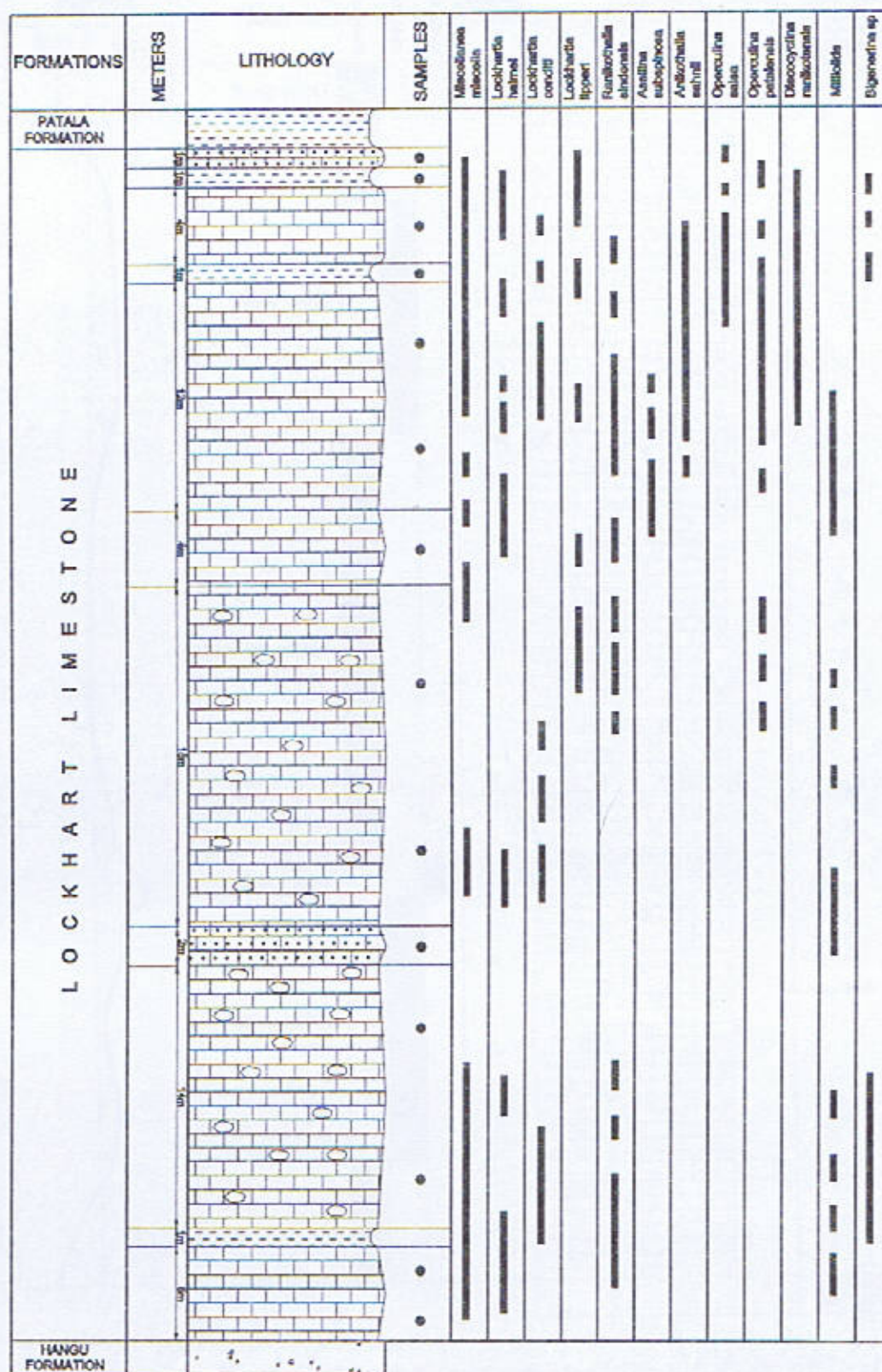


Fig. 3. Vertical range of Formation recorded in Lockhart limestone, Jabri, Hazara



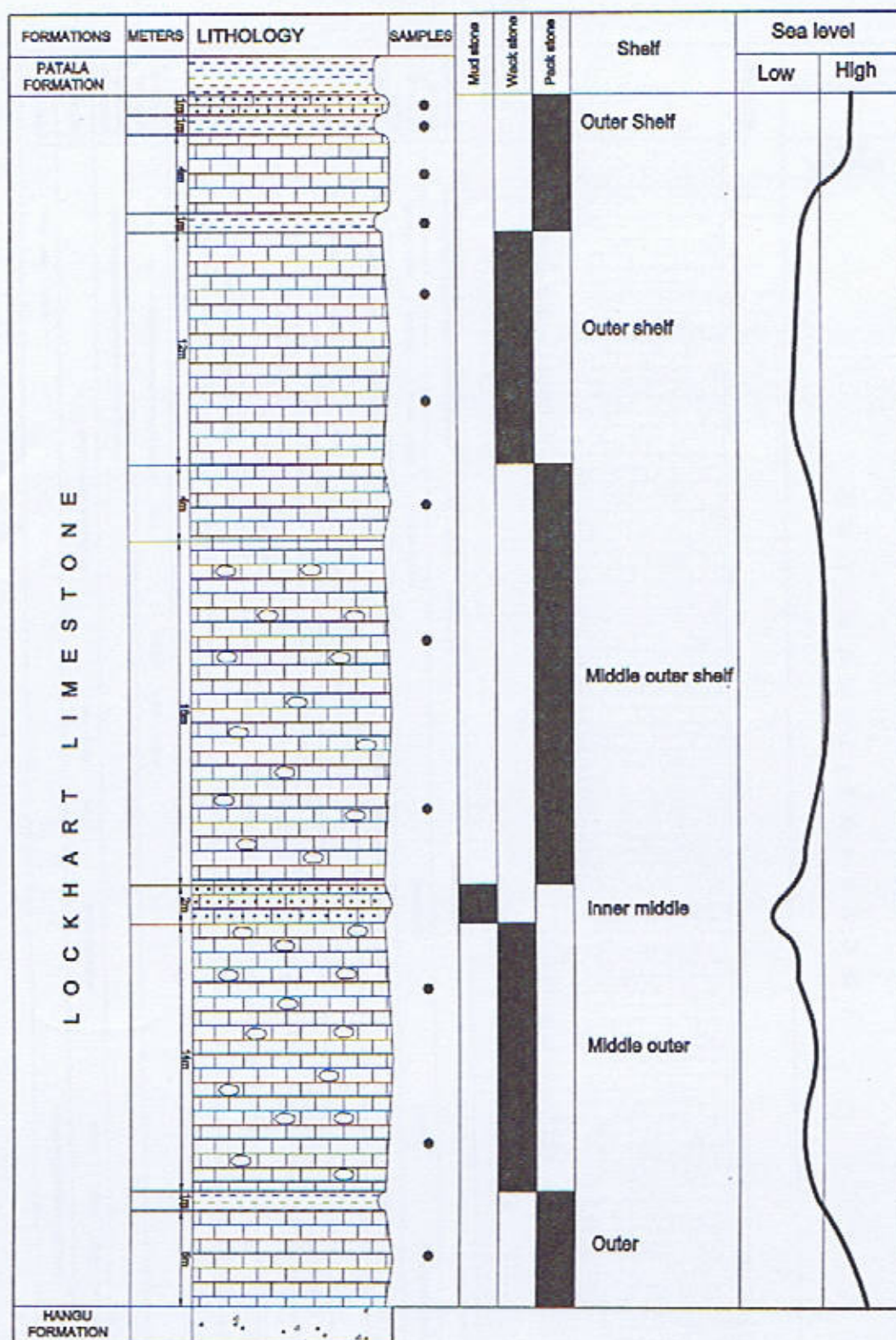


Fig. 4. Showing the microfacies and interperception of subenvironments within the shelf of Lockhart limestone, Jabri, Hazara



## DESCRIPTION OF PLATES

## Plate-1

- A, B *Miscellanea miscella* (d'Archaic & Haime)  
 C, D *Ranikothalia sindensis* (Davies)  
 E Upper- *Ranikothalia sindensis* (Davies)  
 Lower left- *Ranikothalia sahnii* (Davies)  
 Lower right- *Lockhartia tipperi* (Davies)

## Plate-2

- A *Lockhartia haimei* (Davies)  
 B, D *Lockhartia conditi* (Nuttall)  
 C Milliolid  
 E *Operculina patalensis* Davies & Pinfold  
 F *Assilina subspinoso* Davies & Pinfold  
 G *Discocyclina ranikotensis* Davies

## Plate-3

- A, B *Ranikothalia sahnii* (Davies)  
 C *Operculina salsa* Davies & Pinfold  
 D *Lockhartia tipperi* (Davies)  
 E *Bigenerina* sp.  
 F *Discocyclina ranikotensis* Davies

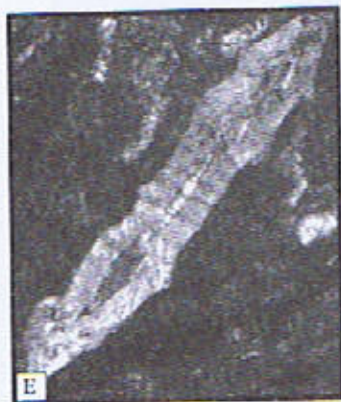
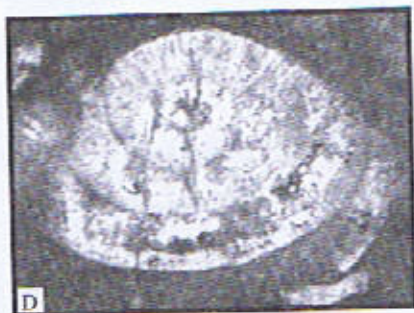
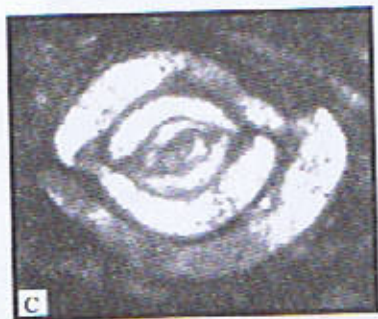
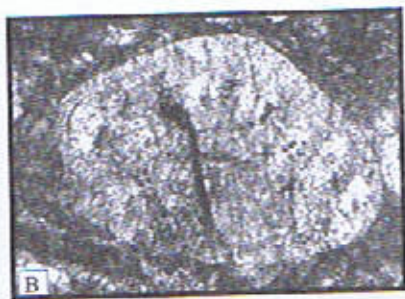


## Plate-1



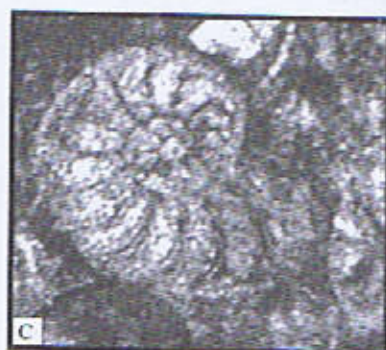
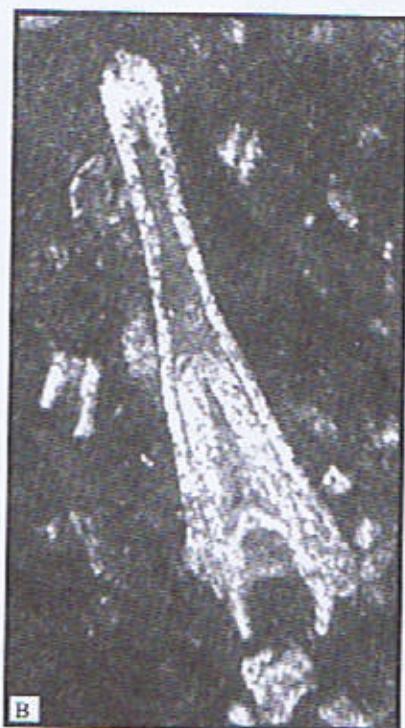


Plate-2





## Plate-3





*Operculina patalensis* Davies & Pinfold  
( Figs. E Plate 2 )

*Operculina patalensis* Davies & Pinfold 1937. Mem. Geol. Surv. India, Pal. Indica, New Series, vol.24(1), pl.5, figs. 6, 17-19, 26.

Remarks: This species is recorded only from the upper most part of the formation.

*Assilina subspinosus* Davies & Pinfold  
( Figs. F Plate 2 )

*Assilina subspinosus* Davies & Pinfold 1937. Mem. Geol. Surv. India, Pal. Indica New Series, vol.24(1), pl.4, figs. 19-20, 23-26.

Remarks: This species is recorded from the middle and upper part of the formation.

*Bigenerina* sp.  
( Fig.E Plate 3 )

Remarks: These are observed only in the upper most part of the formation.

Millioliids  
(Fig.C Plate 2)

Remarks: Millioliids are present in the lower and middle part of the formation.

## CONCLUSION

Ten species of larger foraminifera are recorded from the formation along with millioliids and *Bigenerina* sp. which confirm the Thanetian (Upper Paleocene) age of the Loickhart Limestone. The larger foraminifera are known to characterize the shallow shelf carbonate environments. The variation in faunal assemblage is used to recognize the subenvironments within the shelf, based on the salinity tolerance and habitat of various association of fauna. These subenvironments include inner, middle and outer shelf (Fig.4) where three major type of microfacies are deposited, these are Mudstone, Packstone, and Wackstone.

## REFERENCES

- Butt, A.A. 1972: Problems of stratigraphic nomenclature in the Hazara Distt. N.W.F.P Pakistan. *Punjab University Geol. Bull.* 965-69
- Cotter, G. de P., 1933: The geology of the part of the Attock Distt. *Indian Geol. Surv. Mem.*, 55 63-161
- Davies, L. M., 1930a: The fossil fauna of the Samana Range and some neighbouring area; Part 6, The Paleocene Foraminifera. *Ibid., Mem., Paleont., Indica, New Series, v. 15*, 13p.
- Eames, F.E., 1952a: A contribution to the study of Eocene in the western Pakistan and western India. Part A The geology of standard sections in the western Punjab and in the Kohat Distt., *Geol. Soc. London, Quart. Jour.* 107, 159-172
- Eames F.E. 1952b: A contribution to the study of the Eocene in the western Pakistan and western India. Part B. Description of the faunas of the certain sections and their bearings on the classification and correlation of the Eocene in western Pakistan and western India *Ibid.* 107, 2:173-200.
- Fatmi, A.N. 1973: Lithostratigraphic units of the Kohat-Potwar Province Indus Basin, Pakistan *Mem. Geol. Surv. Pakistan*, 10, 180.
- Latif, M.A. 1970: Explanatory notes on the geology of the southeastern Hazara to accompany the revised geological map- *Jahrb. Geol. Bundesanst.* 15:25-61
- Latif, M.A. 1970a: Explanatory notes on the geology of southern Hazara, to accompany the revised geological map. *Wein Jahrb. Geol. B.A; Sonderb.* 15, 5-20.
- Latif, M.A. 1976: Stratigraphy and micropaleontology of the Galis group of Hazara to Accompany the revised geological map- *Jahrb. Geol. Bull. Punjab University*, 13:1-63
- Middlemiss, C.S., 1896: The geology of Hazara and black mountain *Mem. Geol. Surv. India*, 26, 1-302.
- Mirza, K., Sameeni, S.J., Rashid, S., 2000: Biostratigraphy of the Patala Formation, Jabri area, Hazara, Pakistan. *Geol. Bull. Punj. Univ.* 35, 89-94.
- Munir, H.M. Baig M.S., 2006: Paleogene biostratigraphy of Thattapani, Kotli, Azad Kashmir, northwest sub-Himalayas, Pakistan. *Jour. Himalayan Earth Sc.* 39, 39-48.
- Pinfold, E. S., (1918): Note on structure and stratigraphy in the north-west Punjab; *India Geol. Surv., Recs.*, 3, 137-160.



- Sameeni, S.J. (1993): Microfaunal studies of the Lower Eocene Margala Hill Limestone of the Bandi area, Hazara, Pakistan. *Pak J Geol* **2**(2) & #1) 43-50
- Shahnawaz, R. Sameeni, S.J. et al. 1992: Reconnaissance microfacies studies of the Margala hills Limestone of the Jabri area, southern Hazara Pakistan *jour. Hydrocarbon*, **1**&**2** 53-62
- Shah S.M. I., 1977: Stratigraphy of Pakistan., *Geol Surv. Pak. Mem* **12**, 1-183
- Waagen, W., 1872: Rough section showing the relation of the rocks near Mari (Murree) Punjab. *Mem. Geol. Surv. India*, **5**, (Part-I), 15-18.
- Waagen W and Wynne A.B. 1872: The geology of mount Sirban in Upper Punjab. *Ibid Mem* **9**, 331-350
- Wiess W., 1993: Age Assignment of larger foraminiferal assemblages of Maastrichtian to Eocene age in the norther Pakistan. *Zitteliana* **20**:223-252
- Wynne A B., 1873: Notes from the progress of report on the geology of parts of upper Punjab., *Indian Geol Surv. Recs* **7**(3):59-64
- Wynne A B., 1874: Notes from the progress of report on the geology of parts of upper Punjab., *Indian Geol Surv. Recs.*, **6** (3)64-74
- Wynne A.b., 1877 Notes on the tertiary zone and underlying rocks in the northwest Punjab., *India Geol surv. Recs* **6** (3)59-6, *Geol. Surv. India*, **26**(1) 1-290.



# ENGINEERING PROPERTIES OF POTENTIAL AGGREGATE RESOURCES FROM EASTERN AND CENTRAL SALT RANGE, PAKISTAN

BY

MUHAMMAD MUNAWAR IQBAL GONDAL

Road Research and Material Testing Institute, New Campus, Lahore-54590

NAVEED AHSAN

Institute of Geology, University of the Punjab, Quaid-i-Azam Campus,  
Lahore-54590 Pakistan

AND

AHMAD ZIA JAVID

Road Research and Material Testing Institute, New Campus, Lahore-54590

**Abstract:** A colossal quantity of aggregates derived from rocks and natural gravel are extensively used in the construction of infrastructures. The engineering properties of these aggregates determine their in-service performance. Jutana Formation, Sakeasar Limestone and gravels deposited by streams in Jabbi-Warchha and Katha Saghrul area are crushed for use in ordinary Portland cement and asphalt concrete, unbound and bound pavements, railway ballast and riprap. Present study evaluates engineering properties of these local coarse aggregates for use in roads and concrete. The physical properties of aggregates like specific gravity (2.65), water absorption (0.739%), soundness (4.06%), Los Angeles abrasion value (24.48%), California Bearing Ratio (90.10%) and coating and stripping values conform to available standards thereby indicating that these aggregate deposits are potential aggregate sources for mega projects in the Punjab province.

## INTRODUCTION

Pakistan has an area of 803,950 Sq-Km and a population of around 160 Millions that use 228,206 km of road network through out the country. In 1990s, the then Government took initiative to remodel and reconstruct all the National Highways of Pakistan to provide safe and efficient communication network. In general it is believed that better roads are considered as an imperative component of the Government's poverty alleviation approaches that operate as a mechanism to create jobs (Khan, 2008). According to careful estimates, the transport sector contributes about 10% of total GDP of Pakistan by providing work for about 2 million people and transporting over 90% passengers and goods by roads.

For road construction a large quantity of aggregates (Smith and Collis, 1993) is a prerequisite. In Pakistan, aggregates are produced mainly by quarrying rocks and then crushing (Ahsan et al., 2000, 2000a;

Chaudhry et al., 2000) to required sizes for use in ordinary Portland cement concrete, base, sub base, asphalt concrete, water bound macadam, railway ballast, riprap and fillers. Besides these, gravel and sand produced by natural processes is also used as aggregate (e.g. Neville and Brooks, 1999; Kandhal et al., 2000; Zadi et al., 2008). The in-service performance of above mentioned structures is bracketed with the engineering properties of the aggregate (Neville, 2000). The present study deals with the evaluation of aggregates available in Ara-Basharat-Garibwal area (Jhelum and Chakwal districts), Jabbi-Warchha gravel fan and Katha Saghrul area (district Khushab) for use in ordinary Portland cement, base, sub base and asphalt concrete.

## ARA-BASHARAT-GARIBWAL AREA

### Location and accessibility

The Ara-Basharat-Garibwal area (lat. 32° 40' to 32° 45'N; long. 73° 10' to 73° 25' E, Fig 1) is accessible through Pind Daden (P.D) Khan-Jhelum road and Head Rasool to



Kharian road. Two roads off take from P.D. Khan-Jhelum road, one at Dharyala/Chak Mujahid to Rawal and Ara and the second from P.D. Khan to Gharibwal via Saawal. These roads are in process of widening/improvement.

Presently, a few small crushers located in Chakwal district are potential aggregate source for the area. Besides these, Irrigation Department and Pakistan Railway is using uncrushed and crushed stone aggregate picked from various Nullahs as riprap and rail road ballast, respectively. However, these sources are unable to meet the huge requirements of road sector.

The samples (Smith and Collis, 1993; Baker, and Hendy, 2005) of rock pieces and crush were collected from Irrigation quarry stack, Gharibwal cement factory crushers, from rock out crops falling along the route alignment of Basharat-Ara-Rawal road and railway crusher at Rawal village on Chak Mujahid-Gharibwal factory road.

### Geology

The Salt Range forms steep cliffs and scarps that rise abruptly from the Punjab Plains (Kazmi and Jan, 1997) to the south whereas to the north these slopes are gentler and wide and form hogbacks and cuestas. The rocks exposed in the area (Shah, 1977) belong to Salt Range Formation, Khewra Sandstone, Kussak Formation, Jutana Formation, Baghanwala Formation and Tobra Formation. At places these units are overlain by Tertiary sequence comprised of limestones and shales (Shah, 1977). Besides other localities, in the present study samples were also taken from Jutana Formation and Sakesar Limestone outcrops.

Jutana Formation, Early Mid. Cambrian Late Early Cambrian in age, is composed of cliff forming thick bedded to massive brownish weathering, cream colored to yellowish white sand dolomites to dolomitic sand stone with few shale intercalations. Thickness of this unit at village Jutana/Gharibwal cement factory is 75-90 meter thick. It runs right from Jalalpur to this area at the same level. Pakistan Railway and Punjab Irrigation Department quarries are located in this unit. Sakesar Limestone, early Eocene in age, consists of light grey to off white/cream colour nodular to massive limestone beds (Shah, 1977; Boustani, 2000). In this area it forms hogbacks and cuestas along with steep cliffs. It occurred all along the northern slopes i.e. dip slopes of the Salt Range. The exposures of these limestones are in kilometers width.

## JABBI- WARCHHA AND KATHA SAGHRAL AREA

### Location and accessibility

The potential quarry area of Jabbi-Warcha (lat.  $32^{\circ} 21'$  to  $32^{\circ} 26' N$ ; long.  $72^{\circ} 00'$  to  $72^{\circ} 07' E$ ) and Katha Saghral (latitude  $32^{\circ} 32' N$ ; long.  $72^{\circ} 27' E$ ) are well connected and accessible through existing road network. A 24 feet wide metalled road off takes from Mitha Tiwana at Khushab-Mianwali road and after traversing through plain area leads to Jabbi at 13km distance. The same road with single carriageway turned toward Dhokari, Choa Warchha, and Joins with Qaidabad Warchha road developing a loop with Khushab Mianwali road. The section from Jabbi to Warchha runs over gravel terrace nearly parallel to the Salt Range hills. Punjab Highway Department used hand broken and crushed sub base and base course aggregate from quarries located in Jabbi-Choa-Warchha area for the construction of Khushab-Mianwali road in Khushab district.

At present three small crushers with 2000-3500 ft<sup>3</sup> per day crushing capacity are working in the vicinity of Jabbi. In Katha Saghral area the gravel is manually picked/mined from nullah bed and transported to the crushers. In this area two crushers with the crushing capacity of 1500 to 3500 ft<sup>3</sup> per day are operative. The aggregate is reported to be produced by Pakistan Atomic Energy Commission for its construction works. In addition to this the crushed gravel aggregate is also used for mortar and reinforced concrete in adjoining areas.

The samples of pit run gravel, large sized boulders were collected from nullah bed and gravel fan area, whereas crush samples were collected from the crushing plants installed at Khushab-Chakwal road in Katha Saghral area and crushers located at Jabbi on Jabbi-Mitha-Tiwana road.

### Geology

The relief of the Salt Range in this area varied from 300m to 1522m (Sakesar peak) and 1242m (Khura). The rock units range in age from Eo-Cambrian to Paleogene (Shah, 1977; Kazmi and Jan, 1998) and are comprised of shale, sandstone, limestone, dolomitic limestone, dolomitic sandstones and dolomite. Jabbi to Choa Warchha area is severely disturbed due to diapiric folding. Various small-scale faults are associated with these folds, which resulted into sever rock shattering into blocks, boulders and gravels. Surrakha Wahan and Choa Nullah traverse through this severely shattered area and form alluvial fans.

Jabbi to Warchha fan deposits are one of the largest gravel terraces on the southern side of the Salt Range. These deposits comprise light gray, creamish to off white coloured limestones with subordinate off white quartzite, minor reddish coloured sandstone, dolomitic sandstone and sandy dolomite. The fine ratio in pit-run gravel varies from 4 to 30%. The width



of Jabbi-Warchha gravel fan area varied from 1.5 km to 2.5km approximately and its vertical extent is more than 100 feet.

Similarly, the fan area along the Salt Range in Katha Saghral - Katha Misral is relatively narrow ( $\frac{1}{2}$  km to 1km in width) however large quantity of gravels are deposited in the bed of both these kathas. The gravel fan of Jabbi-Warchha area and gravel terraces of Katha Saghral-Misral are formed by deposition of sub-spherical to sub-angular boulders/gravels shed from adjoining severely shattered Salt Range hills by hill torrents during monsoon.

## LABORATORY TESTING

Characterization of aggregate is of prime importance in selection of good quality and performance bound aggregate for use in construction industry (Fookes et al., 1988; Kandhal and Parker, 1998; Ahsan et al., 2000; Chaudhry et al., 2000, 2006). In order to meet the required standards specific gravity and water absorption (AASHTO T-85), sodium sulphate soundness (AASHTO T-104), Los Angeles abrasion value (AASHTO T-96), modified proctor test (AASHTO T-180), California Bearing Ratio (CBR, AASHTO T-193) and coating and stripping test with 60/70 and 80/100 bitumen (AASHTO T-182) were conducted for determination of physical properties of aggregates of Ara-Basharat-Garibwal area (Jhelum and Chakwal districts), Jabbi- Warchha gravel fan and Katha Saghral area (district Khushab). In addition to this petrographical evaluation of these aggregates were carried out to predict alkali aggregate reaction potential (Navelli, 2000; Chaudhry et al., 2000, 2006).

In the present studies 18 samples from crushers, plants, outcrops and gravel pits were collected to evaluate engineering properties following the test procedures mentioned in the published literature (e.g. AASHTO). Each sample was tested thrice to minimize the error and ensure error free results. However, average of three tests is given against each sample and results are presented in Table 1.

### Specific Gravity and Water Absorption (AASHTO T-85)

Specific gravity is considered a ratio of density of material to density of water and water absorption determines the amount of water that an aggregate can absorb. Specific gravity of crushed aggregate ranges from 2.62 to 2.70 (mean = 2.65) whereas the water absorption varied from 0.445% to 1.308% (mean = 0.739%). All the 18 samples indicate more or less same value of specific gravity while in case of water absorption the samples belonging to Sakesar Limestone

outcrops and Katha Misral pit-run gravel show higher water absorption values. No limit for specific gravity has been specified in the published literature (AASHTO T-85-88; NHA, 1998). In all the samples the water absorption was found well within 2% specified limits (AASHTO T-85-88; NHA, 1998).

### Soundness Test (AASHTO T-104)

This test method is helpful in accessing the soundness/performance of aggregates during intense weathering action (e.g. freeze and thaw, attacks by various salts, etc) especially in the absence of in service records of the aggregates. The %age values obtained after completion of 5 cycles of immersion in the  $\text{Na}_2\text{SO}_4$  solution and subsequently drying ranges from 2.15 to 8.47% (mean is 4.06%) against specified maximum limit of 12% for base course and 10% (maximum) for cement concrete jobs. Two samples obtained from Sakesar Limestone outcrop and railway quarry show a relatively higher value of soundness but within limits mentioned in literature as compared to the other crushed aggregates probably due to insitu weathering.

### Los Angeles Abrasion Test (AASHTO T-96)

In order to work out the toughness and durability of crushed aggregate, Los Angeles abrasion test is recommended in the published literature. The Los Angeles abrasion values (LAV) ranges from 18.60% to 29.40% (mean = 24.48%). The samples collected from Gharibwal cement factory crushers show minimum LAV whereas samples collected from Jabbi, railway crusher, Chukki Whan and Khata Saghral show slightly higher LAVs (27.8% to 29.4%), though within safe limits, as compared to other samples. Mostly pit run gravel indicate such higher values as they contain the boulders derived from both competent and incompetent lithologies. The maximum allowed LAVs of aggregates for sub-base, base course and ordinary Portland cement and asphalt concrete are 50%, 40% and 35%, respectively.

### Modified Proctor Test (AASHTO T-180)

This test is a pre-requisite for executing good quality civil projects specially roads. The samples were tested to evaluate the maximum dry density and optimum moisture content on ratio of 75% coarse and 25% fine. The value of maximum dry density for sub-base ranges from 143.0 lb ft<sup>-3</sup> to 144.8 lb ft<sup>-3</sup> (mean = 144.3 lb ft<sup>-3</sup>) whereas value of maximum dry density for base course varies from 2.227 lb ft<sup>-3</sup> to 2.414 lb ft<sup>-3</sup> (mean = 2.315 lb ft<sup>-3</sup>). The optimum moisture content for these samples varies from 5.4% to 5.6% (mean value is 5.5%).

### CBR Value (AASHTO T-193)

This test method is intended for determination of bearing value of material when subjected to intense loading. Therefore to assess the strength of material under load, CBR test procedure was carried out at 100% compaction level under soaked conditions. The coarse and fine ratios were combined,



**Table 1**  
Engineering Properties of Potential Aggregate Resources from Eastern and Central Salt Range

| Description  | Specific Gravity | Water Absorption % | Sulphate Soundness % | Los Angles Abrasion Value% | Max. Lab. Density pcf | Optimum Moisture Content% | CBR Value %     |  | Area coated 60/70 Grade Bitumen Immersion in water (16-18 hrs) | Area coated 80/100 Grade Bitumen Immersion in water (16-18 hrs) |
|--|------------------|--------------------|----------------------|----------------------------|-----------------------|---------------------------|-----------------|--|--|---|
|  |                  |                    |                      |                            |                       |                           | 100% compaction |  |  |   |
| Surrakha wahan pit-run gravel                                    | 2.67             | 0.588              | 4.42                 | 26.6                       | 144.5                 | 5.4                       | 95.8            |  | Above 95%  | Above 95%   |
| Chukki wahan pit-run gravel                                      | 2.67             | 0.551              | 3.56                 | 27.2                       | 143.0                 | 5.5                       | 96.2            |  | Above 95%  | Above 95%   |
| Chukki wahan boulder   | 2.66             | 0.612              | 3.45                 | 27.1                       | 144.2                 | 5.6                       | 90.2            |  | Above 95%  | Above 95%   |
| Jabbi boulder  | 2.65             | 0.659              | 3.44                 | 28.9                       | 144.5                 | 5.5                       | 83.5            |  | Above 95%  | Above 95%   |
| Jabbi boulder 1  | 2.65             | 0.659              | 3.45                 | 29.4                       | 144.8                 | 5.6                       | 83.4            |  | Above 95%  | Above 95%   |
| Crush (Dr. Hidayat crusher) Jabbi-Mitha Tiwana Road              | 2.66             | 0.586              | 4.28                 | 24.8                       | 144.6                 | 5.4                       | 85.2            |  | Above 95%  | Above 95%   |
| Katha Saghrul pit-run gravel                                     | 2.67             | 0.556              | 4.25                 | 27.3                       | 144.3                 | 5.4                       | 94.1            |  | Above 95%  | Above 95%   |
| Katha Saghrul pit-run gravel A                                   | 2.66             | 0.610              | 4.20                 | 27.6                       | 144.7                 | 5.4                       | 94.2            |  | Above 95%  | Above 95%   |
| Crush (Dr. Hidayat crusher) Katha Saghrul (Khushab Chakwal Road) | 2.66             | 0.920              | 2.15                 | 26.6                       | 144.8                 | 5.5                       | 91.4            |  | Above 95%  | Above 95%   |
| Katha Misral pit-run gravel                                      | 2.65             | 1.218              | 4.36                 | 25.9                       | 144.0                 | 5.6                       | 90.3            |  | Above 95%  | Above 95%   |
| Delomite rock Irrigation Quarry                                  | 2.70             | 0.557              | 4.24                 | 2.61                       | 144.5                 | 5.4                       | 89.9            |  | Above 95%  | Above 95%   |
| Crush Gharibwal cement factory crusher                           | 2.67             | 0.541              | 3.52                 | 20.6                       | 143.0                 | 5.4                       | 91.1            |  | Above 95%  | Above 95%   |
| Crush Gharibwal cement factory crusher                           | 2.68             | 0.445              | 3.67                 | 18.6                       | 144.2                 | 5.5                       | 88.7            |  | Above 95%  | Above 95%   |
| Sakesar lime stone outcrop                                       | 2.66             | 1.117              | 3.46                 | 24.8                       | 144.8                 | 5.6                       | 94.7            |  | Above 95%  | Above 95%   |
| Sakesar lime stone outcrop                                       | 2.62             | 1.020              | 3.11                 | 24.0                       | 144.6                 | 5.5                       | 94.1            |  | Above 95%  | Above 95%   |
| Sakesar lime stone outcrop                                       | 2.64             | 1.308              | 3.86                 | 25.4                       | 144.3                 | 5.6                       | 90.2            |  | Above 95%  | Above 95%   |
| Sakesar lime stone outcrop                                       | 2.65             | 0.690              | 8.47                 | 25.6                       | 144.8                 | 5.6                       | 83.4            |  | Above 95%  | Above 95%   |
| Mixed crush Railway crusher                                      | 2.65             | 0.671              | 5.21                 | 27.8                       | 144.0                 | 5.6                       | 85.2            |  | Above 95%  | Above 95%   |



as they were available in natural deposits. The values ranged from 83.4% to 96.2% at 100% compaction. The normal requirement specified by AASHTO for sub-base and base course is 30% and 80% at 100% compaction, respectively.

#### **Coating and Stripping of Bitumen-Aggregate Mixture (AASHTO T-182)**

This test is primarily conducted to counter check the petrographic analysis towards adhesive properties of certain grade asphalt. Usually it is conducted under typical laboratory conditions following standard specifications, however it may also be conducted at actual temperature prevailing at road surface during extreme hot conditions. Sixteen samples of crush were tested for determining their ability to retain bituminous film (AASHTO T-182) method, in case of 80/100 and 60/70 grade bitumen all the samples at 25°C qualified the test requirements depicting values greater than 95%.

#### **Alkali aggregate reaction potential (ASTM C-295)**

Alkali aggregate reaction is considered a reaction between alkalis in cement and certain rock aggregates (e.g. Smith and Collis, 2001). Besides other engineering properties, petrographic testing is a microscopic examination that evaluates the aggregate material (French, 1991) in respect of deleterious alkali aggregate reaction potential that is believed to be one of the major cause of deterioration in hardened concrete (Lopez-Buendia et al., 2006). Petrographically, Sakeasar Limestone is composed of carbonate, quartz (upto 0.5%) that shows normal optics, hematite/limonite ( $\approx 0.5$ ), clay ( $\approx 1.0\%$ ) and minor dolomite (less than 0.5%). Percentages of constituent minerals indicate that the rock can safely be used as an aggregate with ordinary Portland cement and high alkali cement. Although, crushed rock aggregate of Ghraibwal area contains about 6% quartz but it is non-deleterious as quartz shows normal optics.

Besides these observations, modal analysis of crushed rock aggregates of Jabbi-Warchha area shows the presence of about 2.1% quartzwackes that indicates its potentially deleterious character when used with ordinary Portland cement and high alkali cement. Moreover, Jutana Formation composed of dolomite may show alkali carbonate reaction potential with ordinary Portland cement.

#### **DISCUSSION**

The Jutana Formation is composed of sandy dolomite, dolomitic sandstone, hard and tough to hammer. The physical and petrographical results show that aggregate derived from this formation is suitable

for road sub base and base course. Because of hydrophobic character reflected by above mentioned 95% adhesion value, it gives an excellent binding with bitumen when used in asphalt wearing course. In addition to this Jutana Formation aggregate will provide anti-skidding characteristics to asphalt wearing course as reflected by less polishing value. It is an excellent dimension stone for building construction however, it may not be suitable as cement concrete aggregate due presence of dolomite that may trigger potentially deleterious alkali carbonate reaction.

Sakeasar Limestone outcrops on the back slopes of Salt Range escarpment. It is exposed in a very large area of Bashart and Ara Union Councils. In Basharat Union Council area Sakeasar Limestone outcrops are a potential source of raw material for Ghariwal cement factory that has established its crusher at Sirhadi above village Jutana. However, Sakeasar Limestone outcrops in Ara Union Council has not been leased out by the Mine and Mineral Department, Govt. of Punjab. The engineering properties of the Sakeasar Limestone indicate that this lithostratigraphic unit is hard, tough, and durable with excellent strength properties and being hydrophobic in nature it gives good adhesion characteristics. Therefore this formation is suitable for road sub base, base course, Ordinary Portland cement concrete (PCC/RCC), riprap and railway ballast. However in Ara Union Council area and where substantial reserves of the formation are available, careful planning is required to develop quarries for local construction industry.

Both above described rock units could be mined through open pit excavation. In case of quarrying of Sakeasar Limestone, "the principle potential aggregate source", in Ara Union Council area, the land is required to be reclaimed, which is not just a requirement of environmental protection and conservation but an essential part of financial planning and overall viability of aggregate production. The underlying rock/sediments comprise Patala Formation (Shah, 1977) composed dominantly of shales, so the pits and quarries can successfully be used for agriculture as well as for forestry purpose. Presently the major vegetation is restricted to the shale outcrops and limestone shows sporadic vegetation.

This potential aggregate source area may be developed for quarrying activity either by Govt. or private sector or as a joint venture. It will serve as a cheap and durable aggregate source for civil construction works for Chakwal, Jhelum, Gujrat, Mandi Baha-ud-Din, Gujranwala, Sialkot, Sheikhupura, Lahore and Kasur Districts. These areas are major aggregate consumers since major industrialization is taking place in these areas.

The engineering properties of crushed gravel of Jabbi-Warchha area and Katha Saghr-al-Misral revealed that it qualifies all specified limits indicated in AASHTO for sub base and base course. These deposits predominately comprise hydrophobic carbonaceous rocks (limestone/dolomite) which is



further supplemented by good adhesion with bitumen of 60/70 and 80/100 grade. The hydrophobic nature and good adhesion with bitumen suggests that the crush of these deposits can safely be used in asphalt concrete and surfacing work (Triple surface treatment). The presence of minor impurities like quartzite when crushed along with limestone will act as good anti-skidding material for road surface. The calcitic composition of rock clasts crushed aggregate strongly recommends its use in cement concrete work.

Due to inadequate crushing facility, presently it is not an approved aggregate source of Highway Department for base, asphalt concrete, surfacing and cement concrete. The area under study has good potential for open pit mining and crushers can be installed in gravel fan area of Jabbi-Choa Warchha section as well as along the terraces of both Katha Saghrat and Jabbi Warchha area. The operation cost of crushing activity will be less if plant is installed close to or on to the deposits. These potential quarry sites are easily accessible through existing road network. Moreover, it is strongly suggested that environment friendly quarrying and crushing procedures may be applied.

The area in general is barren with sporadic vegetation due to poor rainfall. The local population has very limited economic activity. If these quarries are developed as potential resources of construction materials, it will definitely serve the needs of public and private sector construction activity in district Khushab, Bhakkar and part of Mianwali. Due to exploitation of

this natural resource, there will be drastic change in the socio-economic conditions of the local populace.

## RECOMMENDATIONS

1. The coarse and fine fraction of both Jutana Formation and Sakesar limestone are suitable aggregates for road construction. However in ordinary Portland cement concrete aggregates derived from Sakesar Limestone should be used.
2. The coarse and fine fraction of gravel from Katha-Saghrat and Jabbi- Warchha qualifies in strength, durability and other associated tests. They are recommended for use in construction works. However, Jabbi- Warchha gravel contains greywackys that have potential for deleterious alkali silica reaction.
3. The pit-run gravel after bringing it into proper grade and size should be used as sub base and base material.
4. For Lahore Sheikhupura, Kasur, Gujranwala, Sialkot, Wazirabad, Gujrat, Mandi Bauha-ud-Din, etc. these aggregates are cheap due to less transportation cost as compared to Kirana Hills and Margalla Hills aggregates.
5. They show excellent bitumen affinity so they are more suitable for road surfacing.
6. The mining should be done with environment friendly procedures.

## ACKNOWLEDGEMENT

The authors would like to acknowledge Mr. Muhammad Akbar for typing this manuscript.

## REFERENCES

- Ahsan, N., I.H. Baloch, M.N., Chaudhry, Ch M. Majid, 2000. Strength Evaluation of Blends of Lawrencepur, Chenab and Ravi Sands with Lockhart and Margala Hill Limestones for use in Concrete. *Special Issue Pak. Muse. Nat. Hist. Pakistan Science Foundation*, pp. 213-240.
- Ahsan, N., M.N. Chaudhry, and M. Muzaffar, Ch. 2000a, Mineralogy, Engineering Properties and Alkali Aggregate Reaction Potential of Maira Sand, Thakot, Pakistan. *Third South Asia Geological Congress*, Lahore, Pakistan Sept. 23-26, 2000, pp. 150-151
- Baker, D., and Hendy, B., 2005. Planning for Sustainable Construction Aggregate Resources in Australia. *The Queensland University of Technology Research Week International Conference*, Brisbane, Australia.
- Boustani, M., 2000. Depositional and diagenetic environments of the (Eocene) Sakesar Limestone in the Salt Range Area, Pakistan. Unpublished Ph. D. Thesis, Quaid-e-Azam University, Islamabad, Pakistan, pp. 1-208.
- Chaudhry, M.N., I.H. Baloch, N. Ahsan, and Ch. M. Majid, 1999. Engineering properties, Mineralogy, Alkali Aggregate Reaction Potential and Provenience of Lawrencepur Sand Pakistan, *Special Issue Pak. Muse. Nat. Hist. Pakistan Science Foundation*, pp. 241-254.
- French, W.J., 1991. Concrete Petrography. *Quarterly Journal of Engineering Geology*, Vol. 3, pp 17-48.
- Kandhal, P.S., Mallick, R.B., and Huner M., 2000. Measuring Bulk Specific Gravity of Fine Aggregates: Development of a New Test Method. *Transportation Research Board, Transportation Research Record*, 1721.



- Kazmi, A.H. and Jan, M.Q., 1997. Geology and Tectonics of Pakistan. Graphic Publishers, Karachi, pp. 1 – 554.
- Khan, R. A., 2008. Role of Construction Sector in Economic Growth: Empirical Evidence from Pakistan Economy. In: *First international conference on construction in developing countries (ICCIDC-I) "Advancing and integrating construction education, research and practice"* August 4-5, 2008, Karachi., Pakistan.
- Liu, H., Kou, S. and Arne, P., 2004. Microscope Rock Texture Characterization and Simulation of Rock Aggregate Properties". *SGU Project* 60-1362.
- Lopez-Buendia, A.M., Climent, V., Verdu, P., 2006. Lithological Influence of Aggregate in the Alkali- Carbonate Reaction. *Cement and Concrete Research*, Elsevier Ltd, Valencia, Spain, Vol. 36.
- Neville, A.M. 2000. Properties of Concrete 4th ed. Pearson Education Asia Pte. Ltd. Edinburgh, U.K. 844p.
- Neville, A.M., and Brooks, J.J., 1999. Concrete Technology Longman Group U.K. First ISE reprint 1999 Edinburgh, U.K. 438p.
- Quiroga, P. N. 2003. The Effect of Aggregate Characteristics on the Performance of Portland Cement Concrete. PhD Dissertation, The University of Texas at Austin, Austin, TX.
- Smith, M. R. and Collis, L. 2001. Aggregates – Sand, Gravel and Crushed Rock Aggregates for Construction Purposes (3rd edition) The Geological Society London. 339p.
- Shah, S.M.I., 1977, Stratigraphy of Pakistan: *Geol. Surv. Pakistan*, Quetta, Mem. No. 12, pp. 138.
- Zaidi, S. M., Rafeeqi, S. F.A., Ali, M. S. and Khan, A. M., 2008. Aggregate characterization - An Important Step towards Addressing Construction Issues in Pakistan. In: *First international conference on construction in developing countries (ICCIDC-I) "Advancing and integrating construction education, research & Practice"* August 4-5, 2008, Karachi., Pakistan.



## GEOCHEMISTRY AND TECTONIC ENVIRONMENTS OF BABUSAR AMPHIBOLITES IN SOUTHEAST KOHISTAN, PAKISTAN.

BY

MUHAMMAD AHMED KHAN, SAIF UR REHMAN, MUHAMMAD FAHAD ULLAH  
Department of Earth Sciences, University of Sargodha, Pakistan

AND

NAVEED AHSAN  
Institute of Geology, University of the Punjab, Quaid-i-Azam Campus,  
Lahore-54590 Pakistan

**Abstract:-** The Kohistan terrane is a good example of young arc crust, sandwiched between the Indian and Karakoram plates. The base is occupied by a major stratiform Sapat ultramafic-gabbroic complex which overrides the crust of the Indian plate along the Indus suture (i.e., the Main Mantle Thrust, MMT). It was intruded into the base of a thick pile of metavolcanics of the Kamila belt, which comprise MORB-type tholeiitic basalts, island-arc tholeiites and calc-alkaline. The Chilas complex comprising ultramafic and gabbro-norite rocks, is also intrusive into the Kamila belt, it is emplaced onto the top of the Kamila belt. The Kamila Amphibolite rocks are intruded by granitoids of different composition. The Kamila belt is a composite mass dominated by amphibolite facies. KAU does not occur as a single, extensive body, field relation show that it is divisible into three linear belts in addition to small patches and screens within or between plutons. These belts are named from south to north as Babusar, Niat and Jal and within the Niat belt, a thin slice named Sumal amphibolites. Present article deals with the brief study of Babusar amphibolites. Babusar amphibolites are generally medium grained, and hypidioblastic to xenoblastic with hornblende composition ranging from 20 to 70%. Eight samples were selected for geochemical studies. All the samples show low  $\text{TiO}_2$  (mean 0.8 wt%) and  $\text{MgO}$  (Mean 5.6 wt%). All the trace elements are also depleted as Nb (0.8 ppm), Y (15.3 ppm), Zr (8.6 ppm) and Ni (18.7 ppm). Babusar amphibolites are tholeiitic and depleted in LIL elements which show normalized trace element patterns consistent with the subduction related component.

### INTRODUCTION

Amphibolites are widespread in the Kohistan sequence and form a prominent belt that extends from Afghanistan in the west, through Bajaur, Dir, Swat, and Indus valley, up to Nanga Parbat in the east. The belt has a maximum width of about 50 km and a length of 300 km. Preliminary studies were performed by Martin et al. (1962) and Davies (1965) in the Swat area and they included the Kohistan amphibolites in their "Upper Swat Hornblende Group" and interpreted them to be a product of metamorphism rather than igneous processes. In contrast, part of the amphibolite belt exposed in the Thak valley was assigned an igneous parentage by Shams (1975), who called them "veined metadiorites". Jan and Kempe (1974) introduced the name "the Kohistan Basic Complex" for the basic rocks of southern Kohistan and recognized the presence of an extensive suite of amphibolites. Jan (1979)

classified the amphibolites into two varieties: (a) massive and homogeneous, and (b) banded and sheared. Tahirkheli and Jan, 1979; Coward et al., 1986 referred these amphibolites as the Kamila amphibolite belt and Jan, 1979, 1988; Bard et al., 1980; Bard, 1983 a, b as the southern amphibolites.

The true thickness of the Kamila amphibolites is still uncertain due to an abundance of intrusive plutonic bodies and intense ductile-brittle shearing. However, the stratigraphic position of the Kamila amphibolites in the Kohistan sequence has become clearer with the delineation of its lower stratigraphic contact in the presently studied area and the upper contact in the Dir-Swat area (Sullivan et al., 1993). Therefore the name "Kamila Amphibolite Unit (KAU)" is used in this paper, which carries a stratigraphic connotation. KAU has a vast distribution in southern Kohistan (Fig.1). It was considered that the unit occupies



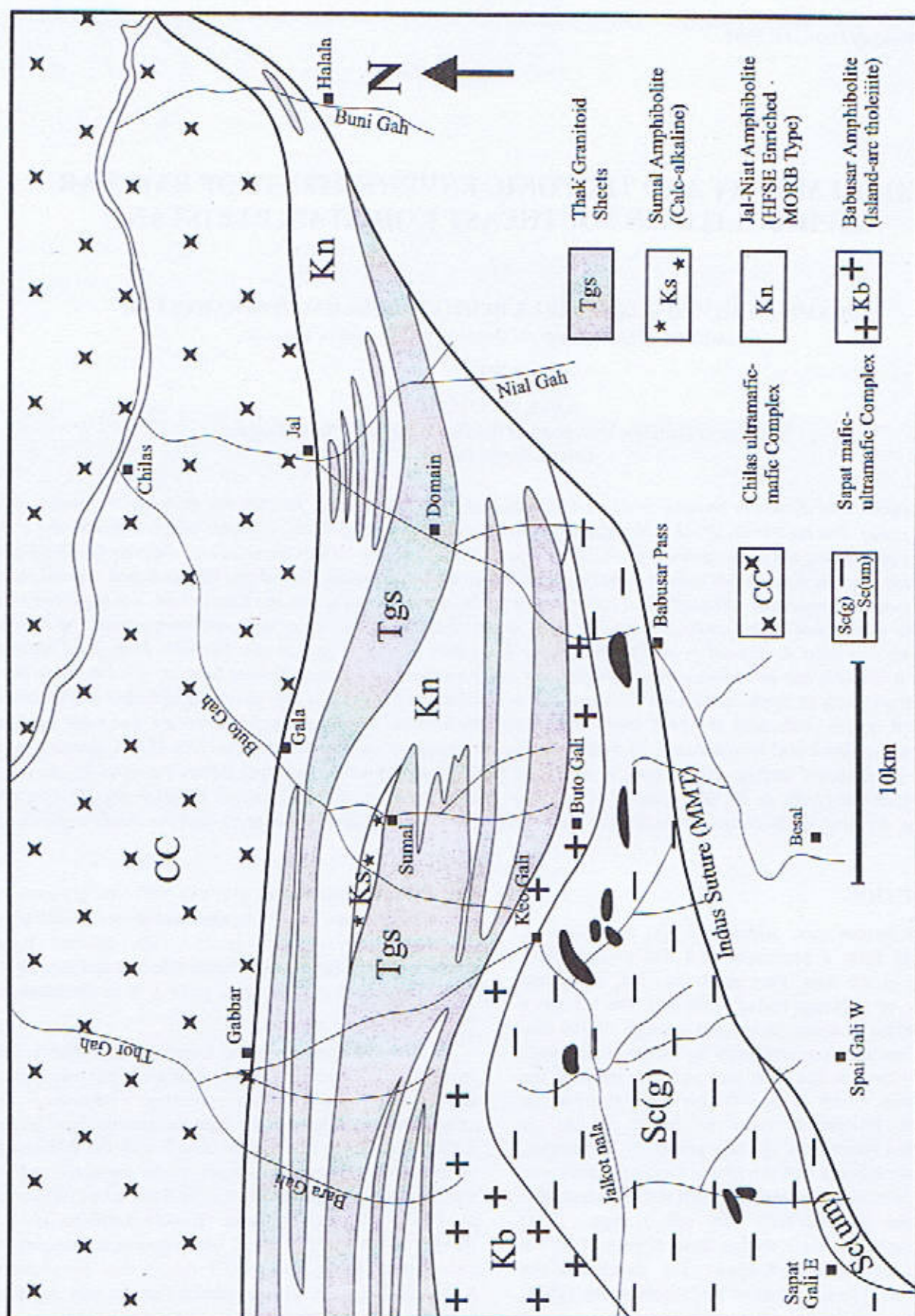


Fig. 1. Geological map of SE Kohistan showing detailed lithological subdivisions, the Sapat complex, the Kamila amphibolite belt and the Thak granitoid sheets (Khan, 1997)



the entire southern part of the Kohistan terrane between the Main Mantle Thrust (MMT) in the south and the Chilas Complex in the north (Tahirkehi and Jan, 1979; Bard et al., 1980). In the Indus valley, the unit is overlying the Jijal Complex which occupies the hanging wall of the MMT. This study has revealed that it is in direct contact with the MMT only in the extreme eastern (i.e., Bunar valley) and western parts of the Kohistan terrane. In the area between the Babusar Pass in the east and the Indus Valley in the west, the unit is separated from the MMT by a basal mafic-ultramafic layered complex in the hanging wall of the MMT, termed the Sapat Complex (Jan et al., 1993). To the north, the unit is bounded by the Chilas Complex, which occupies an axial position in the Kohistan terrane. KAU does not occur as a single, extensive body, field relations show that it is in three main linear belts, in addition to small patches and screens within or between plutons. These belts are named from south to north as Babusar, Niat, and Jal. Within the Niat belt, a thin slice of amphibolites with distinctly different characteristics is named as Sumal amphibolites. Diorites, granodiorites, trondhjemites and granites intrude all these amphibolites.

#### LITHOLOGY AND PETROGRAPHY OF BABUSAR AMPHIBOLITES

The amphibolites are best exposed in the southern part of the study area as east-west belt stretching between the drainage divide of Jalkot Nala and the tributaries of the Indus River at high reaches of Katai gali, Butogah gali, Keo gali, Makheli gali, Shikaro gali and Sherman gali. The width of the belt in the eastern part of the area in the Thak valley is 1.5 km while in the western part near Sherman Gali it is 5 km. The belt has a gradational contact with the basal ultramafic-mafic rocks of Sapat-Babusar Complex to the south. To the north the contact is sharp with intrusive diorites. To the east of Babusar Pass in the Charal gah the belt occurs directly in the hanging wall of the Indus suture. On the fresh surface the rocks are dark grey to dark greenish grey. On weathered surface, they look dark greenish brown. The rocks are strongly foliated, sheared and commonly banded. Foliation is mostly parallel to the banding. The banded aspect of these rocks is due to variations in the proportions of amphibole, epidote and plagioclase + quartz in alternate layers. The bands range from centimeter to over half a meter in thickness. Most of them are less than two centimeters thick and usually have sharp contacts.

The amphibolites are generally medium-grained, and hypidioblastic to xenoblastic. Locally they contain poikiloblasts and porphyroblasts with minor inclusions. Foliation and gneissose banding are common; in some rocks alternating bands of quartz and plagioclase with fine-grained aggregates of amphibole and epidote are present. In foliated varieties flaky minerals are oriented in one

direction; elongation is also seen in quartz and epidote crystals. The banded varieties are mostly finer grained than the homogeneous types some of which are coarse-grained. Variations in texture and mineral proportion are common in both the varieties. They contain hornblende, epidote and plagioclase as the dominant constituents. Chlorite, quartz, sphene, rutile and opaque minerals occur as accessories, while some samples contain biotite, white mica and garnet and a few have clinopyroxene.

The amphibole is mostly hornblende in composition and shows a wide range from 20% to 70% (Table-1), subhedral to anhedral, fresh but some of the large are uranitized at boundaries. Inclusions of quartz and opaque minerals, suggesting post magmatic growth but in some cases these minerals occur only in the central parts. Small inclusions of hornblende within large hornblende crystals are also observed. Hornblende encloses or is enclosed by epidote and it is partly replaced by chlorite, less commonly by epidote, sphene and minor chlorite. It is light green to brownish green and bluish green and displays zoning with bluish green cores and greenish blue margins. Actinolite occurs as long prismatic crystals and in columnar to fibrous aggregates. It is colourless to light green.

The plagioclase ranges from 4% to 23% and is cloudy. It is in the range of andesine ( $An_{40-45}$ ) but in rare cases it is sodic labradorite. Untwinned and anhedral plagioclase are enclosed by quartz and show myrmekitic intergrowth. Inclusions of sericite are common with some apatite; it is replaced by epidote and albite. Epidote is from 8% to 40%, elongated, subhedral as well as anhedral, and has likely formed subsequent to the growth of amphibole. Inclusions of epidote are present in hornblende. It is zoned and displays anomalous blue colour in cores and greenish or brownish in margins. Quartz from 3% to 20%, anhedral and shows strong strain effects. It is in the form of aggregates elongated parallel to the well-developed schistosity of the rocks. Its segregation and straining boundaries suggest that the recrystallization occurred during metamorphism. Sphene, biotite, magnetite or ilmenite are common accessories. Sphene is developed along the fractures, cleavages and along grain boundaries of hornblende. Calcite occurs as minor with a good zoning, bluish green to light green flakes along the margins and within fractures of the hornblende. Opaque minerals occur in the cores and along boundaries of hornblende. Rutile is associated with magnetite, and both may be derived from ilmenite.

#### GEOCHEMISTRY

Eight selected samples from the Babusar amphibolites are used for the evaluation of the geochemical characteristics of these rocks (Table-2). All the samples have low  $TiO_2$  (mean 0.8 wt%) and  $MgO$  (mean 5.6 wt%).



**Table.1**  
Modal composition of Babusar Amphibolite

| Sample No       | A-243 | A-241 | BS-10 | A-31 | BS-18 | A-56 | A-58 | A-59 |
|-----------------|-------|-------|-------|------|-------|------|------|------|
| Amphibole (%)   | 30.0  | 40.0  | 55.0  | 39.0 | 7.0   | 55.0 | 58.0 | 70.0 |
| Plagioclase (%) | 4.0   | 23.0  | 0.0   | 22.0 | 4.0   | 20.0 | 14.0 | 6.0  |
| Epidot (%)      | 8.0   | 22.0  | 24.0  | 24.0 | 40.0  | 8.0  | 11.0 | 9.0  |
| Quartz (%)      | 20.0  | 6.0   | 10.0  | 5.0  | 3.0   | 7.0  | 9.0  | 6.0  |
| Chorite (%)     | 4.0   | 9.0   | 8.0   | 6.0  | 43.0  | 2.0  | 3.0  | 0.0  |
| Magnetite (%)   | 1.0   | 1.0   | 1.0   | 1.0  | 0.0   | 4.0  | 5.0  | 3.0  |
| Sphene (%)      | 3.0   | 2.0   | 2.0   | 1.0  | 3.0   | 4.0  | 6.0  | 6.0  |
| Biotite (%)     | 0.0   | 1.0   | 0.0   | tr   | 0.0   | 0.0  | 0.0  | 0.0  |
| Calcite (%)     | 30.0  | 0.0   | 0.0   | 1.0  | 0.0   | 0.0  | 0.0  | 0.0  |
| Mucovite (%)    | tr    | 2.0   | 0.0   | 1.0  | 0.0   | 0.0  | 0.0  | 0.0  |
| Apatite (%)     | 0.0   | 0.0   | tr    | 0.0  | tr    | 0.0  | 0.0  | tr   |

**Table.2**  
Major and trace element composition of Babusar Amphibolites.

| Sample No                      | BS-3   | BS-7   | BS-8   | BS-9   | BS-10  | BS-11  | BS-18  | BS-19  |
|--------------------------------|--------|--------|--------|--------|--------|--------|--------|--------|
| SiO <sub>2</sub>               | 49.43  | 47.86  | 56.09  | 54.34  | 43.21  | 46.54  | 49.32  | 45.13  |
| TiO <sub>2</sub>               | 1.25   | 0.86   | 0.85   | 0.63   | 0.72   | 1.00   | 0.79   | 0.68   |
| Al <sub>2</sub> O <sub>3</sub> | 15.80  | 20.36  | 15.83  | 17.70  | 19.05  | 17.82  | 18.21  | 18.76  |
| Fe <sub>2</sub> O <sub>3</sub> | 13.98  | 11.95  | 10.89  | 9.67   | 13.47  | 14.75  | 12.50  | 14.25  |
| MgO                            | 5.72   | 4.25   | 4.26   | 4.20   | 7.88   | 6.19   | 4.93   | 7.06   |
| CaO                            | 12.38  | 10.81  | 8.88   | 9.98   | 15.37  | 11.81  | 11.48  | 12.93  |
| Na <sub>2</sub> O              | 0.87   | 3.28   | 2.76   | 3.00   | 0.04   | 1.50   | 2.45   | 0.95   |
| K <sub>2</sub> O               | 0.21   | 0.12   | 0.15   | 0.18   | 0.02   | 0.04   | 0.04   | 0.01   |
| MnO                            | 0.24   | 0.26   | 0.19   | 0.19   | 0.23   | 0.28   | 0.21   | 0.22   |
| P <sub>2</sub> O <sub>5</sub>  | 0.11   | 0.24   | 0.10   | 0.10   | 0.02   | 0.06   | 0.07   | 0.01   |
| Nb                             | 0.70   | 1.70   | 1.00   | 0.50   | 0.60   | 0.20   | 0.90   | 0.20   |
| Zr                             | 15.40  | 25.10  | 8.70   | 11.90  | 1.00   | 5.00   | 5.50   | 3.60   |
| Y                              | 23.10  | 28.90  | 16.80  | 17.30  | 6.30   | 12.50  | 14.80  | 10.80  |
| Sr                             | 252.00 | 296.50 | 154.70 | 167.40 | 148.60 | 167.40 | 200.30 | 141.60 |
| Rb                             | 1.20   | 0.50   | 1.10   | 1.50   | 1.50   | 1.00   | 0.90   | 0.40   |
| Th                             | 0.40   | 0.20   | -0.50  | 0.30   | -0.10  | 0.10   | -0.10  | -0.50  |
| Pb                             | 4.20   | 2.10   | 1.70   | 2.40   | 1.10   | 1.50   | 1.00   | 0.90   |
| Ga                             | 17.90  | 19.00  | 14.50  | 15.40  | 14.80  | 17.20  | 18.00  | 15.80  |
| Zn                             | 115.30 | 110.10 | 92.40  | 85.00  | 88.80  | 126.40 | 100.00 | 99.50  |
| Cu                             | 96.50  | 17.00  | 38.80  | 35.30  | 49.70  | 103.40 | 123.20 | 67.50  |
| Ni                             | 21.80  | 6.30   | 14.00  | 16.60  | 36.40  | 17.90  | 16.60  | 23.00  |
| Cr                             | 28.60  | 4.70   | 34.70  | 36.20  | 82.30  | 41.70  | 36.80  | 88.40  |
| V                              | 498.10 | 148.70 | 299.70 | 247.10 | 464.50 | 414.10 | 395.80 | 439.00 |
| Sc                             | 51.40  | 26.10  | 39.10  | 41.50  | 60.10  | 59.90  | 49.00  | 65.10  |
| Ba                             | 29.50  | 31.50  | 55.30  | 67.60  | 17.60  | 21.60  | 28.50  | 16.90  |
| La                             | 0.60   | 2.90   | 1.50   | 1.30   | -1.40  | 0.10   | -0.20  | -1.30  |
| Ce                             | 6.10   | 10.20  | 3.60   | 4.30   | 1.40   | 2.60   | 2.90   | 3.50   |
| Nd                             | 5.50   | 10.40  | 3.60   | 3.90   | 0.60   | 0.60   | 2.70   | 1.10   |



All the trace elements also are depleted in these rocks, but the elements like Nb (0.7ppm), Y (15.3ppm), Zr (8.6 ppm) and Ni (18.7ppm) are particularly depleted.

### Classification

The amphibolites classify as basalts and basaltic andesites (BS-8 and BS-9) on the  $\text{SiO}_2$ -( $\text{Na}_2\text{O}+\text{K}_2\text{O}$ ) plot of Le Maitre et al. (1989) and one sample (BS-10) plot in the field of microbasalt (Fig.2). On the classification scheme of De La Roche et al. (1980) the analyses range from olivine basalt through tholeiite to andesite basalt. One sample (BS-8) plots in the field of andesite (Fig.3). The Jensen cation plot (Jensen, 1976) supports the above classification of the studied amphibolite rocks (Fig.4). Four samples BS7, 8, 9 and 18) plot in the field of andesite and the rest of the four samples show an affinity with high-Fe tholeiite basalt. On AFM diagram of Irvine and Barager (1971), the amphibolites classify as tholeiites but they display an alkali-enrichment trend (Fig.5). The  $\text{K}_2\text{O}$  content in all the analyses is low ( $< 0.2$  wt%) and the rocks classify on this basis as low-K tholeiites on  $\text{K}_2\text{O}$  versus  $\text{SiO}_2$  diagram (Fig.8) after Le Maitre et al., (1989).

### Fractionation Assemblage

To evaluate the crystallization sequence of Babusar amphibolites, variation diagrams using  $\text{SiO}_2$  as a fractionation index are plotted (Fig.5, Fig.6a & Fig.6b). Depletion of MgO and Ni with advancing fractionation in the studied rocks is indicative of early crystallization of olivine. The depletion of these two elements together with that of Cr, increasing degree of fractionation suggests the igneous parentage of these rocks. The low  $\text{TiO}_2$  and low Zr/ $\text{TiO}_2$  ratios also confirm the igneous past of these amphibolites. The depletion of iron and CaO increasing fractionation warrants the crystallization of an iron oxide and clinopyroxene.  $\text{Na}_2\text{O}$  and Sr variation trend supports this sequence of fractionation.  $\text{Na}_2\text{O}$ ,  $\text{K}_2\text{O}$  and  $\text{P}_2\text{O}_5$  show enrichment with increasing proportions of  $\text{SiO}_2$ . Depletion in  $\text{Al}_2\text{O}_3$  suggests plagioclase crystallization started early in the sequence. Sr is highly compatible with plagioclase and shows enrichment in early fractionation and at ~50 wt%, Sr trend becomes negative. It is likely that the plagioclase crystallizing earlier was calcic to accommodate much Sr, but at ~50 wt% of  $\text{SiO}_2$ , it probably changed its composition.  $\text{TiO}_2$  shows some enrichment in early fractionation and then, because of probable crystallization of ilmenite, shows a decline. On the basis of major and trace element variations it is considered that olivine, clinopyroxene and iron oxide were the earliest crystallizing minerals and joined subsequently by plagioclase. This sequence of crystallizing minerals is mainly responsible for the compositional diversity in the Babusar amphibolites. The crystallization of plagioclase after clinopyroxene in the crystallizing sequence is a characteristic of subduction-related settings than that of mid-ocean ridges (Perfit et al., 1980).

## TRACE-ELEMENT VARIATIONS

The Babusar amphibolites are generally depleted in large-ion lithophile elements like Rb, Pb, Th and K (Table-2). The contents of these elements show an increase with fractionation. Amongst the high-field strength elements (HFSE) Ti concentration is controlled by tholeiitic trend of the studied suite. The amounts of Zr and Y are about eight times higher than those in the chondrites. In some samples the Zr concentration is equal or less than chondrites.

### Ferromagnesian Elements

Ni ranges from 6 ppm to 36 ppm and Cr from 5 ppm to 88 ppm in the studied rocks (Table-2). When plotted against  $\text{SiO}_2$ , the elements like Ni, V, Sc and Cr display decrease in concentration with increasing contents of  $\text{SiO}_2$  (Fig.5). Decrease in Ni with increasing  $\text{SiO}_2$  may be attributed to olivine fractionation and that in Cr to clinopyroxene and Cr-spinel separation.

### Trace-element Patterns as Spidergrams

The Babusar amphibolites have highly spiked trace element pattern characterized by positive peaks for Ba, K, Sr, Ti, and negative anomalies for Rb, Nb and Zr. The patterns have a peculiar shape which resembles the alphabet "W" (Fig.9). These patterns are different from that of the ocean-floor tholeiites and are matching with the island arc tholeiites (Fig.7). The peaks and troughs of arc tholeiites are, in general, corresponding with the amphibolites of this group.

### Tectonic Environment

The Babusar amphibolites are tholeiitic and are depleted in large ion lithophile (LIL) elements, which is a characteristic feature of tholeiitic rocks from mid-ocean ridge and subduction-related environments (island arcs and Andean-type continental margins). Tholeiitic basalts can occur in all the major tectonic settings of magma generation. The depleted contents of LIL elements in the Babusar amphibolites clearly indicate their affinity with within-plate oceanic or continental settings, so the Babusar amphibolites are may be related to either oceanic- or island arc/continental margin environments. The tholeiite series is considered to be the earliest-and in some cases dominating phase of magmatism in island arc /continental margin environments. The island arc basalts are characterized by selective enrichment of elements of low ionic potential (Sr, K, Rb, and Th) and low abundances of elements of high ionic potential (Nb, P, Zr, Ti, and Y) compared to N-type MORB (Fig.9). The enrichment in low ionic potential elements has been attributed to metasomatism of the mantle source of arc basalts by fluids released from the subducted slab. In contrast, the relative depletion in high ionic potential elements has been variably attributed to higher



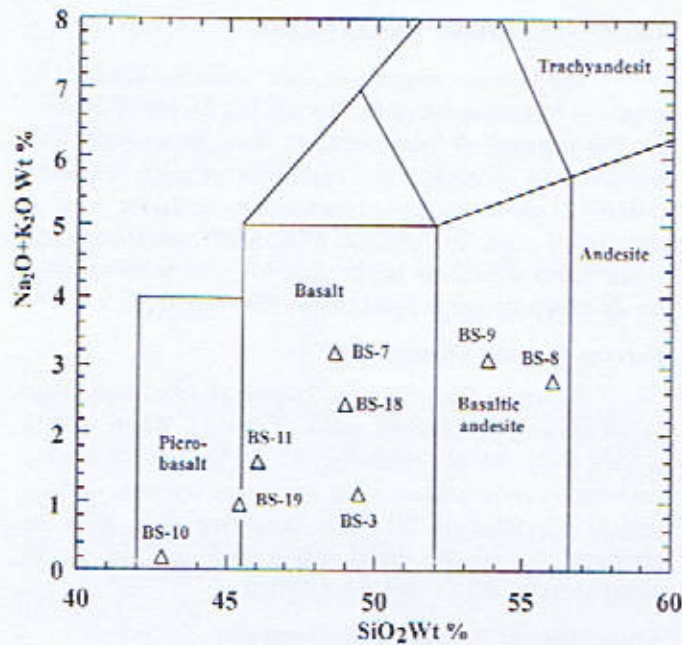


Fig. 2. Chemical classification and nomenclature of Babusar amphibolites using total alkalis versus  $\text{SiO}_2$  (TAS) plot after Le Maitre et al., (1989).

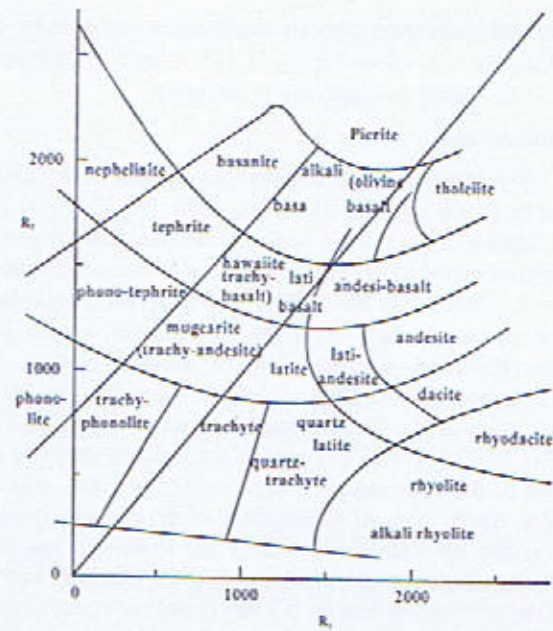


Fig. 3. R1-R2 diagram of Babusar amphibolites after De La Roche et al., (1980).

$$R1 = 4\text{Si} - 11(\text{Na} + \text{K}) - 2(\text{Fe} + \text{Ti}),$$

$$R2 = 6\text{Ca} + 2\text{Mg} + \text{Al}.$$

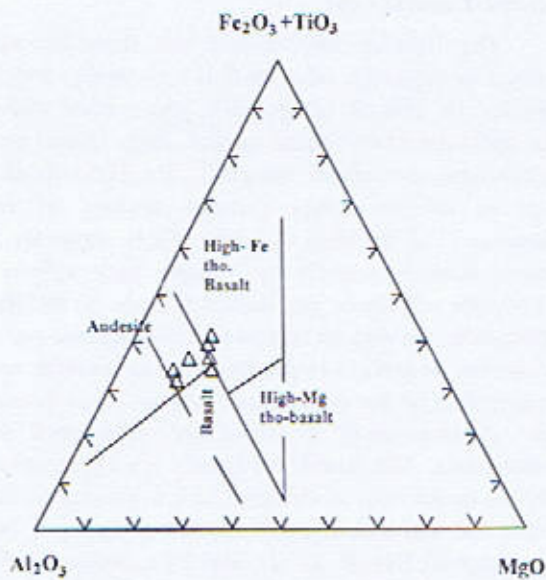


Fig. 4. Ternary plot of classification according to cation percentage of Al, (Fe total + Ti) and Mg after Jensen, (1976).

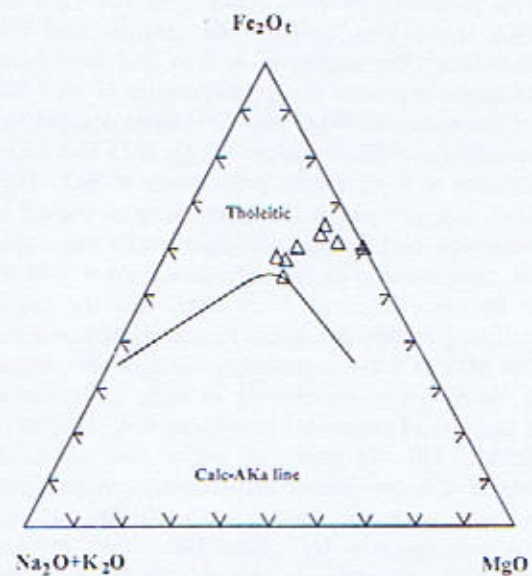


Fig. 5. AFM diagram of studied rocks after Irvine and Barager, (1971)



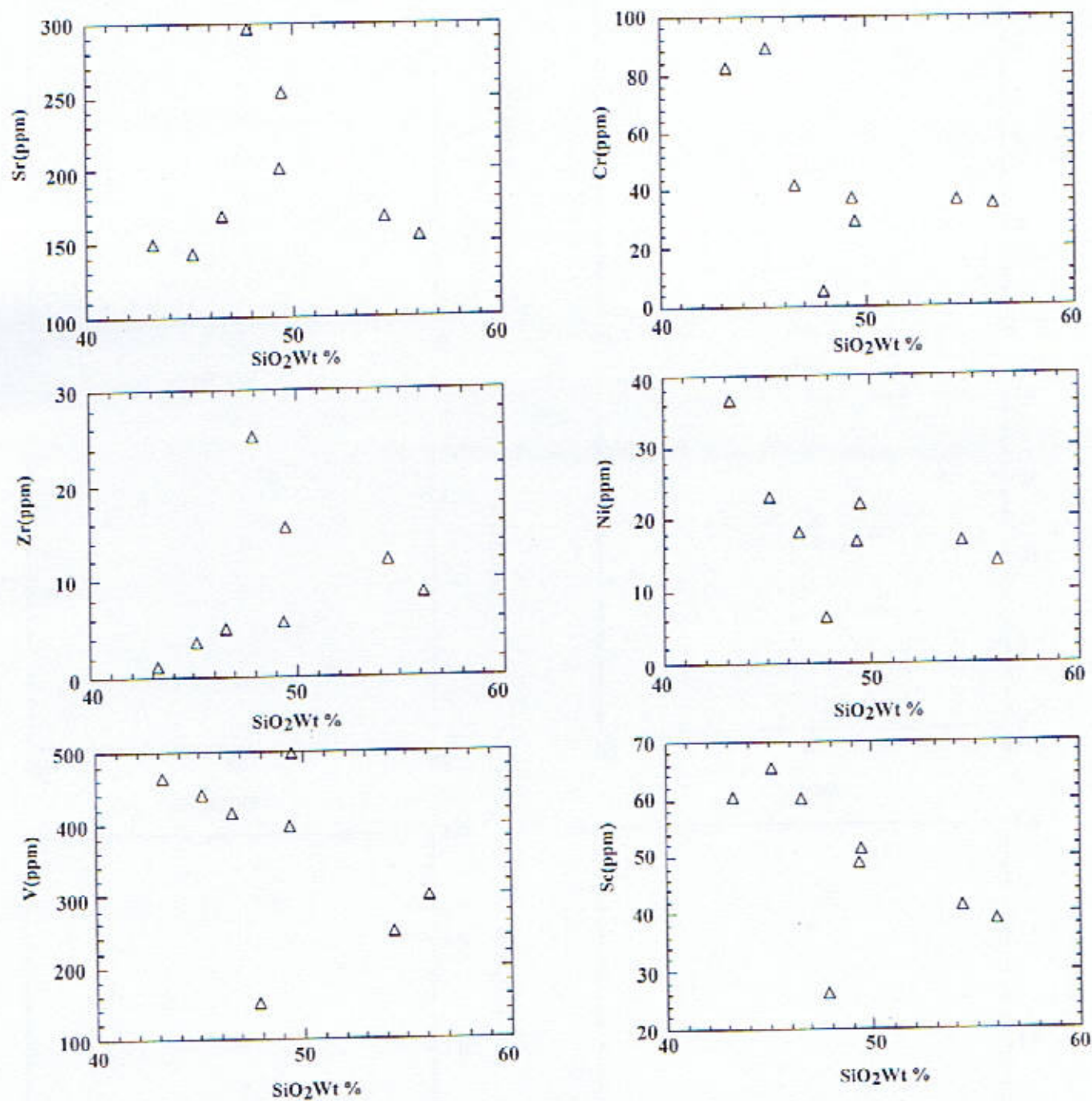


Fig. 5. Binary plots of trace elements versus SiO<sub>2</sub> wt % for Babusar



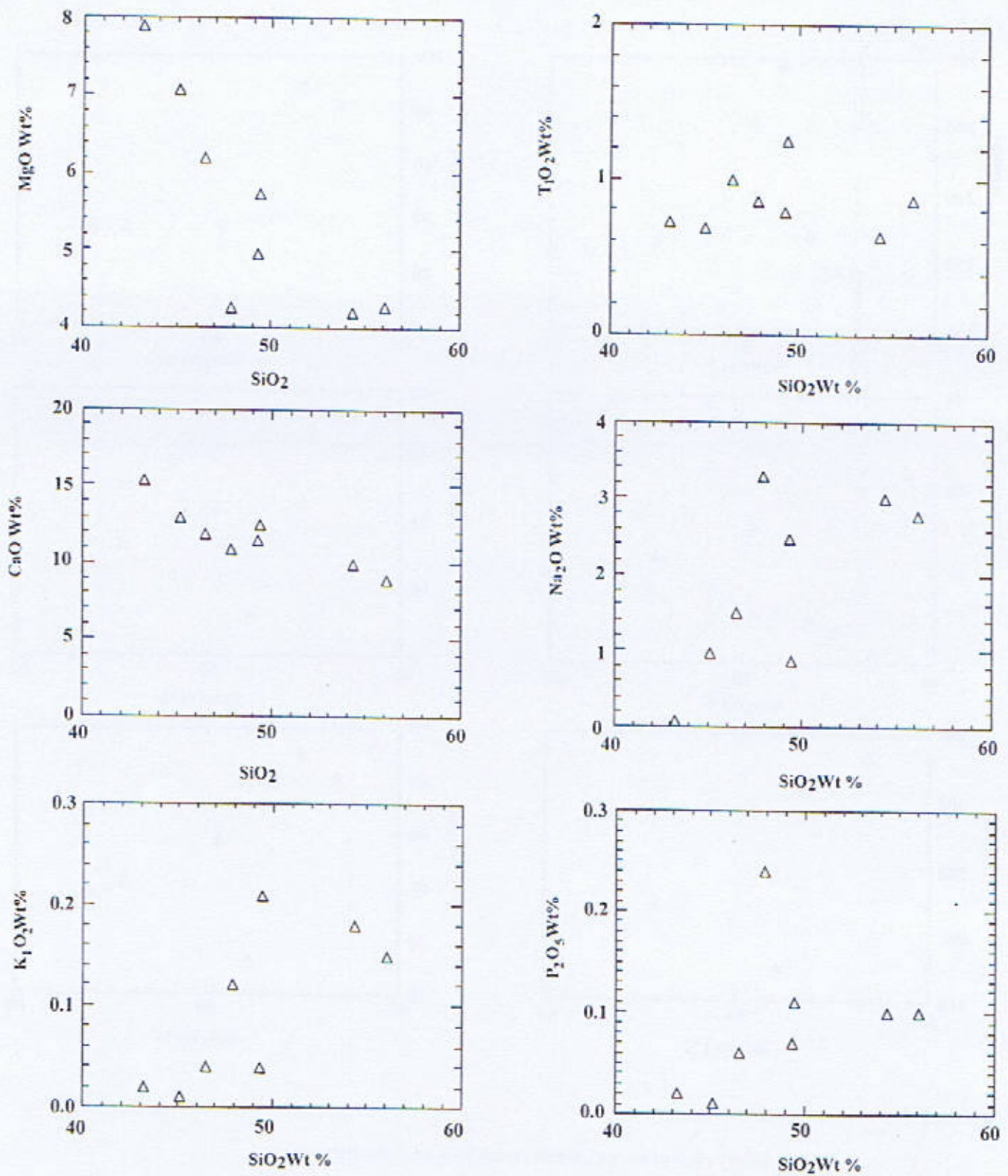


Fig. 6a. Binary Plot of Major oxides versus SiO<sub>2</sub> wt %



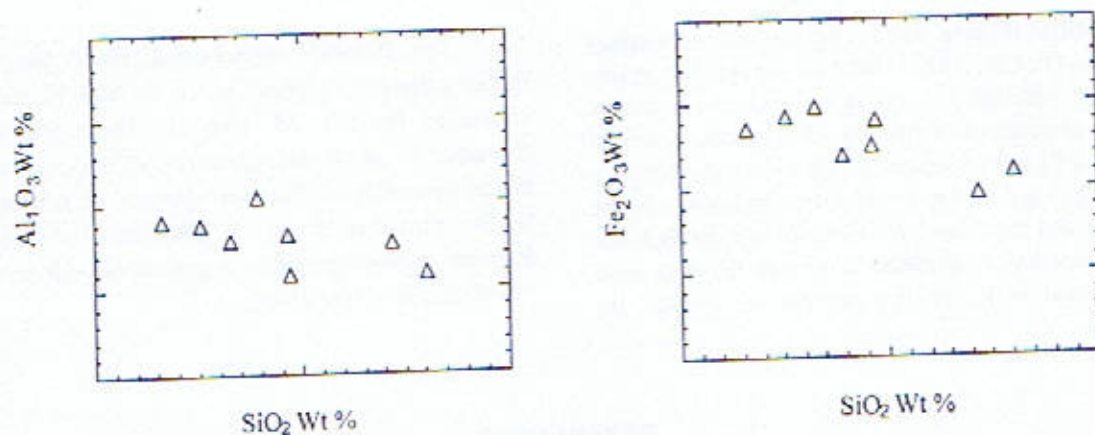


Fig.6b Binary Plot of Major oxides versus  $\text{SiO}_2$  wt %

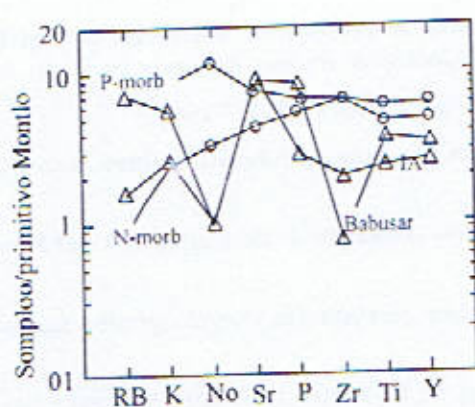


Fig.7 Primordial mantle normalized diagram of Babusar amphibolites showing the spike trace elements pattern and also compared with various tectonic setting after Sun and

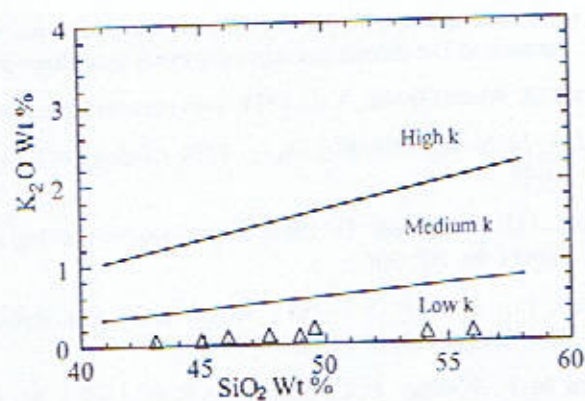


Fig.8 Subdivision of Babusar amphibolites on  $\text{K}_2\text{O}$  versus  $\text{SiO}_2$  wt % diagram after Le Maitre et al (1989).

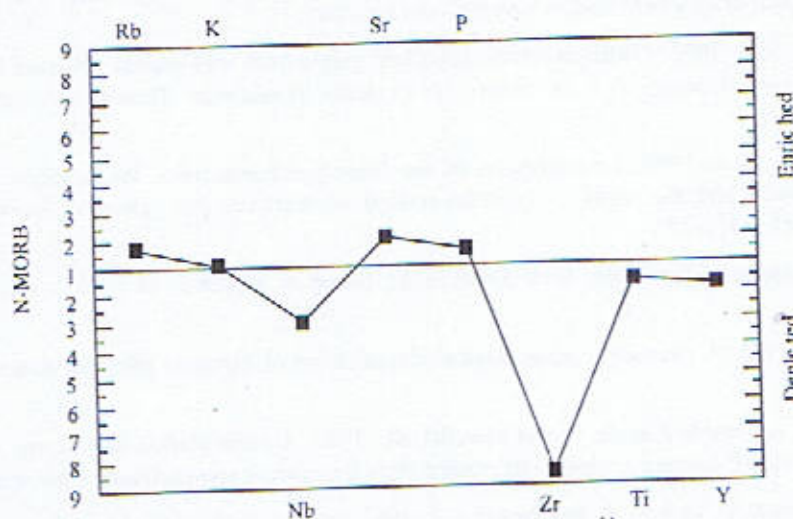


Fig. 9. Diagram showing enrichment of low ionic potential elements (Sr, K, P and Rb) and depletion of high ionic potential elements (Nb, Zr, Ti and Y) in island arc tholeiite and Babusar amphibolites



degrees of partial melting and to the stability of residual mantle phases (Pearce, 1982). N-MORB normalized values of the Babusar amphibolites and oceanic island arc basalts clearly show enrichment in elements of low ionic potential (Rb, K, Sr and P) and depletion in high ionic potential (Nb, Zr, Ti and Y) (Fig.7 & Fig.9). The only difference in the studied rocks and the island arc rocks is that the Babusar amphibolites are highly depleted in Zr and Rb, and show some enrichment in P, but the patterns are broadly the same.

The Babusar amphibolites show the distinctive spiked pattern with peaks at Th, Sr and Y, and negative anomalies for Rb, Nb and Zr. These patterns are a characteristic of all subduction related magmas, attesting to the involvement in their petrogenesis of subduction zone fluids enriched in Sr and Th. The peaks and troughs in the Babusar amphibolites show a general resemblance with the low-K island arc tholeiites.

## REFERENCES

- Barker, F., 1979. Trondhjemite: definition, environment and hypotheses of origin. *Trondhjemites, Dacites, and Related Rocks*, edited by F. Barker. Elsevier, New York, 1-12.
- Butt, K. A., Chaudhry, M. N. and Ashraf, M., 1980. An interpretation of petrotectonic assemblage west of W. Himalayan syntaxis in Dir district and adjoining areas in northern Pakistan. *Geological Bulletin, Peshawar University*, **13**, 79-86.
- Chappell, B. W. and White, A. J., 1974. Two contrasting granite types. *Pacific Geology*, **8**, 173-174.
- Chaudhry, M. N. and Chaudhry, A. G., 1974. Geology of Khagram area, Dir district. *Geological Bulletin, Punjab University*, **11**, 21-43.
- Clemens, J.D. & Vielzeuf, D. 1987. Constraints on melting and magma production in the crust. *Earth and Planetary Science Letters*, **86**, 207-306.
- Clemens, J.D. & Wall, V.J. 1981. Origin and crystallization of some peraluminous (S-type) granitic magmas. *Canadian Mineralogist*, **19**, 111-131.
- Coward, M. P., Windley, B. F., Broughton, R. D., Luff, I. W., Petterson, M. G., Pudsey, C. J., Rex, D. C. and Khan, M. A., 1986. Collision tectonics in the NW Himalayas. In: Coward, M.P. and Ries, A.C. (eds.) *Collision Tectonics*. Geological Society of London, Special Publication, **19**, 203-219.
- Cox, K. G., Bell, J. D. and Pankhurst, R. J., 1979. The interpretation of igneous rocks. *George, Allen and Unwin*, London.
- Crawford, M.B. 1988. Leucogranites of the NW Himalaya: crust-mantle interaction beneath the Karakoram and the magmatic evolution of collisional belts. *PhD thesis, University of Leicester*.
- Crawford, M.B. & Searle, M.P. 1993. Collision-related granitoid magmatism and crustal structure of the Hunza Karakora, North Pakistan. *From Treloar, P.J. & Searle, M.P. (eds) Himalayan Tectonics, Geological Society Special Publication*, **74**, 53-68.
- Crawford, M.B. & Windley, B.F. 1990. Leucogranites of the Himalaya/Karakoram: implications for magmatic evolution within collisional belts and the study of collision-related leucogranite petrogenesis. *Journal of Volcanology and Geothermal Research*, **44**, 1-19.
- Davies, R. G., 1965. The nature of the Upper Swat Hornblende Group of Martin et al. (1962). *Geological Bulletin, Punjab University*, **2**, 51-52.
- Debon, F. and Le Fort, P., 1983. A chemical - mineralogical classification of common plutonic rocks and associations. *Earth Sciences*, **73**, 135-149.
- De La Roche, H., Leterrier, J., Grande Claude, P. and Marchal, M., 1980. A classification of volcanic and plutonic rocks using R1-R2 diagrams and major element analyses - its relationships and current nomenclature. *Chemical Geology*, **29**, 183-210.
- Deniel, C., Vidal, P., Fernandez, A., Le Fort, P. and Pecaat, J. J., 1987. Isotopic study of the Manaslu granite (Himalayas, Nepal): inferences on the age and source of Himalayan leucogranites. *Contributions to the Mineralogy and Petrology*, **96**, 78-92.



- Drummond, M. S. & Defant, M. J., 1990. A model for trondhjemite-tonalite-dacite genesis and crustal growth via slab melting: Archean to modern comparisons. *Journal of Geophysical Research*, **95**, 503-521.
- Evenson, N.M., Hamilton, P.J. and O'Nions, R.K. 1978. Rare-earth abundances in chondritic meteorites. *Geochim. Cosmochim. Acta*, **42**, 1199-1212.
- George, M.T., Nigel, B.W., Harris & Robert W.H. Butler. 1993. The tectonic implications of contrasting granite magmatism between the Kohistan island arc and the Nanga Parbat-Haramosh Massif, Pakistan Himalaya. *From Treloar, P.J. & Searle, M.P. (eds) Himalayan Tectonics, Geological Society Special Publication*, **74**, 173-191.
- Ghazanfar, M., Chaudhry, M. N. and Hussain, M. S., 1991. Geology and petrotectonics of southeast Kohistan, northwest Himalaya, Pakistan. *Kashmir Journal of Geology*, **8 & 9**, 67-97.
- Harris, N.B.W. & Inger, S. 1992. Trace Element modeling of Pelite-derived Granites. *Contributions to Mineralogy and Petrology*, **110**, 46-56.
- Hayden, H.H., 1916. Notes on the geology of the Chitral, Gilgit and Pamirs. *Records of the Geological Survey of India*, **45**, 271-335.
- Honegger, K., Dietrich, V., Frank, W., Gansser, A., Thoni, M. and Trommsdorff, V., 1982. Magmatism and metamorphism in the Ladakh Himalayas the Indus-Tsang-Po Suture Zone. *Earth and Planetary Science Letters*, **60**, 253-292.
- Inger, S & Harris, N. 1993. Geochemical constraints on leucogranite magmatism in the Langtang Valley, Nepal Himalaya. *Journal of Petrology*, **34**, 345-368.
- Ivanac, J. F., Traves, D. M. and King, D., 1956. The geology of the northwest portion of the Gilgit Agency. *Records of the Geological Survey of Pakistan*, **3**, 1-27.
- Jan, M. Q., 1970. Petrography of the upper part of Kohistan and southwestern Gilgit Agency along the Indus and Kandia rivers. *Geological Bulletin, Peshawar University*, **5**, 27-48.
- Jan, M. Q. & Asif, M., 1983. Geochemistry of tonalites and quartz diorites of the Kohistan-Ladakh (Transhimalayan) granitic belt in Swat, N. Pakistan. In: Sham F.A. (ed.) *Granites of Himalayan, Karakorum and Hindu Kush*. Institute of Geology, Punjab University, Lahore, 355-376.
- Jan, M. Q. & Howie, R. A., 1981. The mineralogy and geochemistry of the metamorphosed basic and ultrabasic rocks of the Jijal complex, Kohistan, NW Pakistan. *Journal of Petrology*, **22**, 85-126.
- & Mian, I., 1971. Preliminary geology and petrography of Swat Kohistan. *Geological Bulletin, Peshawar University*, **6**, 1-32.
- Khan, M. A., Khan, M.A and Jan, M. Q., 2003. Trondhjemites in the southeastern part of the Kohistan island-arc terrane, Pakistan: A product of partial melting. *Geol. Bull. Univ. Peshawar*, Vol. 36, 39-48.
- Khan, M. A. 1997. Geology of southeast Kohistan, NW Himalayas, Pakistan. *PhD Thesis, Peshawar University*.
- Le Bas, M. J., Le Maitre, R. W., Streckeisen, A. and Zanettin, B., 1986. A chemical classification of volcanic rocks based on total alkali-silica diagram. *Journal of Petrology*, **27**, 745-750.
- Le Maitre, R. W., Bateman, P., Dudek, A., Keller, J., Lameyre, Le Bas, M. J., Sabine, P. A., Schmid, R., Sorensen, H., Streckeisen, A., Woolley, A. R. and ZANETTIN, B., 1989. A classification of igneous rocks and glossary of terms. *Blackwell, Oxford*.
- Martin, H., 1987. Petrogenesis of Archean Trondhjemites, Tonalites, and Granodiorites from Eastern Finland: Major and Trace Element Geochemistry. *Journal of Petrology*, **23**, Part 5, 921-953.
- O'Connor, J.T. 1965. A classification for quartz-rich igneous rocks based on feldspar ratios. *U.S. Geological Survey, Professional Paper*, **525B**, B9-B4.
- Pearce, J. A., Harris, N. B. W. and Tindle, A. G., 1984. Trace element discrimination diagrams for the tectonic interpretation of Granitic rocks. *Journal of Petrology*, **25**, 956-983.
- Petterson, M. G. & Windley, B. F., 1985. Rb-Sr dating of the Kohistan arc batholith in the Trans Himalaya of N. Pakistan and tectonic implications. *Earth and Planetary Science Letters*, **74**, 54-75.



- Petterson, M. G. & Windley, B. F., 1991. Changing source regions of magmas and crustal growth in the Trans-Himalayas: Evidence from the Chalt volcanics and Kohistan batholith, Kohistan, N. Pakistan. *Earth and Planetary Science Letters*, **102**, 326-346.
- Saunders, A. D., Tarney, J., Marsh, N. G., Wood, D. A. And Panayiotou, A., 1980. Ophiolites as ocean crust or marginal basin crust; a geochemical approach. In: *Ophiolites; Proceedings, International ophiolite symposium*, 193-204.
- Saunders, A. D., Norry, M. J. And Tarney, J., 1988. Origin of MORB and chemically depleted Mantle Reservoirs: trace Element Constraints. *Journal of Petrology Special Lithosphere Issue*, **29**, 415-445.
- Searle, M. P., Rex, A. J., Tirrul, R., Rex, D. C. And Barnicoat, A., 1989. Metamorphic, magmatic and tectonic evolution of the Central Karakoram in the Biafo-Baltoro-Hushe regions of N. Pakistan. In: Malinconico, L. L. and Lillie, R. J. (eds.) *Tectonics of Western Himalayas*. Geological Society of America, Special Paper, **232**, 47-73.
- Searle, M.P., Crawford, M.B. & Rex, A.J. 1992. Field relations, geochemistry, origin and emplacement of the Baltoro granite, central Karakoram. *Transactions of the Royal Society of Edinburgh*, **83**, 519-538.
- Searle, M.P. & Khan, M.A. 1996. Geological map of North Pakistan and adjacent areas of northern Ladakh and, western Tibet.
- Sun, S.-S. & McDonough, W.F. 1989. Chemical and isotopic systematics of oceanic basalts: implications for mantle composition and processes. In: Saunders, A.D. & Norry, M.J. (eds) *Magmatism in the Ocean Basins*. Geological Society, London, *Special Publications*, **42**, 313-345.
- Tahirkheli, R. A. K., And Jan, M. Q. 1979. Geology of Kohistan, Karakoram Himalaya, northern Pakistan. *Geological Bulletin, Peshawar University*, **11** (Special Issue), 187p.
- Tarney, J., Saunders, A. D., Weaver, S. D., Donnellan, N. C. B. and Hendry, G. L. 1979. Minor element geochemistry of basalts from Leg 49. In: Luyendyk, B. P., Cann, J. R. et al. (eds). *Initial Reports of the Deep Sea Drilling Project*, **49**, 660-685.
- Thompson, A.B. 1982. Dehydration melting of pelitic rocks and the generation of H<sub>2</sub>O-undersaturated granitic liquids. *American Journal of Science*, **282**, 1567-1595.
- Treloar, P. J., Brodie, K. H., Coward, M. P., JAN, M. Q., KNIPE, R. J., REX, D. C. and Williams, M. P. 1990. The evolution of the Kamila shear zone, Kohistan, Pakistan. In: Salisbury, M.H. and Fountain, D. M. (eds.) *Exposed Cross-sections of the Continental Crust*. Kluwer Academic Publishers, Amsterdam, 175-214.
- Vigneresse, J.-L. & Burg, J.-P. 2003. The paradoxical aspect of the Himalayan granite In: Singh, S. 2003. Granitoids of the Himalayan Collisional Belt. *Journal of the Virtual Explorer, Electronic Edition*, **11**, Paper 03, ISSN 1441-8142.
- Wickham, S.M. 1987. The segregation and emplacement of granitic magmas. *Journal of the Geological Society, London*, **144**, 281-297.
- Wilson, M., 1989. *Igneous petrogenesis*. Unwin Hyman, London.
- Windley, B. F., 1983. Metamorphism and tectonics of the Himalaya. *Journal of Geological Society of London*, **140**, 849-865.
- Zen, E.-An & Hammarstrom, J.M. 1983. Magmatic epidote and its petrological significance. *Geology*, **12**, 515-518.



## MANGLA EARTHQUAKE OF MARCH 10, 2006: SOURCE PARAMETERS AND NATURE OF THE DERIVED FAULT

BY

**TALAT IQBAL, KARAM KHAN, MUHAMMAD QAISAR, TARIQ MAHMOOD**  
Micro Seismic Studies Programme, Ishfaq Ahmad Research Laboratories P.O. Nilore, Islamabad  
E-mail: talatqbal@hotmail.com

AND

**NASIR AHMAD**  
Institute of Geology, University of the Punjab, Quaid-i-Azam Campus,  
Lahore-54590 Pakistan

**Abstract:-** On March 10, 2006, an earthquake of magnitude  $M_L$  5.0 occurred near Mangla Lake about 95 km south-east of Islamabad. The epicentral area was jolted by the earthquake. One person was killed, 22 injured in Mirpur District. Further, the earthquake was felt widely from Peshawar to Lahore. The well controlled fault plane solution was obtained on the basis of P-wave polarity data of seismic stations of the local seismic network including world wide seismic stations. The fault plane is oriented in NW and SE direction with strike, dip and rake  $293^\circ$ ,  $20^\circ$  and  $117^\circ$  respectively which is in accordance with the local tectonics of the region. On the basis of Landsat Imagery, and seismotectonic analysis, a possibility of a thrust fault is also derived which passes near a small town Kalial where this earthquake occurred can be named as Kalial Thrust.

### INTRODUCTION

A moderate earthquake of Local Magnitude 5.0 occurred in the morning of March 10, 2006 at 07:50 GMT. This earthquake shook the city of Mirpur and Mangla with intensity VII on MMI (Modified Mercalli Intensity) scale (Fig.1). Seismic intensity at Pindori, 15 km almost west of the source near Mangla was VI. It was felt at Bhimbar, Kharian and Gujar Khan with intensity V. The earthquake was located at  $33.10^\circ$  N and  $73.76^\circ$  E at a focal depth of 10 km in the area of Azad Jammu and Kashmir near Mangla Lake in Mirpur District. It was followed by two aftershocks of Local Magnitude 4.0 and 3.0 respectively. The source lies in the area of Mangla Anticline near the town of Mangla. The populated city in the area is Mirpur. This city being on the hanging wall was most affected. One person was killed and 22 injured in the city. It was felt from Peshawar to Lahore. Fault plane solution of this earthquake was determined on the basis of P-wave polarity data by AZMTAK and PMAN (Suetsugu 1997).

### LOCATION PARAMETERS

Micro Seismic Studies Programme (MSSP), an establishment of Pakistan Atomic Energy Commission is operating a seismic network of 25 stations in Pakistan. To get the better coverage for the location of this earthquake, the data of a few nearby global stations was also used. Computer software SEISAN (Havskov, J. and Ottemoller L. 2001) gave the following hypocentral parameters with the Azimuthal coverage of  $288^\circ$ .

|                  |   |
|------------------|---|
| Origin Time      | 07:50:12.94                             |
| Latitude         | $33.10^\circ \pm 4.7\text{km}$          |
| Longitude        | $73.76^\circ \pm 5.7\text{km}$          |
| Depth            | $10\text{km} \pm 4.3\text{km}$          |
| Magnitude, $M_L$ | 5.0, ( $m_b = 4.9$ as reported by USGS) |



The result of location was good showing reasonably small errors in longitude, latitude and depth as it is evident from the error ellipse (Fig.2).

## REGIONAL GEOLOGY

The study area where earthquake occurred is surrounded by the region of low hills composed of Siwalik group of rocks. Material accumulated in the Gangetic geosynclines, where the rate of subsidence kept pace with the rate of deposition until about 20000 feet of material was deposited. The axis of this geosyncline was more northerly than that of geosyncline in which the rivers of the Indus-Ganges plain are depositing their sediments today. The most recent uplifts folded the Siwalik deposits and, to a lesser degree, displaced these along thrust faults. This probably occurred in the middle of the Pliocene Epoch and may be continuing on a lesser scale today. The area is seismically unstable and destructive earthquakes occur from time to time. The great system of thrust faults has, in the past, been considered as a single fault known as the Main Boundary Thrust (MBT). One branch of this major fault, the Bhimbar thrust (Fig. 3), passes at the distance of about 30 km from Mangla Dam whereas on the other hand, eastern termination of Salt Range Thrust lies in the south of Mangla Dam at the distance of 15 km.

## SEISMOTECTONIC ANALYSIS

The earthquake was occurred due to the movement of the fault passing near the town of Kalial. The pre-earthquake satellite imagery and digital elevation model analysis show that the fault existed previously but was not properly investigated. However the surface trace of this fault was marked on map (Searle et. al. 1996)). The recorded instrumental seismic data did not indicate any significant seismic event generated by this fault in the last few decades.

The earthquake area is an active seismic zone where Jhelum Fault, Salt Range Thrust, Main Boundary Thrust (MBT) and Kashmir Thrust are some pronounced seismogenic sources (Kazmi and Jan 1997, Ali et. al. 2008). The analysis of recorded seismic data shows that the area is dominated by low to moderate frequent seismicity at shallow depths (<33 km) Fig. 4 and Fig.5. The significant earthquakes occurring in the surrounding region in the near past are the Pattan earthquake ( $m_b=6.0$ ) of Dec. 28, 1974 (Wayne et. al. 1979), Astor Valley earthquake ( $m_b=6.2$ ) of Nov. 1, 2002 (Mahmood et. al. 2002), Kaghan Valley earthquake ( $M_L=5.6$ ) of Feb. 14, 2004 (Khan et. al. 2004) and Muzaffarabad earthquake ( $M_L=7.0$ ) of Oct. 8, 2005 (Qaisar et. al. 2007).

The Landsat ETM imagery, SRTM Digital Elevation Model (DEM), GPS, GIS and remote sensing alongwith source parameters were utilized in spatial analysis to

understand and mark surface features of the earthquake causative fault. The focal mechanism solution as determined predominantly thrust, striking northwest and dipping northeast, with a slight

strike slip component (Fig. 6) coincides well with the slip nature of the fault and also supported by surface evidences marked through spatial analysis of the area. As the fault passes near the town of Kalial, the fault may be named as Kalial\_thrust fault. The epicentral location was also supported by the intensity survey as maximum intensity was found near Kalial, District Mirpur. The seismic data of the main shock and aftershocks indicated that tectonic movements concentrated on part of Kalial Thrust at shallow depths. The projected surface trace length of the Kalial Thrust is estimated to be about 23 km.

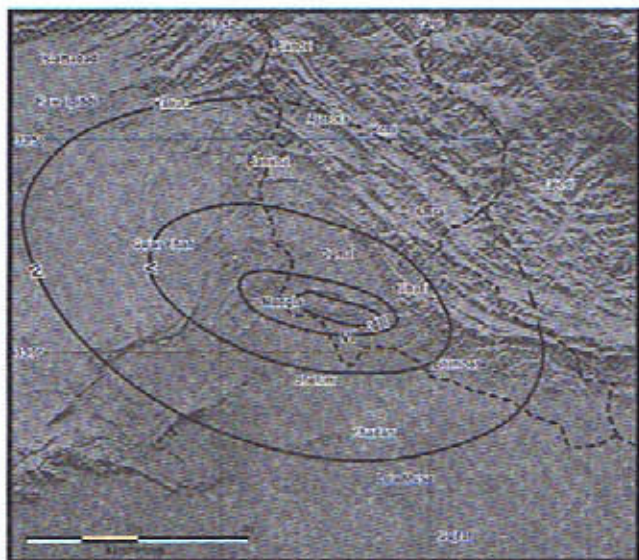
## FAULT PLANE SOLUTION

Fault plane solution of the earthquake on the basis of P-wave polarity data was obtained. The solution was derived using computer codes AZMTAK (Suetsugu, 1997) to calculate the azimuth and take off angle for the seismic stations used in the solution and PMAN (Suetsugu, 1997) to draw the nodal planes on the focal sphere as shown in Fig. 6. The earthquake followed by the two significant aftershocks having Local Magnitude 4.0 and 3.0 respectively. The clear P-wave polarity data of local network along with the seven global seismic stations for the main shock were sufficient to draw the nodal planes, but the aftershock's P-wave polarity data played an additional role in controlling the fault planes. Out of 43 data points used in the composite fault plane solution, 38 were consistent and only 5 remained inconsistent. Thus we got a well-controlled composite fault plane solution of the earthquake. The East-West oriented fault plane dipping towards north gave strike  $293^\circ$ , dip  $20^\circ$  and rake  $117^\circ$ . The fault plane solution clearly shows that the nature of the source is low angle thrusting. The Centroid Moment Tensor (CMT) solution given by the Harvard university is in agreement with the solution obtained in this study.

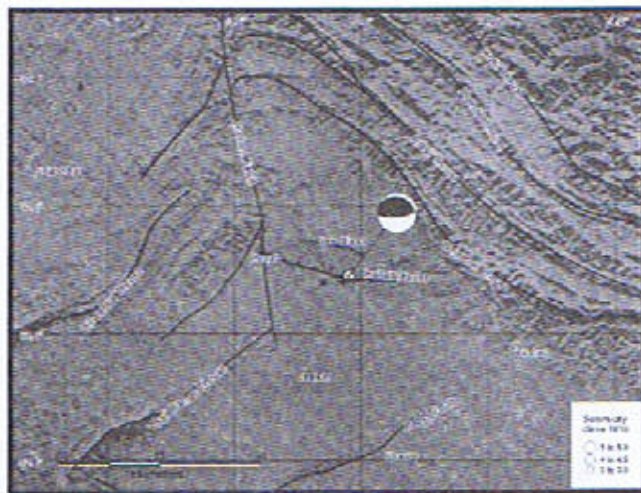
## INTENSITY DISTRIBUTION

A team of MSSP scientists and engineers made the intensity survey of the area affected by the earthquake to understand the mechanism of earthquake and its impacts on civil structure. The survey was based on the effects on land, houses and other buildings through the observations of the people living in the affected area and geology of the area through published maps. The maximum intensity VII on MMI scale occurred near the Mangla in Mirpur district where one person was killed and 22 were injured. The intensity decreased sharply in north south direction as is evident from the contour elongated in the WNW-ESE direction (Fig. 1).





**Fig. 1.** Isoseismals of the Mangla Earthquake of March 10, 2006





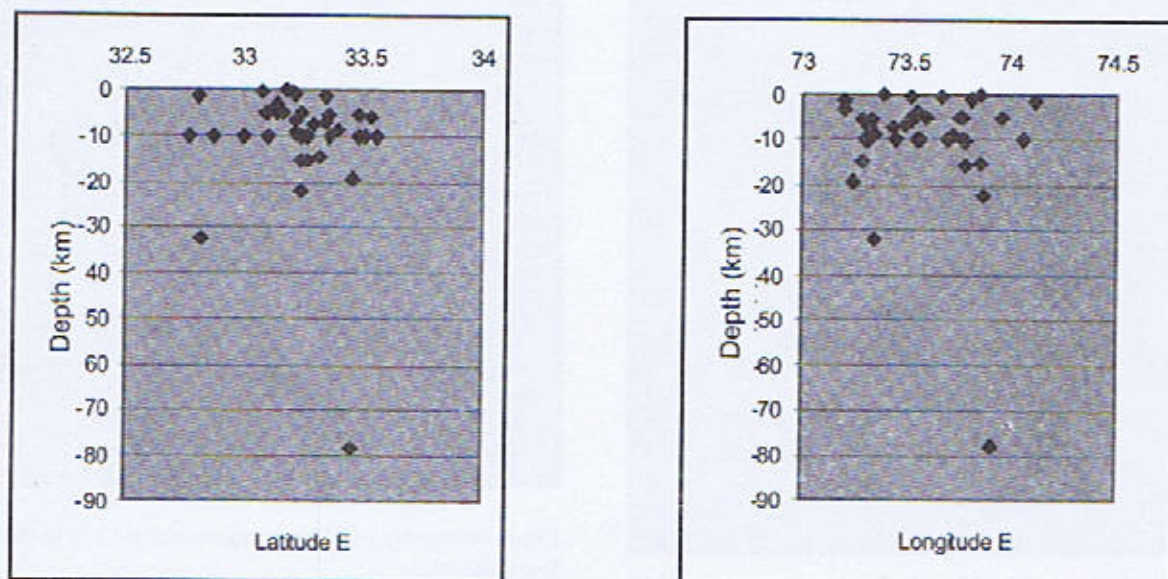


Fig. 5. Variation of Focal depth (km) with Latitude and Longitude

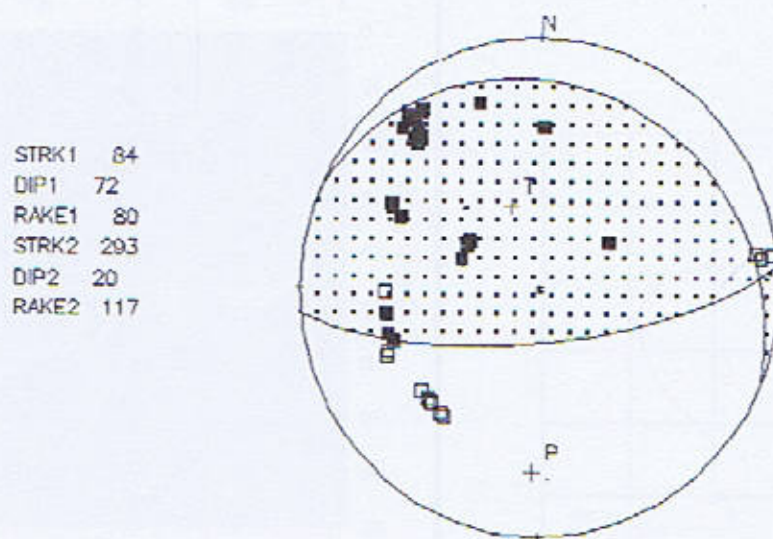


Fig. 6. Fault plane solution of Mangla earthquake



Following is the intensity felt in some well known places in the affected area.

### **Mangla**

Mangla is a well known town in Mirpur district due to Mangla Lake almost 12 km west of the epicenter. That is why the earthquake was named as the Mangla Earthquake. The population of Mangla is more than 3000. The intensive shaking was felt indoor and outdoor. The moderate damage to mud-stone masonry structure and partial damage to concrete structure was seen. The observed intensity was estimated as VII on MMI scale.

### **Mirpur**

It is a well populated city in the earthquake affected area having more than 371000 people living in it. It lies about 10 km NW of the epicenter of the main shock on the hanging wall of the fault plane. Being a populated city, each type of civil structure including very loose masonry structure exists in the city, therefore, it faced severe damage to loose structure and few cracks were seen in concrete structure. It was difficult to stand on the ground due to shaking. The overall observed intensity was same as felt at Mangla, that is VII on MMI scale.

### **Gujar Khan**

It is a densely populated city situated about 48 km WNW of the earthquake epicenter. The population is more than 70,000. There is no damage to civil structure, but many people felt the earthquake even during the outdoor activities. The intensity was estimated between IV and V for Gujar Khan.

### **Bhimber**

Bhimber is a small city, about 29 km ESE of the source with a population of 5500. All types of the civil structure were shook considerably but no damaged was seen in the city. The observed intensity was about IV to V on MMI scale in the city.

### **Jhelum**

Jhelum is an old city which lies almost 18 km south of the epicenter having more than 30,000 populations. The Jhelum is nearer to the source than Gujar Khan and Bhimber, but the earthquake was felt just indoors and household goods like crockery clashes in some houses. It shows that intensity decreases very sharply in north south direction, and hence the observed intensity at Jhelum was IV on MMI scale.

The intensity in some other cities and towns had also been observed and is shown in Fig. 1.

### **CONCLUSION**

An attempt is made to determine the source parameters along with nature of causative fault where the earthquake occurred. The location parameters of the earthquake were found with 288° coverage of seismic stations. The errors found in latitude, longitude and depth were  $\pm 4.7$ ,  $\pm 5.7$  and  $\pm 4.3$  km respectively which shows very small uncertainty in location. This earthquake is followed by the two aftershocks along with the spread of seismicity (Fig. 3) which shows that there is a reasonable concentration of the earthquakes in the vicinity of the current event. A well controlled fault plane solution of the earthquake shows that the nature of the causative fault is low angle thrusting with a very small strike-slip component which is in accordance with the structural trend in the area. On the basis of the above facts and that the large earthquakes are always associated with some fault, indicating the presence of subsurface low angle thrust fault near the town of Kalial may be named as Kalial Thrust fault.

### **ACKNOWLEDGEMENTS**

The authors wish to thank Mr. Naseem Ahmed and Muhammad Ali Shah for their valuable help in this study.

### **REFERENCES**

- Ali, Z., Qaisar, M., Mahmood, T., Shah, M. A., Iqbal, T., Serva, L., Michetti, A.M. and Burton, P. W. 2009. The Muzaffarabad, Pakistan, earthquake of 8 October 2005: surface faulting, environmental effects and macroseismic intensity. *Palaeoseismology: Historical and Prehistorical Records of Earthquake Ground Effects for Seismic Hazard Assessment* (Reicherter, K., Michetti, A.M. & Silva, P.G. editors). The Geological Society, London, Special Publications, 316, 155-172. DOI: 10.1144/SP316.9 0305-8719/09/\$15.00 © The Geological Society of London 2009
- Havskov, J., and Ottemoller L., 2001. *SEISAN: The Earthquake Analysis Software. Version 7.2*. University of Bergen, Bergen, Norway.
- Kazmi, A. H., and Jan, M. Q., 1997. *Geology and Tectonics of Pakistan* Graphic Publisher ; Karachi p. 124.
- Khan, S.A., Khan, K., Iqbal, Z., Mahmood, T., and Z. Ali. The Kaghan Valley Earthquakes of February 14, 2004: Source Mechanism and Regional Neotectonics. PAEC



- Mahmood, T., Ali, Z., Khan, K., Iqbal, T., Hakim, A., Khan, S.A. and M. Qaisar, 2004.
- Mahmood, T., Qaisar, M. and Ali, Z., 2002. Source mechanism of Astor Valley Earthquake of November 20, 2002 inferred from teleseismic body wave. *Geol. Bull. Univ. Peshawar*, Vol. 35, 2002.
- Qaisar, M., Daud, M., Ali, Z. and Tariq Mahmood, 2007. Muzaffarabad earthquake of October 8, 2005: Seismological aspects. Special Edition of Transactions of the International Academy of Sciences H&E, ICSD/IAS, Baku-Innsbruck, Azerbaijan. p 332-337.
- Report No. MSSP-71/2004.
- Searle, M. P. and Asif Khan, M. 1996. Geological map of North Pakistan and adjacent areas of northern Ladakh and western Tibet
- Suetsugu, D., 1997. Source Mechanism Practice. Lecture notes. International Institute of Seismology and Earthquake Engineering, Tsukuba, Japan 1997.
- The Kaghan Valley Earthquake of February 14, 2004: Intensity Survey and Geotectonics. PAEC Report No. MSSP-72/2004.
- Wayne, D., 1979. A summary of Field and Seismic Observations of the Pattan Earthquake of 28 December 1974. *Geodynamics of Pakistan: Geological Survey of Pakistan, Quetta, 1979.*



## PALEOCURRENT ANALYSIS OF DHOK PATHAN FORMATION, FROM THATHI NORTHEASTERN POTWAR DIST. RAWALPINDI

BY

SYED MAHMOOD ALI SHAH, AMER HAFEEZ AND NAVEED AHMAD

Institute of Geology, Quaid-e-Azam Campus, University of the Punjab, Lahore-54790

Shah061@gmail.com

**Abstract:** *Paleocurrent studies of the Dhok Pathan Formation was comprehensively carried out around Thathi village in northeastern Potwar. In the study area trough cross bedding was used to collect the data. A total of 50 sampling station were selected for the collection of data. Data was corrected for tectonic tilt and plotted on the rose diagram for the paleoflow and source direction of the Dhok Pathan Formation. The analysis shows that source is from northwest direction and paleoflow was in southeast direction.*

### INTRODUCTION

Paleocurrent analysis involves using sedimentary structures to determine the direction of flow or orientation of flow like that of a river, a group of streams within a basin, the wind direction within a region, or the direction of oceanic currents. Individual sedimentary structures tell you the flow direction at that geographic point and at that instant in time but in solving true regional scale problems we need to look statistically at populations of sedimentary structures (Boggs, 1995). These will give us a collective average of the current directions within a region over a period of time. All sedimentary structures did not provide flow direction information and even those that do, do not provide the same kind of information. For those that do provide flow information we have those that point down stream (down flow direction) like asymmetric ripples and trough cross-bedding and we have those like tool marks (skips, groves, and prods) and parting lineation that give us a current orientation, but we can not go upstream from downstream.

"Siwaliks" of Meddlicot (1864) are the fluvial deposits formed in the foothills of the Himalaya mountain i.e. foreland basin. Potwar is part of this foreland basin (Fig.2) and Siwaliks stretch nearly to all of the Potwar. Siwaliks are of Late Miocene Chinji Formation, Early Pliocene Nagri Formation, Early to Middle Pliocene Dhok Pathan Formation and the Late Pliocene to Early Pleistocene Soan Formation (Shah, 1977). All these formations are mainly composed of sandstone, shale, claystone and conglomerate and pebbles. Dhok Pathan as a

part of lower Siwaliks is comprised of monotonous cyclic alternations of sandstone and claystone and minor alternations of yellowish brown siltstone & conglomerates in the form of lenses and layers. Good exposures of trough cross bedding (Plate 1) are present in the study area which is the part of the Jabbar Anticline. The main purpose of the study is to know the paleocurrent direction of the Dhok Pathan Formation.

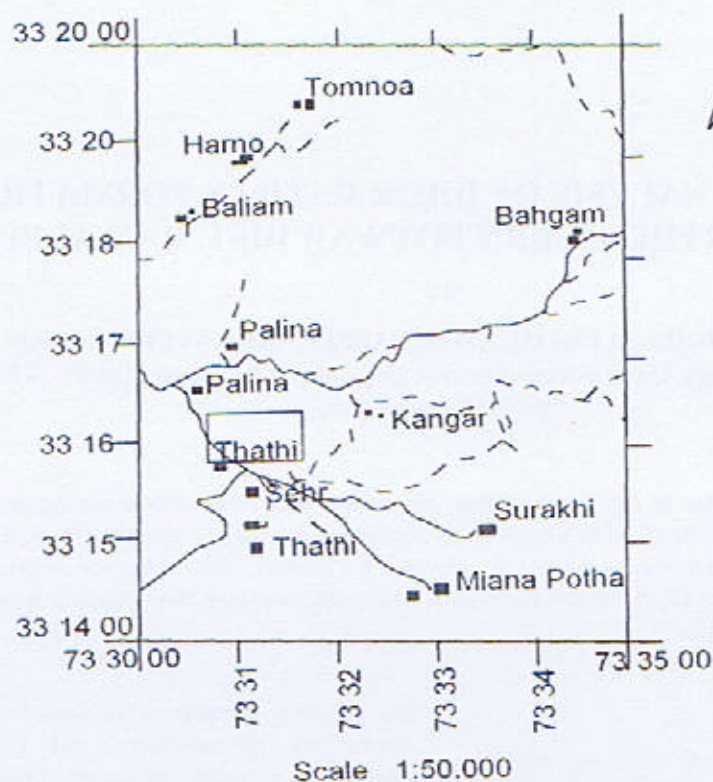
### METHODOLOGY

Following Steps were carried out in the study of paleocurrent analysis of the Dhok Pathan Formation from the surroundings of the Thathi village northeastern Potwar (Fig. 1).

### COLLECTION OF DATA

The way to ascertain a paleocurrent direction is first to go into the field and gather the data, that is make measurements with the Brunton Compass on the orientation of the structure. For those that point down stream we record the down current direction while for those which only give us a stream orientation we record the bearing for that trend expressed as so many degrees east of north or west of north. We do this for all available structures within the area of interest (allowing for time constraints of course if the region has a generous supply of structures). This is recorded in field book. Cross bedding data were collected from the sandstone units, which contained well preserved trough cross beds for paleocurrent flow direction. Total 50 sampling stations were selected for the collection of data.





Accessibility Map of the Study Area  
Fig.1 Location Map of Thathi Area

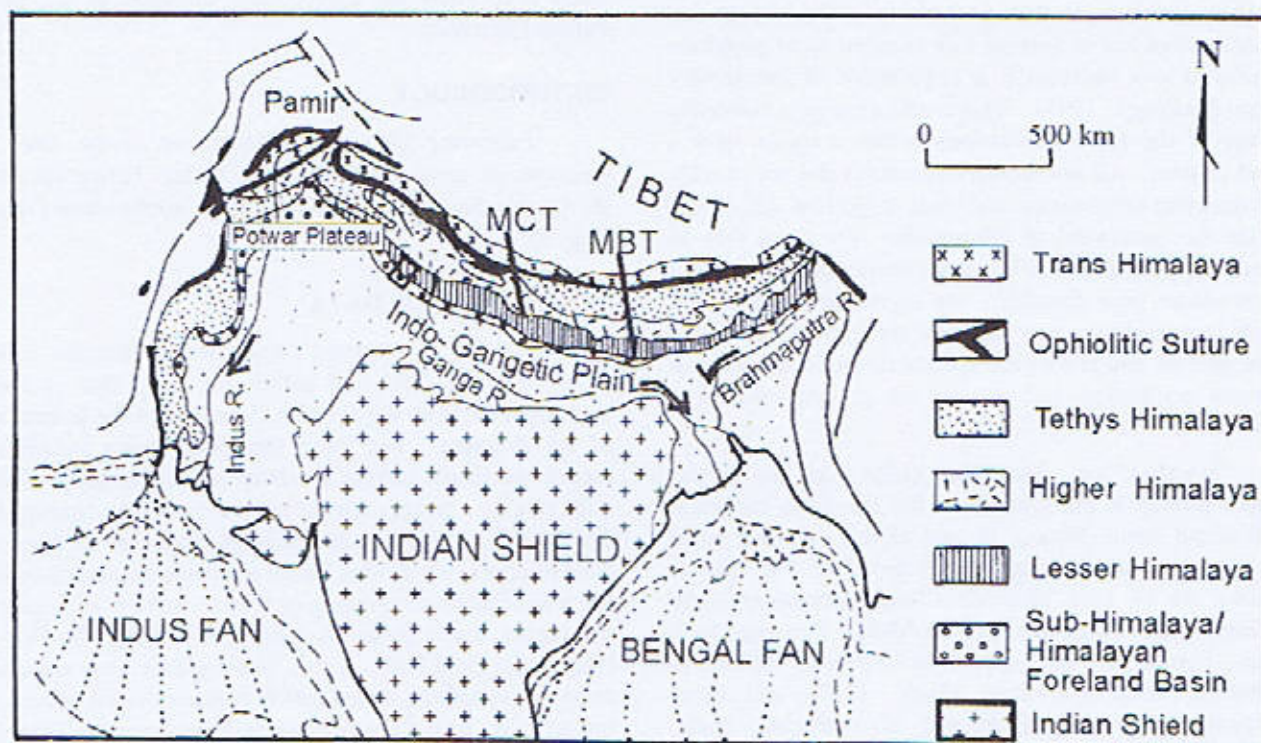


Fig.2 Simplified geological map of the Potwar (after Rohtash Kumar, 2003)



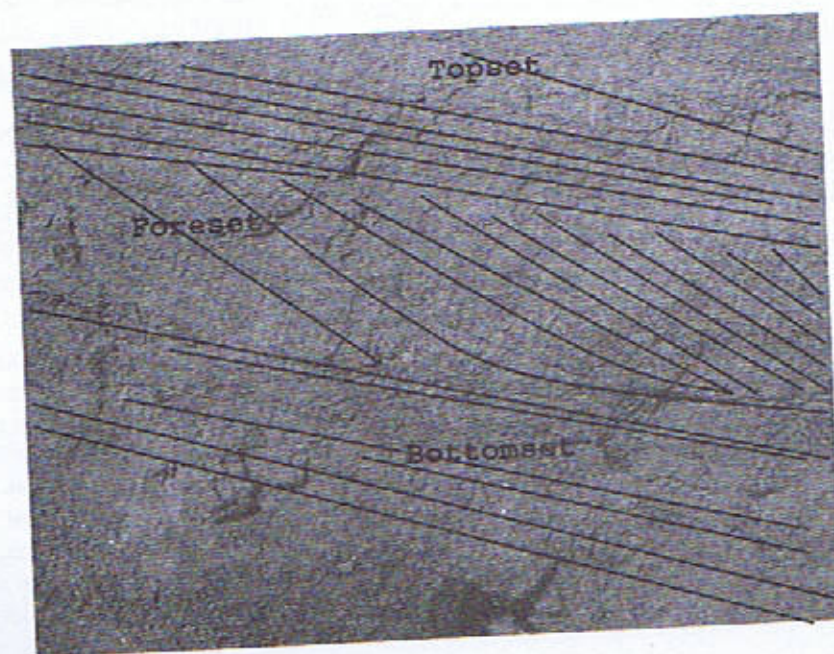


Plate1 Cross bedding in Dhok Pathan Formation near Sehr Village

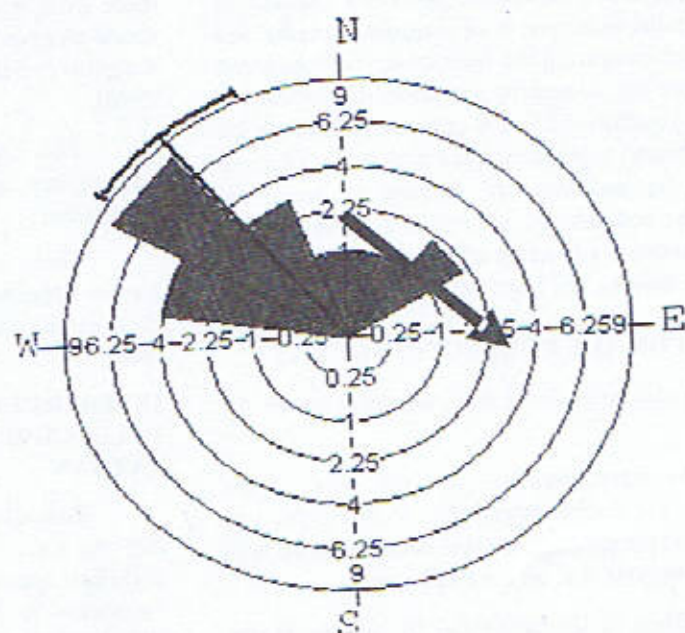


Fig. 3 Paleocurrent Direction of Dhok Pathan Formation



## CORRECTION OF DATA FOR TECTONIC TILT

Data are commonly collected from folded or tilted sequences and must be corrected in order to restore the bedding to its original horizontal position. The study area is part of the Northern Potwar Deformed Zone (NPDZ), in which the Jabbar Anticline lies, so the data should be corrected for tectonic tilt. This is done by rotating a line or plane about a horizontal axis using stereographic projection (Lidholm, 1987).

If the structural dip is less than  $25^\circ$  the measured azimuth of linear structures need no correction. If the dip exceeds  $25^\circ$  the effects of tilting must be removed. This can be done with a stereonet.

The situation for planar structures (e.g. cross bedding) is different, because even very low tectonic dip values (anything greater  $5^\circ$ ) may introduce an appreciable error. As is the case for linear structures, rotation can be done using stereographic projection. The procedure is more complicated in the case of steeply plunging folds, and double rotation may be required. If the plunge is less than  $10^\circ$  or if the dip is less than  $45^\circ$ , no correction for the plunge is necessary.

If the beds from which you are making paleocurrent measurements are not horizontally lying then you must correct for their structural orientation. If the bed dips more than 15 degrees you need to do this, if not don't bother. Making the correction involves using a stereonet and a sheet of tracing paper or clear acetate film known usually as the plot sheet. In the field, you must measure the strike and the dip of the bed containing the sedimentary structure and you must measure the orientation and down dip rotation of the sedimentary structure. You are defining the orientation in space of the bed as a planar surface with a line of strike and a line of dip and you are defining in space the orientation of the sedimentary structures apparent current direction or orientation (direction of plunge) as a compass direction and a rotation (dip) from the horizontal.

## PROCEDURE FOR THE CORRECTION OF DATA

Plot the poles of bedding and cross bedding on the stereogram.

Rotate the stereogram so that the pole of the bedding, B, comes to the equatorial line. In doing this you will also rotate CB the pole of the cross bedding. Mark both points on the stereogram (i.e. on the tracing paper).

Bring bedding to the horizontal by shifting B, the pole of the bedding to the centre of the stereogram. Move CB the pole of the cross bedding, the same number of degrees in the same direction along the nearest small circle (dashed lines).

Rotate the stereogram back, so that its N-S line coincides with the N-S line on the stereonet. To read the dip direction, draw a line from the pole, through the center, to the edge of the stereonet.

All these steps are shown in the Fig.4.

## GRAPHIC PRESENTATION OF DIRECTIONAL DATA

In practice there are two approaches that are used for graphic presentation of the directional data. These are current rose or rose diagram and vector mean the later is not applied in this study.

A popular device for presenting directional data is the current rose or rose diagram, which is a histogram converted to a circular distribution. Various class intervals are used but a  $30^\circ$  interval will meet most needs. It is better to plot the observations in each class than to plot the total number of observations. The class interval with the most observations is the modal class. When measurements of structures which show direction of movement are plotted (e.g. cross beds and flute casts) the rose diagram indicates the direction towards which the current moved. Most distribution produce a single dominant mode (unimodal), although some have two or more sub equal modes (bimodal, polymodal). In the case of structures which show line of movement, each measurement is represented by two opposite azimuth values (e.g.  $30^\circ$  and  $210^\circ$ ). The resulting current rose consists of two reflected halves. Measurements made from several different structures may be plotted on a single composite rose diagram also called a composite ray diagram radial line diagram or spoke diagram (Potter, 1978).

This method was adopted in the study of paleocurrent analysis of Dhok Pathan and Lower Soan Formations.

There is another method called Vector Mean and Vector Magnitude but not adopted in this study but brief description of this method is given below in the following text.

## INTERPRETATION OF ROSE DIAGRAM FOR THE PALEOCURRENT ANALYSIS OF THE DHOK PATHAN

Rose diagram of the Dhok Pathan Formation showed that its source was from the NW direction while the paleoflow was in SE direction. The age of the Dhok Pathan Formation is Early to Middle Pliocene. At that time Himalayan orogeny was on its climax and the Indian Plate was rotating in anticlock wise direction. The tectonically raised high relief and climatic change caused the great influx of sediments from the Kohistan Island Arc deposited in the foreland basin (Potwar Plateau) resulting in thick pile



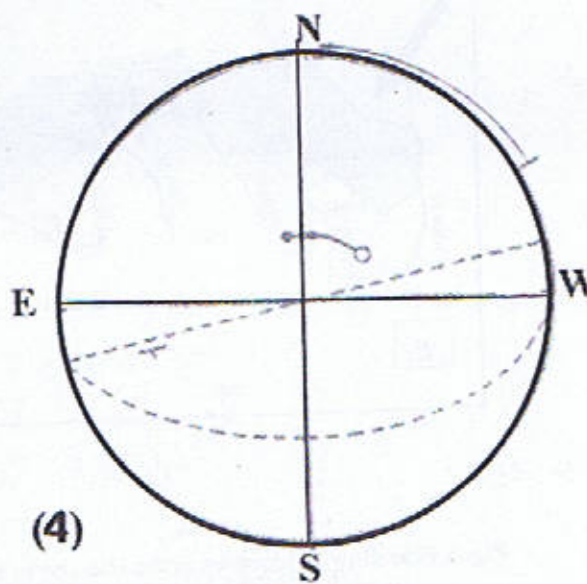
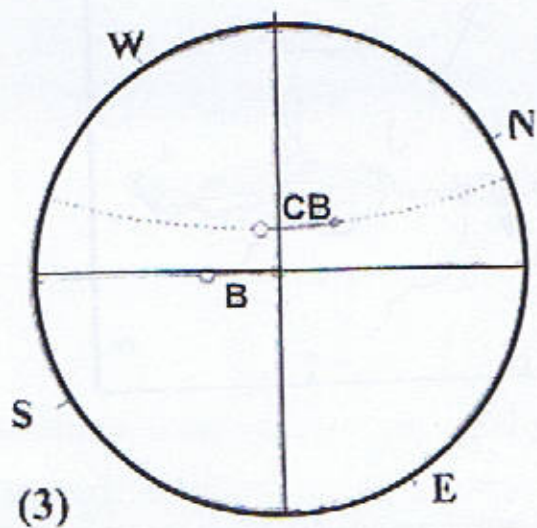
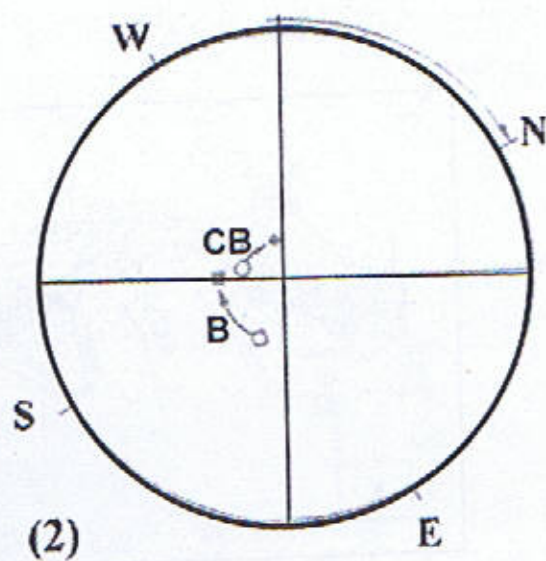
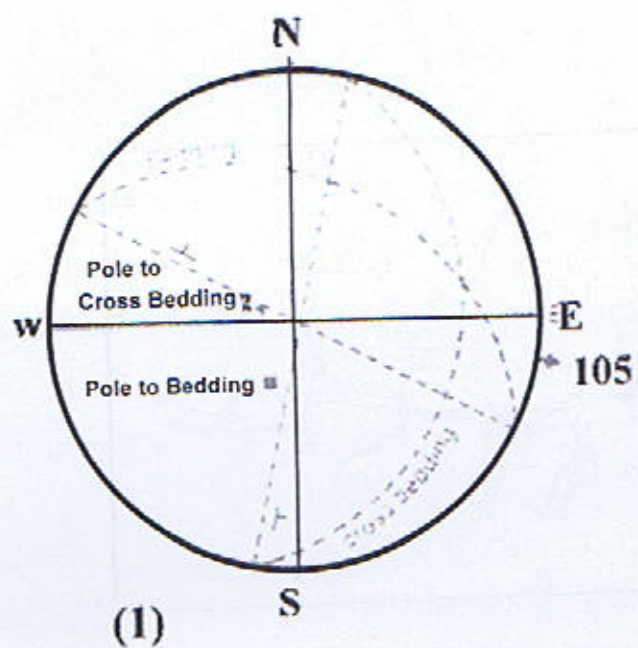


Fig. 4 Showing steps involved in the correction of data



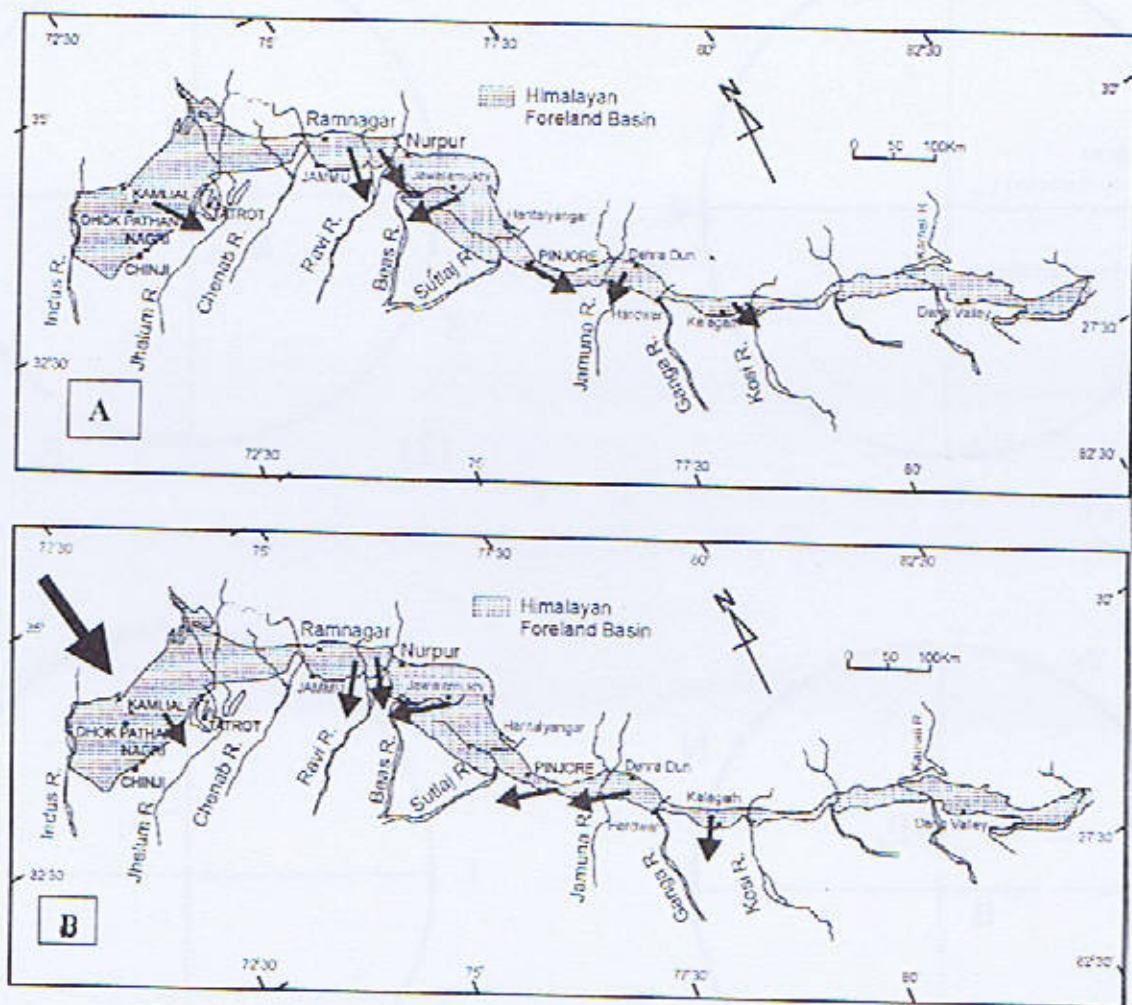


Fig. 5 Paleoflow orientation in the Himalayan Foreland Basin A- variability in paleoflow around 10 Ma B- Variability in paleoflow around 5Ma. Change in paleoflow around 5 Ma is related to the activity along MBT (after Rohtash Kumar, 2003).



of Siwaliks. The paleoflow model of the Dhok Pathan formation is mentioned in the Fig. 3 & 5.

## CONCLUSION

Paleocurrent data of the Dhok Pathan Formation was comprehensively studied from cross bedding exposures around the Thathi village in northeastern Potwar. Totally 50 sampling stations was corrected for tectonic tilt. Data was plotted on rose diagram for the paleoflow and source direction of the Dhok Pathan Formation. The analysis shows that the source was from northeast direction and paleoflow was in southeast direction.

## ACKNOWLEDGEMENT

The authors are grateful to Mr. Abdul Qadir, Director Atomic Energy Mineral Centre Karachi and Mr. Mumtaz Farooq for their guidance and interest to carry out this study in the area, as well authorizing to publish this paper. The authors also express their gratitude to Professor Dr. Muhammad Ashraf for his review of the manuscript. Sincere thanks are also due to Professor Dr. Nasir Ahmad, Director of the Institute of Geology, Punjab University, Lahore for moral encouragement.

## REFERENCES

- Boggs, S. Jr., (1995). Principles of Sedimentation and Stratigraphy 2<sup>nd</sup> ed. Merrill Publishing, Columbus, Ohio.
- Lindholm Roy C. (1987). A Practical Approach to Sedimentology Allen &. Inc., 8 Winchester Place, Winchester, mass. 01890, USA the U.S. company of Unwin Hymin Ltd. P.43-47
- Meddlicot, H.B. (1864). On the geological structure and relation of southern portion of Himalayan ranges between the river Ganges and Ravee: *India Geol. Surv., Mem.*, 3, pt. 2, pp. 1-212
- Potter, P.E. and F.J Pettijohn, (1978). Paleocurrent and Basin Analysis. Academic Press, New York
- Rohtash K., Sumit K. G and Satish J. S (2003). Mio-Pliocene Sedimentation history in the northwestern part of the Himalayan Foreland Basin, India. *Cur. Scie* 84, No.8
- Shah, S.M.I., (1977). Stratigraphy of Pakistan. *Mem. Geol. Surv.* 12 P. 92-93



## SEDIMENTOLOGY OF DHOK PATHAN FORMATION FROM THATHI AREA, NORTHEAST POTWAR DISTRICT RAWALPINDI

BY

SYED MAHMOOD ALI SHAH AND AMER HAFEEZ

Institute of Geology, Quaid-e-Azam Campus, Punjab University, Lahore  
shah061@gmail.com

**Abstract:** The Dhok Pathan Formation of Early to Middle Pliocene age exposed at Thathi area, northeast Potwar district, Rawalpindi was selected for sedimentological studies. The formation is composed of alternating beds of sandstone and clays in 1:1 ratio with minor intercalations of siltstone and intraformational conglomerates which are abundant in upper part. Lithofacies and petrographical studies revealed that sandstone is feldspathic litharenites and formation has provenance of the Kohistan Island Arc. The lithofacies studies suggests that formation is deposited in a fluvial environment in a wide depression in front of the rising Himalayas.

### INTRODUCTION

The Potwar Plateau is constituted by a less internally deformed fold and thrust belt having a width of approximately 150 km in N-S direction. It is bounded to the south by Salt Range Thrust and to the north by the Kalachitta-Margalla Hill Range. Indus River forms its western limit whereas the Jhelum River marks its eastern boundary (Kazmi and Jan 1997). There is a marked difference in the tectonic style of north western, south western and eastern Potwar. The northern part of Potwar Plateau, also referred to as the Northern Potwar Deformed Zone (NPDZ) lies between the Main Boundary Thrust and the Soan Syncline. It is more intensely deformed than the southern part, which is known Southern Potwar Deformed Zone (SPDZ) (Jaswal et.al. 1997). As part of foreland basin Potwar hosted mollase deposits named as "Siwaliks" of Meddlicot (1864) are the fluvial deposits formed in the foothills of the Himalaya mountain. Siwaliks are of Late Miocene Chinji Formation, Early Pliocene Nagri Formation, Early to Middle Pliocene Dhok Pathan Formation and the Late Pliocene to Early Pleistocene Soan Formation (Shah, 1977).

The "Upper Manchar" of Blandford (1876), Dhok Pathan of Pilgrim (1913) and Dhok Pathan Formation of Cotter (1913) was adopted as such by the Stratigraphic Committee of Pakistan in 1967. The name is derived from the village of Dhok Pathan in the Attock district (lat. 33°07'N; long 72°14'E) is the type locality of formation. The formation is widely distributed through Indus Basin

and Quetta region of the Calcareous Zone of the Northern Axial Belt. The formation is 1330m thick at the Gaud River which is the principal reference section and 1500m at the Thathi (Fig.1) area which has been our area of study. Where it was mapped and measured first time (Fig.2).

A very rich vertebrate fauna has been recorded from the Dhok Pathan Formation of the Kohat-Potwar province, (Pascoe 1963). The formation is less fossiliferous in the lower Indus basin and Quetta region. Some of the important fossils are: *Indarctos salmontanus*, *Arctamphicyon lydekkeri*, *Ictitherium indicum*, *Mastodon browni*, *Dicoryphochoerus titanoides* and *Hydasphitherium megacephalum*. The fauna indicates Early to Middle Pliocene age. The formation has transitional contact with the underlying Nagri formation and conformable with the Soan formation in the study area.

### LITHOLOGY

The formation is composed of monotonous cyclic alternations of sandstones & clays. Sandstone is grey, light grey, white, reddish brown, occasionally brownish grey, brown or buff thick bedded, calcareous, moderately cemented, soft and cross bedded. Clay is orange, brown, dull red or reddish brown; occasionally rusty orange, greenish yellow, yellowish grey, or chocolate coloured, calcareous and sandy. They are in 1:1 ratio.

Minor intercalations of yellowish brown siltstone are common. Conglomerates in the form of lenses & layers (channel beds) (Plate 1B) are the essential part of the upper part.



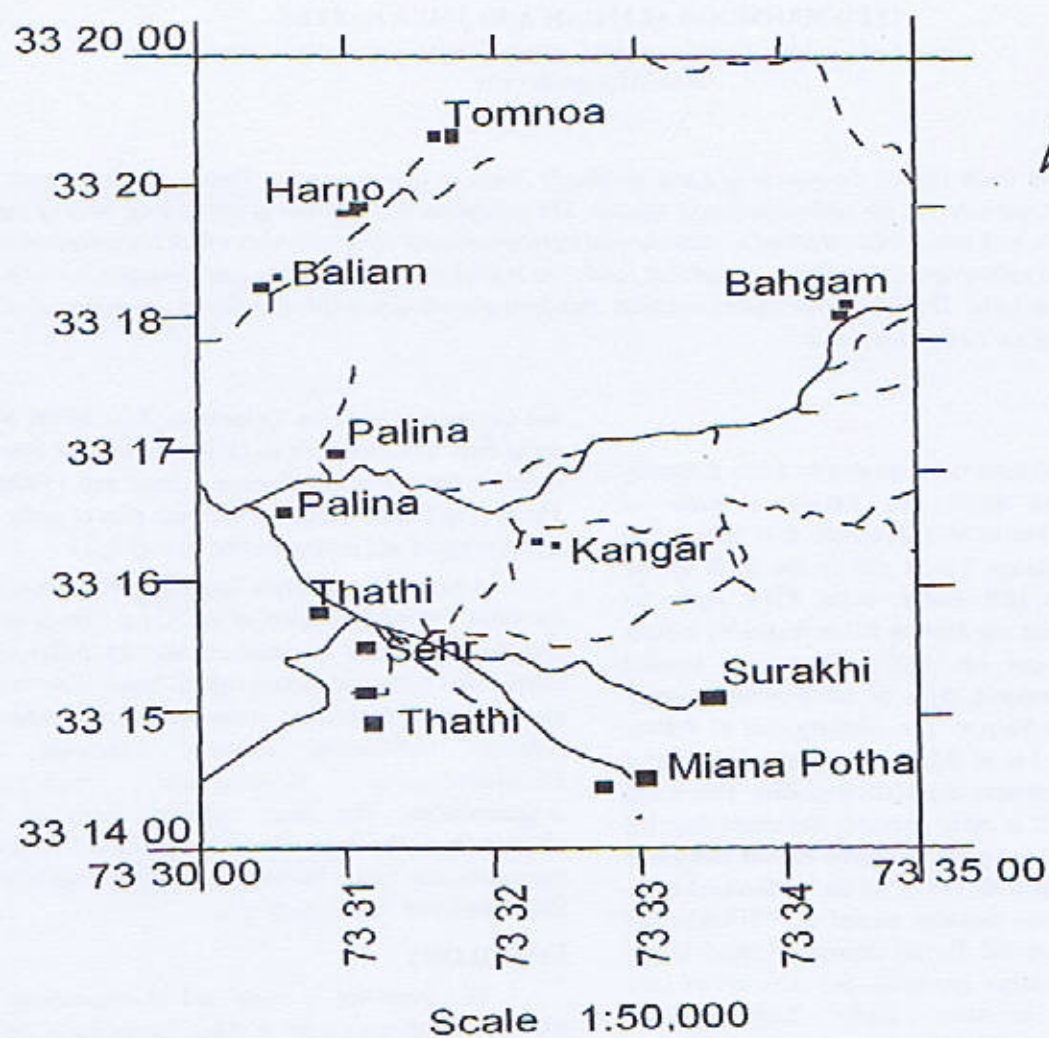


Fig.1 Location Map of Thathi Area



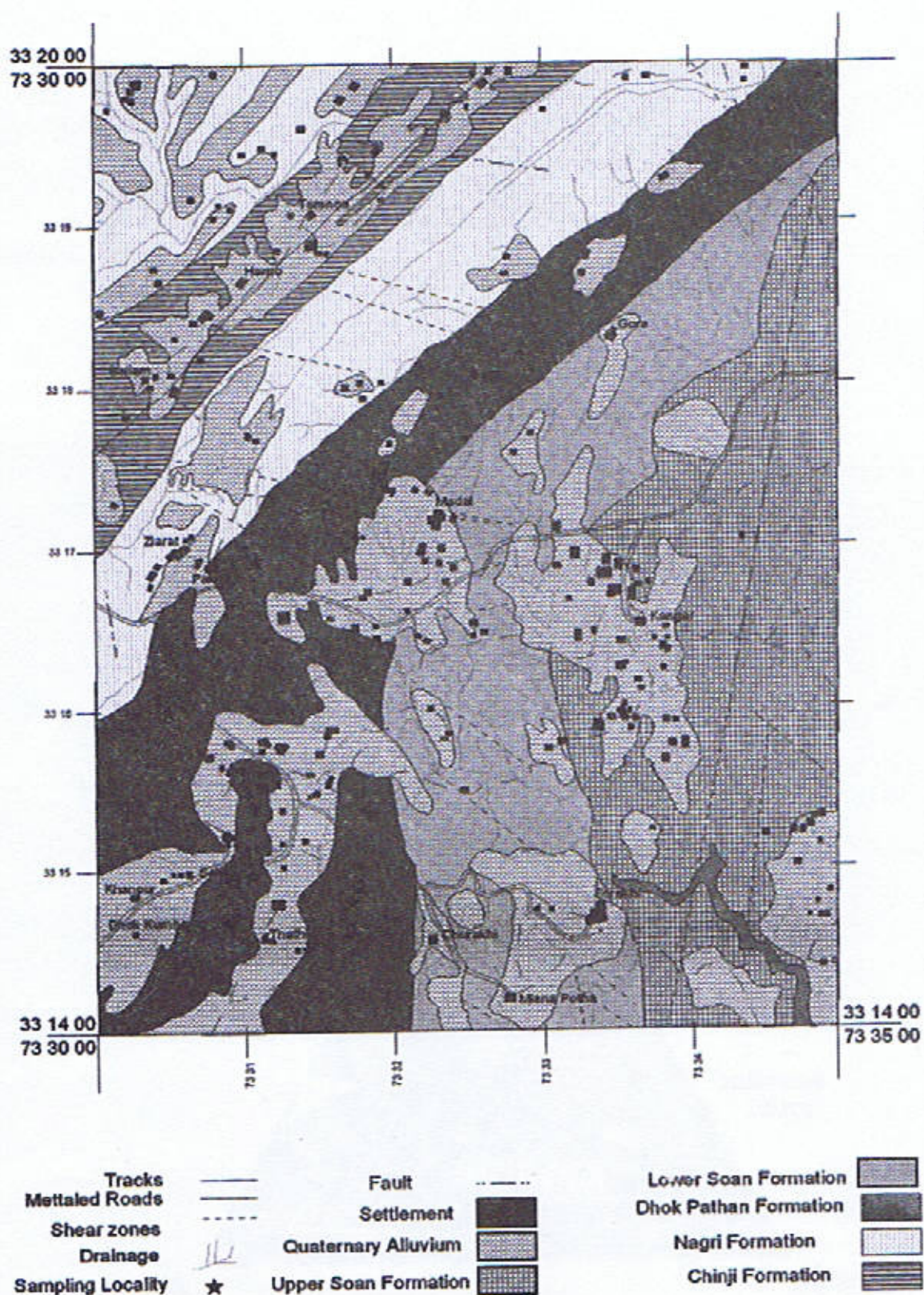


Fig. 2 Lithostructural map of area



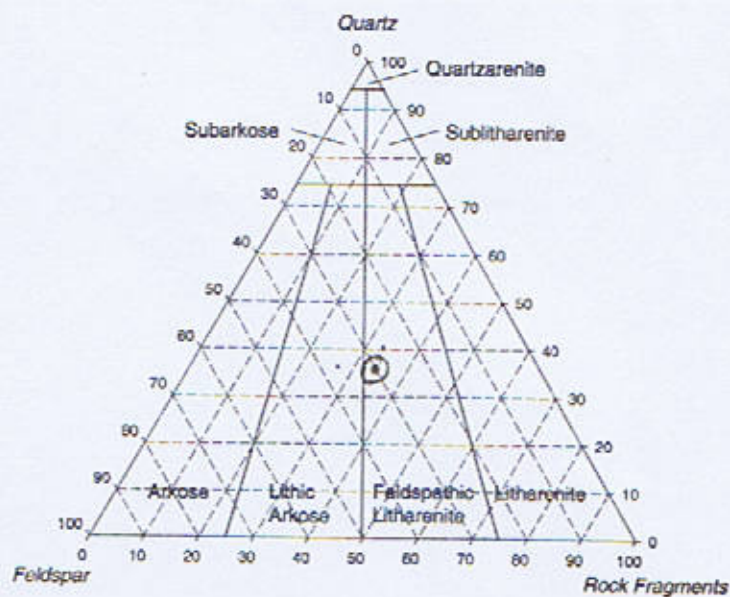


Fig. 3 Ternary diagram showing sandstone classification nomenclature

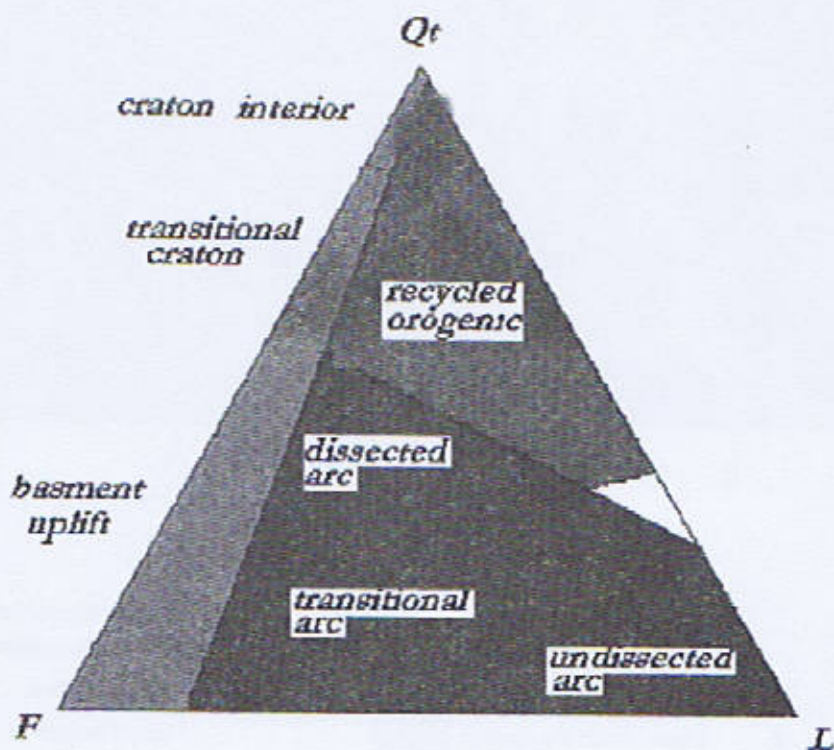


Fig. 4 Diagram showing provenance of Dhok Pathan F





A Conglomerates & Pebbles in channel bed of Dhok Pathan Formation



B Hematitic alteration in Dhok Pathan Formation



## PETROGRAPHY

The sandstone of the Dhok Pathan Formation is medium to coarse grained, friable, poorly sorted and are immature both mineralogically. The average framework composition of the Dhok Pathan Formation is quartz varies from 32-39 percent, K-feldspar varies from 7-12 percent, plagioclase varies from 5-10 percent and rock fragments varies from 20-38 percent. Muscovite and biotite are also present and ranges from 1-3 percent. Chert ranges from traces to 2 percent.

The major alterations observed during thin section study are.

1. Hematite in the form of thin layers (Plate 1A).
2. Feldspar to sericite and kaolinite
3. Amphibole to chlorite

The QFL diagram after Folk (1976) shows that the sandstone is feldspathic litharenite (Fig. 3).

## TEXTURE

The fabric is mostly feldspathic litharenites. The detrital constituent is medium to coarse grained but generally show mixture of grain sizes. Framework grains are mostly angular to subangular. Calcite act as cement with minor iron oxides.

## CLAY MINERALOGY

The bulk mineralogy of all the investigated samples is mainly composed of quartz as dominant phase, subsequently calcite, orthoclase, albite, montmorillonite, clinocllore (chlorite) and illite. The mineral composition throughout the shale is consistent, only one sample Das-10 shows the presence of gypsum, since the sample was dried at 70°C. The gypsum lost 1/2 molecule of H<sub>2</sub>O and restructure as Bassanite.

Less than two micro friction indicates the presence of montmorillonite, Illite, Clinocllore (chlorite). On glycolation the peak shifting of Montmorillonite from 15 Angstrom 17 Angstrom conform the presence of montmorillonite.

The fine grained nature of shales constituents and the absence of other mineral specially Feldspar suggests that material has come from the long distance and during the transportation only quartz and clay minerals were deposited at their final destination. It is also possible that this shale has been redeposited at the site of presence.

## PROVENANCE

The quartz grains of the Dhok Pathan Formation are mostly angular to subangular, occasionally polycrystalline; display normal to undulatory extinction suggests mainly

metamorphic origin. The inclusion of zircon in some of the quartz crystals and presence of myrmekitic texture in some of feldspar grains suggest that source was plutonic. Some quartz grains show fracturing which possibly is related to the intense tectonic activity.

The QFL provenance discrimination diagram (Dickinson, 1985) shows that Dhok Pathan Formation has a dissected arc provenance (Fig. 4). The detrital material of the Dhok Pathan Formation was contributed by a dissected arc during Early to Middle Pliocene located to the north of the Potwar basin and paleodrainage was from northeast direction. Thus the source of Dhok Pathan Formation is mainly laid in Kohistan Island Arc with contribution from basement rocks exposed by the uplift at the back of MCT.

## DEPOSITIONAL ENVIRONMENT

Sandstones represent deposits of levees, crevasse channels and splays, floodplain channels, and large sheet floods. Laminated mudstones represent floodplain and lacustrine deposits. Lakes were both perennial and short-lived, and likely less than 10m deep with maximum fetches on the order of a few tens of kilometers. Trace fossils and body fossils within all facies indicate the former existence of terrestrial vertebrates, molluscs (bivalves and gastropods), arthropods (including insects), worms, aquatic fauna (e.g. fish, turtles, and crocodiles), trees, bushes, grasses, and aquatic flora. Palaeoenvironmental reconstructions are consistent with previous palaeoclimatic interpretations of monsoonal conditions.

## CONCLUSIONS

1. Dhok Pathan Formation is composed mainly of sandstone and shale in 1:1 ratio.
2. Intraformational conglomerates or channel beds are also present and abundant in upper part of formation.
3. Petrographical studies shows that cementing material of the formation is mainly calcite.
4. QFL diagram reveals that sandstone is feldspathic litharenite.
5. Petrographical analysis results that the provenance of the formation was from a dissected arc i.e. Kohistan Island Arc in the north of the Potwar basin.
6. The lithofacies studies suggests that formation is deposited in fluvial environment.

## ACKNOWLEDGEMENT

The authors express their gratitude to Dr. Khurshid Alam Butt, Ex. Director General Atomic Energy Mineral Centre, Lahore for permission to carry out their study in the area under the professional guidance of Mr. Abdul Qadir and Mr. Mumtaz Farooq Energy Mineral Centre, Lahore, as



well as authorizing to publish this paper. The authors are also thankful to Dr. Mohammad Ashraf for the review of the manuscript. Thanks are also due to Professor Dr. Nasir

Ahmad, Director of the Institute of Geology, Punjab University, Lahore for moral encouragement and support.

## REFERENCES

- Blandford, W. T., (1876). "Note on the Geology of the Sind": *Ibid.*, Recs., 9, pp 8-22
- Cotter G. de P., (1933). "The Geology of the part of the Attock District". *India Geol. Surv., Mem.*, 55 pp. 63-161
- Dickinson, W.R., (1985). "Interpreting Provenance, relations from Detrital Models of Sandstone". In: G.G. Zuffa (ed), *Provenance of Arenite*, Nato series, Riedel, Dordrecht, 148:33-361
- Folk, R. L., (1974). "Petrology of Sedimentary Rocks". Hemphill's, Austin, Texas
- Jaswal, T.M., Lillie, R.J. and Lawrence, R.D., (1997). "Structure and Evolution of the Northern Potwar Deformed Zone, Pakistan" *Amer. Assoc. Petrol Geol. Bull.* 81, p308-352
- Kazmi, A.H., Jan, M.Q (1997), "*Geology and Tectonics of Pakistan*" Graphic Publishers. p 139
- Meddlicot, H.B. (1864). "On the Geological structure and relation of southern portion of Himalayan Ranges between the River Ganges and Ravee": *India Geol. Surv., Mem.*, 3, pt. 2, pp. 1-212
- Pascoe, E. H., (1963). "*A manual of Geology of India and Burma*". 3: *Ibid* Calcutta, pp.1344-2130.
- Pilgrim, G. E., (1910). "Preliminary notes on a revised classification of the Tertiary fresh water deposits of India": *India Geol. Surv., Recs.*, 40, pt. 3, pp. 185-205
- Shah, S.M.I., (1977). "Stratigraphy of Pakistan". *Mem. Geol. Surv.* 12: P. 92-93



## TEACHING STAFF LIST OF THE INSTITUTE OF GEOLOGY, UNIVERSITY OF THE PUNJAB 2 0 0 9

| <u>No.</u> | <u>Name and Qualifications</u>  | <u>Designation</u>                | <u>Field of Specialization</u>  |
|------------|---|-----------------------------------|---|
| 1          | <b>Dr. Nasir Ahmed</b><br>M.Sc. (Pb), Ph.D (Leeds)  | Professor<br>(Director)           | Environmental Science   |
| 2.         | <b>Dr. Akhtar Ali Saleemi</b><br>M.Sc. (Pb), M.Sc. (Leicester),<br>Ph.D. (Leicester)                                  | Professor                         | Mineralogy, Petrology, Industrial<br>Mineralogy                               |
| 3.         | <b>Dr. Riaz Ahmad Sheikh</b><br>B.Sc. (Hons), M.Sc. (Pb), D.I.C.,<br>Ph.D (Imperial College)                          | Professor                         | Structure & Petroleum Geology,<br>Sedimentology, Regional Tectonics           |
| 4.         | <b>Dr. Muhammad Saeed Farooq</b><br>M.Sc. (Pb), Ph.D. (Pb)  | Professor                         | Engineering Geology, Geohydrology   |
| 5.         | <b>Mr. Umar Farooq</b><br>M.Sc. (Pb), M.Sc., D.I.C. (Imperial<br>College), GTC (Japan)                                | Associate Professor               | Exploration Geophysics  |
| 6.         | <b>Dr. Zahid Karim Khan</b><br>M.Sc. (Pb) PGD (Delft), Ph.D. (Pb)   | Associate Professor               | Engineering Geology, Geohydrology,<br>Aggregate Materials                     |
| 7.         | <b>Dr. Nazir Ahmad</b><br>M.Sc. (Pb), Ph.D. (Leicester)   | Associate Professor               | Structural & Petroleum Geology, Mapping,<br>Sedimentology, Regional Tectonics |
| 8.         | <b>Dr. Syed Alim Ahmad</b><br>M.Sc. (Pb), Ph.D (Pb)   | Associate Professor               | Mineralogy, Petrology   |
| 9.         | <b>Dr. Shahid Jameel Sameeni</b><br>M.Sc. (Pb), Ph.D. (Pb.), COMETT-<br>EUCOR Micropal (Basel), Post-Doc<br>(Berkley) | Associate Professor               | Biostratigraphy, Micropaleontology,<br>Paleobiology, Paleocology              |
| 10         | <b>Mr. Sajid Rashid</b><br>M.Sc. (Pb)   | Assistant Professor<br>(on leave) | Engineering Geology, Geohydrology   |
| 11.        | <b>Syed Mahmood Ali Shah</b><br>M.Sc. (Pb)  | Assistant Professor               | Mineralogy, Petrology   |
| 12.        | <b>Dr. Naveed Ahsan</b><br>M.Sc. (Pb), Ph.D. (Pb)   | Assistant Professor               | Structural & Petroleum Geology, Tectonics                                     |
| 13.        | <b>Dr. Shahid Ghazi</b><br>M.Sc. (Pb) Ph.D. (Leeds)   | Assistant Professor               | Petroleum Exploration Sedimentology &<br>Sequence Stratigraphy                |



- |     |  |                        |   |
|-----|--|------------------------|---|
| 14. | <b>Mr. Mustansar Naeem</b><br>M.Sc. (Pb)               | Assistant Professor    | Engineering Geology                                 |
| 15. | <b>Mr. Abdus Sattar</b><br>M.Sc. (Pb)                  | Assistant Professor    | Geochemistry, Mineralogy                            |
| 16. | <b>Dr. Abdur Rauf Nizami</b><br>M.Sc. (Pb), Ph.D. (Pb) | Assistant Professor    | Petroleum Geology, Remote Sensing,<br>Sedimentology |
| 17. | <b>Mr. Zia ud Din</b><br>M.Sc. (Pb)                    | Assistant Professor    | Geophysics  |
| 18. | <b>Mr. Kamran Mirza</b><br>M.Sc. (Pb)                  | Assistant Professor    | Micropaleontology, Stratigraphy,<br>Sedimentology   |
| 19. | <b>Mr. Sohail Akram</b><br>M.Sc. (Pb)                  | Lecturer<br>(on leave) | Engineering Geology, Geohydrology                   |



**NON TEACHING STAFF MEMBERS LIST OF  
THE INSTITUTE OF GEOLOGY, UNIVERSITY OF THE PUNJAB  
2009**

| <u>Sr. No.</u> | <u>Name of Employee</u>    | <u>Designation</u>  |
|----------------|----------------------------|---------------------|
| 1.             | Sharafat Ali Khan          | Librarian           |
| 2.             | Basher ul Islam            | Admin. Officer      |
| 3.             | Aurangzeb Bhatti           | Store Supervisor    |
| 4.             | Nadeem Younas              | Private Secretary   |
| 5.             | Sarfraz Ahmad              | Office Assistant    |
| 6.             | Khurshid Ali               | Office Assistant    |
| 7.             | Liaqat Ali                 | Junior Technician   |
| 8.             | Sami Ullah Khan            | Junior Technician   |
| 9.             | Tasneem Ahmad Khan         | Draftsman           |
| 10.            | Muhammad Ilyas             | Head Lab. Assistant |
| 11.            | Safdar Ali Bhatti          | Sr. Clerk           |
| 12.            | Liaqat Ali                 | Lab. Attendant      |
| 13.            | Muhammad Farrukh Javed     | Sr. Clerk           |
| 14.            | Ali Akbar Sindhu           | Sr. Clerk           |
| 15.            | Muhammad Bashir            | Junior Clerk        |
| 16.            | Shaukat Ali                | Junior Clerk        |
| 17.            | Muhammad Jahanzeb          | Driver              |
| 18.            | Muhammad Riaz              | Driver              |
| 19.            | Hafiz Malik Muhammad Nazir | Lab. Attendant      |
| 20.            | Haq Nawaz                  | Lab. Attendant      |
| 21.            | Syed Qaim Ali Shah         | Junior Clerk        |
| 22.            | Ghulam Mustafa             | Lab. Attendant      |
| 23.            | Nazir Ahmad                | Lab. Attendant      |
| 24.            | Muhammad Rafi              | Lab. Attendant      |



|     |                         |                     |
|-----|-------------------------|---------------------|
| 25. | Arshad Ali              | Attendant           |
| 26. | Syed Sajid Hussain Shah | Qulli               |
| 27. | Muhammad Ramzan         | Naib Qasid          |
| 28. | Shabbir Ali             | Naib Qasid          |
| 29. | Muhammad Imran          | Naib Qasid          |
| 30. | Asad Ahmad              | Lab. Attendant      |
| 31. | Malik Muhammad Nasir    | Naib Qasid          |
| 32. | Syed Asif Ali           | Machine Assistant   |
| 33. | Muhammad Irfan          | Semi-Skilled worker |
| 34. | Sohail Iqbal            | Naib Qasid          |
| 35. | Qudrat Ullah            | Lab. Attendant      |
| 36. | Abdul Waqar             | Lab. Attendant      |
| 37. | Javed Masih             | Lab. Attendant      |